2012

Driving Cycle Properties and their Influence on Fuel Consumption and Emissions

Oscar Francisco Delgado-Neira
West Virginia University

Driving Cycle Properties and their Influence on Fuel Consumption and Emissions

Oscar Francisco Delgado-Neira

Dissertation submitted to the

Benjamin M. Statler College of Engineering and Mineral Resources

West Virginia University

In partial fulfillment of the requirements

for the degree of

Doctor of Philosophy

In

Mechanical Engineering

Gregory J. Thompson, Ph.D., Chair

Christopher M. Atkinson, Sc.D.

Nigel N. Clark, Ph.D.

David R. Martinelli, Ph.D.

W. Scott Wayne, Ph.D.

Department of Mechanical and Aerospace Engineering

Morgantown, West Virginia

2012

Keywords: Modeling, Fuel Economy, Greenhouse Gases, Regulations, NOx Emissions, Driving Cycles.

Abstract

Driving Cycle Properties and their Influence on Fuel Consumption and Emissions

Oscar Francisco Delgado-Neira

When developing regulations or preparing emissions inventory models for on-road mobile sources, it is of critical importance to obtain representative values of fuel consumption and emissions rates that accurately represent the vehicle behavior for varying vehicle operation. Unfortunately, fuel consumption and emissions are often only known for a few test cycles which generally represent limited types of vehicle activity. It is known that distance-specific emissions and vehicle fuel consumption strongly depend on the vehicle activity and this dependency causes difficulties when trying to estimate fuel consumption and emissions over different vehicle activity than the original test cycle(s). The central hypothesis of this research is that linear relationships exist between metrics that quantify vehicle activity and the resulting emissions and fuel consumption. These metrics are calculated on the basis of vehicle speed-time traces and are termed driving cycle properties. A methodology of linear interpolation in the properties' space is used to calculate appropriate linear combination weights for varying vehicle activities in order to predict fuel consumption and emissions over "unseen" driving cycles or in-use routes. The proposed modeling approach and method evaluation provides accurate oxides of nitrogen and fuel consumption inventory data estimations for diverse vehicle operation using either chassis dynamometer or in-use data collected with portable emission measurement systems. The predictive accuracy of the in-use model was improved when using grade-related metrics. Fuel consumption average prediction errors of 5.7% and 3.6% were obtained for chassis dynamometer data and in-use data, respectively. Oxides of nitrogen average prediction errors of 10.2% and 7.2% were obtained for chassis dynamometer data and in-use data, respectively. The prediction errors were slightly higher than the run-to-run variations found in chassis or in-use testing.

Acknowledgements

My Ph.D. has been a very enriching journey. Five years of my life and lots of different people and experiences after, I am very proud and happy of making the decision to come to WVU. First of all, I would like to express my gratitude to my advisor, Dr. Gregory Thompson, for his excellent guidance, support, and patience during these years. He always encouraged me to do good work and provided me with a good atmosphere and plenty of opportunities to do research and teaching. I think we make a good team and hope to keep our collaboration and friendship in the future.

I also want to thank Dr. Nigel Clark for helping me shape the original idea for this dissertation. His advice and important contributions to this study are appreciated as well as his friendliness and collegiality. I would also like to express my gratitude to my committee members, Dr. Chris Atkinson, Dr. David Martinelli, and Dr. Scott Wayne for their time, constructive comments, and valuable input.

I also had many interesting and inspiring discussions about my dissertation work with my friends Fritz Campo and John Rivas. The many people of the CAFEE group have provided a very professional, yet fun work environment. I want to thank them as well.

My parents and grandparents deserve special recognition for raising me and taught me the values of responsibility and hard work. I can't imagine where I would be without their support and example.

Finally, I would like to thank my wife for her love, support, and patience, as well as for sharing this journey with me from the beginning to the end, in both good and bad times.

Table of Contents

List of Tables

List of Figures

Nomenclature

ANL	Argonne National Laboratory
bhp	Brake Horsepower
CAA	Clean Air Act
CAFE	Corporate Average Fuel Economy
CAFEE	Center for Alternative Fuels, Engines, and Emissions
CARB	California Air Resource Board
CBD	Central Business District
CFD	Computational Fluid Dynamics
CMEM	Comprehensive Modal Emissions Model
CO	Carbon Monoxide
CO_2	Carbon Dioxide
COV	Coefficient of Variance
CRC	Coordinating Research Council
DOE	Department of Energy
DOT	Department of Transportation
DPF	Diesel Particulate Filter
EIA	Energy Information Administration
EPA	Environmental Protection Agency
ER	Emission Rate
FC	Fuel Consumption
FTP	Federal Test Procedure
g	Grams
GEM	Greenhouse Gas Emissions Model
GHG	Greenhouse Gas
GVWR	Gross Vehicle Weight Rating
HC	Hydrocarbons
HD	Heavy Duty
HDDT	Heavy Heavy-Duty Diesel Truck Schedule
HWFET	Highway Fuel Economy Test
hp	Horsepower
LSFC	Load Specific Fuel Consumption
MD	Medium Duty
MEMS	Mobile Emissions Measurement System
MOVES	Motor Vehicle Emissions Simulator
MY	Model Year
mph	Miles per hour
NHTSA	National Highway Traffic Safety Administration
NMHC	Non Methane Hydrocarbons
NN	Neural Networks
NRC	National Research Council
NOx	Oxides of Nitrogen
PM	Particulate Matter
PSAT	Powertrain System Analysis Toolkit
PEMS	Portable Emissions Measurement Systems

Re	Reynolds Number
SCR	Selective Catalytic Reduction
SET	Supplemental Emissions Test
SIP	State Implementation Plan
THC	Total Hydrocarbons
US	United States
VSP	Vehicle Specific Power

1 Introduction

Heavy-duty diesel engines are the primary power source in the United States (US), and elsewhere, to move goods and services. Although these engines provide the means for economic growth and prosperity, they produce emissions harmful to human health and the environment (Sydbom et al., 2001). The primary emissions species of concern from heavy-duty diesel engines have been particulate matter (PM) and oxides of nitrogen (NOx) and these two exhaust species have been reduced nearly two orders of magnitude between the late 1980's and the latest regulations change in 2010 in the US (CFR, 2008). It is unlikely that heavy-duty diesel engine PM and NOx emissions will be reduced from their 2010 limits in the future. The next major regulatory step will concern fuel consumption and greenhouse gas (GHG) emissions (US EPA and NHTSA, 2011). Liquid fuel consumption by medium-duty (MD) and heavy-duty (HD) vehicles[1] represents 26 percent of all US liquid transportation fuels consumed and has increased more rapidly than consumption by other sectors (NRC, 2010).

The Energy Independence and Security Act, Section 108, was passed in 2007 and requires the US Department of Transportation (DOT), for the first time in history, to establish fuel consumption standards for MD and HD vehicles. In December 2009, the US Environmental Protection Agency (EPA) formally declared that GHG emissions endanger public health and the environment within the meaning of the Clean Air Act, a decision that compels EPA to consider establishing first-ever GHG emissions standards for new motor vehicles, including MD and HD vehicles (NRC, 2010). The trucks, buses, and work vehicles included under this regulation are the fastest-growing contributor to the transport sector's GHG emissions, currently representing about 22 percent of the sector's emissions (US EPA, 2010a).

[1] Vehicles in the US are classified based on the DOT classification using gross vehicle weight rating (GVWR). Light-duty passenger vehicles and light-duty trucks (Classes 1 and 2a) have a GVWR less than 8,500 pounds and are covered by the GHG and Corporate Average Fuel Economy (CAFE) standards. The remaining classes (Class 2b to Class 8, see Table 1) are the subject of upcoming regulations and for the purposes of this document, the term medium- and heavy-duty (MD and HD) will be used for them. Note that a different classification by EPA may be found in which vehicles with GVWR between 8,500 and 19,500 lbs (Classes 2b to 5) are considered light heavy-duty, vehicles with GVWR between 19,500 and 33,000 (Classes 6 and 7) are considered medium heavy-duty, and vehicles with GVWR greater than 33,000 pounds (Class 8) are considered heavy heavy-duty.

It is necessary to consider how fuel consumption and GHG emissions for MD and HD vehicles can be regulated. These vehicles are used in almost every sector of the economy, in a large number of different configurations (e.g. pickup trucks, refuse trucks, delivery vehicles, transit buses, long haul tractor trailers) and their duty cycles vary greatly from low speed, stop and go urban operation to higher speed operation on suburban roads and highways. In order to promulgate standards for fuel consumption or GHG emissions, regulatory agencies should address the duty cycles that characterize different types of vehicles and their wide range of applications. The number and complexity of MD and HD engine-vehicle configurations and duty cycles would inevitably lead to the use of computer simulation as a cost-effective means to calculate fuel consumption and emissions. It is therefore desirable to develop an accurate method to estimate fuel consumption and emissions over various duty cycle scenarios, based on a limited number of required tests. The method should achieve fidelity between certification values and real-world results, in order to assure the beneficial impact of the regulations.

This research was directed towards developing and verifying a mathematical-empirical methodology for prediction of MD and HD vehicle fuel consumption and emissions during operation over new or "unseen" vehicle activity based on fuel consumption and emissions data which had been gathered from operation on known chassis dynamometer cycles or in-use routes data. Statistical properties of those cycles or routes (statistical descriptors of vehicle activity) were used. The technique focused on defined properties and their relationship to fuel consumption and emissions to develop predictions from a more fundamental approach as compared to other statistical approaches such as linear or non-linear regression of continuous data. The technique may prove useful within regulatory analyses and inventory models, reducing the number of required tests, and providing a means for translating emissions and fuel consumption data between diverse types of vehicle activity.

1.1 Issues Regarding Future Fuel Consumption and GHG Regulations

The following sections discuss issues regarding MD and HD vehicles emissions and fuel consumption models that should be assessed in order to develop appropriate inputs and to define methods to evaluate the outputs. Although the end goal is to develop a model that is targeted to fuel consumption and GHG regulations, specific requirements of present or pending regulations are not presented here so that a general model can be developed.

1.1.1 Vehicle Activity-Emissions Dependency

When developing fuel consumption and emissions models, it is of critical importance to obtain representative data that accurately represent the vehicle behavior for a particular vehicle operation. Unfortunately, fuel consumption and emissions are often measured using only a few test cycles which represents only a few average speed and specific types of activity. Engine operation envelopes and transient behavior differ between test cycles or in-use operation and affect vehicle-out average emissions. It is known that distance-specific emissions and vehicle fuel consumption strongly depend on the driving cycle used during testing (Clark et al., 2002b). Road grade (Zhang and Frey, 2006) and weight (Frey et al., 2007) also affect fuel consumption and emissions. This dependence imparts difficulties when trying to estimate fuel consumption and emissions over new, unseen vehicle activity, or when trying to compare emissions or fuel consumption between vehicles that were not tested on the same, or similar, cycle or route. Moreover, some engine dynamometer or chassis dynamometer driving cycles may be criticized in that they are not necessarily representative of a real-world, present-day fleet and vehicle's activity.

1.1.2 Computer Simulation Issues

The diversity of the MD and HD fleet in terms of configurations and duty cycles would inevitably lead to the use of computer simulation as a cost-effective means to estimate fuel consumption and emissions. A computational fluid dynamics (CFD) model with full emissions modeling could provide detailed emissions information but is computationally expensive and not a mature technology that lends itself to the modeling required as a regulatory tool. Simulations using complete vehicle models may be too complex and require detailed input parameters (component models, control strategies, and engine maps among others) to be useful for regulatory control due to the vast amount of information needed from diverse vehicle populations. Additionally, availability of model input data may restrict application of these complex models. For example, control strategies often are proprietary and accurate component models information usually are only available to users of commercial software. Rather than develop a model based upon specific input parameters for which data may not likely to be readily available, it is important to seek surrogate variables that are related to the key physical variable of interest but for which data may be more readily available (e.g. vehicle speed-time traces and test-bench measurements).

1.1.3 Test Cycles and Weighting Method

From a regulatory perspective, one desirable approach to MD and HD vehicle fuel consumption and GHG emissions testing would be to use the same test cycles to test all the vehicles, regardless of type, and using an appropriate weighting method to project fuel consumption and emissions over a wider envelope of vehicle activity. This would be similar to current EPA fuel economy and emissions testing of light-duty vehicles, which uses five different test cycles to determine City, Highway and combined fuel economy ratings for every vehicle model[2]. For ease of implementation of this method and to reduce overall costs there is a strong desire to minimize the number of test cycles required for any MD and HD vehicle fuel economy regulations. There must be a judicious selection of test cycles in order to provide a wide range of vehicle activity. For example, if all testing and modeling was done on a slow speed urban test cycle manufacturers would have little incentive to improve vehicle aerodynamics, but would have a large incentive to incorporate a hybrid drive train. There is a need for appropriate selection of test cycles for MD and HD vehicles. If weighing factors are to be applied to estimate fuel consumption and emissions, it is desirable to know how they should be calculated to provide physically meaningful estimations.

With the above considerations (emissions being dependent on test cycle, diversity of MD and HD fleet, lack of availability of input parameters for modeling, complexity of actual simulation software, need for appropriate selection and weighing of test cycles) in mind, this dissertation proposes a modeling framework that allows prediction of fuel consumption and emissions over a wide envelope of vehicle activity based on measurements over a few predetermined test cycles, using simple but robust inputs, and providing a physically meaningful way to weight emissions and fuel consumption results. The developed methodology will prove useful for upcoming GHG and fuel efficiency regulations and will help complement the current inventory models for translation of emissions between driving cycles or in-use routes, representing diverse types of vehicle activity.

---

[2] For pre-2008 model year vehicles, the FTP-75 and HWFET cycles were used to determine city and highway fuel economy, respectively. Combined fuel economy was determined by weighting the city fuel economy at 55 percent and the highway fuel economy at 45 percent using harmonic averaging. For 2008 and later model year vehicles, the EPA updated the test procedures to include a mixture of five separate driving cycles including the HWFET (highway), FTP-75 (city), US-06 (high speed, aggressive driving), SC-03 (air conditioning), and cold temperature FTP-75 (Federal Register, 2009).

1.2 Hypothesis and Objectives

The central hypothesis of this proposed research is that the relationship between vehicle activity and emissions can be modeled through the use of chassis dynamometer driving cycles' or in-use routes' properties. The underlying assumption is that fuel consumption and emissions vary in the same way as the driving cycle or in-use route properties. These properties are related to the power consumption of the vehicle via the external loads placed on the vehicle, and can be used for calculating appropriate linear combination weights for different vehicle activities, in order to predict fuel consumption and emissions over new or "unseen" driving cycles or in-use routes.

This research was based on a modeling methodology to predict fuel consumption and emissions over unseen cycles or in-use routes using measurements performed over other cycles or routes, and their properties. The objective of this study is to perform a model evaluation to increase both the predictive ability and the application level of the modeling methodology. The specific objectives of this study are:

- Perform a model analysis to describe and understand it from a mathematical perspective. This objective also includes a variability analysis of the input parameters used, and a sensitivity analysis of the modeling methodology. The outcome of this objective provided a starting point for further development of the model.
- Identify the most suitable properties for translation of fuel consumption and NOx emissions between different types of vehicle activity.
- Generate guidelines for appropriate selection of chassis dynamometer cycles to be used within the modeling methodology.
- Extend the methodology to in-use data gathered with portable emissions measurement systems (PEMS) and provide guidelines for appropriate selection of routes and metrics.

1.3 Structure of the Dissertation

A review of relevant literature is presented in Chapter 2. A description and mathematical analysis of the modeling methodology is presented in Chapter 3. The results of the variability and sensitivity analyses are given in Chapter 4. The data used and the methodology followed are presented in Chapter 5. The results are presented and discussed in Chapter 6. A summary of the study and conclusions, including recommendations for further work, are given in Chapter 7. Appendix A describes the calculation of cycle and route properties. Appendices B and C provide information about the chassis dynamometer cycles

and the in-use routes used in this study, respectively. A decision-making structure (flowchart) is presented in Appendix D as a reference guide for application of the modeling methodology.

Please note that while the general terms emissions and GHG emissions are used throughout this document, only carbon dioxide (CO_2) (as a surrogate for fuel consumption) and NOx are examined in this work for HD diesel and natural gas-fueled vehicles. While other emissions are of interest from a regulated and GHG emissions perspective, only these two emissions are examined herein to explore this model development.

1.4 Contribution

This dissertation will present the following contributions:

- The level of accuracy achieved with the methodology reduces the requirement of vehicle testing over representative cycles (aimed at reproducing real world operating conditions) and reduces testing requirements. A limited number of baseline test cycles would be sufficient to predict emissions and fuel consumption for a broad range of vehicle activity. In this way, a unique set of driving cycles can be used by regulatory agencies to test different configurations of MD and HD vehicles, and then apply a different weighting of the emissions and fuel consumption results depending on vehicle vocation.
- Another contribution of this proposed research is broadening the application level of the methodology by assessing its use with in-use data gathered with PEMS. This can generate a new approach for local emissions inventory allowing users to access real-world emissions from a vehicle that is operated over a roadway route that may be very different from the schedules used for initial emissions and fuel consumption characterization.
- Metrics were developed to include directly measurable parameters to capture the dependence of MD and HD vehicle emissions on and fuel consumption for in-use driving conditions. Specifically, the influence of grade on the model.
- The results of this research have been disseminated in two peer-reviewed papers, together with two presentations at conferences, to date.

2 Literature Review

Vehicle fuel consumption and engine out NOx emissions are directly related to the vehicle power consumption which depends heavily on the speed time trace or cycle under which the vehicle has been driven. Other regulated emissions for MD and HD engines include carbon monoxide (CO), total hydrocarbons (THC) or non-methane hydrocarbons (NMHC), and total particulate matter (TPM) and these emissions species generally are more dependent on transient engine activity. It is therefore necessary to develop methods to accurately estimate fuel consumption and emissions from individual vehicles on any driving cycle. The general theme of this study is the modeling of fuel consumption and emissions (NOx) of heavy-duty vehicles over new or unseen activity, based on driving cycle properties. With that in mind, the literature review includes an overview of the MD and HD fleet, a discussion of the road load equation, cycle properties, general regulations of emissions and fuel consumption for MD and HD vehicles, and a summary of prior approaches for prediction of fuel consumption and emissions.

2.1 Heavy-duty Fleet Overview

According to the US Department of Energy (DOE), Energy Information Administration, US consumption of liquid fuels totals 19 million barrels per day (EIA, 2011). The transportation sector accounts for 71% of that total. This sector's energy consumption grew at an average rate of 1.2% from 1975 to 2009 and is expected to account for 73% of total liquid fuel consumption in 2035. Heavy truck fuel consumption is expected to increase 23% between 2009 and 2020 because of economic growth drivers for freight transportation (EIA 2011). Because of the energy density that petroleum fuels provide, there are no apparent alternatives energy sources, such as total electrification of MD and HD vehicles, in the near future.

Heavy-duty vehicles are classified by weight, based on the gross vehicle weight rating (GVWR), which is the maximum in-service weight set by the manufacturer. Table 1 shows the classification of MD and HD vehicles with some of their applications. Passenger cars, minivans, and pick-up trucks with less than 8,500 lb GVWR are considered light-duty vehicles. Unlike the light-duty segment whose primary mission tends to focus on transporting passengers for personal travel, the heavy-duty segment is very diverse in terms of types of vehicles and usage patterns. For example Class 2B and 3 vehicles are mainly heavy-duty pickup trucks that may be primarily used for personal transportation to and from work with an average annual mileage of 15,000 miles and maximum payloads of about 5,000 lb, while Class 7 and 8

combination tractors used for freight transportation can travel more than 150,000 miles per year carrying up to 50,000 lb of payload (EPA, 2011). In between those classes, one can find a wide range of applications or vocations including shuttle vans, delivery trucks, transit buses and refuse trucks. Usage pattern also contributes to fleet diversity. For example, Class 8 combination tractors may operate as short-haul, typically into metropolitan areas or as long-haul travelling longer distances between cities and states.

The US Energy Information Administration (EIA, 2011) estimates that Class 2b vehicles achieved approximately 14.5 to 15.6 mpg in 2010, Class 3 to 6 vehicles achieved about 7.9 mpg, and Class 8 freight hauling trucks achieved approximately 6.1 mpg. Note that fuel economy in units of distance per unit volume of fuel consumed may not sufficiently describe a vehicle's vocation and that a further normalization of fuel economy with the number of passengers transported, as for buses, or with the amount (volume or weight) of cargo transported, as for trucks, may be necessary to truly evaluate the efficacy of a specific vehicle technology.

Table 1 US MD and HD vehicle classes (NRC, 2010)

Class	Applications	Typical Payload (lb)	GVWR (lbs)
2b	Large Pick-Up, Utility Van	3,700	8,501-10,000
3	Utility Van, Mini-Bus	5,250	10,001-14,000
4	City Delivery, Large Walk-in	7,250	14,001-16,000
5	City Delivery, Large Walk-in	8,700	16,001-19,500
6	City Delivery, School Bus	11,500	19,501-26,000
7	City Bus, Tractor-Trailer	18,500	26,001-33,000
8	City Bus, Tractor Trailer	50,000	33,001-80,000

Heavy-duty vehicles defined as Classes 2b through 8 make up only about 5% of the vehicles on the road but they account for about 10% of the vehicle miles traveled and for about 25% of the fuel consumed (NRC, 2010). Figures 1, 2, and 3 shows the distribution of 2007 US MD and HD fleet in terms of number, miles traveled, and fuel consumed, respectively. Class 8 trucks are mostly tractor semitrailers operating on trip lengths greater than 100 miles. Class 8 trucks represent about 21% of the MD and HD fleet. They are also the largest CO_2 emitters[3] and fuel users accounting for about 50% of miles travelled and about

[3] In distance-specific units (g/mile).

67% of all commercial truck fuel used. Class 6 box trucks, which are typically used in urban deliveries rank second in fuel use with about 13% of total fuel use.

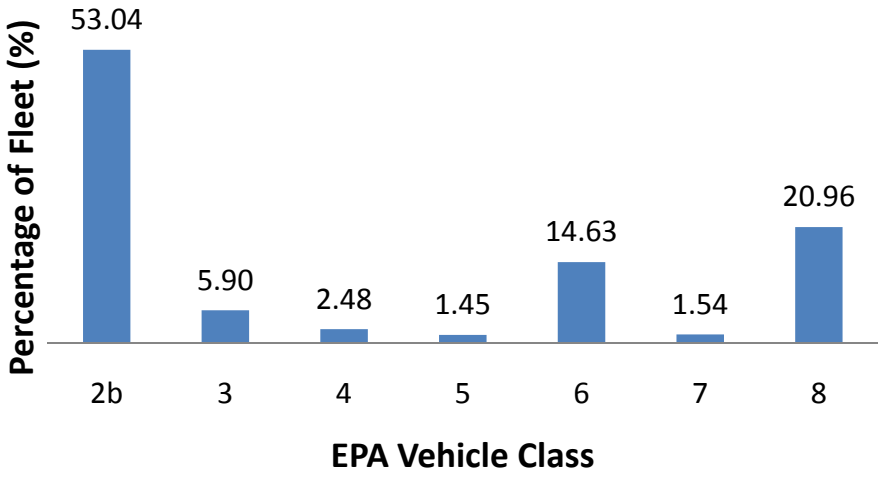

Figure 1 MD and HD fleet distribution, total fleet: 11.69 million (NRC, 2010)

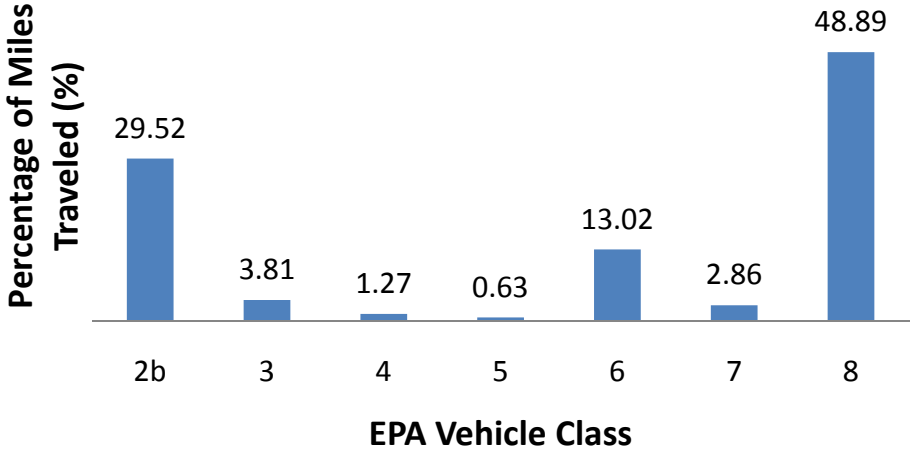

Figure 2 MD and HD fleet miles traveled distribution, total miles traveled: 315 billion (NRC, 2010)

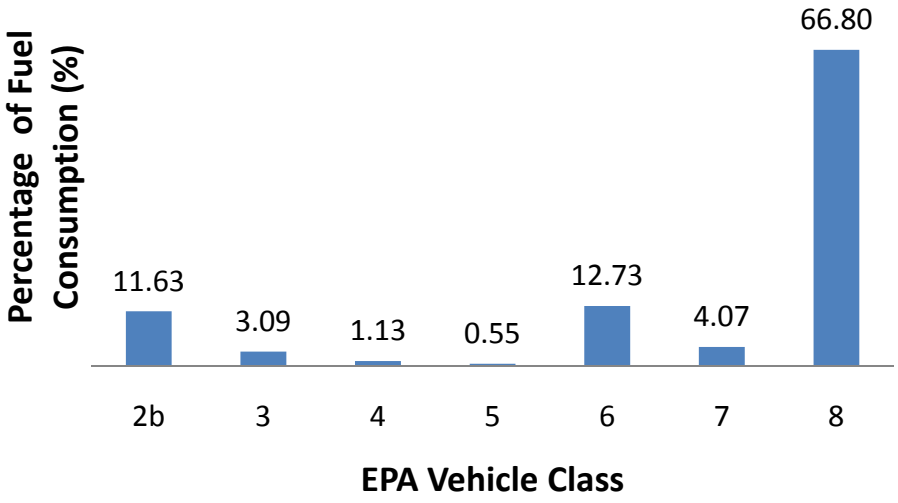

Figure 3 MD and HD fleet fuel consumption distribution, total consumption: 47.28 billion gallons (NRC, 2010)

2.2 Road Load Equation

Vehicle fuel consumption and emissions depend on vehicle power demand as the vehicle is driven. The power requirement for a given vehicle can be calculated from the road load equation which includes rolling resistance, aerodynamic drag, road grade and inertial power required to accelerate the vehicle. Equation 1 shows the road load equation where P represents the propulsion power demanded by the vehicle at the drive wheels, m is the mass of the vehicle, μ represents the coefficient of rolling resistance[4], g is the acceleration due to gravity, V is the instantaneous velocity, ρ is the ambient air density, A is the frontal cross sectional area of vehicle, C_D is the aerodynamic drag coefficient[5], θ is the road inclination, and t is time. Rotational inertia of the wheels, tires and axles may be taken into account

[4] The rolling resistance coefficient μ is affected by many parameters including vehicle speed, tire structure, tire material, wear, temperature, inflation pressure and load, aspect ratio and radius, road conditions, side slip angle, and tractive and braking forces (Genta et al, 1997). The tire rolling loss force is both elastic and hysteretic. The rubber compounds in the tire are subjected to deformations and dissipate energy into heat causing the tire to heat up. To overcome this loss of energy, additional fuel must be consumed.

[5] The aerodynamic drag coefficient C_D is nearly constant for fully developed turbulent flows, condition that is determined by the Reynolds number of the flow. A critical value of $Re=2x10^6$ is suggested by (SAE, 1981).

by adding an equivalent mass to the vehicle's total mass but has been neglected here since it was assumed to be approximately 5% contribution[6] (Giannelli, et al., 2005).

Usually, chassis dynamometer testing is executed assuming level grade neglecting the contribution of road grade. Most of the chassis dynamometer test cycles do not include road grade. When the simulated terrain is flat, the dynamometer will pose a load on the vehicle simulating aerodynamic and rolling resistance, while flywheels can simulate vehicle inertia. During acceleration the inertial masses load the drivetrain and they provide motoring while decelerating. If grade is to be included, a similar way of storing and releasing energy should be considered. The dynamometer should have enough capacity to provide the retarding and motoring loads associated with the grade.

$$P = \mu mgVcos\theta + \frac{1}{2}\rho AC_D V^3 + mV\frac{dV}{dt} + mgVsin\theta \quad (1)$$

The contribution of each major element of the road load equation to the overall vehicle power demand will change based on the duty cycle or in-use activity. For example, Table 2 shows the percentage contributions of rolling resistance, aerodynamic drag, inertial power, and grade for the in-use routes considered in this study[7]. Only positive accelerations and grades were considered for the calculation since decelerations and downhill slopes were assumed to be "closed throttle" operation with zero fueling and hence zero emissions. On average, the contributions are ranked in the following order: road grade (36.3%), inertial power (24.7%), rolling resistance (24.1%), and aerodynamic drag (14.9%). Rolling resistance presented the least variability over the routes with a COV of about 8%, while aerodynamic drag showed the highest variability over the routes with a COV of about 30% for the routes examined here. The importance of grade cannot be underestimated.

[6] A rotating mass term multiplier (1+ε) is usually factored with the vehicle mass to account for this contribution. The term is assumed to be constant. However, it increases in lower speed gears (Gillespie, 1992). US EPA and NHTSA, (2011) suggest adding 125 lbm per tire to account for rotational inertia of HD vehicles.

[7] See Section 5.2.2

Table 2 Contribution of road load power components to total positive power demand

Route	Percentage of total power demand (%)			
	Rolling	**Aerodynamic**	**Inertial**	**Grade**
WashPA2	25.8	11.1	26.6	36.5
WashPA1	24.5	8.0	31.4	36.0
BM2Sab	24.3	14.3	24.2	37.2
Sab2BM	21.1	13.1	19.7	46.1
Sab2SW	22.2	17.4	26.1	34.3
SW2Sab	23.3	18.3	25.9	32.4
WashPA3	27.6	22.2	18.9	31.4
AVERAGE	***24.1***	***14.9***	***24.7***	***36.3***
COV (%)	***8.3***	***29.7***	***16.2***	***12.3***

2.3 Cycles and Routes

A drive or test cycle can be defined as a prescribed speed trace that the vehicle must reproduce as a function of time. A cycle has defined test duration and target distance, and it may or may not include grade. A different kind of schedule is a drive route which is distance based, similar to how a vehicle would be driven in the streets or on a test track (Nine et al., 1999). A route has defined total distance but completion time may change depending upon vehicle performance (e.g. power/weight ratio) and traffic interruptions.

Cycles and routes are useful in providing a like-to-like comparison of emissions from different engine or vehicle technologies. However, it is important to recognize that while both chassis and in-use testing are intended to provide real world information on emissions, no single test can describe all of the conditions that any vehicle or group of vehicles would experience during actual service. The choice of driving cycle (or route) will have a significant effect on vehicle performance. A vehicle's fuel efficiency is highly dependent on duty cycles or activities (Clark et al., 2002a). Emissions results from chassis-dynamometer testing represent specific driving conditions set by the test schedule (speed-time or speed-distance) and are not easily extrapolated for other drive cycles (Cappiello et al., 2002). For example, McKain et al. (2000) compared hybrid and diesel transit buses and found that the driving cycle influenced the

advantage of hybrid buses over conventional buses. Part of the scope of this study was to find a way to translate fuel consumption and emissions between different types of vehicle activity.

2.4 Cycle and Route Properties

A useful way to characterize vehicle activity over a cycle or a route is by means of its properties, such as average velocity, standard deviation of velocity, average acceleration, and stops per distance. These metrics provide some information that the speed-time trace cannot give by itself. The most important metric to analyze fuel consumption and emissions is believed to be average velocity, because in Equation 1 velocity appears in each term. Average velocity is a robust indicator of the type of activity exhibited during a given cycle. A low average velocity may represent a very transient cycle similar to what is expected in city traffic while a high average velocity may represent a more steady behavior similar to what is expected in highway driving. However, two very dissimilar cycles can have the same average velocity and other metrics (e.g. standard deviation of speed or number of stops per mile) should be considered to account for the different amounts of transient behavior (frequency and magnitude of changes of the speed trace) (Delgado et al., 2012).

Extensive properties depend on the size of the vehicle activity and they are exemplified by metrics such as cycle time length or distance. If a test cycle is run twice "back-to-back," and treated as one cycle, the values of its extensive properties would be doubled. On the other hand, intensive properties do not depend on the size. The objective of this study was to predict fuel use or emissions in time-specific units of grams per second and hence only intensive properties were used in this study. An equivalent approach would be to use extensive cycle properties to predict fuel use or emissions in mass (an extensive property), rather than mass rate.

Cycle properties are also used in test cycle development. Data collection is performed by measuring driving patterns in the field (target data) and the objective is to develop a test cycle to represent accurately the target data. For a test cycle to be representative, the values of its properties should match the values of the measured driving patterns.

2.5 Emissions Regulations

In the US, engines for on-road, HD vehicle automotive applications are certified over the engine dynamometer-based Federal Test Procedure (FTP). For the purposes of regulation, emissions are measured in energy-specific units such as grams per brake horsepower-hour (g/bhp-hr). Brake-specific units represent a measure of work performed, so expressing emissions in this way allows comparison of engines of different sizes. Heavy-duty diesel engines must comply with the EPA emissions standards presented in Table 3. It can be seen that PM and NOx emissions standards have become steadily stricter over the last decade and have seen nearly two orders of magnitude reduction in NOx and PM over the last two decades. The diesel engine industry has responded with fundamental technology improvements that have allowed diesel engines to meet these standards. In order to comply with the 0.01 g/bhp-hr PM standard, diesel particulate filters (DPF) have been implemented in the exhaust stream and have been proven to reduce engine-out PM levels by over 90% (Hiranuma et al., 2003). The 0.2 g/bhp-hr NOx standard is being met with the implementation of advanced combustion control, exhaust gas recirculation, and or selective catalytic reduction (SCR) urea injection systems.

For HD engine emissions certification, only the engine, separate from the vehicle, is tested using an engine dynamometer test facility. Heavy-duty chassis dynamometer vehicle tests, and in-use testing using PEMS measure fuel economy and emissions for the vehicle as a system and are used primarily for technology evaluation and comparison in the US. It is noted that HD engine manufacturers are obligated to use PEMS as part of their emissions compliance. Several chassis test cycles exist for both light-duty (LD) and HD vehicles.

Table 3 Summary of EPA emissions standards for HD diesel engines

Engine Model Year	CO (g/bhp-hr)	HC (g/bhp-hr)	NMHC (g/bhp-hr)	NO_x (g/bhp-hr)	PM (g/bhp-hr)
1988	15.5	1.3		10.7	0.60
1990	15.5	1.3		6.0	0.60
1991	15.5	1.3		5.0	0.25
1994	15.5	1.3		5.0	0.10
1998	15.5	1.3		4.0	0.10
2004[A]	15.5	1.3	0.5	2.5[B]	0.10
2007	15.5		0.14	1.2-1.5[C]	0.01
2010	15.5		0.14	0.2	0.01

A – Moved to Oct. 2002

B – NMHC + NO_x

C – Family Emission Limit (FEL) as a phase-in towards 0.2 g/bhp·hr

2.6 Fuel Efficiency and GHG Regulations

In August 2011, the EPA and the NHTSA finalized the first-ever program in the US to reduce GHG emissions and improve fuel efficiency of MD and HD vehicles. The agencies worked collaboratively to deliver regulations under their respective authorities: the EPA developed GHG emission standards under the Clean Air Act, and NHTSA developed fuel efficiency standards under the 2007 Energy Independence and Security Act. The EPA program will begin in model year 2014, while the NHTSA program will become mandatory starting in model year 2016. Three regulatory classes were considered for this program:

- Class 7 and 8 tractor trucks: tractor manufacturers would be required to certify their vehicles using Greenhouse gas Emission Model (GEM) simulation model, and would be required to install certified engines in their tractors. Nine separate standards were considered based on combinations of three categories of vehicles (Class 7, Class 8 day cab, and Class 8 sleeper cab) and three roof height categories (low, medium, and high).The standard for MY 2017 represents a 9% to 23% improvement over the MY 2010 values. The engines would be certified using the SET test cycle.
- Class 2B and Class 3 Commercial pickups and vans: Unlike the tractor category, the agencies will use chassis dynamometer for certification of these classes as complete vehicles in a fashion

similar to light-duty passenger vehicle GHG and CAFE program[8]. There will be no separate regulation for their engines.

- Class 2B-8 Vocational Vehicles: This category includes the MD and HD vehicles that are not classified as a tractor or HD pickup or van and include bucket trucks, urban delivery vehicles, refuse trucks, and buses. As with the tractors, separate vehicle and engine standards exist, and the GEM software will be used for vehicles. The engine regulation for vocational vehicles is identical to the program for tractors' engines with the only difference of the test cycle used[9]. The standard for MY 2017 represents a 6% to 9% improvement over the MY 2010 values.

The respective metrics for the EPA and NHTSA programs are grams of CO_2 per ton-mile and gallons of fuel per 1,000 ton-miles[10]. For light-duty vehicles, the corporate average fuel economy (CAFE) program uses miles per gallon (mpg). This measure is not the appropriate measure for MD and HD vehicles. A partially loaded vehicle would consume less fuel per mile than a fully loaded one, but this would not be an accurate measurement of the fuel efficiency of moving goods (or passengers). However, normalizing fuel consumption by the payload and using the calculation of gallon/ton-mile (load specific fuel consumption (LSFC)) the fully loaded vehicle would have a much lower LSFC than the partially loaded one, reflecting the actual ability to accomplish the task.

As mentioned in the previous chapter, current EPA HD certification focuses on criteria pollutants (i.e., NOx, PM, NMHC, CO) emitted from engine tests rather than from chassis tests. The testing burden from a small number of engine configurations is manageable from a compliance and certification point of view. In order to extend the certification to the full vehicle level, however, there must be another approach other than full vehicle testing for every potential vehicle configuration. Because of the multitude of truck combinations and applications, the agencies decided that manufacturers must certify

[8] Fuel economy results from the light-duty FTP (city) and the HFET (highway) are combined to determine the vehicle's fuel economy to be used for Corporate Average Fuel Economy (CAFE) using the following equation

$$mpg_{combined} = \frac{1}{\frac{0.55}{mpg_{FTP}} + \frac{0.45}{mpg_{HFET}}}$$

[9] Vocational vehicles would be required to meet their respective standards based on the heavy-duty FTP rather than the steady-state SET test cycle.

[10] A ton-mile is defined as a metric ton of freight transported one mile. The standards in the EPA and NHTSA programs are identical, based on an emission factor of 10,180 grams of CO_2 per gallon of diesel fuel.

their vehicles using the GEM computer simulation model. A more detailed discussion of the GEM model can be found in Section 2.9. The use of a vehicle simulation to assess vehicle efficiency would align with many large truck manufacturers' approach to employ computer simulations for whole vehicle efficiency assessment and would reduce the potential testing burden incurred by this broad and diverse market sector to a manageable level (Lee et al., 2011).

Engine testing for compliance with GHG and fuel efficiency regulations will occur simultaneously with testing for criteria pollutants. Three more pollutants: CO_2, methane (CH_4), and nitrous oxide (N_2O), must be measured and reported[11]. Engines will be categorized as light-heavy (Classes 2B-5), medium heavy (Classes 6 and 7), and heavy-heavy (Class 8) based on the vehicle class in which they are going to be used (EPA and NHTSA, 2011).

2.7 Emission Modeling Techniques

To assess air quality benefits of transportation control and emissions regulation, researchers and regulators need accurate methods of predicting emissions from the current on-road vehicle fleet and the ability to track changes to the emission inventory. Emission models can be categorized based on their level of temporal and vehicular aggregation. For example, at the lowest aggregation level, microscopic (or instantaneous) models produce continuous (usually, second-by second) emission rates for specific individual vehicles while macroscopic levels aggregate emissions over the entire fleet for a given regional network. The following describe some relevant macroscopic and microscopic models.

2.7.1 Macroscopic Models

In the US, the procedure for estimating vehicle emissions for a fleet of heavy-duty vehicles has relied traditionally on mobile source emission-factor models such as US EPA's MOBILE and California Air Resources Board's EMFAC. These models, along with the COPERT model developed by the European Environmental Agency (Ntziachristos and Samaras, 2000), are classified as macroscopic emission models. Emission factors in distance-specific units such as g/mile (calculated from engine emissions certification data in energy-specific units of g/bhp-hr) are multiplied by the activity variable of vehicle

[11] Greenhouse gas standards, also known as carbon dioxide equivalent standards, include non-CO_2 emissions according to their global warming potential factors: 1 for CO_2, 23 for CH_4, and 296 for N_2O (EPA, 2011).

miles traveled (VMT) to predict the amount of emissions that will be associated with operation of a given fleet over a given time period. These models make use of average speed as input to produce activity-specific emission factors.

Macroscopic models involve broad simplifications of physical processes involved in regulated emissions formation. An important drawback of the average speed methodology is that instantaneous speed fluctuation plays a great part in the resulting emissions generation. For the same average speed, one can observe widely different transient operation (number and magnitude of accelerations and decelerations), each resulting in very different fuel consumption and emission levels. The extent of transient operation can be quantitatively measured by means of various properties or statistical descriptors of vehicle operation. It has been recognized that models based on the average speed from fixed driving cycles do not adequately capture the effects of driving and vehicle dynamics on emissions (NRC, 2010), and fail to account for real world driving characteristics (Fomunung et al., 1999). Therefore, their applicability is limited to estimate and forecast emission inventories of large areas and over long time periods.

Another concern with these models is that they base their analysis on emissions certification tests (e.g. FTP cycle) which are based on vehicle behavior that may not be relevant to today's vehicle usage (Clark et al., 2003).

2.7.2 Microscopic Models

Microscopic models aim to provide a more precise description of vehicle energy consumption and emissions production by relating them to vehicle operation during a series of short time steps (i.e. second by second). This approach takes into account the transient operation of vehicles, which helps capture the effects of different instantaneous speed and acceleration profiles on vehicle emissions, thereby representing more accurately real driving conditions. In principle, instantaneous models allow the user to calculate emissions for any vehicle operation profile, and therefore new emission factors can be generated without the need for further testing. This detail represents an advantage when trying to analyze a few vehicles over a small number of types of activity; however, it will be a cumbersome task to try to estimate all possible combinations of vehicles and corresponding operational envelopes to calculate an emissions inventory for a given region due to the need to capture each vehicle's physical design.

When developing microscopic models, correct time alignment of instantaneous power and the emissions constituent should be implemented. The engine or vehicle (axle) power is measured instantaneously, yet the resulting emissions are measured after a time delay of the gas traveling from the engine to the analysis bench. Also, in addition to time delay, an effect defined as "smearing" or time diffusion of the gaseous emissions data occurs. This arises from axial mixing in the exhaust transfer tube, dilution tunnel, and sampling lines and from the response of the analyzers (Clark et al., 2003).

Microscopic models can be classified into activity-based models, regression-based models, load-based models and non-linear models. Various approaches exist for the prediction of heavy-duty vehicle emissions and are discussed next.

2.7.2.1 Activity Based Models (Speed-Acceleration Binning)

Activity based models are based on emission maps that contain the average emission rates for every combination of speed and acceleration in the driving cycle used for the emission test. For a given vehicle, the speed governs the road load losses (the ratio between aerodynamic losses and rolling resistance losses), and the product of speed and acceleration governs the instantaneous inertial power demand. These models are convenient to interface with activity data from transportation models.

Kern (2000) used data collected by West Virginia University (WVU) transportable laboratory to obtain emissions factors in distance-specific units (grams per mile). Emissions were then categorized by vehicle instantaneous speed and acceleration. Given a drive cycle, time fractions in each of the speed-acceleration bins were calculated, and the fractions were coupled with the emissions rate bins (in grams per second) to estimate total emissions. Prediction errors were as low as 5%.

Clark et al. (2003) used data from WVU transportable heavy-duty chassis dynamometer to create an instantaneous emissions model using a speed-acceleration binning technique. The research provided tabular factors for use with vehicle activity information to describe the instantaneous emissions from heavy-duty vehicles. Emission mass rate values in grams per second for determined vehicle types and model year were binned according to the speed and acceleration of the vehicle, and it was shown that the emissions could be predicted with reasonable accuracy by applying this table to the original activity data. The test cycle used was found to have a significant effect on the emissions value predicted.

Weinblatt et al. (2003) presented a procedure for estimating the emissions of HD vehicles combining second-by-second speed and acceleration data from in-use operation with data on average emission rates. Validation tests provided NOx differences of only two to four percent between measured and predicted values for urban operation. NOx emissions estimates predicted using study results for rural operation were lower (by 10 to 15 percent) than those predicted using the study results for urban operation. These rural estimates provided a poorer fit to the measured values obtained using urban test cycles. NOx speed-correction factors were developed showing differences with the factors generated by EPAs MOBILE6.

Gajendran (2005) studied the effects of various parameters (driving schedule, vehicle weight, and off-cycle injection strategy) on heavy-duty diesel emissions. A set of emission factor tables with speed-acceleration based emissions was generated for prediction of HD diesel vehicle emissions inventory. The methodology was validated using measured emissions data from chassis dynamometer testing available in the WVU database. The main interest was on NOx emissions, but HC and CO emissions were also considered. A drive cycle with high average speed (Inventory Highway Cycle at 36.94 mph average speed) was developed to extend the database which was limited on high speed information.

Frey et al. (2008) developed a methodology for estimating roadway link-based[12] emission rates to evaluate the effects of vehicle activity and operation on emissions from heavy-duty trucks. A speed-acceleration modal emission approach was developed from a database gathered via PEMS for single rear-axle and tandem-axle dump trucks. Speed profiles were categorized by facility type (arterial or freeway) and link mean speed. Five acceleration ranges and 13 speed ranges were constructed from the database. Idling was categorized as a separate mode. Modal average emission rates were then estimated by using second-by-second PEMS measurements. Link-based emission rates were estimated by averaging emission rates for all links on the same roadway type and across all speed profiles within a pre-specified range of link mean speed. Link emission rates were estimated as shown in Equation 2, where i=speed-acceleration mode index, j=link index, k=speed profile run index, $t_{i,j,k}$=time spent in speed –acceleration mode i on link j for run k(s), $T_{j,k}$= total travel time spent on link j for run k (s), ER_i=modal

[12] A link is defined as a roadway segment between two junctions.

average emission rate for speed-acceleration mode i, and $E_{j,k}$=link average emission rate for run k on link j.

$$E_{j,k} = \sum_{i=1} \left\{ \left(\frac{t_{i,j,k}}{T_{j,k}} \right) \times ER_i \right\} \quad (2)$$

The modal approach was compared with results from the MOBILE6 model for a range of average speeds on different roadway types. The results indicated that NOx emission rates appear to increase with link mean speeds in both methods. However, the link-based estimates were less sensitive to mean link speed than were MOBILE6 results.

Although relatively easy to generate and use, emissions maps are not satisfactory because they can be highly sensitive to the driving cycle (Cappiello et al., 2002; Clark et al., 2003). Another downfall of such modal approach is the need for a wide range of vehicle-operating conditions to fill the bins in the lookup tables, which usually requires testing time (Barth et al. 2004). Another limitation is that the lookup tables assume that there is no time dependence in the emissions response to the vehicle operation, and it is known that vehicle operating history can have a significant role in instantaneous emission values.

Additional problems arise when the speed-acceleration profile of the vehicle for which an emissions factor is to be determined encounters hills or grades. The extent to which grade affects the emissions is hidden because the vast majority of the test schedules used to date on chassis dynamometers do not have provisions for simulating hills or terrain and grade is just neglected (Thompson et al., 2004). As a vehicle is travelling uphill, the acceleration is usually low, while the axle power demand is high as compared to the vehicle travelling on level ground. The full-power emissions data that are gathered on the dynamometer are generally at high accelerations. This means that the predicted emissions of the vehicle ascending the grade will be lower than the actual emissions produced. This will hold true for emissions species that correlate well with axle power, such as CO_2 or NOx (Clark et al., 2003). Likewise, the emissions predicted when the vehicle descends a hill will be higher than the actual emissions produced because the vehicle can attain a relatively high rate of change of speed, for which there is emissions data at full power. Similar difficulties will be encountered trying to find convenient methods to introduce weight effects or accessory use in this type of modeling.

2.7.2.2 Regression Models

Regression-based models typically employ functions of instantaneous vehicle speed and acceleration as explanatory variables. These models overcome some limitations of the emission maps (activity-based models), such as sparseness and non-flexibility, but can lack a physical interpretation and can also over fit the calibration data as they typically use a large number of explanatory variables (Cappiello et al., 2002).

Ramamurthy et al. (1998) used an approach where emissions data were related to the instantaneous power output from the vehicle rear axle. Instantaneous chassis dynamometer emissions data for a particular vehicle were processed to yield the instantaneous emissions mass rate in grams per second as a function of a single variable: drive axle power. Before attempting correlation, a time alignment or shifting between the emissions and axle power data was performed. The researchers found the approach to be successful for modeling of NOx and CO_2 emissions from diesel vehicles but difficulties arose for the cases of CO and HC emissions. It was found also that the approach cannot account for "off-cycle" injection timing.

Ahn et al. (2002) developed log-transformed polynomial regression models to predict fuel consumption and emission rates for LD vehicles and LD trucks. Instantaneous vehicle speed and acceleration measurements were used as explanatory variables. The statistical results indicated a good fit for fuel consumption estimates (R^2=0.99), an average fit for NOx estimates (R^2=0.80), and a relatively poor fit (R^2 below 0.75) for HC and CO emission estimates. The model was enhanced by separating positive and negative acceleration levels to achieve R^2 in excess of 0.92 for all emissions. The model was then incorporated within a microscopic traffic simulation model to demonstrate its applicability.

Rakha et al., (2004) developed the Virginia Tech microscopic energy and emission model (VT-Micro). The model was based on regression with numerous polynomial combinations of speed and acceleration levels. Specifically, linear, quadratic, cubic, and 4^{th} power terms of speed and acceleration were examined using chassis dynamometer data collected at the Oak Ridge National Laboratory (ORNL). The final regression model included a combination of linear, quadratic, and cubic speed and acceleration terms because it provided the least number of terms with a relatively good fit to the original data with an R^2 value in excess of 0.92. This method has a significant advantage over emission data collected from

a few driving cycles because it is difficult to cover the entire vehicle operational envelope with only a few driving cycles.

Krishnamurthy (2006) used Multivariate Adaptive Regression Splines (MARS) to predict NOx emissions for heavy-duty diesel engines using inputs from the electronic control unit (ECU) broadcast. The ECU parameters used were engine speed, engine torque, injection timing, fueling rate, manifold air temperature and pressure, and coolant and oil temperatures. NOx data were collected with the on-road emissions testing capabilities of the WVU's Mobile Emissions Measurement System (MEMS), and the vehicles were tested over urban and highway routes. The prediction uncertainty of the models was at most ± 20%.

2.7.2.3 Load-Based Models

Power demand is a key variable that explains the vehicle fuel consumption rate and emissions rate for some pollutant species. Load-based models are usually based on the road load equation and focus on the physical phenomena that generate emissions. These models incorporate a detailed physical approach, which defines the variables and parameters that should be included when modeling fuel consumption or emissions. Load-based models can be quite complex and, when applied to the entire flow of vehicles in a network over a period of time, the computational effort can be high.

Some researchers have made use of the correlation between vehicle power and emissions. Yanowitz et al. (2002) developed a model of a HD vehicle driveline with automatic transmission for estimating engine speed and load from vehicle speed. The model was validated using both chassis dynamometer and engine dynamometer emissions tests. A load-based model using engine test data was used to predict chassis dynamometer NOx, PM, CO and HC emissions. The researchers found that NOx emissions were proportional to engine power on a second-by-second basis. HC emissions were not well predicted by the engine test although there was not consistent bias. CO emissions were reasonably consistent between the engine and the chassis tests, and the engine certification test consistently underestimated PM emissions on a brake-specific work basis.

Barth et al. (2004) created the Comprehensive Modal Emissions Model CMEM at the University of California, Riverside. They developed a HD diesel truck model that used a parameterized physical approach in which the entire emissions process was broken down into different components that

correspond to physical phenomena associated with vehicle operation and emission production. The modal instantaneous emission model used a power-demand approach that incorporated grade, variable weight and variable fuel injection strategies. The complete emissions model was composed of six modules as indicated by the six boxes in Figure 4. The modules predicted engine power, engine speed, air-to-fuel ratio, fuel use, and engine-out emissions among others. The model required a fair amount of input parameters including vehicle and operation variables (e.g. second-by-second speed, acceleration, road grade, accessory use) as well as model calibrated parameters (such as cold start coefficients, and engine friction factors). A total of 31 static parameters were needed for the different sub models. Depending on the specific parameter, the values were determined either directly from measurements or on the basis of several regression equations. The model predicted NOx emissions with relative errors between 15% and 31%.

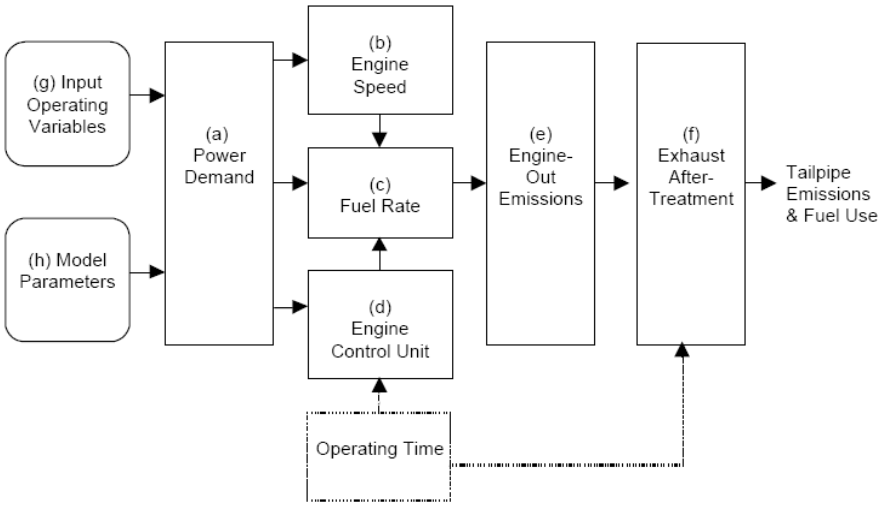

Figure 4 CMEM model structure (Barth, 2004)

Giannelli et al., (2005) developed the Physical Emission Rate Estimator (PERE) to supplement the limited heavy-duty vehicle data used in EPA's Motor Vehicle Emission Simulator (MOVES). PERE is a road load-based model that combines vehicle tractive power with power train parameters specific to the class of vehicle (weight, shape, engine type, transmission). The authors presented the road load, engine, and transmission parameters used. These parameters were used to predict fuel consumption and CO_2 mass rate emissions within 10% of measured values for different vehicles on individual vehicle trips.

Frey et al. (2007) used a road load based model to estimate transit bus fuel consumption and emissions as a function of the power demand for given transit bus activities and environmental conditions. The approach made use of vehicle specific power (VSP) (tractive power per unit mass of the vehicle), a variable that is highly correlated with vehicle emissions and was originally reported by Jimenez-Palacios (Jimenez-Palacios, 1999). The VSP values were binned in different modes and cycle fuel consumption was calculated as shown in Equation 3 where k is a specific VSP mode. The same method was used to estimate emissions. Fuel consumption predictions with relative errors lower than 10% when compared to experimental observations were observed.

$$Fuel\ Consumption\ (gal) = \sum_k (fuel\ consumption\ rate, gal/s)_k \cdot (time\ spent\ in\ mode, s)_k \quad (3)$$

Zhai et al. (2008) used VSP modes to estimate roadway link average emission rates for diesel-fueled transit buses based on link mean speeds from data gathered by a PEMS. Validation of VSP modeling approach for CO_2 resulted in individual errors from -16% to 24%, and from -29% to 104% for NOx, a substantial inter-vehicle variability. VSP modal average emission rates and the time spent in the corresponding VSP modes were used to make aggregate estimates of total and average emission rates for a road link. The authors reported fleet emission estimate errors of 2% and 17% for CO_2 and NOx, respectively. Some studies have indicated that a bias is likely when using VSP as the only parameter of driving conditions to simulate vehicular emissions, particularly under high- or low-speed driving conditions (Wang and Fu, 2010). In addition, VSP alone cannot directly correlate with transportation demand models which usual output is average speed.

2.7.2.3.1 Dynamic Vehicle Simulators

Dynamic vehicle simulators are systems-based models that represent all vehicles' components and interactions. ADVISOR (Wipke et al., 1999) and PSAT (Karbowski et al., 2010) have been used for modeling energy consumption and emissions. Driving schedules are input to these tools to simulate dynamic vehicle operation and the corresponding dynamic power flows and energy losses within the powertrain. These models simulate fuel consumption and performance in greater detail by accounting for transient behaviour and control. They are capable of great accuracy compared to the other models described. Wipke et al. (1999) quote ADVISOR errors of less than 1% for vehicle performance and less than 2% for vehicle energy use. Ciccarelli and Toossi (2002) performed simulation studies using ADVISOR software to evaluate potential fuel savings and reduced emissions from hybrid buses in Long Beach, CA.

Wang et al. (2010) constructed a PSAT model of a heavy-duty truck. The truck modeled was an over-the-road Peterbilt tractor truck with a 410kW 1996 Caterpillar 3406E non-EGR engine. Figure 5 shows a schematic of a vehicle model in PSAT. Fuel rate was predicted by using a lookup table in terms of engine torque and engine speed. NOx emissions were predicted as a function of engine power, speed, torque and their derivatives. The model was validated against actual test data showing results within 5% relative error. These full system simulations models are ideally suited to development of hardware and control systems (Simpson, 2005). However, these models require component models (e.g. control strategy, engine model, fuel maps, emissions maps, transmission model) in order to simulate performance. The availability of detailed well-validated component performance maps is somewhat limited. These performance maps are usually produced through steady-state testing, requiring a fair amount of testing time and resources to be developed. Due to their steady-state nature, some models are not useful to simulate dynamic effects. Other issues of these models include the need to buy specialized software and their computational intensity (especially when many vehicles or technologies are to be compared). Additional advantages and disadvantages of dynamic vehicle simulators can be found in the paper by Gao et al. (Gao et al., 2007).

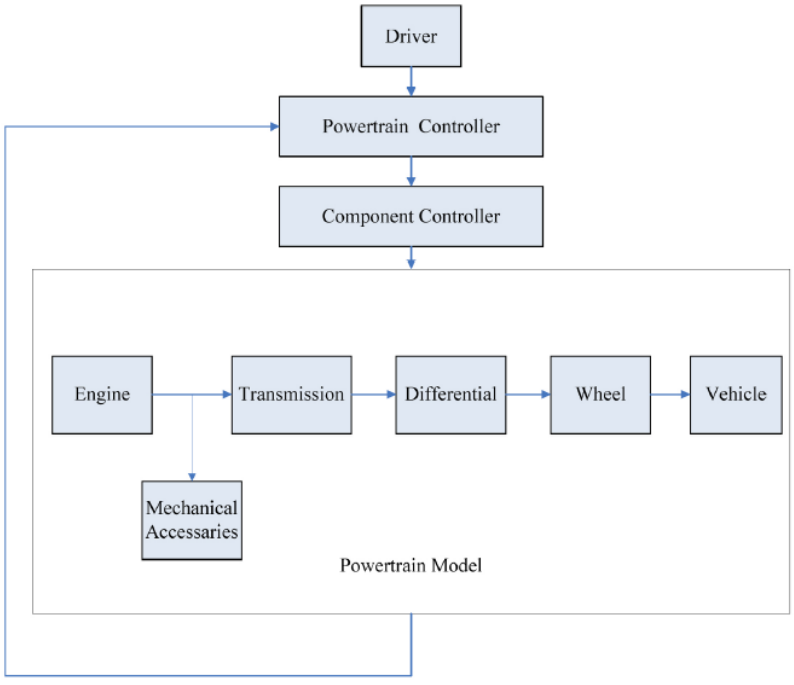

Figure 5 PSAT schematic vehicle model (Wang et al., 2010)

2.7.2.3.2 Lumped-Parameters Models

Simpler models that avoid the need for dynamic simulation by using lumped-parameters or cycle-averaged values obviate the need for specialized software or detailed performance maps. Development of a lumped parameter model begins with the fundamental physics equations that describe the energy requirement of a vehicle. Their primary limitation is their lack of accuracy. The inaccuracy can arise from simplifying assumptions that facilitate a more convenient model but introduce errors (Simpson, 2005). Some models do not normally include a model of the driving pattern and therefore cannot model dynamic effects that would easily be reproduced with a driving cycle, for example Sovran and Blaser (Sovran and Blaser, 2003) required the energy consumption at the wheels as an input and therefore could not readily consider the dependence of this quantity on the nature of the driving pattern. Errors in the range of 10 to 20% could be expected (Simpson, 2005).

A method which characterizes fuel consumption and emissions according to driving situations was developed by de Haan and Keller (de Haan and Keller, 2004). Fuel consumption and emission factors for a newly measured driving pattern were determined by finding the linear combination of driving patterns which produces the closest match to the new pattern, using up to three existing patterns of known fuel consumption and emissions factors. The matching procedure involved finding the combination of predefined patterns that most closely approached the distribution (frequency plots were used) of average speed and inertial power (product of speed and acceleration) of the new pattern.

Emission factors of the new pattern were estimated by adding the corresponding emission factors of the matching combination of driving patterns as shown in Equation 4, where X, Y, and Z are proportions of predefined patterns in the combination. One advantage of this model is that properties of the vehicles do not need to be known. They reported average absolute relative errors for gasoline and diesel passenger vehicles of 42% for CO, 8% for CO_2 and fuel consumption, 41% for HC and 20% for NOx. The bias was reported as 17% for CO, -3% for CO_2 and fuel consumption, 21% for HC and 4% for NOx. A good emission prediction may be expected for driving cycles that are situated among driving patterns for which measurements are available. However, should a driving pattern be extreme (with respect to the kinematic parameters adopted) with regard to the available driving patterns, the method actually must extrapolate rather than interpolate. This will lead to a decrease in prediction ability.

$$EF_{new\ pattern} = X \cdot EF_{pattern\ 1} + Y \cdot EF_{pattern\ 2} + Z \cdot EF_{pattern\ 3} \quad (4)$$

2.7.2.4 Non-linear Models

Artificial neural networks (NN) have been used to predict fuel consumption and emissions. NN are more appropriate when imprecise or fuzzy correlation exists between variables. NN can identify highly non-linear relations between multiple input and output data, making them suitable for emissions prediction. A black-box modeling approach between input and output variables is used, rather than hypothesize the physical relationship between input and output. Trained with adequate amount of relevant data, a suitably configured NN will mimic the function and future events can be predicted. As limitations, NN models require a large amount of training data (second-by-second) and the black box modeling approach make it difficult to understand the inherent physical process occurring.

Traver et al. (1999) explored the feasibility of using in-cylinder pressure-based variables to predict gaseous exhaust emissions levels for a HD diesel engine using NN. The networks were trained with data at steady-state conditions and then validated on real-time data obtained from the transient FTP cycle. NOx and CO_2 emissions were shown to respond very well to the method. Thompson et al. (2000) used a large number of engine dynamometer data inputs for NN emissions prediction. The inputs included engine speed, intake air temperature and pressure, exhaust temperature, oil and coolant temperature, injection pressure and pulse width, start of injection and accelerator position. These inputs allowed prediction of NOx, CO_2, CO, HC and PM emissions. Prediction errors for CO_2 and NOx were lower than 5.1% and 7.7%, respectively. Tóth-Nagy et al. (2006) used NN to model CO_2 and NOx emissions in conventional and hybrid vehicles. The NN models were trained with data from engine dynamometer tests of two HD diesel engines. Inputs to the models were engine speed and torque and their first derivatives over 5 and 10 seconds. A model scaling approach was performed assuming that emissions scale with power. The NN proved to be extremely robust in extrapolating and the non-scaled approach was used in final simulations with ADVISOR software for operation of a tractor truck and a series hybrid-electric bus. It was found that the main error factor for the bus simulation was the hybrid control strategy. It was also found that accessory loads also have a considerable impact on simulation results. Bedick (2009) developed an NN heavy-duty diesel engine model that estimated NO_x, exhaust temperature and volumetric flow using inputs to the model of engine speed, engine torque, oil temperature, and turbocharger boost pressure.

Morris (2011) developed a modular NN model to predict in-use diesel emissions. Two modules were trained independently, the first module was trained with data from in-use testing, and the second module was trained with data from engine dynamometer testing. The first module predicted engine speed and torque associated with the inputs of road grade and vehicle speed and fed those outputs to the second NN which predicted the emitted quantities of NOx, CO_2, HC, and CO. The NN predictions were not unique because they depended on the type of training used, and the randomized sample for internal validation during the training algorithm. Average prediction errors of 6% for NOx and 15% for CO_2 were reported when the NN were trained with data from the same route that was being predicted.

2.8 MOVES

The US EPA developed a modal activity-based mobile source emission model named the Motor Vehicle Emission Simulator (MOVES). The model estimates emissions of on-road and non-road sources for multiple scale analysis, from fine-scale analysis to national emissions inventory estimation. The model is used by state and local agencies to calculate emission factors and emission inventories for state implementation plans (SIP) and transportation conformity purposes. EPA has also included information regarding the use of MOVES for estimating mobile source air toxic and greenhouse gas emissions. Although there are no SIP or conformity requirements for these emissions, MOVES 2010 (latest version) is EPA's best tool for estimating air toxic and greenhouse gas emissions from on road mobile sources (US EPA, 2010b). Most earlier heavy-duty emission rates were based on certification tests of then new, mid-1990's engines. For the newer engine models, EPA has included data on more than 400 in-use trucks, including chassis dynamometer data and data obtained with on-road measurement equipment (US EPA, 2010b). This allowed the EPA to better understand how real HD vehicles pollute at a range of driving conditions.

Figure 6 shows the general structure of MOVES. MOVES is based on four major functions: an activity generator, a source bin distribution generator, an operating mode distribution generator, and an emissions calculator. The activity generator estimates total activity in source hours operating (SHO) based on vehicle population and vehicle miles travelled information. The source bin distribution generator classifies vehicles into different source bins, defined as combinations of vehicle class, model year, vehicle weight, engine size, and fuel type. The operating mode distribution generator classifies vehicle operating modes into different bins associated with VSP and speed. Finally, the emissions

calculator develops weighted emission rates based on modal-based emission rates and the source bin and operating mode distributions (Koupal et al., 2003).

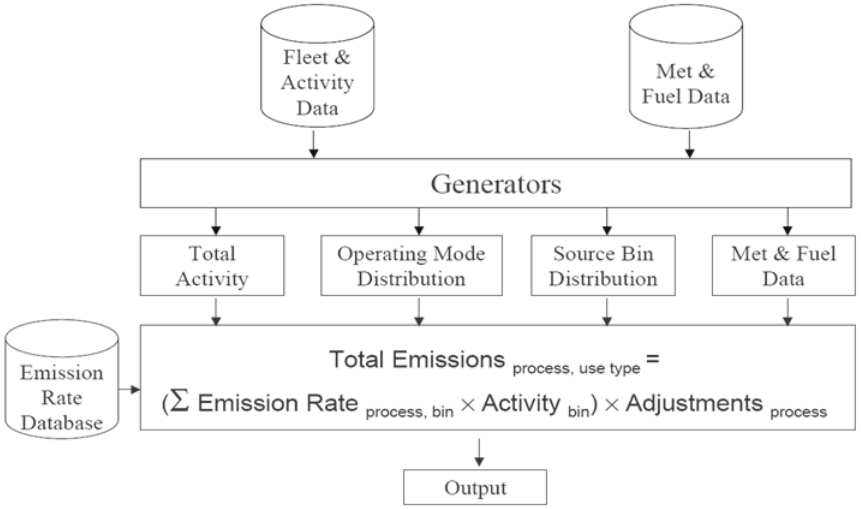

Figure 6 General model structure of MOVES (Koupal et al., 2003)

To characterize the relationship between vehicle activity and energy consumption, MOVES uses a binning approach. The basic concept to characterize vehicle activity is VSP or the related concept scaled tractive power (STP). These metrics are the key to define operating modes in MOVES. Both VSP and STP represent tractive power needed to move the vehicle and are calculated in a similar way. Equations 5 and 6 show the formulas for calculating VSP and STP, respectively. The calculations only differ in how they are scaled. The VSP parameter is used for LD vehicles and the STP parameter is used for HD vehicles (US EPA, 2010c).

$$VSP = \frac{A \cdot v + B \cdot v^2 + C \cdot v^3}{M} + (a + g \sin\theta) \cdot v \quad (5)$$

$$STP = \frac{A \cdot v + B \cdot v^2 + C \cdot v^3 + M(a + g \sin\theta) \cdot v}{f_{scale}} \quad (6)$$

In Equations 5 and 6, the parameters A, B, and C are track road load coefficients, representing rolling resistance, rotational resistance and aerodynamic drag in units of [kW·s/m], [kW·s^2/m^2] and [kW·s^3/m^3],

respectively. M is the vehicle mass in metric tons (t)[13], f_{scale} is a scaling factor named fixed mass factor (17.1 t), g is the acceleration due to gravity (9.8 m/s^2), v is the vehicle speed in m/s, a is the vehicle acceleration in m/s^2 and sin θ is the road grade.

For HD vehicles, EPA used the relationships of road load coefficient to vehicle mass from a study by Petrushov (Petrushov, 1997). The mid-point mass for the source bin was used as the vehicle mass and A, B, and C coefficients were computed for each source bin. The final road load coefficients for all source types are listed in Table 4 (US EPA, 2010c).

Table 4 Road load parameters (US EPA, 2010c)

Source Type	A (kW-s/m)	B ($kW\text{-}s^2/m^2$)	C ($kW\text{-}s^3/m^3$)	M (t)	f_{scale} (t)
Intercity Bus	1.30	0	0.003715	19.59	17.1
Transit Bus	1.09	0	0.003587	16.56	17.1
School Bus	0.75	0	0.002176	9.07	17.1
Refuse Truck	1.42	0	0.003572	20.68	17.1
Single Unit Short-haul Truck	0.56	0	0.001603	7.64	17.1
Single Unit Long-haul Truck	0.50	0	0.001474	6.25	17.1
Motor Home	0.62	0	0.002105	6.73	17.1
Combination Short-haul Truck	1.96	0	0.004031	29.33	17.1
Combination Long-haul Truck	2.08	0	0.004188	31.40	17.1

Due to the limited HD vehicle data, MOVES rates need to be supplemented with rates determined with PERE. This model combines vehicle tractive power with powertrain parameters specific to the class of vehicle (weight, shape, engine type, and transmission). PERE takes vehicle input parameters, then runs the simulation through driving cycles defined by the user and outputs second-by-second fuel consumption rates. The model was validated to diverse engine technologies and in most cases the predictions were within 10% relative error. Additional details about PERE can be found elsewhere (US EPA, 2004a; Giannelli et al, 2005).

[13] 1t = 1,000 kg = 2,204.6 lb

2.9 GEM

As mentioned in Section 2.6, EPA and NHTSA are going to make use of a simulation model as the primary tool to certify MD and HD vehicles GHG emissions and fuel efficiency. GEM is a forward-looking MATLAB/Simulink-based tool that uses the same physical principles as other existing vehicle simulation models to derive governing equations which describe the engine, the powertrain, and the vehicle. The equations are then integrated in time to calculate transient speed and torque. Finally, the model makes use of steady state fuel maps to predict fuel consumption and CO_2 emissions.

The model contains pre-defined parameters and component files that cannot be modified by the end users (only by the agencies) to accommodate their vehicle-specific information. These parameters include electrical loads, engine maps, transmission configurations, frontal area, and payload weight. For tractors, inputs to the model include data on aerodynamics, tire rolling resistance, weight reduction, and extended idle reduction. Only tire rolling resistance is used for vocational (2B-8) vehicles. The model also predefines the applicable drive cycles: the Transient mode of the HHDDT cycle, a constant speed cycle at 55 mph and a constant speed cycle at 65 mph. Therefore, manufacturers cannot select alternative drive cycles.

To demonstrate compliance with new vehicle standards, manufacturers of vocational truck chassis and combination tractors are required to obtain vehicle-specific parameters and component data via required test procedures. Manufacturers then input vehicle-specific parameters and component data to run GEM which evaluates and reports CO_2 emissions and fuel consumption based on required inputs applicable to each subcategory (e.g. tire rolling resistance, tractor aerodynamics as well as features that reduce idling, vehicle speed and mass) (Lee, 2011). The model architecture consists of six systems: ambient, driver, electric, engine, transmission, and vehicle. Some of the systems consist of components, each of which represents a physical entity that makes up the system. Table 5 shows the overall structure of GEM (Lee, 2011).

Table 5 Structure of GEM (Lee, 2011)

System	Components
Ambient	N/A
Driver	N/A
Electric	Accessory
Engine	Cylinder (fuel map), Accessory
Transmission	Clutch, Gear
Vehicle	Drive shaft, Differential, Final drive, Axle, Tire, Chassis

Based on the general truck usage pattern, the agencies have defined three sets of cycle weighting factors for use in the regulations. Table 6 shows that these weightings are specific to sleeper cabs (typically > 100 miles cruising), day cab (<~100 miles cruising), and vocational vehicles (stop and go operation).

Table 6 GEM weighing factors (US EPA and NHTSA, 2011)

Drive Cycle	Sleeper Cab	Day Cab	Vocational Vehicle
Transient	5	19	42
55mph Cruise	9	17	21
65mph Cruise	86	64	37

This author has identified some issues with the current regulations:

- For vocational vehicles (Classes 2B to 8), the only input to GEM is rolling resistance. It is clear that these vehicles mostly operate in an urban setting with transient rather than steady state operation. However, some operation may be at high continuous cruising speeds (Table 6 suggests that vocational vehicles operate 58% of the time at high speed cruise). Possible benefits of aerodynamic devices in terms of GHG emissions and fuel consumption may be negated by this rule.
- The user cannot specify the fuel maps. The simulation is carried out using a standard engine for each vehicle class (a single fuel map for all the vehicles within a given subcategory) regardless of the vehicle or engine manufacturer. Research in advanced combustion methods to reduce GHG and fuel consumption may not be simulated if the user cannot specify the fuel map, or if different fuel maps are used for different manufacturers.

- Steady state tests may underestimate fuel consumption. Presence of road grade and traffic congestion impedes the HD trucks to achieve actual steady state in real-world operation.
- As currently configured, GEM can only simulate vehicles with standard drivetrains and cannot be used to certify hybrid vehicles for compliance with fuel and GHG standards. Hybrid control and other technologies that can potentially achieve GHG emission and fuel consumption reductions are not included in the GEM model. Manufacturers of hybrid vehicles may choose to certify their vehicles using either full vehicle chassis dynamometer testing, engine dynamometer testing with a hybrid system or powertrain testing.

3 Model Description: Linear Interpolation in the Properties' Space

3.1 Overview

A method for predicting emissions for transient HD vehicle activity based on information from measured chassis dynamometer test cycles was presented by Taylor et al. (2004). Four dissimilar modes were used to generate emission predictions for 11 heavy-duty vehicles over the US HD urban dynamometer driving schedule (UDDS). The emissions for the predicted schedule were a linear combination of emissions from the four different predictive modes. The relative weightings were based on properties of the modes. The properties used were average speed, number of stops per unit distance, percentage idle, and average kinetic energy. Errors for CO_2 and NOx prediction did not exceed 15% and 7%, respectively. Clark et al. (2010) further explored the methodology using average velocity, average inertial power and average acceleration as metrics. The average error between predicted and measured cycle emissions for CO_2 and NOx were 4.2% and 7.8%, respectively.

The methodology involves identifying the most important properties (metrics) of a cycle and developing a technique which proportions emissions for an "unseen" cycle based on emissions from cycle data using those metrics for weighting. The weighting factors for the linear combination of cycles were determined by posing a simultaneous set of equations based on cycle properties. In this way each baseline cycle will contribute to a percentage of the emissions of the unseen cycle. The number (N) of baseline test cycles determines the number of simultaneous equations and, hence, the number of properties that can be used. One of the equations will always constrain the sum of the coefficients to be equal to one, so there will be N-1 properties that are used to solve the N simultaneous equations. In each case, the predicted emissions (CO_2 emissions mass rate in g/s as a surrogate of fuel consumption[14]

[14] Fuel consumption is preferred to fuel economy. Fuel economy (in miles per gallon for example) is not a robust metric for judging the fuel efficiency of a HD vehicle. It depends heavily on the average speed of the cycle used and it has a non-linear relationship with fuel consumption that may generate misunderstandings in terms of actual savings (e.g. a 100% percent increase in fuel economy correspond to 50% decrease in fuel consumption). Fuel consumption is the fundamental measure of fuel efficiency in the current regulations (NRC, 2010).

or NOx mass rate in g/s in this study) would be a weighted summation of the measured emissions from the baseline cycles.

3.2 Model Description

Assume that emissions measurements (cycle averaged CO_2 or NOx emissions mass rates in g/s) for three different test cycles are available and one wants to estimate emissions for a fourth, different cycle. The three measured cycles are termed the "baseline cycles" and the predicted cycle is termed an "unseen cycle." The baseline cycles form the basis to estimate emissions for the unseen cycle. Each baseline cycle will have weighting factors (w_i) that defines the relative proportion of that cycle to the unseen cycle in terms of the metrics used. It is expected that these weighting factors also can be employed to estimate the unseen cycle emissions and fuel consumption. Two cycle properties should be used for a unique solution because the number of baseline cycles is three. Note that a different number of metrics and baseline cycles may have been used.

The prediction method consists of posing a set of three linearly independent simultaneous equations, based on the selected cycle properties, to calculate the weights of each baseline cycle to the "unseen" cycle. The three unknowns are the weighting factors for each baseline cycle. The equation set is shown in matrix form in Equation 7. The first two equations are linear combinations using two different properties (P_1 and P_2). The first equation uses P_1, the second equation uses P_2, and the third equation constrains the weights to sum to unity. Various metrics could be used. One specific objective of this study is to find the most suitable metrics to predict fuel consumption and NOx emissions.

$$\begin{bmatrix} P_1^{cycle1} & P_1^{cycle2} & P_1^{cycle3} \\ P_2^{cycle1} & P_2^{cycle2} & P_2^{cycle3} \\ 1 & 1 & 1 \end{bmatrix} \begin{bmatrix} w^{cycle1} \\ w^{cycle2} \\ w^{cycle3} \end{bmatrix} = \begin{bmatrix} P_1^{unseen\ cycle} \\ P_2^{unseen\ cycle} \\ 1 \end{bmatrix} \quad (7)$$

The next step is to solve the simultaneous equations to obtain the weighting factors. Once the weighting factors are calculated, they are used to calculate the emission rate (ER), or the fuel consumption (FC)[15] for the "unseen" cycle as shown in Equations 8 and 9, respectively.

[15] Properties, emission rates (ER), and fuel consumption (FC) are not expressed as continuous functions (i.e. second-by-second). They are expressed as averages over a certain vehicle activity (driving cycle or in-use route).

$$ER_{unseen\ cycle} = w_{cycle1} ER_{cycle1} + w_{cycle2}\, ER_{cycle2} + w_{cycle3} ER_{cycle3} \quad (8)$$

$$FC_{unseen\ cycle} = w_{cycle1} FC_{cycle1} + w_{cycle2}\, FC_{cycle2} + w_{cycle3} FC_{cycle3} \quad (9)$$

Note that no regression technique is required for the method, which relies solely on the linear association of vehicle emissions with activity parameters. As such, any non-linear relationship between the metrics and test cycle data will be modeled as a linear system. Note that the selected metric could be non-linear and an example is square of velocity (V^2). However, the key to successful prediction is the adequate selection of both cycle properties and baseline cycles to be used in the model. Additionally, the original data must be precise and, preferably, accurate if the model is to be used to provide real-world analysis results.

3.3 Geometric Explanation

Solving a system of three equations and three unknowns as shown in the previous section example is equivalent to finding the equation of a plane in a three dimensional space. The concept used to predict emissions or fuel consumption is shown graphically in Figure 7. In this figure the cycle properties (P_1 and P_2) and the measured fuel consumption (FC) from a vehicle operating on three different "baseline cycles" are shown as points in three-dimensional space. The plane formed by connecting these three points forms a solution set for the interpolated fuel consumption from the same vehicle operating over any other route. In this way, fuel consumption can be determined for any unseen route using its values of properties to then project upwards vertically until intersecting the plane. The value of fuel consumption where the vertical line intersects the plane represents the projected or estimated fuel consumption from that route. Emission rates may be estimated using the emissions data with the same method.

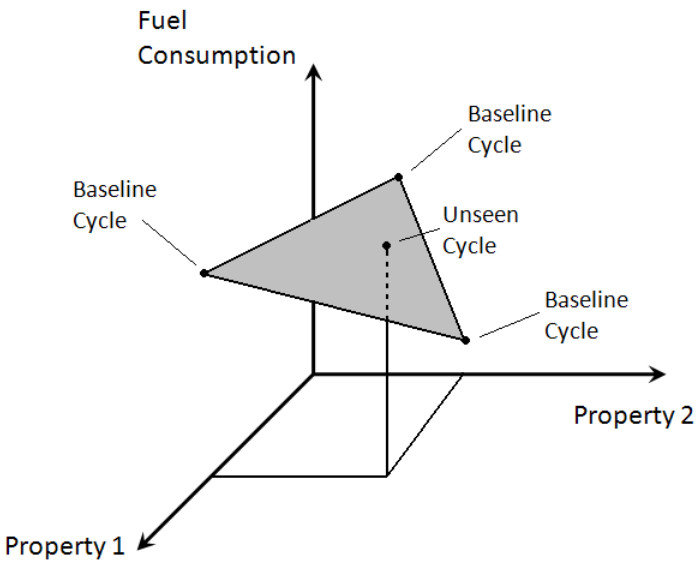

Figure 7 Geometric interpretation of the linear interpolation method

3.4 Plane Equation

The modeling approach simplifies the real world surface (which may be curvilinear) to a plane, using minimum information. The plane is unique because one and only one plane can cross through any three points (unless the points are collinear). Equation 10 is the general equation of a plane in the three-dimensional space shown in Figure 7. Variables A, B, C, and D for a particular plane may be determined using equations 11 to 14[16]. Once the plane equation is obtained, it may be used for FC prediction of "unseen" activity by knowledge of its properties. Note that the equation of the plane depends only on the metrics and FC of the baseline cycles (the variables A, B, C, and D do not depend on any unseen cycle parameters). This is because the equation of the plane only depends on the three points that define that plane (i.e. baseline cycle information only). The plane equation (rearranged in Equation 15) can be used to predict other cycle's fuel consumption (or emissions) a priori, by just knowing these new cycle's properties (P_1 and P_2 for any unseen cycle).

$$A \cdot P_1 + B \cdot P_2 + C \cdot FC + D = 0 \tag{10}$$

$$A = P_2^{bc1} \cdot \left(FC^{bc2} - FC^{bc3}\right) + P_2^{bc2} \cdot \left(FC^{bc3} - FC^{bc1}\right) + P_2^{bc3} \cdot \left(FC^{bc1} - FC^{bc2}\right) \tag{11}$$

[16] Superscript bc means baseline cycle.

$$B = FC^{bc1} \cdot \left(P_1^{bc2} - P_1^{bc3}\right) + FC^{bc2} \cdot \left(P_1^{bc3} - P_1^{bc1}\right) + FC^{bc3} \cdot \left(P_1^{bc1} - P_1^{bc2}\right) \quad (12)$$

$$C = P_1^{bc1} \cdot \left(P_2^{bc2} - P_2^{bc3}\right) + P_1^{bc2} \cdot \left(P_2^{bc3} - P_2^{bc1}\right) + P_1^{bc3} \cdot \left(P_2^{bc1} - P_2^{bc2}\right) \quad (13)$$

$$D = -\left[P_1^{bc1} \cdot \left(P_2^{bc2} FC^{bc3} - P_2^{bc3} FC^{bc2}\right) + P_1^{bc2} \cdot \left(P_2^{bc3} FC^{bc1} - P_2^{bc1} FC^{bc3}\right) + P_1^{bc3} \cdot \left(P_2^{bc1} FC^{bc2} - P_2^{bc2} FC^{bc1}\right)\right] \quad (14)$$

$$FC = \left(\frac{A}{-C}\right) \cdot P_1 + \left(\frac{B}{-C}\right) \cdot P_2 + \left(\frac{D}{-C}\right) \quad (15)$$

3.5 Extrapolation and Weight Coefficients

In general, interpolation is more accurate than extrapolation. Extrapolation is based on pure speculation of the effect of the parameter being estimated. Interpolation, at minimum, bounds the effect since the effect under intermediate conditions will fall between the two conditions tested. However, the method may use extrapolation, for example predicting points on the plane but outside the triangle shown in Figure 7. As with other models, extrapolation should be exercised with caution. Trying to predict vehicle activity that is very dissimilar to the baseline cycles used to create the model may produce unrepresentative results. Therefore, it is desirable to use baseline cycles that cover a wide envelope of vehicle activity to avoid performing extrapolations, or at least extrapolations far outside the bounds defined by the data.

Negative weights will result if the cycle being predicted is outside the region defined by the baseline cycles. Equations 16 and 17 show the set of equations to be solved for a simplified case where only two baseline cycles are available. Figure 8 shows a two-dimensional illustration of the method. Baseline cycles 1 and 2 are used to generate the equation of a line. In this case the number of baseline cycles is two so only one property (P in Equation 16). The weight coefficient of baseline cycle 2 (w_2) is illustrated as an arrow and has a value of 0 at point 1 and a value of 1 at point 2. If the cycle being predicted is between the two baseline cycles (point a in the Figure), w_2 will have a value between 0 and 1 and both weight coefficients are positive. On the other hand, if the predicted cycle is outside the region defined

by the baseline cycles (point b in the Figure), one of the weight coefficients (w_2) will have a value greater than 1 making the other weight coefficient (w_1) to be negative.

$$\begin{bmatrix} P^{cycle1} & P^{cycle2} \\ 1 & 1 \end{bmatrix} \begin{bmatrix} w^{cycle1} \\ w^{cycle2} \end{bmatrix} = \begin{bmatrix} P^{unseen\ cycle} \\ 1 \end{bmatrix} \tag{16}$$

$$FC_{unseen\ cycle} = w_{cycle1} FC_{cycle1} + w_{cycle2}\, FC_{cycle2} \tag{17}$$

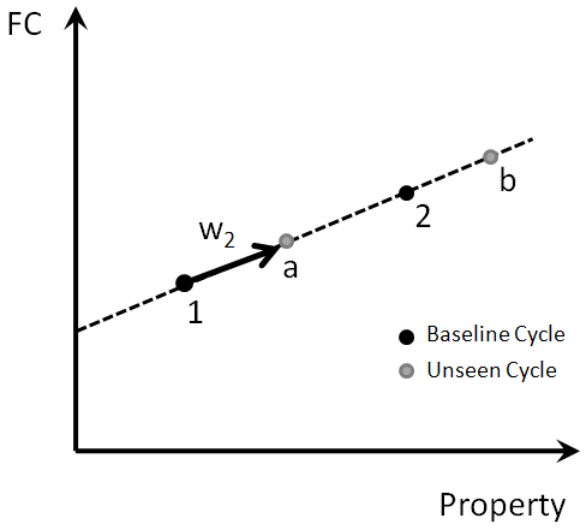

Figure 8 Geometric interpretation of a two-dimensional simplified model

Considering the three-dimensional case (Equation 7), note that the solution of the system of three simultaneous equations does not depend on fuel consumption or emission rates values. The weights only depend on the properties (P_1 and P_2) of baseline and unseen cycles. With this in mind Figure 9 illustrates a two dimensional projection of the plane in the properties axis. Dotted lines represent the points in the region where one of the weight coefficients has a value of zero. It can be seen that six different regions of extrapolation occur; each one is shown with its corresponding signs of the weight coefficients (w_1, w_2, w_3) within the parentheses. Any unseen cycle outside the triangular region determined by baselines cycles 1, 2, and 3 will result in either one or two of the weight coefficients to be negative.

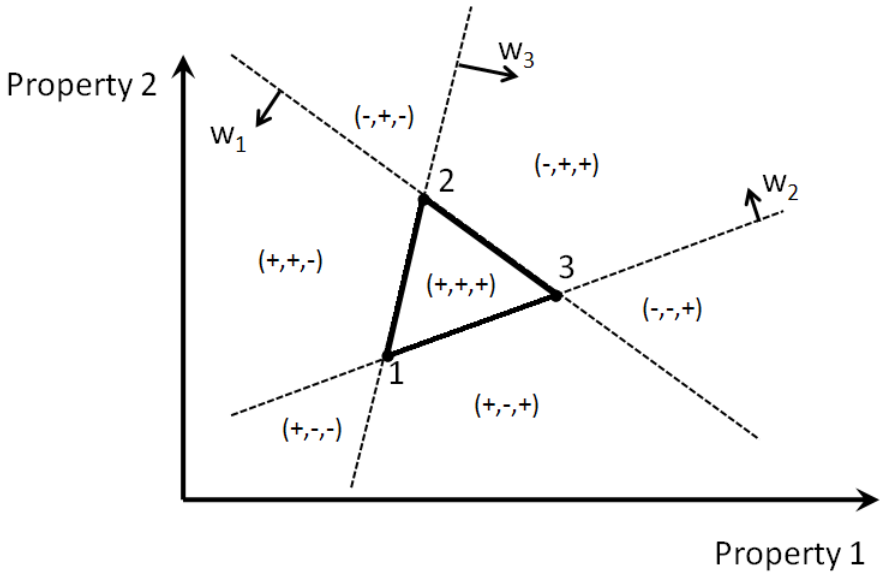

Figure 9 Weight coefficients signs[17]

By inspection of Figure 9, one can find regions outside the triangle where unseen cycle properties are bounded by the values of properties for the baseline cycles (think of a rectangular box where the triangle is inscribed within this box). Going from a 1-dimensional space to a 2-dimensional space the interpolation region is smaller than expected. In general, adding dimensions to the model (i.e. adding another baseline cycle and property) makes the interpolation region smaller to the whole space. Figure 10 shows the interpolation regions in 2-dimensional space and 3-dimensional space. The ratio between the areas of the triangle and the circle is 0.4135 as calculated in Equation 18[18]. The ratio between the volumes of the tetrahedron and the sphere is 0.1225 as calculated in Equation 19[19]. For the 1-dimensional case, if the baseline cycles are at the extreme boundaries of the space, all the space corresponds to an interpolation region and the ratio would be equal to 1. It is clear that adding dimensions to the model will reduce the region of interpolation with respect to the whole space. This fact can explain the occurrence of diminishing returns in accuracy when trying to add more than three baseline cycles to the model.

[17] Sign within the parentheses represent the sign for each weight (w_1, w_2, w_3).

[18] The side of an equilateral triangle inscribed in a circle of radius r=1 is $a=3/\sqrt{3}$.

[19] The side of a regular tetrahedron inscribed in a sphere of radius r=1 is $a=\sqrt{\frac{8}{3}}$.

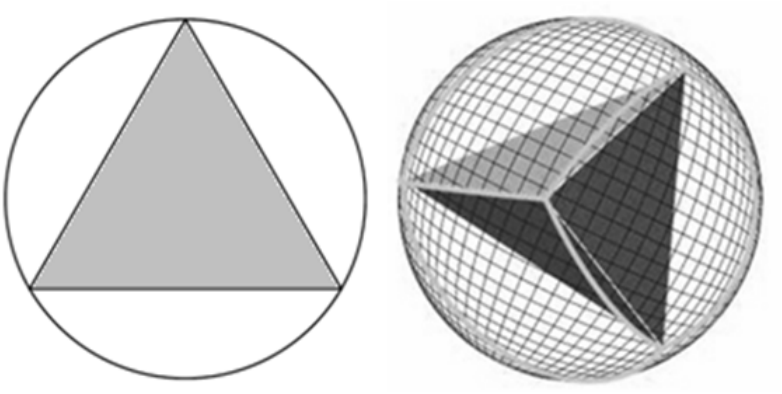

Figure 10 Interpolation regions in two and three dimensions[20]

$$\frac{Area\ triangle}{Area\ circle} = \frac{\frac{\sqrt{3}}{4}a^2}{\pi r^2} = 0.4135 \quad (18)$$

$$\frac{Volume\ tetrahedron}{Volume\ sphere} = \frac{\frac{\sqrt{2}}{12}a^3}{\frac{4}{3}\pi r^3} = 0.1225 \quad (19)$$

It is expected for the model to experience a loss of accuracy due to extrapolation. The magnitude of that loss will be higher if the predicted cycle is farther from the interpolation region. A good metric to quantify the magnitude of extrapolation (i.e. distance from the triangle or tetrahedron) is the absolute value of the highest weight coefficient. If no extrapolation occurs, weight coefficients' absolute values will be less than one. If extrapolation occurs, one or more weight coefficient absolute values will be greater than one. The longer the distance to the interpolation region, the larger the absolute value of the weight coefficients. An extrapolation parameter could be defined as shown in Equation 20.

$$Extrapolation\ Parameter = \begin{cases} 0 & if\ |w_{max}| \leq 1 \\ |w_{max}| - 1 & if\ |w_{max}| > 1 \end{cases} \quad (20)$$

Figure 11 shows a scatter plot of the absolute percentage error versus the extrapolation parameter for the prediction of CO_2 mass rate for a representative case[21]. Although the regression coefficient shown (R^2=0.54) is not conclusive, the general trend observed for this and many other models is that

[20] Source: http://www.math.ubc.ca/~cass/courses/m308-03b/projects-03b/wagner/Webpage.htm

[21] Predictions using average road load power and aerodynamic speed as properties and all possible combinations of cycles available for bus 41 described in Section 5.1

attempting heavier extrapolations (higher extrapolation parameter values) caused larger prediction errors.

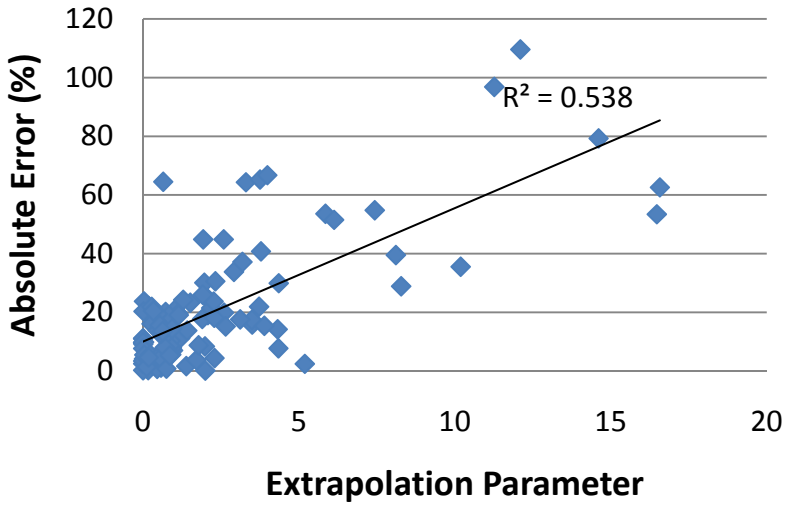

Figure 11 Relationship between extrapolation and absolute error

3.6 Ill-Posed Models

The main idea of the model is to produce a plane (or a multidimensional hyper plane) that fits well through the activity-emissions data. Ill-posed models may generate high prediction errors. In general, one may identify an ill-posed model when the absolute values of one or more of the weight coefficients are far greater than one.

An ill-posed model will occur when the property values of two or more baseline cycles are close to each other causing the system to be near singular. Another non-desirable case is when the metrics for one baseline cycle are a linear combination of other baseline cycles (e.g. metrics for one baseline cycle having twice the value of other baseline cycle). That will create a non-independent base and therefore a singular (i.e. without solution) system. In terms of the metrics, choosing two very similar metrics will not create a singular system; the only effect is that the model will behave as if it had one dimension less than the original one due to redundant information being input.

3.7 Preliminary Work

The modeling methodology was detailed by Delgado et al. (2012) focusing on the fuel consumption predictive capabilities of the model. The motivation for this research was to predict fuel consumption of a vehicle exercised over new or unseen cycles using limited chassis dynamometer data so as to reduce heavy-duty chassis dynamometer operation costs. Nine driving cycle properties and their combinations were used to predict fuel consumption for 56 heavy-duty vehicles over the UDDS cycle, based on measurements from up to four different baseline driving cycles (Idle, Creep, Transient, and Cruise modes of the Heavy Heavy-Duty Diesel Truck (HHDDT) schedule). Data were acquired as part of the Coordinating Research Council (CRC) E-55/59 program (Clark et al., 2007b) conducted in California. The results showed that average velocity and average positive acceleration were suitable for the translation of fuel consumption between cycles, producing the lowest prediction error among the cases considered (4.3% relative error). Parity plots for fuel economy and CO_2 mass rate predictions using the recommended baseline cycles of Idle, Transient, and Cruise are shown in Figures 12 and 13, respectively.

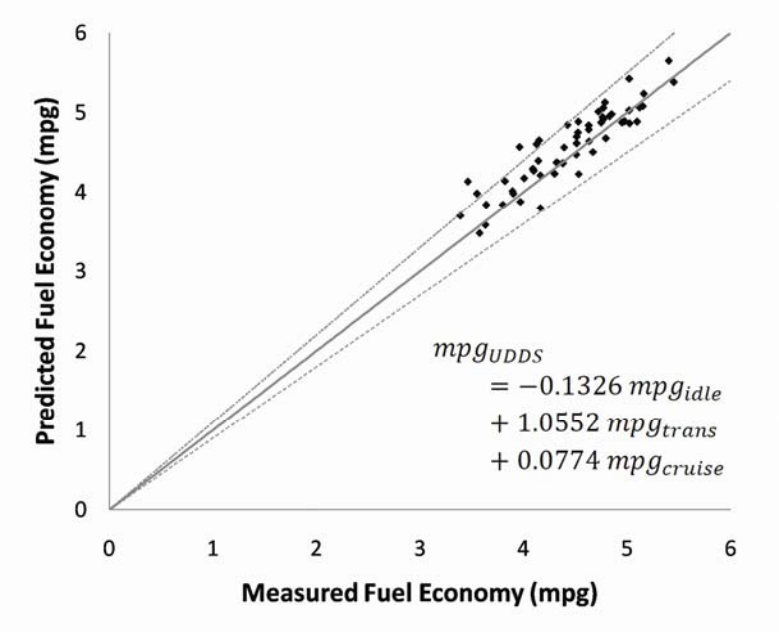

Figure 12 Results for fuel economy (mpg) prediction for 56 trucks using Idle, Transient, and Cruise modes of the HHDDT schedule as baseline cycles and average speed and average positive acceleration as metrics (Delgado et al., 2012)

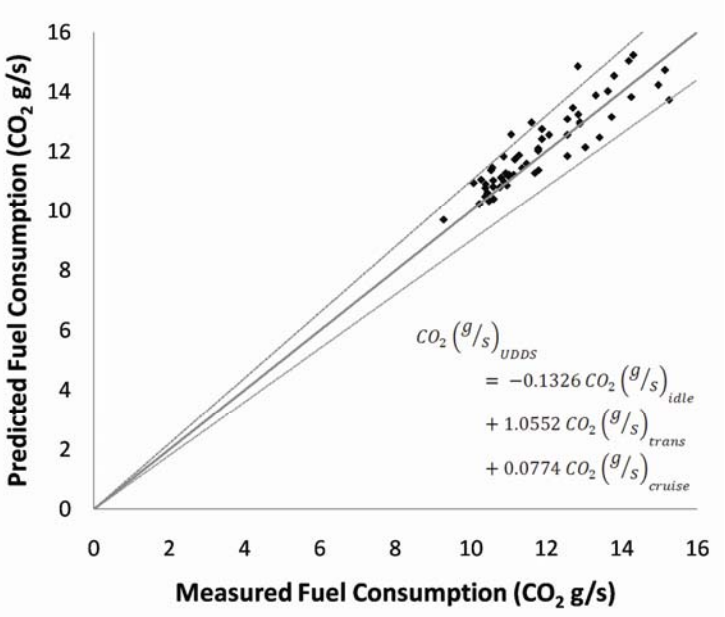

Figure 13 Results for CO_2 mass rate prediction as fuel consumption surrogate. Prediction for 56 trucks using Idle, Transient, and Cruise modes of the HHDDT schedule as baseline cycles and average speed and average positive acceleration as metrics (Delgado et al., 2012)

The plots show measured and predicted values, as well as the equation used for prediction. The solid line represents the parity line and the dashed lines represent the limits of ±10% error in the prediction. Note that the weighting factors are the same for CO_2 and for fuel economy prediction (using the same metrics and the same baseline cycles), but the Idle cycle information is lost in the fuel economy prediction because of the zero fuel economy value for the Idle cycle. Based on this finding, it was recommended that the prediction be made in terms of CO_2 mass rate, or equivalent units of fuel mass flow rate. One may then compute fuel economy using average cycle speed. It was found also that if another metric (and baseline cycle) was to be added to the model, it was recommended to use the number of stops per unit of distance as the additional metric (Delgado et al., 2012).

Delgado et al. (2011) applied the methodology for a set of five transit buses with diverse technologies (conventional diesel, compressed natural gas, and diesel hybrid buses) over an extended set of up to 17 chassis dynamometer cycles. This was the first attempt of using the method to predict emissions over diverse driving cycles. The technique worked well for CO_2 mass rate prediction as can be seen in Figure 14. The parity plot shows that vehicles of a chosen category can be evaluated using a limited number of cycles with sufficiently different properties, and behavior of any cycle in a wide envelope can be predicted. Appropriate cycle selection is important to assure model accuracy and to define cycles which

should be used if the methodology was ever to be used for regulatory purposes. It was found that baseline cycles must include the Idle cycle, along with a relatively slow transient cycle and a relatively high speed cycle, preferably with an average velocity at or above the average velocity of the unseen cycle.

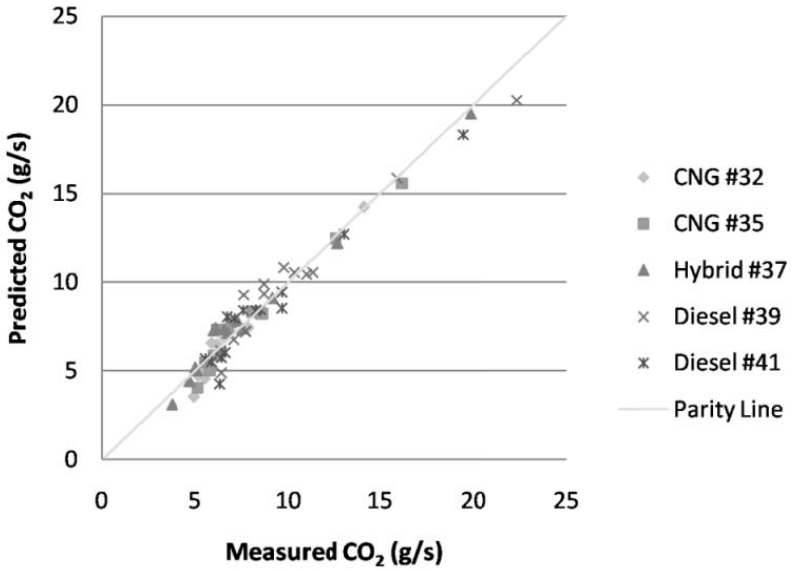

Figure 14 Parity plot for prediction of CO_2 mass rate using Idle, OCTA, and KCM as baseline cycles and average velocity and average positive acceleration as metrics (Delgado et al., 2011a)

The same metrics and baseline cycles used for the prediction of CO_2 were used to predict NOx emissions. Figure 15 shows a parity plot of NOx emissions mass rate measured versus predicted values for all the predictions. Overall results were poorer than the previous CO_2 prediction (with an average NOx rate error of 20.4% over the five buses compared to about 10% for CO_2). However, there was no attempt in this study to optimize NOx prediction or to explore other metrics in order to increase the NOx predictive ability.

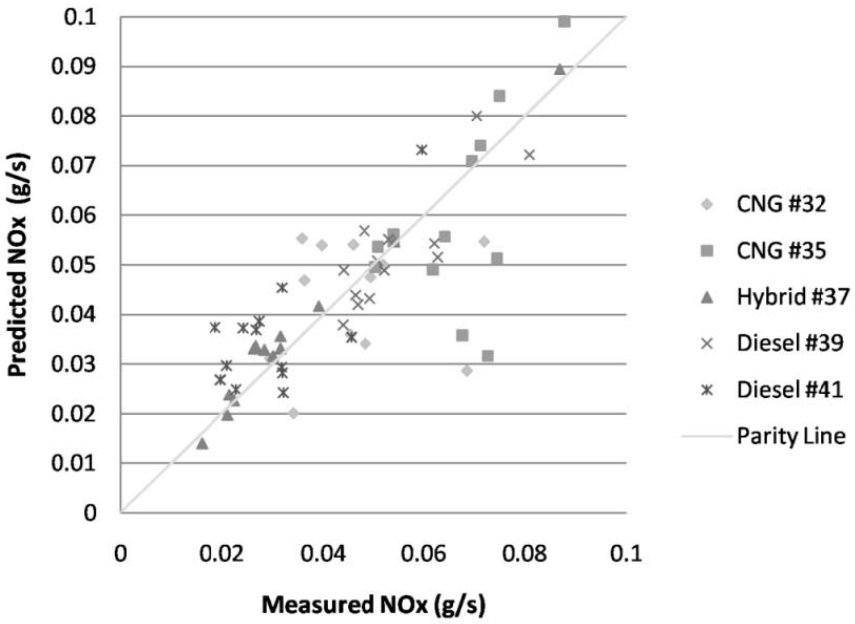

Figure 15 Parity plot for prediction of NOx mass rate using Idle, OCTA, and KCM as baseline cycles and average velocity and average positive acceleration as metrics (Delgado et al., 2011a)

4 Variability and Sensitivity Analysis

This chapter starts with a description of the modeling methodology from a mathematical perspective. Then, an assessment of causes of error (variability) in emissions measurement and properties estimation which are the inputs to the model is presented. The chapter ends with a sensitivity analysis of the response of the model with respect to variability in its inputs.

4.1 Causes of Error

As shown in Equation 8, Section 3.2, the model inputs include cycles' or routes' properties and emissions measurements. Several sources of variability go into the model due to metrics estimation and from the measured data. The linear model could not be expected to be better than variations between measured data sets. Uncertainty may arise from many sources. For this specific modeling approach, these sources can be divided into experimental uncertainties and modeling uncertainties.

4.1.1 Experimental Uncertainties

Experimental uncertainties will inevitably appear and affect model response. The model is calibrated with data that contains measurement errors. Thus, it is very important to quantify the variability or statistical uncertainty that will occur when performing repeated tests. It is noted that all models must contend with experimental uncertainties and data quality in general.

Emissions and fuel consumption data will usually vary from test to test due to random variation in the data collection process and due to engine and or vehicle operator variations. The fuel consumption and emissions measurements from the baseline cycles or routes are an important part of the model. Uncertainties due to measurements propagate through the model and affect uncertainties of any simulated results.

4.1.1.1 Driver Performance

Even though vehicles are tested with respect to a given speed time profile, the test driver will deviate from the set speed trace and such deviations can lead to test-to-test variability. For example, Figure 16 compares the relationship between the actual and target speed employed for a HD truck[22] over the

[22] CRC E55/59 Program, Vehicle ID 23 (Clark et al., 2007b).

UDDS cycle on a chassis dynamometer. Drivers were instructed to follow the scheduled trace as closely as possible without driving in a fashion uncharacteristic of real-world operation. The response time of the driver, when trying to follow the speed-time trace, as well as the capability (or lack thereof) of the vehicle to achieve the desired accelerations, creates small variations in time and speed at certain points. Adherence of the driver to the test cycle target speeds may be analyzed via regression of the data[23]. Customarily, WVU manages data quality by ensuring that the distance travelled during the test cycle is within 5% of the target distance (Wayne et al., 2004) to account for vehicles that may be underpowered. Automatic transmissions would reduce driver control effects because there were no direct driver shift choices, and they provide the ability to follow test schedules with higher accelerations closely because of the interfacing of the transmission with the engine control during shifting.

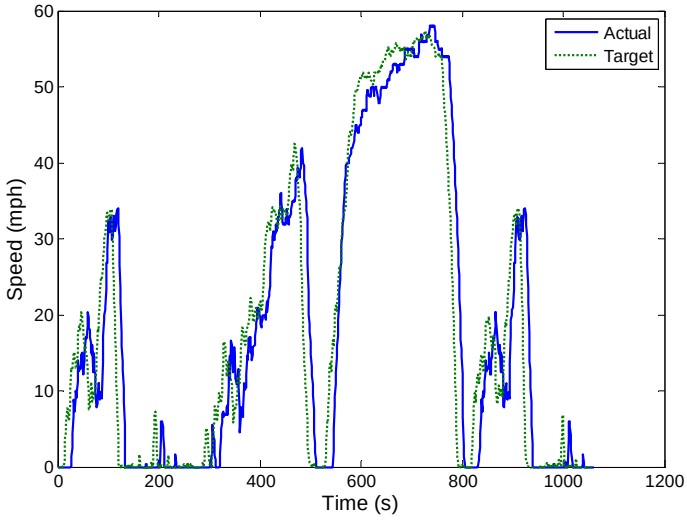

Figure 16 Comparison of the actual and target speed for a chassis dynamometer test over the UDDS cycle

For in-use testing, driving style (e.g. aggressiveness of driving) will have an effect on resultant emissions. Test-to-test repeatability is considerably more difficult when following a predefined driving route than when following speed-time traces on a chassis dynamometer because of external influences such as

[23] SAE J2711 recommended practice (SAE, 2002): Target speed (x) and actual speed (y) should be charted in 1Hz increments and a trend line inserted with a zero intercept. If the resulting trend line has a slope that varies from unity by more than 10% or an R^2 of less than 0.8 the test run should be considered an invalid representation of that test cycle.

traffic congestion, environmental conditions (wind, wet roads, and visibility), and the need to pay attention to driving the vehicle in a safe manner. As an example, Figure 17 shows speed-distance traces and altitude-distance traces for three repeated tests of WashPA3 route for an over-the-road HD truck[24]. The traces are similar to each other but some discrepancies indicate that different traffic conditions were encountered for each test. Note that there is variability in the altitude-distance trace due to variations in the speed and altitude data from the GPS system.

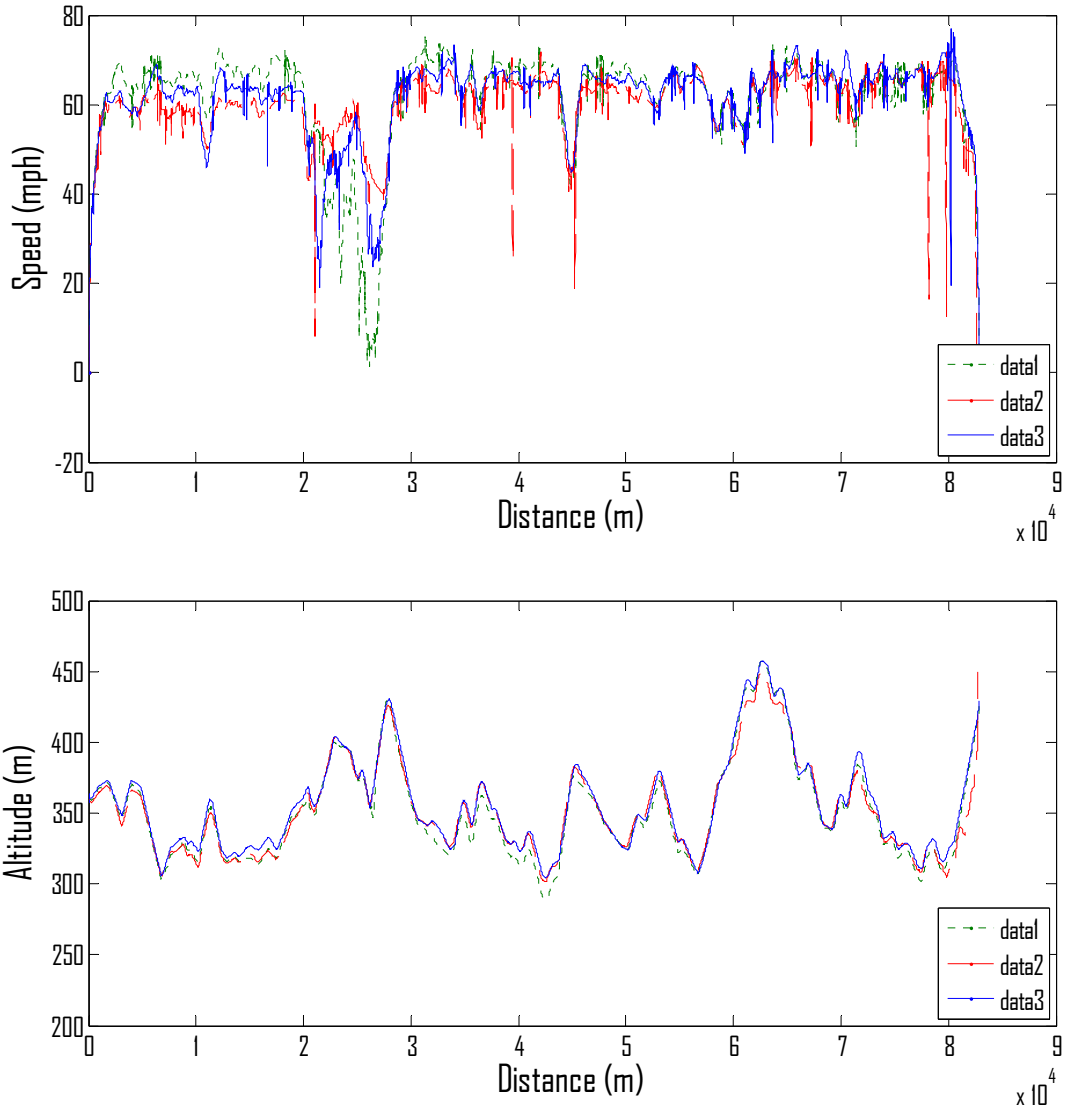

Figure 17 Speed-distance and altitude-distance traces for three in-use tests over WashPA3 route

[24] Vehicle ID N in Table 16.

4.1.1.2 Thermal Loads/Accessories

Engine cooling systems and air conditioning (AC) loads may have an impact on the emissions and fuel consumption of HD vehicles. Because of the difficulty to compare one test to another when the operating variables that affect AC loads are not completely controlled (ambient temperature, ambient humidity, heat transfer coefficients, thermal loads, etc.) the recommended practice for measuring fuel economy and emissions for HD vehicles (SAE, 2002) does not recommend that testing be conducted with the AC in operation. However, the engine cooling fan of a HD vehicle could take up substantial power (up to 30 hp) and its operation will depend on uncontrollable factors such as ambient temperature. Other vehicle accessories such as pumps or electrical devices can add some variation in the emissions data because they require power to operate. Auxiliary load demanded from the engine of a HD vehicle might be in the range of 5 hp to about 40 hp (Clark et al., 2007a).

4.1.1.3 Off-Cycle Behaviour

Off cycle behavior refers to emissions that occur in actual operation but that are not captured over the test procedure used to determine compliance with the standards. For HD trucks model years prior to 1999, advanced injection timing at steady cruise was implemented for various HD manufacturers in order to improve fuel economy with a corresponding substantial rise (order of 200%) in NOx emissions. As a result, the vehicles emitted NOx at two different levels at the same power output and engine speed. Figure 18 shows NOx versus CO_2 (fuel rate) for an in-use trip[25] where two different trends can be identified. Vora et al. (2004) concluded that due to differing injection timing strategies, it is impractical to attempt to predict Cruise Mode emissions from Transient Mode data, and vice-versa, for the case of NOx. Earlier model year vehicles with mechanical fuel injection avoid the influence of “off cycle “effects but could be varied if mechanical adjustments were made to the fueling system outside the original manufacturing setting.

The United States and six heavy-duty diesel engine manufacturers entered into individual agreements known as Consent Decrees. The Consent Decrees required that the six engine manufacturers cease the employment of defeat devices that altered their injection timing during certification testing

[25] WashPA3 route. See section 5.2.

(Krishnamurthy, 2000). Additional emission testing requirements were also introduced, including the Supplemental Emission Test (SET)[26] and the Not-to-Exceed (NTE) testing[27].

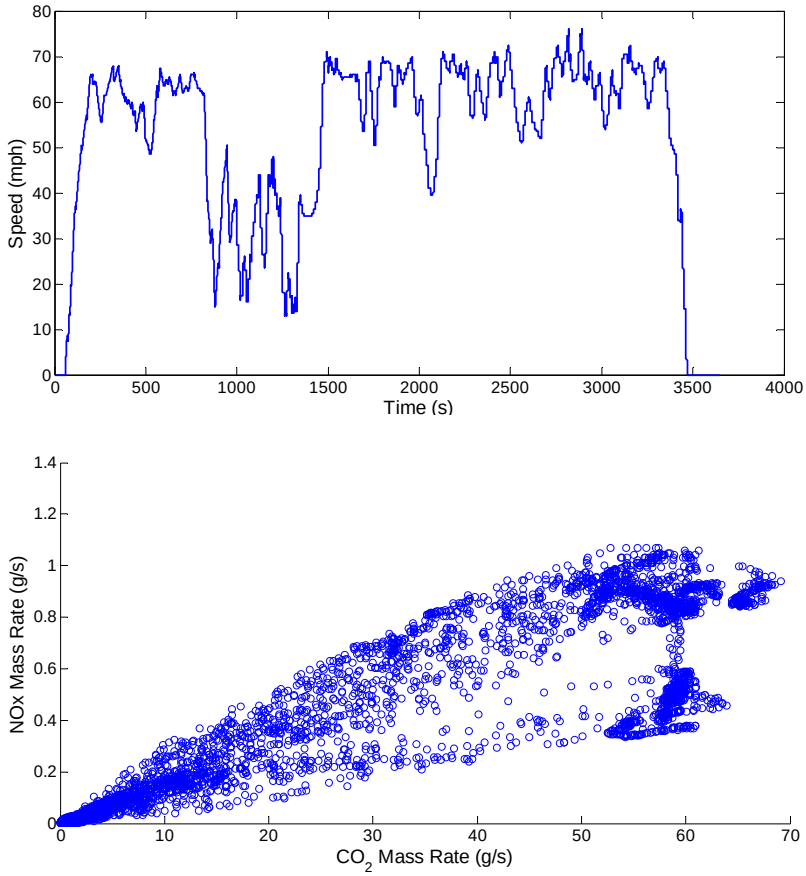

Figure 18 Off-cycle NOx emissions over WashPA3 route

4.1.1.4 Air/Fuel Ratios

NOx production is dependent on the degree of throttling on spark ignited engines. For compressed natural gas (CNG) vehicles, NOx may vary from run-to-run due to air/fuel ratio variations (Wayne et al., 2004). Also, NOx varies substantially with load, so that an engine at 1200 rpm, 180 Nm will yield very different NOx at 1800 rpm, 120 Nm, even though the power is the same. Figure 19 shows brake-specific

[26] A steady-state test to ensure that heavy-duty engine emissions are controlled during steady-state type driving.

[27] Driving of any type that could occur within the bounds of a pre-defined NTE control area for at least 30 seconds of continuous operation under steady-state or transient conditions.

NOx emissions at lean operation for a 1.6L lean-burn CNG engine as discussed in Einewall et al. (Einewall et al., 2005). Note that higher levels of NOx may be emitted as the engine air-to-fuel ratios approach stoichiometric conditions.

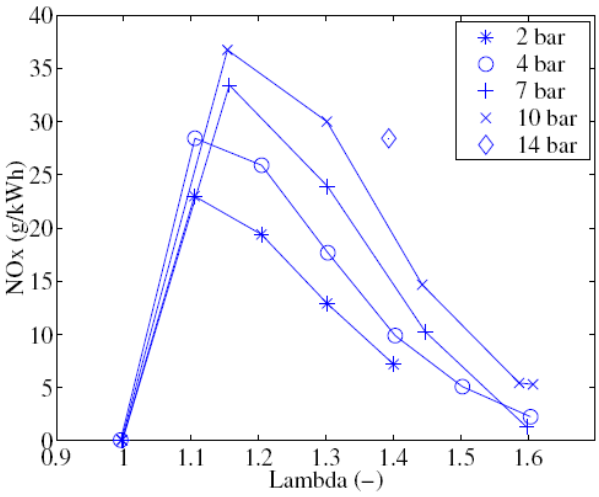

Figure 19 Brake-specific NOx emissions after the catalyst for various load cases (Einewall et al., 2005)

Another possible source of NOx variability for lean-burn natural gas engines is the use of aftertreatment. If an oxidation catalyst is used, large NO_2/NOx ratios may result, causing additional uncertainty in NOx emissions measurements because the chemiluminescence technique was developed for low NO_2/NOx ratios (Olsen et al., 2010).

4.1.1.5 Idle

A large number of heavy-duty vehicles spend their time idling in traffic, during deliveries, and at truck stops. Electronically controlled engines may have different engine timing strategies that are temperature sensitive during idle and this could have affected emission results from test to test.

4.1.2 Model Uncertainties

Model uncertainties or errors could arise when a limited number of descriptors (i.e. less than the optimum number of descriptors) are used within the model. For example, when using models with only one cycle or route property as input, it would be difficult to capture both the steady-state losses and the transient nature losses. The description of complex phenomena may be incomplete if the model does not have a sufficient set of explanatory variables.

Model errors can occur when the actual functional form of the properties-emissions relationship is different to the functional form specified by the model (a plane in this work). This may occur when one or more relevant cycle properties are omitted, or one or more unsuitable metrics are included. If unsuitable variables are included, the estimation will be inefficient in terms of number of test required. The user must be aware that some emission species present non-linear functionality with respect to power demand and are more strongly a function of the frequency and severity of the transients in vehicle activity (e.g. PM).

Model uncertainty should not be confused with model repeatability. No random component is involved in the modeling approach used in this study (as may be the case for NN modeling to cite an example). Therefore, if the proposed model is run several times with the same inputs the output will always be the same.

4.2 Variability Analysis

In order to understand the impact uncertainties have on the model, a variability analysis was performed to quantify the typical variation levels of model's input parameters. It is important to determine the variation between measured data sets in order to understand the achievable accuracy of the model.

4.2.1 Variability in Chassis Dynamometer Testing

Measurement error may be determined statistically from run-to-run variations. The level of variation in emission measurements between different runs determines the maximum achievable accuracy of the predictive model. In other words, if run-to-run variability is 20%, it cannot be expected for any model to predict with errors lower than 20%. A summary of chassis dynamometer data from 15 over the road class 8 trucks[28] was examined in order to determine typical test-to-test variation in measured emissions values. CO_2 and NOx mass rate emissions values for multiple runs (between three and five) of a particular cycle were averaged, and their standard deviations and coefficients of variation (COV) were calculated. Tables 7 and 8 show COV values for CO_2 and NOx measurements, respectively. The COV for

[28] The data used were gathered as part of the CRC E55/E59 program, which was created to characterize heavy-duty trucks emissions in California. The model year for this set ranged from 1973 to 2005, and engine power ranged from 200hp to 530hp (Clark et al., 2007b). See Section 5.1.2 for a description of the chassis dynamometer cycles.

the measured CO_2 values ranged from 0.1% to about 23%, while the COV values for the measured NOx ranged from 0.4% to about 93%. It can be seen in Table 7 that the average variation in CO_2 measurements was about 4.4%. It is evident that the test cycle influences the expected variation with higher variations at lower average speeds. Idle cycle variability may be explained by test-to-test differences in ambient conditions and cooling fan (and or any other accessories) operation (Khan et al., 2006). Table 8 shows that NOx variability was higher than CO_2 with an average of 11.3%. Again, the variability increased for lower speed cycles with the exception of the cruise cycle (off-cycle behavior may explain this fact). Test-to-test variability for a set of chassis dynamometer data from transit buses (see Section 5.1) from the WMATA emission testing program (Melendez et al., 2005; Wayne et al., 2008) was estimated at about 11% for NOx mass rate (g/s) and 4% for CO_2 mass rate (g/s). However, not enough repeated tests were available to calculate reliable COV values. Customarily, WVU manages data quality by ensuring that the COV on NOx and CO_2 emissions between runs are below 5% (Wayne et al., 2004).

Table 7 Variability analysis of CO_2 emissions from chassis dynamometer testing

	COV of measured CO_2 (%)					
Vehicle ID	**Idle**	**Creep**	**Trans**	**UDDS**	**Cruise**	**Average**
10	10.2	7.2	0.8	2.4	0.5	***4.2***
14	8.9	10.1	0.9	1.8	0.5	***4.4***
15	15.0	9.1	0.2	0.7	1.6	***5.3***
16	9.6	6.4	5.9	5.5	7.4	***7.0***
17	12.2	11.9	4.3	3.5	1.7	***6.7***
18	8.3	2.5	1.6	3.9	0.5	***3.4***
19	22.5	4.9	1.6	0.9	0.1	***6.0***
20	13.3	2.6	4.4	0.9	0.6	***4.4***
21	6.4	4.3	1.0	1.1	0.5	***2.7***
22	9.5	0.8	4.0	1.9	1.2	***3.5***
23	8.4	8.1	1.5	0.8	0.4	***3.9***
24	2.4	6.1	1.2	0.3	0.6	***2.1***
25	3.0	1.8	1.5	0.4	0.1	***1.3***
28	12.4	9.5	3.9	4.2	4.0	***6.8***
45	4.7	3.8	3.3	4.1	3.4	***3.9***
Average	***9.8***	***5.9***	***2.4***	***2.2***	***1.5***	***4.4***

Table 8 Variability analysis of NOx emissions from chassis dynamometer testing

	COV of measured NOx (%)					
Vehicle ID	**Idle**	**Creep**	**Trans**	**UDDS**	**Cruise**	***Average***
10	21.2	10.1	6.1	11.9	19.0	***12.3***
14	92.9	47.4	1.6	1.3	0.4	***35.8***
15	72.8	6.2	4.6	0.5	2.1	***21.0***
16	38.2	4.5	12.4	5.3	16.2	***15.1***
17	36.9	9.4	4.5	3.1	1.6	***13.5***
18	7.0	5.2	2.1	3.2	1.4	***4.4***
19	55.1	3.1	1.7	1.9	1.3	***15.5***
20	4.1	2.9	3.6	0.7	2.3	***2.8***
21	29.0	1.6	2.2	3.7	2.5	***9.1***
22	12.4	7.6	6.2	2.1	2.2	***7.1***
23	20.7	12.6	7.7	3.3	1.8	***11.1***
24	6.7	9.5	5.5	2.3	6.4	***6.0***
25	10.5	5.1	4.0	4.2	7.0	***6.0***
28	25.5	20.6	15.0	9.5	22.8	***17.6***
45	10.6	10.3	3.6	5.5	18.3	***7.5***
Average	***29.6***	***10.4***	***5.4***	***3.9***	***7.0***	***11.3***

4.2.2 Variability in In-Use Testing

Variability of in-use testing data is expected to be higher than for chassis dynamometer data. A summary of in-use data gathered with WVU's MEMS from 13 over the road class 8 trucks over eight different routes[29] was examined in order to determine typical test-to-test variation in measured emissions values. The engines in these vehicles were pre-2002 (pre-EGR) model year. CO_2 and NOx mass rate emissions values for multiple runs (between three and five) of a particular route were averaged, and their standard deviations and coefficients of variation (COV) were calculated. Tables 9 and 10 show the COV values for CO_2 and NOx emissions measurements, respectively. The COV for the measured CO_2 values ranged from 3.0% to 13.3%, for different routes, with an average COV of 6.4%. The COV values for the measured NOx ranged from 4.7% to 18.3% for different routes, with an average of 8.6%. The emissions data were collected during different testing periods on the same route. Differences between tests could be due to various factors such as ambient weather conditions, traffic conditions, and different driving styles for different drivers. Idle "route" data were extracted from idle portions of the

[29] See Section 5.2.2

routes. These stationary portions may occur at different ambient and or engine conditions, explaining the higher emissions variability observed for the Idle routes. Note that the average variability in the in-use route NOx data in Table 10 (8.6%) is lower than that of the chassis dynamometer NOx data in Table 8 (11.3%). A possible explanation may be the total distance traveled where chassis dynamometer testing typically occurs within a 10 mile distance whereas the in-use testing occurred over tens of miles. The longer in-use test duration may provide a more accurate representation of the NOx emissions data.

Table 9 Variability analysis of CO_2 emissions from in-use testing

	COV of measured CO_2 (%)								
Vehicle ID	**Idle**	**WashPA2**	**WashPA1**	**BM2Sab**	**Sab2BM**	**Sab2SW**	**SW2Sab**	**WashPA3**	**Average**
12	11.7	16.4	4.0	3.9	8.1	12.9	2.0	3.5	***7.8***
17	22.0	9.5	3.0	0.7	5.3	4.4	3.2	5.6	***6.7***
21	9.3	3.1	10.8	6.5	3.1	4.1	5.5	4.0	***5.8***
24	11.2	7.2	11.4	5.9	3.2	13.6	0.9	8.1	***7.7***
25	12.4	0.4	3.2	4.2	17.2	6.2	1.8	0.7	***5.8***
26	10.5	6.1	9.9	9.1	6.7	9.5	1.0	1.4	***6.8***
27	12.2	5.4	6.0	4.6	6.0	3.5	3.2	2.2	***5.4***
28	11.2	13.4	2.7	2.5	4.7	5.9	1.7	7.2	***6.2***
29	17.0	9.7	4.3	6.7	3.7	9.9	1.6	6.4	***7.4***
32	25.1	7.1	6.4	2.6	3.7	1.9	5.5	12.4	***8.1***
37	6.3	7.5	5.1	4.1	6.8	5.4	3.7	2.1	***5.1***
42	12.7	7.8	4.7	7.1	2.3	3.7	5.9	4.8	***6.1***
44	10.8	7.9	0.6	7.9	5.0	0.6	2.9	3.1	***4.9***
Average	***13.3***	***7.8***	***5.5***	***5.1***	***5.8***	***6.3***	***3.0***	***4.7***	***6.4***

Table 10 Variability analysis of NOx emissions from in-use testing

	COV of measured NOx (%)								
Vehicle ID	**Idle**	**WashPA2**	**WashPA1**	**BM2Sab**	**Sab2BM**	**Sab2SW**	**SW2Sab**	**WashPA3**	**Average**
12	20.1	18.2	4.8	4.7	10.7	13.1	8.5	6.3	**10.8**
17	16.2	10.7	7.1	1.1	5.2	10.3	3.1	11.1	**8.1**
21	19.8	4.6	18.3	10.9	5.6	1.9	4.2	5.7	**8.9**
24	11.6	11.9	11.7	7.3	6.6	12.6	3.6	7.2	**9.1**
25	11.5	6.6	15.1	5.9	14.7	4.4	10.1	3.2	**8.9**
26	10.5	4.9	4.5	5.4	5.7	8.7	4.0	3.5	**5.9**
27	23.8	6.4	15.2	4.6	6.1	6.3	5.9	0.4	**8.6**
28	17.6	17.4	8.7	7.0	3.4	4.1	3.6	11.1	**9.1**
29	17.7	13.7	4.2	6.6	2.5	15.1	6.9	6.8	**9.2**
32	36.1	9.8	15.1	7.1	3.9	5.1	2.8	10.0	**11.2**
37	18.3	11.3	6.0	4.3	9.1	5.4	1.9	2.8	**7.4**
42	16.4	9.8	2.7	6.9	3.5	3.9	6.2	9.9	**7.4**
44	18.7	10.6	3.6	6.9	7.4	1.9	0.6	5.1	**6.9**
Average	**18.3**	**10.4**	**9.0**	**6.1**	**6.5**	**7.1**	**4.7**	**6.4**	**8.6**

4.2.3 Variability of Properties

Repeatability of in-use routes was analyzed to provide some level of understanding of the variability in calculated properties due to test-to-test variability. It is noted that in-use testing is relatively new (since about 2000 in its present requirements) and there is limited understanding to the variability in this form of emissions testing. The analysis was done using in-use data for a HD truck[30] for which up to five repeated tests were available. Tables 11 and 12 show the variability of calculated properties over repeated tests of Sab2SW and SW2Sab highway routes[31], respectively. Average speed COV was 6.41% for Sab2SW route and 2.14% for SW2Sab suggesting that the variation may be route dependent. The property with the highest variability for the tests considered was standard deviation of speed with a COV of 9.64%. In-use variability is expected to be higher than chassis dynamometer variability because the speed-time trace is not fixed since in-use speed depends on various uncontrollable parameters such as traffic congestion and road conditions. Vehicle day-to-day variability due to varying ambient

[30] Vehicle ID 29 in Tables 9 and 10.

[31] Information on the routes can be found in Section 5.2.2. Section 5.3 (see Table 18) summarizes the properties used in this study.

conditions may also influence emissions, and metrics estimations. Note that the variations presented may be route and or vehicle dependent. Therefore, other routes (and or vehicles) could have resulted in more or less variability than the values reported here.

Table 11 Variability of calculated properties Sab2SW route

Route ID	Run ID	Route Properties							Measured FE and Emissions		
		AvSpeed (mph)	StdSpeed (mph)	AvPosAcc (mph/s)	ChPower (W/kg)	AvPosRLP (kW)	StdRLP (kW)	AvClimbRate (m/s)	FE (mpg)	CO_2 (g/s)	NOx (g/s)
Sab2SW	1	46.44	25.32	0.22	3.80	206.0	347.6	0.33	4.45	29.24	0.32
	2	46.36	23.57	0.23	3.90	208.5	357.7	0.32	4.28	30.35	0.32
	3	41.05	26.57	0.19	3.28	175.2	318.4	0.28	4.72	24.38	0.26
	4	47.48	21.29	0.24	3.91	208.4	349.2	0.33	4.13	32.18	0.26
	5	48.78	21.65	0.23	3.81	208.2	333.2	0.34	4.60	29.68	0.37
Average		***46.02***	***23.68***	***0.22***	***3.74***	***201.3***	***341.2***	***0.32***	***4.44***	***29.17***	***0.31***
Std. Dev.		***2.95***	***2.28***	***0.02***	***0.26***	***14.6***	***15.5***	***0.03***	***0.24***	***2.90***	***0.05***
COV (%)		***6.41***	***9.64***	***8.81***	***6.98***	***7.26***	***4.54***	***8.01***	***5.32***	***9.95***	***15.12***

Table 12 Variability of calculated properties SW2Sab route

Route ID	Run ID	Route Properties							Measured FE and Emissions		
		AvSpeed (mph)	StdSpeed (mph)	AvPosAcc (mph/s)	ChPower (W/kg)	AvPosRLP (kW)	StdRLP (kW)	AvClimbRate (m/s)	FE (mpg)	CO_2 (g/s)	NOx (g/s)
SW2Sab	1	48.08	24.48	0.22	3.29	186.7	318.8	0.30	4.90	27.48	0.32
	2	49.90	22.61	0.21	3.32	189.9	313.4	0.31	4.93	28.33	0.35
	3	49.82	23.52	0.22	3.41	192.9	321.2	0.31	5.04	27.67	0.35
	4	47.83	22.44	0.24	3.21	181.7	304.8	0.29	4.70	28.53	0.30
	5	48.00	22.68	0.22	3.05	175.2	291.9	0.29	4.80	28.01	0.32
Average		***48.73***	***23.14***	***0.22***	***3.26***	***185.3***	***310.0***	***0.30***	***4.87***	***28.00***	***0.32***
Std. Dev.		***1.04***	***0.86***	***0.01***	***0.14***	***7.01***	***11.95***	***0.01***	***0.13***	***0.44***	***0.02***
COV (%)		***2.14***	***3.69***	***5.16***	***4.21***	***3.78***	***3.86***	***3.58***	***2.72***	***1.56***	***6.95***

4.3 Sensitivity Analysis

An essential step when developing a modeling methodology is to analyze the model sensitivity to variations in input parameters. A sensitivity analysis provides insight into the internal function of a

model and helps to develop understanding and intuition on how the variation of the input parameters propagates through the model.

The input parameters to the model may be divided into three groups: (1) emissions (or fuel consumption) measurements over the baseline cycles, (2) cycle's properties for the unseen cycle, and (3) cycle's properties for baseline cycles. There are many ways to do sensitivity analyses. An analytical sensitivity analysis based on partial derivative was done for the inputs of groups (1) and (2) because those terms appear explicitly in equations 21 and 22. For group (3), the input-output is somewhat more complicated so an empirical sensitivity analysis was conducted for a "typical" model.

4.3.1 Sensitivity to Emissions Measurements and Unseen Cycle Properties

The model output can be written mathematically in two equivalent ways. Equations 21 and 22 represent the model for the case of prediction of fuel consumption (FC) using three baseline cycles. Equation 21 shows the relationship between model output (predicted FC) and the inputs of measured FC. On the other hand, Equation 22 shows the relationship between model output (predicted FC) and the inputs of baseline cycles' (or routes') properties. The equations are equivalent and are just two different ways of representing the model (the equation of the plane defined by the three baseline cycles).

$$FC_{unseen} = w_1 \cdot FC_1 + w_2 \cdot FC_2 + w_3 \cdot FC_3 \quad (21)$$

$$FC_{unseen} = A \cdot P_1 + B \cdot P_2 + C \quad (22)$$

Sensitivity functions for the model can be defined in terms of partial derivatives. The absolute-sensitivity of the function F to variations in the parameter x is given by Equation 23 (Smith et al., 2008).

$$S_x^F = \frac{\partial F}{\partial x} \quad (23)$$

The relative-sensitivity of the function F to variations in the parameter x is defined by Equation 24 (Smith et al., 2008).

$$\bar{S}_x^F = \left| \frac{\Delta F/F}{\Delta x/x} \right| \quad (24)$$

The sensitivity functions are used to calculate changes in the output due to changes in the inputs or model parameters. They are useful to compare the effects that different parameters have on the output of the model. The absolute sensitivity functions show the most important parameters for a fixed size change in the parameters, while the relative-sensitivity functions show the most important parameters for a certain percent change in the parameters (if the relative-sensitivity function has a value of 10, that means that 1% change in the input parameter produces a 10% change in the output of the model).

For the model under study the absolute sensitivity functions for the measured FC (Equations 25, 26, and 27), and for the unseen cycle properties (Equations 28 and 29) are calculated from Equations 21 and 22, respectively. The analytic sensitivity functions for the measured fuel consumptions and the unseen cycle properties are constants so the sensitivities to changes on these parameters do not depend on the variability of other input parameters. Note that the linear interpolation methodology produces a different model for each attempted (unseen cycle) prediction, and therefore these constants will be different for each prediction made.

$$\frac{\partial FC_{unseen}}{\partial FC_1} = w_1 \tag{25}$$

$$\frac{\partial FC_{unseen}}{\partial FC_2} = w_2 \tag{26}$$

$$\frac{\partial FC_{unseen}}{\partial FC_3} = w_3 \tag{27}$$

$$\frac{\partial FC_{unseen}}{\partial P_1} = A \tag{28}$$

$$\frac{\partial FC_{unseen}}{\partial P_2} = B \tag{29}$$

Because of the linear nature of the model (a plane in this case), the partial derivatives at each point will remain constant regardless of where the point is in the surface. Variations in emission measurements and input properties will affect the outcome of the model in a linear fashion. For example, if fuel consumption for all the baseline cycles varies by 10%, the unseen cycle predicted fuel consumption will

also vary by 10%. If the level of variation is different for each baseline cycle, the expected variation will depend on the relative weights of the baseline activity but its value will never surpass the level of variation of the most variable measurement.

4.3.2 Sensitivity to Baseline Cycle Properties

Variations in properties of the baseline cycle values will affect the calculation of the weight coefficients of the baseline cycles. At the same time, the changes to the weight coefficients are going to affect the output of the model (predicted FC for the unseen cycle). Due to the fact that the equations describing the input-output relationship in this case are complicated (for this specific example there are three equations and three unknowns) a static sensitivity test was applied where a ±10% variation was applied to the property values and the change in predicted values was calculated and analyzed. A "typical" case was selected for illustration purposes. One should have in mind that the methodology produces a different model per each attempted prediction. The weight coefficients will vary for each prediction and performing an individual sensitivity analysis for each model will prove cumbersome.

Vehicle J (see Section 5.2.1, Table 16) was selected for this part of the study. A model was generated using three baseline routes (Idle, WashPA2, and WashPA3) and two route properties (standard deviation of speed, and average positive road load power). CO_2 mass rate emissions for five different routes were predicted. Baseline properties were varied +/-10% one metric at a time. The sensitivity analysis results for this "typical" model are summarized in Table 13. It can be seen that the sensitivity factors (SF) varied from 0.15 to 0.85. The model seems to be more sensitive to road load power (SF from 0.64 to 0.85) than to standard deviation of speed (SF between 0.15 and 0.24). Individual prediction errors varied from 1.69% to 8.82% for the different cases. Weight coefficient values showed more sensitivity varying from 7% to 148%. Note that if all the metrics (baseline and unseen) were varied the model would have produced the same results (being a linear model, the new system of equations would be the same as the original system multiplied by some factor). The use of relative-sensitivity functions in this case allows a comparison of parameters' changes on model outputs because they are dimensionless normalized functions. One drawback of using the partial derivative to quantify the influence of an input parameter is that the partial derivative is influenced by the units of measurement of the parameter.

Table 13 Static sensitivity analysis for a "typical" case

	Variation (%)		Weight coefficients			Unseen Route	CO_2 mass rate (g/s)		Error (%)	SF
	StdSpeed	AvPosRLP	w_1	w_2	w_3		Measured	Predicted		
Base Case	0	0	0.15	0.58	0.27	WashPA1	23.3	21.4	-8.3	0
	0	0	-0.07	0.82	0.25	BM2Sab	27.0	25.3	-6.2	0
	0	0	-0.14	0.32	0.82	Sab2BM	39.0	33.3	-14.7	0
	0	0	-0.24	0.40	0.83	Sab2SW	34.6	35.2	1.8	0
	0	0	-0.16	0.38	0.79	SW2Sab	32.1	33.3	3.7	0
Varying standard deviation of speed	10	0	0.22	0.44	0.34	WashPA1	23.3	21.0	-10.0	0.19
	10	0	0.01	0.64	0.34	BM2Sab	27.0	24.8	-8.1	0.20
	10	0	-0.06	0.14	0.92	Sab2BM	39.0	32.8	-16.0	0.15
	10	0	-0.14	0.20	0.94	Sab2SW	34.6	34.6	0.2	0.16
	10	0	-0.08	0.19	0.89	SW2Sab	32.1	32.7	2.1	0.16
	-10	0	0.07	0.76	0.17	WashPA1	23.3	21.9	-6.2	0.23
	-10	0	-0.17	1.05	0.13	BM2Sab	27.0	26.0	-3.9	0.24
	-10	0	-0.25	0.55	0.70	Sab2BM	39.0	33.9	-13.1	0.19
	-10	0	-0.35	0.65	0.70	Sab2SW	34.6	35.9	3.7	0.19
	-10	0	-0.27	0.61	0.66	SW2Sab	32.1	33.9	5.7	0.19
Varying average positive road load power	0	10	0.16	0.67	0.17	WashPA1	23.3	20.0	-14.1	0.64
	0	10	-0.06	0.93	0.13	BM2Sab	27.0	23.7	-12.2	0.64
	0	10	-0.13	0.48	0.65	Sab2BM	39.0	31.0	-20.7	0.70
	0	10	-0.22	0.57	0.65	Sab2SW	34.6	32.7	-5.3	0.70
	0	10	-0.14	0.53	0.61	SW2Sab	32.1	30.9	-3.5	0.70
	0	-10	0.14	0.47	0.39	WashPA1	23.3	23.0	-1.1	0.78
	0	-10	-0.09	0.69	0.39	BM2Sab	27.0	27.3	1.1	0.78
	0	-10	-0.17	0.14	1.03	Sab2BM	39.0	36.1	-7.4	0.85
	0	-10	-0.26	0.20	1.06	Sab2SW	34.6	38.2	10.5	0.85
	0	-10	-0.19	0.19	1.00	SW2Sab	32.1	36.1	12.5	0.85

5 Methodology

This chapter describes the data sources, the properties used, and the approach followed to find the most suitable model parameters (properties and baseline cycles) for translation of fuel consumption and NOx emissions between different types of vehicle activity.

Two main data sources were selected and employed in this study. The first data set is representative of measurements performed with a chassis dynamometer. The second data set is representative of in-use measurements performed with PEMS units. The criterion for selection of these data sources was the availability of measurements of fuel consumption and emissions over sufficiently diverse driving activity. Acknowledgement is given to the engineers, staff, faculty, and graduate students that were associated with the testing campaigns within the Center for Alternative Fuels, Engines, and Emissions (CAFEE) within WVU.

5.1 Chassis Dynamometer Data

The linear interpolation method was applied to previously published data gathered using the WVU heavy-duty chassis dynamometer. The data were available from the Washington Metropolitan Area Transit Authority (WMATA) emission testing program[32] (Melendez et al 2005; Wayne et al 2008). Note that preliminary chassis dynamometer modeling was documented in published studies (Taylor et al., 2004; Clark et al., 2010; and Delgado et al., 2012) for on-road Class 8 tractors using data from the CRC E55/E59 program and provided the foundation for the start of this work. This study used the CRC E55/E59 data to estimate test-to-test variability of chassis dynamometer (Section 4.2.1). However, the WMATA data was preferred over the CRC data for method development due to the availability of a more diverse set of test cycles.

5.1.1 Vehicles Used

Chassis dynamometer data from two diesel buses, two lean-burn spark-ignited compressed natural gas buses, and one hybrid-electric diesel bus tested over sixteen or seventeen different driving cycles were used. The buses were tested at a simulated inertia weight representing the empty vehicle curb weight

[32] The US DOE and the US DOT sponsored the WVU CAFEE to conduct the program in cooperation with WMATA.

plus one half of the maximum passenger load[33]. Table 14 provides information on the buses. Note that different aftertreatment devices were used. The two CNG buses were equipped with catalytic converters, the diesel hybrid had an Engelhard DPX particulate filter, the DDC diesel engine had a Johnson-Matthey Catalyzed Continuously Regenerating Technology (CCRT) particulate system, and the Cummins diesel engine had a catalytic converter.

Table 14 Transit buses analyzed in this study

Bus ID	Technology	Manufacturer	Bus Type & MY	Engine Type & MY	Aftertreatment	GVW (kg)	Available Cycles
32	CNG	John Deere	Orion 2005	RG6081 2005	Catalytic converter	19,334	16
35	CNG	Cummins	Orion 2005	Cummins CG280 2005	Catalytic converter	19,334	16
37	Hybrid	Allison	New Flyer 2005	Cummins ISL280 2005	Engelhard DPX	18,416	16
39	Diesel	DDC	Orion 1992	DDC S50 2003	Johnson-Matthey CCRT	17,896	17
41	Diesel	Cummins	New Flyer 2006	Cummins ISM280 2006	Catalytic converter	18,416	17

Bus emissions were characterized with WVUs Transportable Heavy-Duty Vehicle Emissions Testing Laboratory (Translab). The Translab consisted of a chassis dynamometer, an emissions analyzer trailer, and a mobile workshop to support them. Detailed description of the Translab can be found elsewhere (Clark et al., 1995).

5.1.2 Cycles Used

The seventeen available chassis dynamometer cycles are listed in Table 15. Some cycles are representative of typical transit bus operation in different metropolitan areas. Average velocities ranged from 0 mph (Idle cycle) to about 44 mph for the Commuter cycle. Average positive acceleration is included as a measure of transient behavior or "aggressiveness" of the cycle and it ranges from 0 mph/s to about 0.5mph/s. Speed-time traces of these cycles, as well as average values of their properties are

[33] Between 34,555lbs and 37,076lbs.

provided in Appendix B. Additional information about the cycles can be found elsewhere (Wayne et al., 2004; Wayne et al., 2008).

Table 15 Average measured properties for five buses over chassis dynamometer cycles

No	Cycle Name	Cycle ID	Average Velocity (mph)	Av. Positive Acceleration (mph/s)	Stops per Distance (stops/mile)
1	CARB Idle Cycle	Idle	0.00	0.00	0.00
2	New York Bus Cycle	NYBus	3.54	0.25	18.71
3	Paris Bus Cycle (ADEME-RATP)	PARIS	6.68	0.32	12.40
4	Manhattan Bus Cycle	Manhattan	6.86	0.37	9.76
5	Washington Metro Transit Authority Cycle	WMATA	8.43	0.30	6.26
6	New York Composite Cycle	NY-Comp	8.75	0.15	7.21
7	Orange County Transit Authority Cycle	OCTA	12.22	0.41	4.87
8	Central Business District Cycle	CBD	13.08	0.52	6.80
9	Braunschweig City Bus Cycle	BRAUN	13.88	0.45	4.19
10	City Suburban Heavy Vehicle Cycle	CSHVC	14.02	0.27	2.29
11	Beeline Cycle (WCDOT)	Beeline	14.03	0.43	3.73
12	European Transient Cycle Urban	ETCURBAN	14.11	0.28	1.92
13	CARB Transient Cycle	TRANS	15.33	0.28	1.69
14	HD Urban Dynamometer Driving Schedule	UDDS	18.71	0.20	2.04
15	King County Metro Bus Cycle (w/o grade)	KCM	23.35	0.41	1.85
16	Arterial Cycle	ART	25.58	0.55	1.47
17	Commuter Cycle	COMM	44.37	0.18	0.17

5.2 In-use Data

In-use emissions measurements collected using PEMS represent real world conditions more accurately than chassis dynamometer or engine dynamometer testing, arguably being the most realistic method to determine exhaust emissions over a certain driving route. However, both the route followed and the traffic situation that the vehicle encounters will influence measured emissions and fuel consumption. In addition to the data obtained by chassis dynamometer testing using the transportable laboratory, data

obtained with WVU MEMS was also employed in the development and validation of the modeling methodology for this study.

5.2.1 Vehicles Used

In-use data for eighteen over-the-road heavy-duty trucks with GVWR of 80,000 lbs were selected for this study. Engine displacement ranged between 10.8 L to 14.6 L. The trucks were driven over up to eight predefined routes consisting of city, suburban, and highway driving. Additional information about the vehicles and engines is given in Table 16. Note that all of the vehicles used in the in-use model development had engines with no specific emissions control devices such as exhaust gas recirculation (EGR), variable geometry turbochargers, or exhaust aftertreatment.

Table 16 Vehicles and engine data used in model development and validation

Veh. ID	Veh. Manuf.	Veh. Model Year	Engine Model Year	Test Weight (lb)	Odometer (miles)
A	Peterbilt	1996	1996	77940	3872427
B	Kenworth	1997	1996	77520	484619
C	Freightliner	1995	1995	79060	600877
D	Kenworth	1998	1998	79040	452680
E	Peterbilt	1996	1996	78060	332150
F	Freightliner	1995	1995	78120	12029
G	Navistar	1995	1995	78960	666088
H	Peterbilt	1999	1998	77900	378311
I	Kenworth	1998	1998	79520	478751
J	Peterbilt	1998	1998	78900	554404
K	Peterbilt	1998	1998	77900	476764
L	International	1999	1998	79180	598165
M	International	1998	1997	77960	625372
N	Volvo	1997	1997	76980	445332
O	Peterbilt	1997	1997	76860	482358
P	Freightliner	1999	1998	78680	176566
Q	Navistar	1996	1996	79480	519795
R	Navistar	1998	1998	78300	507857

The data was gathered with WVU's MEMS. The MEMS consisted of an exhaust gas sample conditioning system and emissions gas analyzers for NO_X and CO_2 concentrations, a data acquisition system, an exhaust flow-rate measurement device, ECU interface hardware, ambient condition sensors and a global positioning system (GPS) receiver. Emissions results were reported in time-specific (g/s), distance-specific (g/mi or g/km), and brake-specific (g/kW-hr) units. Figure 20 shows a schematic of the MEMS

setup (Shade, 2000). Additional details regarding the MEMS test equipment may be found elsewhere (Gautam et al., 2000a; Gautam et al. 2000b; Gautam et al. 2001)).

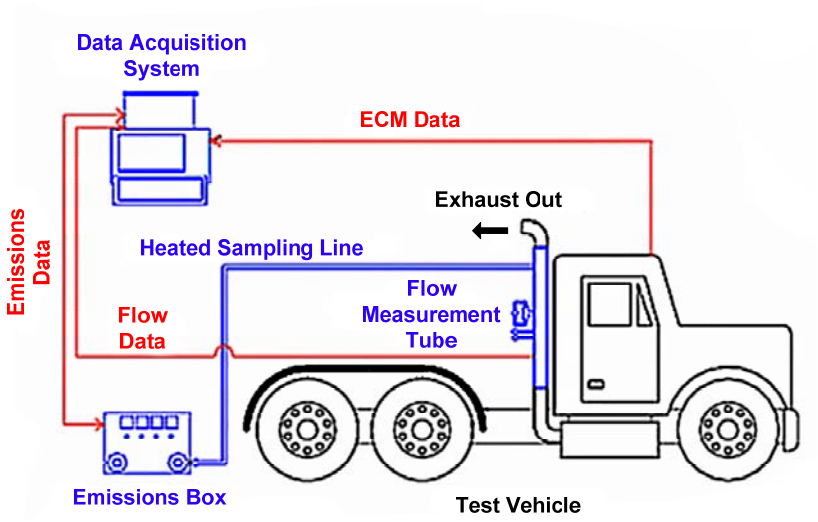

Figure 20 Schematic of MEMS (Shade, 2000)

5.2.2 Routes Used

Eight routes were considered for this study. The routes were developed during Phase II of the "Consent Decree" project. The short description of each route provided by Gautam et al. (Gautam et al. 2000b) is reproduced below.

Saltwell Route:

This route was split into outbound (Sab2SW) and return (SW2Sab) journeys. The route originated at the WVU Sabraton facility located in Morgantown, WV, close to an entrance ramp accessing I-68 west. The route proceeded to I-79, and followed I-79 south to the turnaround point at the I-79 Saltwell Rd. exit near Clarksburg, WV. The total distance was 58.7 miles (94.5 km). The interstate was posted at 70 mph (113 km/h), but there were two curves with advisory signs below that speed. The maximum variation in altitude was encountered during the route was about 500 ft (152 m) over a distance of 5 miles (8 km).

Bruceton Mills Route:

This route was also divided into outbound (Sab2BM) and return (BM2Sab) journeys. The route originated at the WVU Sabraton facility close to entrance ramp on I-68 east, and continued on I-68 where a climb of a sustained 5% grade existed, followed by transient road grades to the turnaround point at Bruceton Mills, WV. The total distance was 39.7 miles. The interstate was posted at 70 mph (113 km/h), but the 5% descent on the return journey was posted at 50 mph (80 km/h) for trucks and was preceded by a mandatory truck stop for checking brakes. In the high speed freeway operation, dramatic reductions in vehicle speed were encountered as the vehicle climbed the hills along the route. In the case of this route, truck speed restrictions and necessary precautions during the steep descent on the return leg of the journey reduced the operating speed on I-68 westbound. These two routes have a significant hill climb during each route and provided sustained (>10 minutes) high power emissions data.

Washington/Pittsburgh Route:

This route originated in Washington, PA, which is located near the intersection of I-70 and I-79. The route proceeded from Washington on US Rte. 19 north through suburban areas toward Pittsburgh, followed PA State Rte. 51 (US truck Rte. 19) to I-279 south, to I-79 south, and then returned to the first rest area in West Virginia along this interstate. The route was divided into three legs. The first leg (WashPA1) and second leg (WashPA2) proceed through suburban roads with speed limits between 25 mph to 45 mph (40 km/h to 72 km/h), and interstate portions with 55mph (89 km/h) speed limit. The final leg (WashPA3) consisted of all highway driving with a transition from 55 mph to 65 mph (89 km/h to 105 km/h).

Idle Data:

Based on the recommendations of previous research (Delgado et al., 2012), idle emissions should be used in the model. With this in mind, CO_2 and NOx emissions from the idle (stationary) portions of the aforementioned routes were extracted from the in-use data to develop the “Idle route.” This route was used as a baseline route in the modeling approach. Idle information is of key importance in this kind of modeling because it represents the lower boundary of vehicle activity and generally the lowest mass rate emissions.

Speed-time traces, altitude-time traces, and average property values for these routes are presented in Appendix C. A summary of the routes and some representative properties is provided in Table 17. Values of properties were averaged over 18 vehicles. The table is sorted in terms of increasing average speed. WashPA1 and WashPA2 routes have the lowest average speed because a significant amount of the route goes through city and suburban driving with low posted speed limits. Sab2BM and BM2Sab routes have relatively low average vehicle speeds (due to low speed hill descent and long hill ascents) even though posted speed limit is 70 mph (113 km/h) for a large portion of these routes. The hill climbs of these routes place a significant load on the vehicle's engine. Note the strong difference in characteristic power between Sab2BM (general uphill driving) and BM2Sab (general downhill driving). Hill ascents produce higher distance-specific emission levels than hill descents because of the increased emissions produced while travelling uphill which are not necessarily fully compensated by a corresponding reduction in emissions when travelling downhill. The BM2Sab route had a slightly lower average vehicle speed than the Sab2BM due to the difference in elevation change between these two routes. The Sab2SW and SW2Sab were also highway routes with a majority of the posted speed limit at 70 mph (113 km/h). However, these two routes had rolling hills with less duration of hill climbs than the Bruceton Mills routes. Note that the average positive acceleration has different units in this table as compared to the data presented in Table 15. The model is insensitive to the units as long as consistent units are used for a given vehicle analysis.

Table 17 Routes and representative properties

Route Name	Distance (km)	Average Speed (km/h)	Average Positive Acceleration (m/s^2)	Characteristic Power (m^2/s^3)
Idle	0	0	0	0
WashPA2	36.9	41.7	0.25	0.52
WashPA1	19.3	42.0	0.27	0.57
BM2Sab	31.9	57.3	0.22	0.47
Sab2BM	32.5	57.9	0.20	0.70
Sab2SW	46.8	75.5	0.24	0.46
SW2Sab	47.2	77.4	0.23	0.41
WashPA3	82.9	83.5	0.15	0.36

5.3 Properties Used

Different combinations of properties may be used to describe vehicle activity in the model. Delgado et al. applied the method to chassis dynamometer data for heavy-duty trucks (Delgado et al., 2012) and transit buses (Delgado et al., 2011a), and recommended the use of average speed and average positive acceleration as properties. One of the purposes of this study was to investigate an extended set of metrics including grade-related metrics and road load-related metrics. Properties such as average velocity and average positive acceleration (Equations 30 and 31, respectively) depend only on the speed-time trace. However, PEMS provides altitude data that can be used to calculate road grade. Road grade related properties may be used within the modeling methodology to account for the "hilliness" of the route. For example, Delgado et al. (Delgado et al., 2011b) derived a property named "characteristic power" (Equation 32) that represents the positive mechanical energy supplied per unit mass per unit time to accelerate and/or raise the vehicle.

$$AvSpeed = \bar{v} = \frac{1}{T}\int v_i\, dt \approx \frac{x}{T} \text{ [mph]} \quad (30)$$

$$AbsPosAcc = \overline{a_+} = \frac{1}{T}\int a_+ dt \approx \frac{\sum a_{i,a>0}}{n} \text{ [mph/s]} \quad (31)$$

$$ChPow = \frac{1}{T}\sum_{i=2}^{N}\left[\frac{1}{2}\left(V_i^2 - V_{i-1}^2\right) + g(h_i - h_{i-1})\right]^+ \text{ [m}^2\text{/s}^3\text{ or W/kg]} \quad (32)$$

Cycle and route properties help quantify a particular vehicle activity through capturing the main features of the recorded speed-time, and in some cases, speed-altitude-time profiles. A literature review was conducted to select a set of candidate properties that may be used to translate fuel consumption and NOx emissions between driving cycles or in-use routes. Initially, a set of 74 properties was considered. Table 18 presents a summary of the properties. A classification framework of the variables is also provided using eight different groups: speed related metrics, acceleration related metrics, variation of acceleration, driving mode, power demand, variation of power, grade related metrics and other. This classification is somewhat arbitrary because some metrics could pertain to two different groups. For example, average of speed to the second power and standard deviation of speed carry essentially the same information but they are classified in two different groups. Most of the variables in Table 18 are self explanatory. However, detailed equations for calculation of properties are provided in Appendix A.

Table 18 Properties used in this study

		Property Name	Units	Abbreviation
Speed related	1	Average speed	mph	AvSpeed
	2	Average driving speed	mph	AvDriSpeed
	3	Relative positive speed	none	RPS
	4	Relative square speed	m/s	RSS
	5	Relative positive square speed	m/s	RPSS
	6	Relative cubic speed	m^2/s^2	RCS
	7	Relative positive cubic speed	m^2/s^2	RPCS
	8	Average of speed to the 1.5 power	$mph^{1.5}$	$AvSpeed^{1.5}$
	9	Average of speed to the 2 power	mph^2	$AvSpeed^2$
	10	Average of speed to the 2.5 power	$mph^{2.5}$	$AvSpeed^{2.5}$
	11	Average of speed to the 3 power	mph^3	$AvSpeed^3$
	12	Average of speed to the 3.5 power	$mph^{3.5}$	$AvSpeed^{3.5}$
	13	Average of speed to the 4 power	mph^4	$AvSpeed^4$
Acceleration related	14	Standard deviation speed	mph	StdSpeed
	15	Coefficient of variation speed	%	CovSpeed
	16	Interquartile range speed	mph	IqrSpeed
	17	Root mean square speed	mph	RmsSpeed
	18	Standard deviation driving speed	mph	StdDriSpeed
	19	Coefficient of variation driving speed	%	CovDriSpeed
	20	Average acceleration	mph/s	AvAcc
	21	Average positive acceleration	mph/s	AvPosAcc
	22	Average negative acceleration	mph/s	AvNegAcc
	23	Average acceleration squared	mph^2/s^2	$AvAcc^2$
	24	Indicator factor	s^{-1}	IF
Variation of Acceleration	25	Standard deviation acceleration	mph/s	StdAcc
	26	Interquartile range acceleration	mph/s	IqrAcc
	27	Root mean square acceleration	mph/s	RmsAcc
	28	Standard deviation positive acceleration	mph/s	StdPosAcc
	29	Coefficient of variation positive acceleration	%	CovPosAcc
	30	Standard deviation negative acceleration	mph/s	StdNegAcc
	31	Coefficient of variation negative acceleration	mph/s	CovNegAcc
	32	Jerk	mph/s^2	Jerk
	33	Number of accelerations per unit distance	$mile^{-1}$	FreqAccD
	34	Number of accelerations per unit time	s^{-1}	FreqAccT
Driving mode	35	Percent time at idle	%	PercIdle
	36	Percent time accelerating	%	PercAcc
	37	Percent time decelerating	%	PercDecel
	38	Kinetic intensity	km^{-1}	KI

		Property Name	Units	Abbreviation
	39	Number of stops per unit distance	$mile^{-1}$	FreqStopsD
Power demand	40	Relative positive acceleration	m/s^2	RPA
	41	Inertial power surrogate	m^2/s^3	IPS
	42	Positive kinetic energy	m/s^2	PKE
	43	Inertial power	kW	InePow
	44	Rolling resistance power	kW	RolPow
	45	Drag power surrogate	m^3/s^4	DPS
	46	Aerodynamic resistance power	kW	AeroPow
	47	Aerodynamic and rolling resistance power	kW	AeroRolPow
	48	Characteristic acceleration	m/s^2	ChAcc
	49	Characteristic power	m^2/s^3 or W/kg	ChPower
	50	Characteristic energy	m^2/s^2 or J/kg	ChEnergy
	51	Average positive road load power	kW	AvPosRLP
	52	Average positive vehicle specific power	W/kg	AvPosVSP
	53	Petrushov power	kW	AvPet
Variation of power	54	Standard deviation road load power	kW	StdRLP
	55	Coeficcient of variation road load power	%	CovRLP
	56	Time derivative of road load power	W/s	dRLP/dt
	57	Standard deviation inertial power	kW	StdInePow
	58	Coefficient of variation inertial power	%	CovInePow
Grade related	59	Average positive grade	%	AvPosGrade
	60	Average negative grade	%	AvNegGrade
	61	Average climb rate	m/s	AvClimbRate
	62	Average grade	%	AvGrade
	63	Standard deviation grade	%	StdGrade
	64	Average ascent	%	AvAsc
	65	Average descent	%	AvDes
	66	Altitude change per distance	%	AltDistance
	67	Grade power	kW	GradePow
Other	68	Average of (acceleration * $speed^3$)	m^4/s^5	Acc^1Speed^3
	69	Average of ($acceleration^2$ * speed)	m^3/s^5	Acc^2Speed^1
	70	Average of ($acceleration^2$ * $speed^2$)	m^4/s^6	Acc^2Speed^2
	71	Average of ($acceleration^2$ * $speed^3$)	m^5/s^7	$Accel^2Speed^3$
	72	Average of ($acceleration^3$ * speed)	m^4/s^7	Acc^3Speed^1
	73	Average of ($acceleration^3$ * $speed^2$)	m^5/s^8	Acc^3Speed^2
	74	Average of ($acceleration^3$ * $speed^3$)	m^6/s^9	Acc^3Speed^3

A computer application was generated in MATLAB to calculate the selected properties. The software was designed to read a file containing time-speed-altitude information as input. The program applies

smoothing functions[34] to speed-time traces before calculation of acceleration values, and to altitude-distance traces before calculation of grade. The time resolution of the input file can vary and the calculation of some metrics can be sensitive to such differences. Consistency is important in order to be able to compare different cycles and the same time resolution has been used. For each vehicle considered the data used in model development (route properties, route average CO_2 (g/s), and route average NOx (g/s)) was an average of measured data from available emissions test runs.

5.3.1 Speed Related Metrics

As discussed previously, vehicle speed is a fundamental parameter to describe vehicle activity. This category includes properties that are calculated solely by using time-speed values. Average speed is a robust indicator of the type of activity exhibited during a given cycle. A low average speed can represent a very transient cycle, similar to what is expected in city traffic, while a high average speed can represent a more steady behavior, similar to what is expected in highway driving.

Average driving speed excludes the segments in which the vehicle is stationary (it can be calculated based on the values of average speed and percent idle). Relative positive speed (RPS), relative square speed (RSS), and relative positive square speed (RPSS) are parameters related to rolling resistance (Smit et al., 2006). Relative cubic speed (RCS) and relative positive cubic speed (RPCS) are parameters related to aerodynamic resistance (Smit et al., 2006). RCS is related to aerodynamic speed (O'Keefe et al., 2007), a property defined as the square root of the ratio of average cubic speed to average speed that is linked to the impact of aerodynamic resistance on vehicle fuel usage. Simpson (2005) suggested that average speed, aerodynamic speed and characteristic acceleration form an orthogonal and independent coordinate set that quantifies the multiple dimensions of a driving cycle.

[34] A Savitzky-Golay smoothing filter was used and is a generalized moving average. The method essentially performs a local polynomial regression of degree k (user selected) on a series of values of at least k+1 points which are treated as being equally spaced in the series to determine the smoothed value for each point. The main advantage of this approach is that it reduces the distortion of essential features of the data like peak heights and width, which are usually "flattened" by other techniques (like moving averages), while the efficiency of the suppression of random noise is effectively unchanged.

Rolling resistance force is proportional to speed, aerodynamic drag force and rolling resistance power are proportional to squared speed, and aerodynamic resistance power is proportional to cubed speed. In order to explore all these factors, average speeds to the n power when n equals 1.5 to 4 in 0.5 increments were also explored and included in this category.

5.3.2 Acceleration Related Metrics

For the same average speed, one can observe widely different instantaneous speed and acceleration profiles, each resulting in different fuel consumption and emission levels. Transient vehicle operation (duration and magnitude of acceleration/deceleration events) implies transient engine operation, and for engines with cooled EGR, emissions and fuel efficiency may be affected by the degree of transient behavior, even at the same instantaneous power level (Delgado et al, 2011a).

Acceleration-related metrics such as standard deviation of speed, interquartile range[35] of speed, or average positive acceleration are used to quantify the magnitude of transient behavior. Accelerations were calculated from speed-time traces using a central differences scheme after smoothing of the speed-time trace. The only metric in this category which name is not self explanatory is the indicator factor. Zervas and Bikas (2008) analyzed the impact of driving cycle on NOx and PM for light-duty diesel vehicles and found a cycle property (indicator factor) that normalizes the acceleration events by their corresponding average speeds. They found that indicator factor showed better correlation with emissions than average velocity.

5.3.3 Metrics Quantifying Variation in Acceleration

This category includes various statistical parameters that quantify the frequency of changes in acceleration during driving activity. These metrics are not directly linked to the road load equation but were included in this study because they also quantify transient behaviour and the severity of vehicle activity. These metrics can provide additional information to the model. For example, a given value of

[35] The interquartile (IQR) range is a measure of statistical dispersion. Unlike total range, IQR is a robust statistic and is preferred to the total range. It represents the distance between the 25th percentile and the 75th percentile being essentially the range of the middle 50% of the data. Because it uses the middle 50%, it is not affected by outliers or extreme values.

standard deviation of speed can be higher for a speed profile with one large speed change compared to a speed profile with several small changes.

Frequencies of acceleration metrics were also included in this category. The number of accelerations greater than 2mph/s[36] was used to calculate frequency of accelerations per unit time and per unit distance.

5.3.4 Driving Mode Metrics

This category includes metrics that quantify the amount of time expended in a certain driving mode. Any data point with velocity below a threshold of 0.5mph was considered to be an idle event to account for possible noise in the velocity data. The same threshold was used for the calculation of number of stops per unit distance[37].

Kinetic Intensity (KI) is defined as the ratio between characteristic acceleration and aerodynamic speed. It measures the fractions of energy availability for regeneration. This is important to quantify potential fuel economy improvements for hybrid vehicles (O'Keefe et al., 2007). KI can be useful to characterize cycles based on their degree of start-stop behavior. Figure 21 shows different cycles by characteristic acceleration and aerodynamic speed. The kinetic intensity is overlaid as lines in the figure. Two speed-time traces with very distinct characteristics (and KI values) are shown.

[36] Kern (2000) considered accelerations greater than 2mph/s as heavy accelerations into a binning methodology approach.

[37] Stops per distance for Idle mode was set to a value of zero by default.

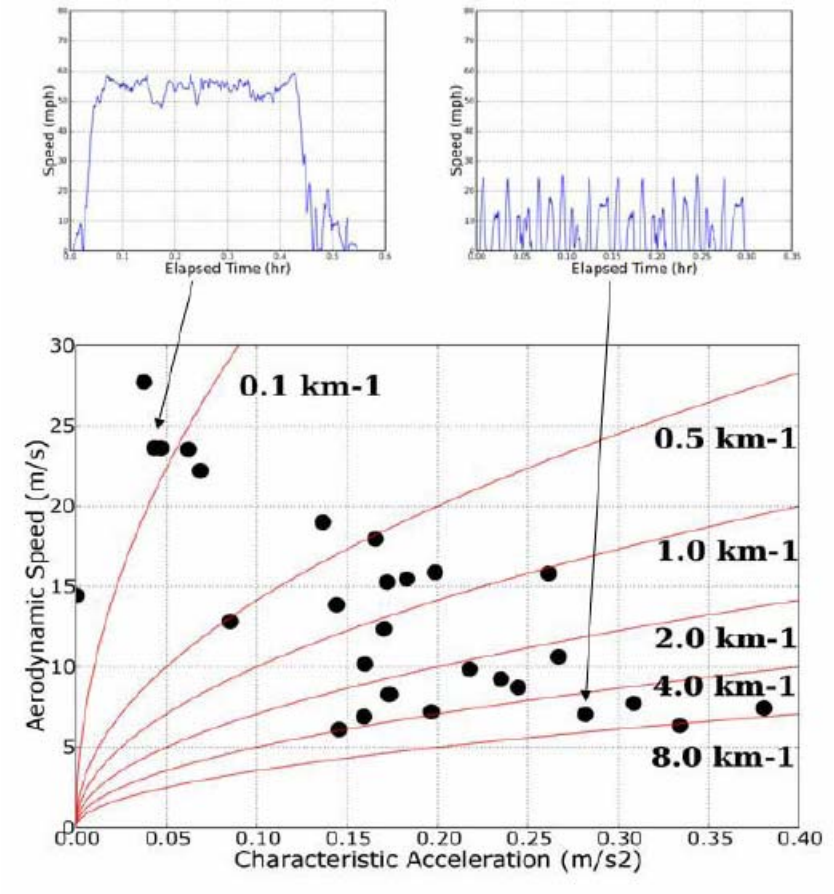

Figure 21 Cycle characterization using kinetic intensity (O'Keefe et al., 2007)

5.3.5 Power Demand Metrics

Power demand metrics are related to one or more of the components of the road load equation so they have a physical connection to energy use. Some power demand metrics require knowledge of parameters such as weight, aerodynamic drag coefficient, rolling resistance coefficient, or frontal area. Relative positive acceleration (RPA) represents the distance-averaged inertial power per unit mass (Smit et al., 2006). IPS represents the time-averaged inertial power per unit mass (Fomunung, 1999). Drag power surrogate (DPA) was defined as time-averaged product of acceleration and squared velocity (Fomunung, 1999). Positive kinetic energy (PKE) represents the change in kinetic energy per unit distance which is a measure of acceleration work required. Krishnamurthy et al. (2006) developed a modal emissions model that used this parameter as a quantitative measure to distinguish between different driving modes (acceleration, deceleration, and cruise). O'Keefe et al. (2007) derived characteristic acceleration (ChAccel). It is the integrated positive mechanical energy (kinetic and

potential energy) supplied per unit mass per unit distance. This metric measures the inertial work to accelerate and/or raise the vehicle per unit mass per unit distance over the cycle. It is the positive part of specific kinetic and potential energy per distance associated with moving the vehicle over a duty cycle. If no grade information is available, characteristic acceleration is equivalent to PKE. Delgado et al. (2011) derived characteristic power (ChPower). It is the integrated positive mechanical energy supplied per unit mass per unit time. Characteristic energy (ChEnergy) is the integrated positive mechanical energy supplied per unit mass per unit time.

Average positive road load power (AvPosRLP) has been defined and calculated here using the road load equation for an average or "generic" bus or truck (depending on the vehicle being simulated). The idea was to keep input parameters to a minimum so estimations based on "average" parameters were made for vehicle mass, rolling resistance coefficient and aerodynamic drag coefficient so as to provide a wider-ranging model parameter that could model groups of vehicles. Individual components of the road load equation were also calculated and their positive portions integrated to calculate inertial power (InePow), aerodynamic resistance power (AeroPow). Aerodynamic and rolling resistances were added to define AeroRolPow[38]. Table 19 shows the parameters for such "generic" vehicles[39].

Table 19 Road load parameters for "generic" vehicles

Parameter	Units	Truck	Bus
m	kg	25,400	16,800
C_D	-	0.79	0.79
Area	m^2	7.7	7.4
μ	-	0.008	0.008

VSP is consistently identified as an explanatory variable that is highly correlated with emissions (Zhai et al., 2008) and was also selected to be included in the model of fuel consumption and NOx emissions.

[38] AeroRolPow = AeroPow + RolPow. These two terms were combined because they only depend on velocity, not on acceleration. These metrics account for steady losses and not for transient behavior.

[39] For Class 8 trucks, the frontal areas for high, mid, and low roof were estimated to be 10.4, 7.7, and 6.9m^2, respectively. Typical C_DA values for Class 8 trucks vary from 5.1 to 7.6m^2 (US EPA and NHTSA, 2011). For the "generic" truck a value of C_DA=6.1m^2 was selected.

An equation (Eq. 33) based on empirical tractive load parameters (a, b, and c) discussed in (US EPA, 2005) and (Petrushov, 1997) was used to calculate a property that represents tractive power without including grade or inertial power. This metric was termed "Petrushov power" (AvPet). Dynamometer testing usually uses this kind of empirically determined parameters. They are determined from track coast-down tests. The "a" coefficient corresponds to the tire rolling resistance term. The "b" term tends to be small and describes higher order rolling resistance factors. The "c" term represents the aerodynamic drag coefficient terms. Table 20 lists the values of the coefficients for buses and heavy-duty trucks from (Petrushov, 1997). Comparisons made in (US EPA, 2005) revealed that the tractor-trailer numbers are about 35% smaller than those typical values reported in the US fleet.

$$Power = av + bv^2 + cv^3 \quad (33)$$

Table 20 Road load parameters (Petrushov, 1997)[40]

Parameter	Units	Trucks	Buses
a	$kW \cdot \frac{s}{m}$	$\frac{0.0661M}{2204.6}$	$\frac{0.0643M}{2204.6}$
b	$kW \cdot \frac{s^2}{m^2}$	0	0
c	$kW \cdot \frac{s^3}{m^3}$	$2.89 + \frac{4.21 \times 10^{-5} M}{2204.6}$	$3.22 + \frac{5.06 \times 10^{-5} M}{2204.6}$

5.3.6 Metrics Quantifying Variation in Power Demand

This category includes statistical parameters that quantify variation in power related metrics. The time derivative of road load power was proposed by Yanowitz et al. (Yanowitz et al, 2002) as an appropriate parameter to determine test severity in terms of rate of increase in power demand and to predict PM mass rate emissions.

[40] M is mass in tonnes.

5.3.7 Road Grade Metrics

Road gradients introduce both positive and negative power demands depending on topography. Part of the energy used to overcome positive gradients is then partially recovered during hill descents. Andrei, (Andrei, 2001) concluded that road grade has a modest but significant effect on NO_x and CO_2 emissions, especially when the road grade is greater than 2%. The effect on other pollutants such as CO and PM is more substantial because these emissions increase near full engine load.

Grade power (GradePow) represents the road grade component of the road load equation. When the calculated values of power are negative, the engine is absorbing power and it is expected that no fueling occur during these periods for a compression-ignition engine. Negative values of power were set to zero to calculate this metric. Climb rate represents the average velocity of ascent normalized by total time of the trip (Post et al., 1984).

Average positive grade (AvPosGrade) and average ascent (AvAsc) account only for the positive grade portions of driving activity. The difference between them is that AvPosGrade normalizes the data dividing by the total distance of the route, while AvAsc normalized the data dividing by distance traveled going uphill. A similar difference occurs between average negative grade (AvNegGrade) and average descent (AvDes). Figure 22 presents altitude-distance traces for two simplified routes (unrealistic grades of 100% were selected for illustrating purposes). Calculated metrics for both routes are presented in Table 21. Note that for both grades the average grade is 0% because they start and end at the same altitude.

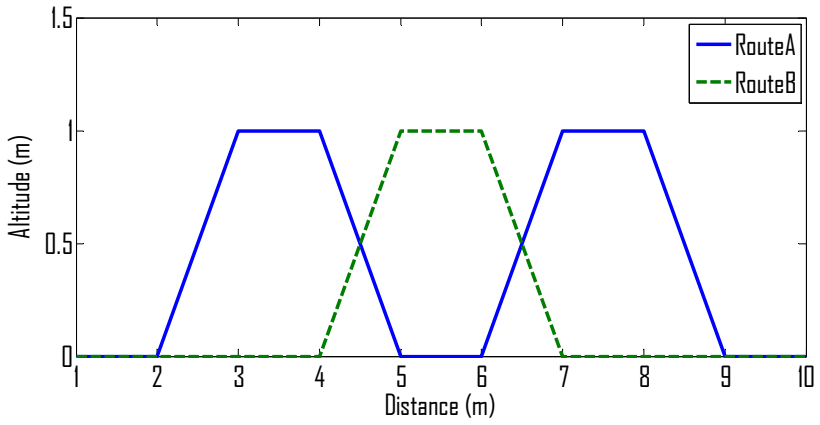

Figure 22 Altitude-distance traces for two simplified routes

Table 21 Calculated grade related metrics

Property	Route A	Route B
AvPosGrade (%)	20	10
AvAsc (%)	100	100
AvNegGrade (%)	-20	-10
AvDes (%)	-100	-100
AvGrade (%)	0	0

The chassis testing performed on WVU's chassis dynamometer uses power absorbers and inertial flywheels to provide a load to the vehicle based on the road load equation. For this equation it is assumed that there are no hills, and the load is calculated for flat, level terrain. Grade related metrics were not calculated for chassis dynamometer data. Details about road grade calculation are provided in the next section.

5.3.7.1 Road Grade Calculation

Altitude may be calculated from atmospheric pressure measurements. Equation 34 was used to determine the altitude as a function of the measured atmospheric pressure.

$$h = \frac{T_o}{L}\left(\left(\frac{P}{P_o}\right)^{-LR/g} - 1\right) \quad \text{(m)} \qquad (34)$$

In the above equation h represents the altitude, T_o represents the standard temperature, R is the universal gas constant for air, L is the standard temperature lapse rate, P_o is the standard pressure, and g represents gravitational acceleration. The derivation of Equation 34 is based on a subset of the International Standard Atmosphere (ISA) model formulated by the International Civil Aviation Organization (ICAO). The main assumptions are hydrostatic equilibrium, perfect gas, gravity independence of altitude, and constant lapse rate (PSAS, 2004). The lapse rate is defined as the rate of temperature decrease in the atmosphere with increasing altitude. The ISA assumes a constant lapse rate between 0 and 11km altitude. Table 22 shows the atmospheric parameters used in the calculation in SI units. Equation 35 displays the final equation used for calculation of altitude based on absolute pressure.

Table 22 Atmospheric parameters

Symbol	Value	Unit	Description
P_o	101325	Pa	Pressure at zero altitude (base pressure)
T_o	288.15	K	Temperature at zero altitude
g	9.80665	m/s^2	Acceleration due to gravity
L	-0.0065	K/m	Lapse rate
R	287.053	J/kg K	Gas constant for air

$$h = 44330.8 - 4946.54\, P^{0.1902632} \quad \text{(m)} \qquad (35)$$

Some of the assumptions done in the derivation of Equation 35 can affect the accuracy of altitude calculation. In the real atmosphere, significant variation is observed in base pressure, temperature, and lapse rate. Lapse rate can change, for example, when there is a temperature inversion near the ground. The perfect gas assumption is highly accurate for air; however, the behavior of a perfect gas is influenced by the constant R, which in turns depends on mean molecular weight. The composition of the lower atmosphere is approximately constant, but a very wet atmosphere may have water content high enough to appreciably lower the atmospheric density, thus changing the R value and influencing the accuracy of the calculations. Finally, the parameters chosen for ISA are based on averages near 45° latitude. The accuracy will decline near the poles or the equator.

The geometric relationships for calculation of grade are shown in Figure 23. The change in elevation ($\Delta h=h_2-h_1$) during the time interval between consecutive time steps ($\Delta t=t_2-t_1$) is calculated based on altitude data. The hypotenuse of the triangle represents the actual traveled distance (Δs). The traveled distance is determined by employing Equation 36, which is the product of vehicle speed and the time interval. The horizontal displacement (Δx) is calculated by the relationship shown in Equation 37. The road grade is then the slope of the distance traveled, whose calculation is shown as Equation 38. If the road grade (in % units) is known, Equation 39 can be used to calculate the angle of inclination.

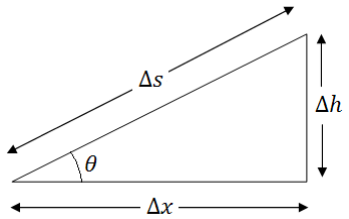

Figure 23 Diagram of relationship between distance traveled and altitude change

$$\Delta s = \bar{v} \cdot \Delta t \tag{36}$$

$$\Delta x = \sqrt{\Delta s^2 - \Delta h^2} \tag{37}$$

$$Grade\ (\%) = \frac{\Delta h}{\Delta x} \times 100 \tag{38}$$

$$\theta = \tan^{-1}\left(\frac{\Delta h}{\Delta x}\right) = \tan^{-1}\left(\frac{Grade(\%)}{100}\right) \tag{39}$$

Some instantaneous grade values resulted in completely unrealistic values, so the data was post-processed to eliminate such values replacing them with values of grade at the previous time step. Additionally, a distance-based Savitsky-golay filter was applied to reduce the noise of the calculated grade trace.

5.3.8 Other Metrics

Combination of speed and acceleration with exponentials raised up to the third power were explored. The units of these metrics suggest that assigning physical meaning to them is fraught with difficulty.

5.3.9 Equivalent Metrics

Some of the metrics in Table 18 have different definitions but produce equivalent results when used within the modeling methodology. This occurs when one metric is the result of other metric being multiplied by a constant factor. For example, IPS multiplied by vehicle mass is equivalent to InePow; AvSpeed multiplied by the factor μm (rolling resistance coefficient multiplied by vehicle mass) is equivalent to RolPow; climb rate multiplied by the factor mg (vehicle mass multiplied by acceleration of gravity) is equivalent to GradePow. Similarly, AvPosVSP, and AvPosRLP produce essentially the same

results. Note that the model is independent of the set of units being used. Converting the properties to other set of units is equivalent to multiply them by a constant factor.

5.4 Approach

The linear interpolation methodology was applied to predict fuel consumption and NOx mass rates for the following cases:

- Chassis dynamometer data
    - 2 baseline cycles
    - 3 baseline cycles
- In-use data gathered with PEMS
    - 2 baseline routes
    - 3 baseline routes

Initially, a software routine was developed to open each test file, retrieve necessary information, and calculate the 74 properties listed in Table 18. Properties requiring grade information were not calculated for chassis dynamometer data. However, properties such as characteristic power or average positive road load power, which use both speed-time trace information and altitude information, were calculated for both data sets (for chassis dynamometer only the speed-time trace was used).

The calculated properties and measured emissions from both data sets were then used to find the most suitable combinations of properties and baseline cycles (or routes) to be used within the modeling methodology. A program was developed using MATLAB to perform an "all-possible subsets" selection procedure in which linear models were developed using different combinations of metrics and baseline cycles (or routes) and then used to predict CO_2 and NOx mass rate emissions for the remaining cycles (or routes) of the dataset. This step was performed to develop models using two or three baseline cycles, as well as using two or three baseline routes.

Analysis of the results was performed next. Because of the nature of the modeling methodology, trying to identify the most suitable metrics without taking into consideration the selection of baseline cycles proved to be difficult and not efficient. As discussed in Chapter 4, the key to successful prediction is the adequate selection of both cycle properties and baseline cycles to be used in the model. An independent study of cycle metrics is not feasible because metrics performance depends on the baseline cycles

selected. In the same way, an independent analysis of baseline cycles cannot be done without specifying the cycle property to be used. With this in mind, the analyses were preformed focusing in both factors (properties and cycles) at the same time. Prediction results from all possible combinations were filtered and organized using Microsoft Excel's pivot table functionality to obtain error matrices. Error matrices columns represented cycle combinations and their rows represented metrics combinations. These matrices were further analyzed using a MATLAB routine to identify combinations of columns and rows that consistently produced "satisfactory" results. Figure 24 graphically illustrates the process followed by the routine. The routine takes as input the error matrix (Figure 24a), and ask the user for a value of acceptable error (i.e. threshold value). Then, the routine perform the following steps:

1. Error values above the threshold value are replaced by zeros. The resultant matrix only contains values below the threshold value (10% in Figure 24b).
2. Columns and rows with only zero values (without predictions below the threshold value) are removed. The resultant matrix size is lower than the original one (Figure 24c).
3. The number of zeros in the columns and rows is counted. If a given column or row has more than 50% zero values, that column or row is removed. A matrix of reduced size with only well populated rows or columns remain (Figure 24d). The selected rows and columns are considered suitable or satisfactory cases.

This routine allowed discarding of metrics and route combinations that were not suitable to achieve good accuracy levels in the predictions. The threshold or criteria to identify "satisfactory" results was varied for each group of predictions, depending on the emission being predicted (CO_2 or NOx), the type of measurement equipment (chassis dynamometer or PEMS), and the number of baseline cycles being used (two or three). Generally, the threshold values used for in-use data were lower than the ones used for chassis dynamometer data, and the threshold values used when using three baseline activities were lower than when using two baseline activities. Different levels of accuracy were expected for the different groups of predictions and that justifies the use of different threshold levels for each one of them. In general, predictions were deemed satisfactory when they produced errors close to the estimated run-to-run variations of the measured data.

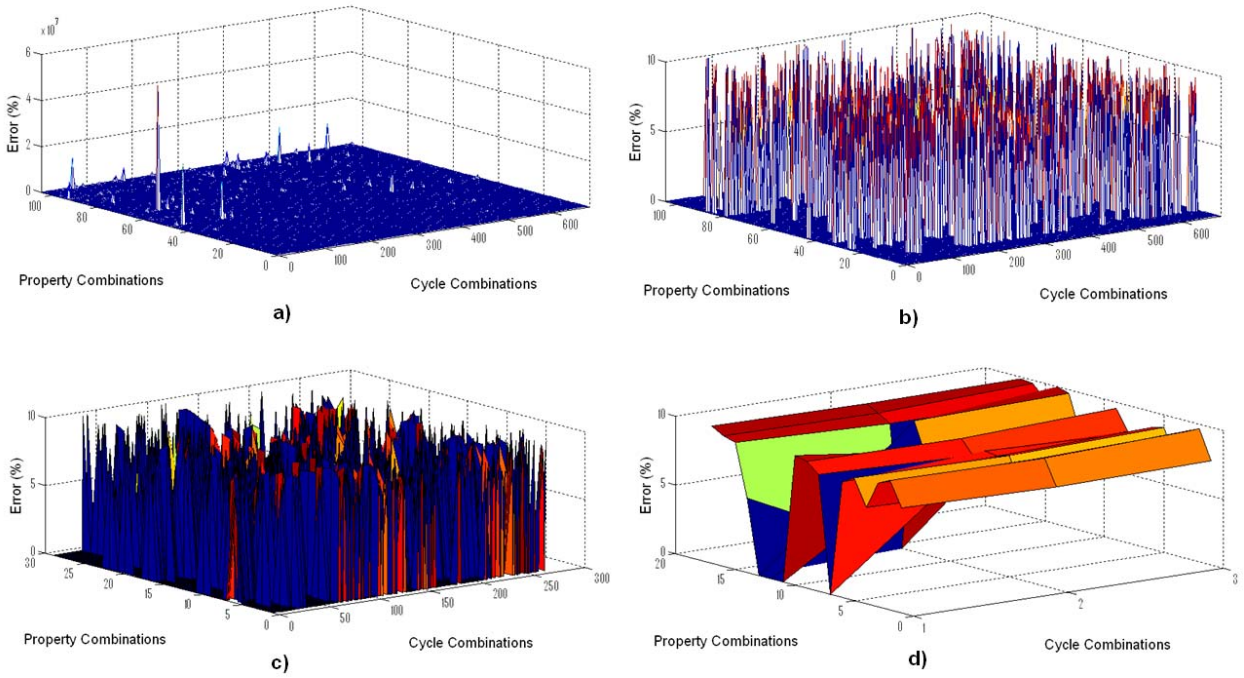

Figure 24 Error matrix routine steps

a) Original matrix, b) cases with errors below threshold are identified, c) rows and columns without satisfactory results are eliminated, and d) only well populated cases remain

5.5 Goodness of Fit Criteria

For each vehicle, CO_2 and NOx mass rate emissions for each individual test run were predicted and compared to actual measured emissions. An accurate model generates predictions that are close to "true" values. The main criterion to evaluate the goodness of fit between the experimentally-measured data and the model-predicted data for a given model was the average absolute percentage error (Equation 40, where x_p are predicted values and x_e are experimental values). Bias is the tendency for emission estimates to be, on average, consistently higher or consistently lower than "true" emission values. The average of the (signed) percentage error (Equation 41) was also calculated as a measure of bias in the predictions. A low value of both parameters may also imply precision (small range of errors). Parity plots will be presented for some predictions in order to show the actual precision and bias of the predictions. Be aware than the average values presented in this document usually are calculated on the basis of a different number of predictions (e.g. while seventeen chassis dynamometer cycles were available, only eight in-use routes were available and hence the number of predicted cycles and predicted routes are different).

$$Average\ Absolute\ Percentage\ Error = \frac{1}{n}\sum_{i=1}^{n}\frac{|x_p - x_e|_i}{(x_e)_i} \times 100\% \quad (40)$$

$$Average\ Percentage\ Error\ (Bias) = \frac{1}{n}\sum_{i=1}^{n}\frac{(x_p - x_e)_i}{(x_e)_i} \times 100\% \quad (41)$$

6 Results and Discussion

6.1 Effect of Number of Baseline Cycles or Routes

As a first step, an exploratory analysis was conducted to find the effect of the number of baseline cycles (or routes) used on the predictive capabilities of the model. The combinations of baseline cycles or routes and their properties that produced the lowest average percent error were identified. The average percent error of these cases provided an estimation of the highest achievable predictive accuracy. Figure 25 shows the minimum predictive error achieved when using two, three, and four baseline cycles or routes for prediction of CO_2 and NOx mass rates for both data sets[41]. Accuracy of the model was expected to increase when adding new baseline cycles or routes because additional information is being used. When the number of baseline cycles (or routes) was increased from two to three, the predictive accuracy increased for all the cases (CO_2 and NOx prediction for chassis dynamometer and in-use data). However, diminishing returns on CO_2 predictive accuracy were obtained when the number of baseline cycles (or routes) was increased from three to four. Moreover, predictive errors for NOx increased when adding a fourth baseline cycle or route. It was discussed in Section 3.5 that adding additional baseline cycles to the model increased the chances of performing extrapolations rather than interpolations. It is expected for the model to experience a loss of accuracy due to extrapolation. Another possible explanation of this behavior is that two cycle properties (or routes) are enough to describe vehicle activity, and using a third property may provide redundant information to the model. Based on this exploratory analysis, the methodology should be used with a maximum of three baseline activity measurements.

[41] It is worth mentioning that the averages were calculated over different number of predictions, depending on the number of baseline activity used and the data set used. For example, the average error for in-use CO_2 with two baseline cycles represents six predictions (eight routes available) while the average error for chassis CO_2 with two baseline cycles represents 15 predictions (17 cycles available).

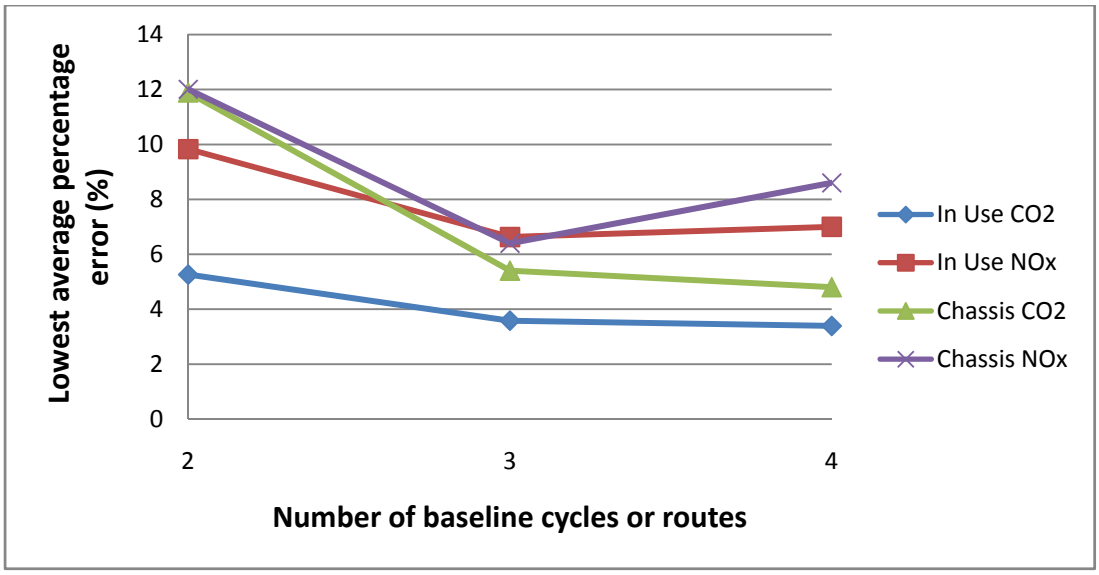

Figure 25 Effect of adding baseline cycles/routes to the linear model

6.2 Predictions Using Chassis Dynamometer Data

The following sections discuss the results of applying the methodology to chassis dynamometer data with a focus on the identification of suitable cycle properties. Fuel consumption and NOx mass rate predictions were performed on the basis of two and three baseline cycles. The data set included up to seventeen different cycles for three different vehicle technologies (diesel, lean-burn CNG and diesel hybrid buses). Fuel consumption predictions were consistent across the different technologies. However, NOx mass rates for lean-burn CNG buses were more difficult to predict accurately. A dedicated section is provided with the objective to find appropriate metrics to predict NOx emissions for lean-burn CNG vehicles.

6.2.1 Fuel Consumption Prediction Using Two Baseline Cycles

The method was applied using all possible combinations of two baseline cycles and one cycle property to predict CO_2 mass rate emissions over the remaining fourteen or fifteen cycles for the five transit buses. Figure 26 shows the distribution of absolute percentage error for a total of 702,241 predictions. Note that while about 80% of the predictions produced errors lower than 100%, about 12% of the predictions produced errors higher than 200%. This was expected because not all the metrics are suitable to be used for fuel consumption prediction. Moreover, some combinations of baseline cycles

may produce an "ill-posed" set of equations if they are too similar to each other or if "significant" extrapolation is used in the cycle's predicted emissions.

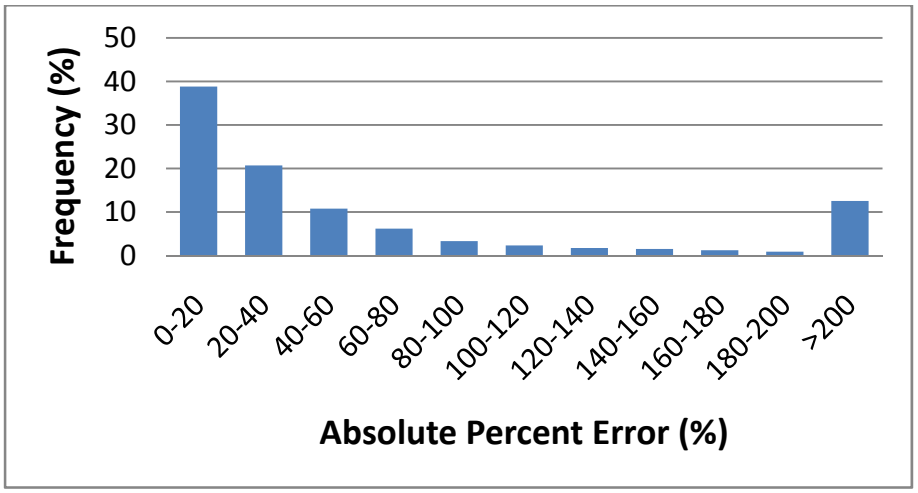

Figure 26 Distribution of error for fuel consumption prediction of five transit buses using two baseline cycles

In order to identify the most suitable metrics and combinations of two baseline cycles the results were filtered and organized using Microsoft Excel's pivot tables. A matrix of average absolute percentage error[42] was generated where rows represent the cycle property used and columns represent the cycle combinations used. The obtained matrix[43] was further analyzed in order to identify columns and rows with consistently "good" results. The MATLAB routine described in Section 5.4 was used to identify the cases that consistently produced errors lower than 20%. Table 23 summarizes the average absolute percentage error for the combination of metrics and baseline cycles that consistently produced predictions with average absolute error below the threshold of 20% for the five transit buses.

From Table 23 it was evident that metrics related to power demand such as characteristic power[44], average positive road load power, and inertial power have good potential to be used within the modeling methodology for fuel consumption prediction. Interestingly, metrics related to the transient behavior of the cycle such as standard deviation of road load power, standard deviation of inertial

[42] Average of 72 predictions: 14 or 15 "unseen" cycles for five transit buses.

[43] Matrix size: 68 x 136.

[44] Note that characteristic power for chassis dynamometer data is calculated without using altitude data. This metric is therefore equivalent to PKE.

power and root mean square of velocity also showed to be suitable to be used in the model when used along with the baseline cycles in the table. Average speed has been consistently identified as a suitable metric (Delgado et al., 2011). However, it was found that the use of average driving speed (idle portions removed) produced better fuel consumption predictions than average speed.

Table 23 Average absolute percentage error (%) of predicted fuel consumption for five transit buses using two baseline cycles with a 20% threshold value

Property	Baseline Cycles										
	Idle OCTA	Idle BRAUN	Idle KCM	Idle CSHVC	Idle Beeline	Idle ETCURB	Idle WMATA	Idle TRANS	PARIS OCTA	PARIS BRAUN	*AVERAGE*
ChPower	12.3	13.3	14.4	13.2	15.4	12.0	11.9	12.1	15.2	15.5	***13.5***
AvPosRLP	14.5	12.5	14.0	13.4	12.5	12.6	18.0	14.1	14.5	14.6	***14.1***
StdRLP	12.4	12.5	14.1	13.3	15.0	16.2	15.0	14.1	15.0	14.7	***14.2***
AvDriSpeed	13.9	13.6	12.6	15.8	15.3	17.2	12.9	15.0	16.6	16.2	***14.9***
StdInePow	13.2	13.3	17.1	13.7	15.6	17.0	15.9	14.3	15.7	15.3	***15.1***
RmsSpeed	14.6	14.2	13.5	17.4	14.2	16.1	13.3	18.1	16.4	16.3	***15.4***
RSS	15.5	16.0	13.7	18.6	13.7	14.2	15.6	18.3	16.3	17.4	***15.9***
RPSS	14.8	13.8	13.2	18.3	13.1	13.0	14.7	22.5	18.2	17.9	***16.0***
IPS	16.3	18.4	18.3	16.6	18.5	16.5	17.2	16.7	18.1	18.7	***17.5***
AvSpeed	17.6	16.9	14.9	17.5	21.7	23.6	25.1	19.0	18.3	18.0	***19.3***
AVERAGE	***14.5***	***14.5***	***14.6***	***15.8***	***15.5***	***15.8***	***16.0***	***16.4***	***16.4***	***16.5***	***15.6***

The combination of the Idle cycle with a transient cycle of intermediate average speed is observed for most of the cases presented in Table 23. The Paris cycle (a low average speed, highly transient cycle) seemed to be a good choice to replace Idle cycle if measured idle data is not available.

The previous analysis was based only on the average absolute error. Nothing has been mentioned regarding possible bias and outliers in the predictions. In order to visualize more clearly the results obtained for the different properties, Figure 27 show box and whisker plots[45] for the distribution of prediction errors for each of the cycle properties presented in Table 23. Each box plot represents one property evaluated with all the combinations of baseline cycles that contain Idle presented in Table 23

[45] On each box, the central red line is the median, the edges of the box are the 25th and 75th percentiles, the whiskers extend to the most extreme data points not considered outliers, and outliers are plotted individually with a red "+" sign. By default, an outlier is a value that is more than 1.5 times the interquartile range (IQR) away from the top or bottom of the box.

(576 predictions for the five transit buses). The results are biased, with predicted CO_2 mass rates being consistently lower than the corresponding measured values. This may be attributed to the fact that the models are too simple (i.e. equations of a line) to capture the correct activity-consumption relationship. Note that although characteristic power produced the lowest percentage error, it also produced outliers with percent errors as high as 60%. The AvDriSpeed, RmsSpeed, and IPS metrics exhibited relatively low error ranges, < ±40%, with no defined outliers.

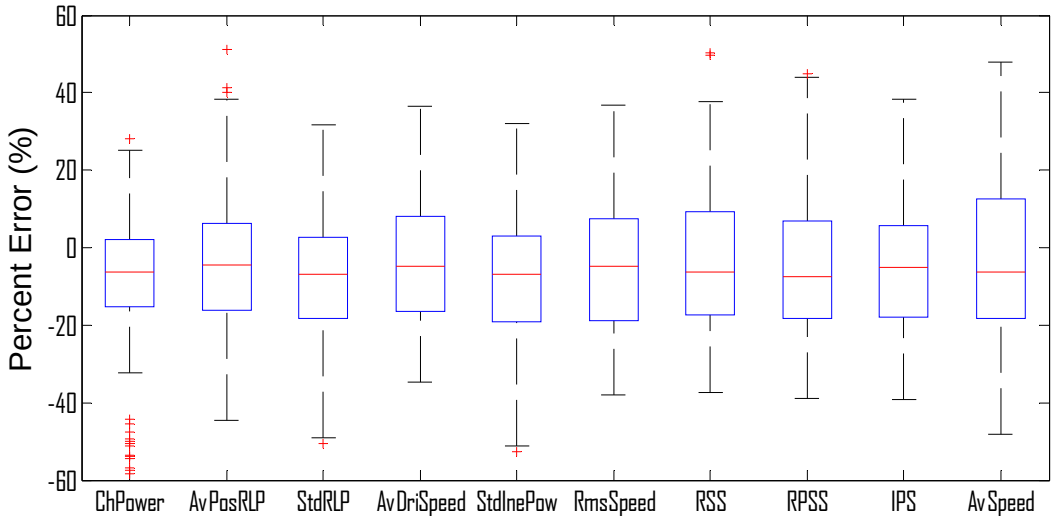

Figure 27 Box plots showing distribution of percent error for CO_2 mass rate predictions for five transit buses using different metrics

A reasonably good fuel consumption prediction should follow three criteria (Delgado et al., 2012): First, that at least 50% of the observations are within ±10% error limits; second, that the maximum errors are bounded by ±20% error; and third, that the value of 0% error is bounded by the interquartile range (not showing any bias). An illustration of the bias in the predictions is shown in Figure 28. CO_2 mass rates were predicted using Idle and KCM as baseline cycles, and average positive road load power as metric. The parity plot shows that the prediction is far from being satisfactory with 38 out of 72 of the predictions being outside the ±10% error bounds. Prediction errors as high as 45% were observed for individual cycles. The model predictive ability is limited because only one parameter is being used. Additional baseline cycles (and properties) should be included in the model to overcome this limitation. No satisfactory results (based on the aforementioned criteria) were obtained in this study when using just one property and two baseline cycles even when using an apparently suitable combination of two

cycles and one cycle property. The next section explores the addition of one more property and baseline cycle to the model.

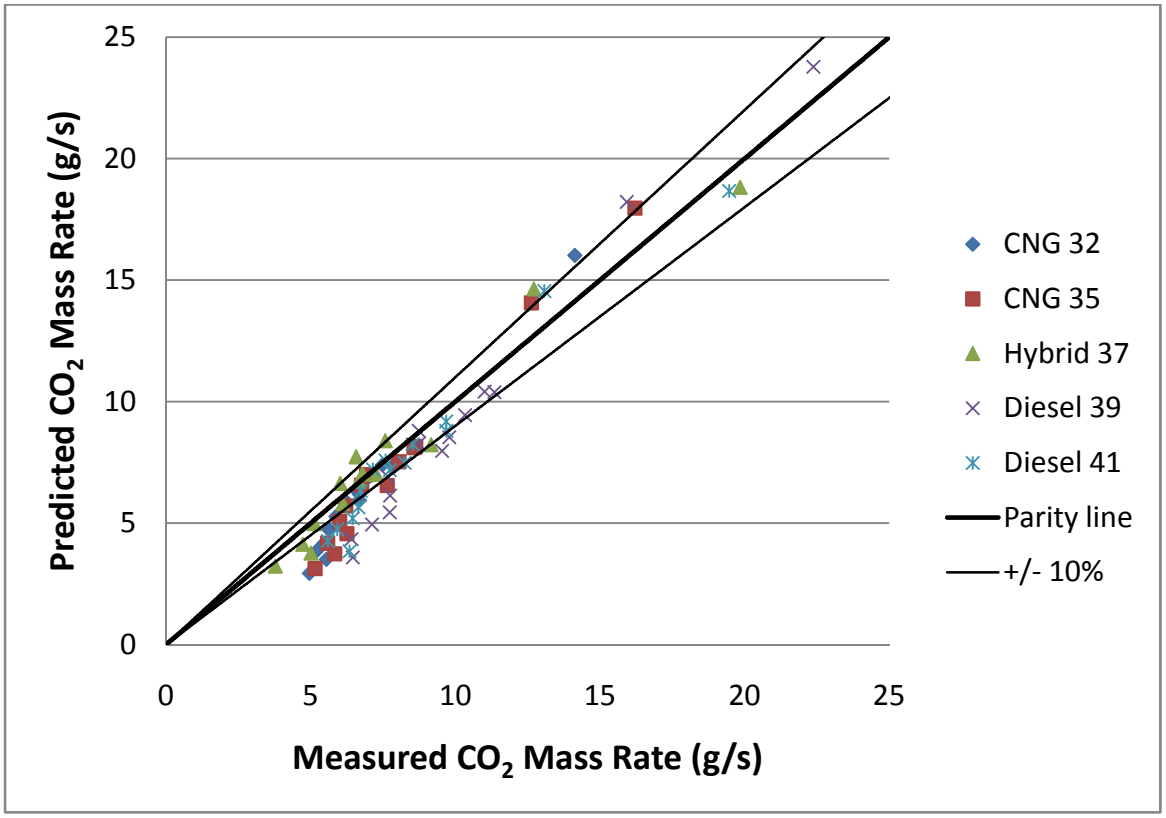

Figure 28 Results for CO_2 mass rate prediction for five transit buses using Idle and KCM as baseline cycles and AvPosRLP as property

6.2.2 Fuel Consumption Prediction Using Three Baseline Cycles

The method was applied using all possible combinations of three baseline cycles and two cycle properties to predict CO_2 mass rate emissions over the remaining fourteen cycles for the diesel buses 39 and 41 in Table 14. Based on the results observed in Section 6.2.1 for the different technologies (diesel, diesel hybrid, and CNG), only data from diesel buses were considered. Nearly two million predictions were made. Figure 29 shows the distribution of absolute percentage error of the predictions for the diesel buses. The overall results show better predictive accuracy when compared with the predictions made with only two baseline cycles. The number of predictions within 20% absolute error increased from 38% to about 50% when adding a third baseline cycle while 85% of the predictions produced errors lower than 100% (80% for two baseline cycles). The use of a third baseline cycle did not avoid the occurrence of ill-posed models. About 8% of the predictions produced errors higher than 200%.

However, the percentage of errors at that level was reduced when compared to the value of 12% obtained when using two baseline cycles.

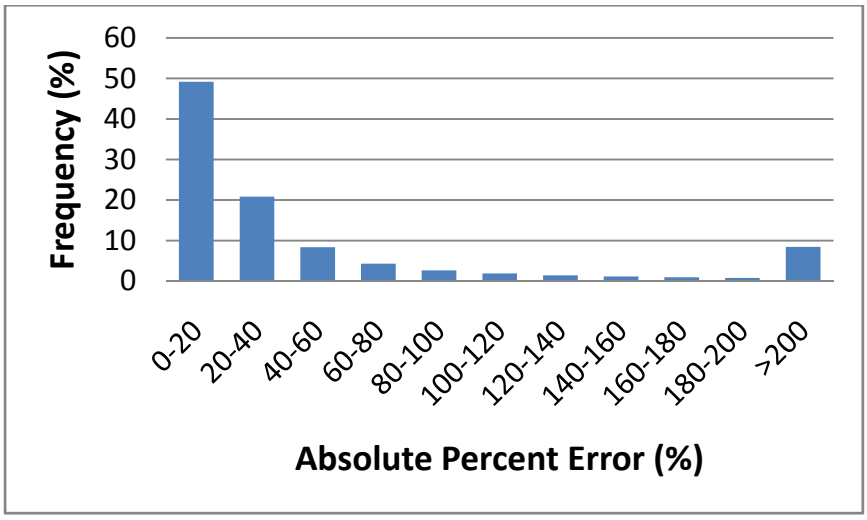

Figure 29 Distribution of error for fuel consumption prediction of two diesel buses using three baseline cycles

In order to identify the most suitable metrics and combinations when using three baseline cycles the results were filtered and organized using Microsoft Excel's pivot tables. A matrix of average absolute percentage error[46] was generated in which rows represent the cycle property used and columns represent the cycle combinations used. The obtained matrix[47] was further analyzed using the routine discussed in Section 5.4 in order to identify columns and rows with consistently good results. Better predictions were expected when adding a third baseline cycle, so a lower threshold value of 12% was selected to perform the processing of the error matrix. Table 24 shows the identified cases (property combinations and baseline cycle combinations) that generally produced errors lower than 12%.

Average positive acceleration was identified as a suitable metric for translation of fuel consumption since it appears in most of the cases presented in Table 24. This is an interesting finding because that metric did not produce satisfactory results when used in the two-baseline cycles models. AvPosAcc does not have enough predictive capabilities by itself, but seems to produce suitable combinations when used along with speed-related metrics such as average driving speed, RCS or RSS. Power-related metrics

[46] Average of 28 predictions: 14 "unseen" cycles for 2 vehicles.

[47] Matrix size: 105 x 680.

that produced consistently good results include characteristic power and aerodynamic and rolling resistance power. Interestingly, most of the combinations include either a speed-related metric or a power-related metric, along with a metric that quantifies transient behavior such as average positive acceleration, standard deviation of power, or root mean square of speed.

Table 24 Average absolute percentage error (%) of predicted fuel consumption for two diesel buses using three baseline cycles with a 12% threshold value

			Baseline Cycles							
			Idle BRAUN UDDS	Idle OCTA UDDS	Idle BRAUN KCM	Idle OCTA KCM	Idle UDDS WMATA	Idle Manhattan UDDS	Idle CBD UDDS	AVERAGE
Properties	AeroRolPow	AvPosAcc	7.13	6.92	5.83	5.72	9.02	7.06	8.92	***7.23***
	RCS	AvPosAcc	7.16	7.29	6.79	6.90	7.36	7.31	8.18	***7.28***
	AvDriSpeed	AvPosAcc	6.76	7.02	8.08	8.37	6.90	7.03	7.02	***7.31***
	$AvSpeed^{1.5}$	AvPosAcc	8.69	8.34	7.14	6.88	9.62	8.66	9.49	***8.40***
	RSS	AvPosAcc	8.14	8.16	11.23	11.46	12.02	7.93	8.03	***9.57***
	RPSS	AvPosAcc	7.99	8.19	12.78	12.71	10.78	7.77	8.18	***9.77***
	AvDriSpeed	StdRLP	8.54	8.90	8.94	9.49	9.07	11.64	12.18	***9.82***
	AvDriSpeed	ChPower	8.80	9.13	9.30	9.88	9.06	12.95	10.62	***9.96***
	ChPower	RmsSpeed	9.30	9.69	9.61	10.30	9.59	13.68	11.24	***10.49***
	AeroRolPow	StdRLP	9.52	9.76	9.62	9.89	9.56	12.50	12.86	***10.53***
	RSS	ChPower	9.16	9.56	10.95	11.12	10.59	12.22	12.08	***10.81***
	AVERAGE		***8.29***	***8.45***	***9.12***	***9.34***	***9.42***	***9.89***	***9.89***	***9.20***

At first glance, the only identifiable trend in the baseline cycle combinations of Table 24 is that all of them include the Idle cycle. The remaining two cycles include cycles with different levels of average speed and transient behavior. Table 25 shows the values of AeroRolPow and AvPosAcc for the two non-idle baseline cycles for the seven cycle combinations shown in Table 24. Highlighted cells represent the highest property value of the two cycles. Opposite relative values for different metrics (resembling a checkerboard pattern) were observed between the different baseline cycle pairs. Use of linearly independent cycles (in terms of their properties) should avoid ill-posed models. If two properties are used, it will be better to select baseline activity with relative metrics values opposite to each other. For example, it is better to use a baseline cycle with relatively low speed and high acceleration and another baseline cycle with relatively high speed and low acceleration than using one baseline cycle with relatively low speed and low acceleration and another with relatively high speed and high acceleration. The former case will avoid baseline cycles to be multiple of each other (i.e. linearly dependent). The

terms “low” and “high” are relative to the chassis dynamometer cycles or in-use routes that are to be predicted and good engineering judgement is needed to quantify these terms.

Table 25 Relative property values for non-idle baseline cycles

	Baseline Cycles	AvPosAcc (mph/s)	AeroRolPow (kW)
1	BRAUN	0.80	10.62
	UDDS	0.35	22.21
2	OCTA	0.73	8.95
	UDDS	0.35	22.21
3	BRAUN	0.80	10.62
	KCM	0.72	26.08
4	OCTA	0.73	8.95
	KCM	0.72	26.08
5	UDDS	0.35	22.21
	WMATA	0.59	6.28
6	Manhattan	0.70	4.57
	UDDS	0.35	22.21
7	CBD	0.96	9.05
	UDDS	0.35	22.21

With the objective of assessing possible bias and outliers in the predictions, Figure 30 show box and whisker plots for the distribution of prediction errors for each combination of metrics presented in Table 24. Each box represents a total of 196 predictions. As discussed in Section 6.2.1, for a reasonably good fuel consumption prediction at least 50% of the observations should be within ±10% error limits, the maximum errors should be bounded by ±20% error, and the value of 0% error should be bounded by the interquartile range (not showing any bias). In addition to the AeroRolPow and AvPosAcc metrics, average driving speed and average positive acceleration comply with the requirements. These results are consistent with a previously published study[48] (Delgado et al., 2012).

[48] The study suggested the use of average speed and average positive acceleration. Average driving speed was not studied.

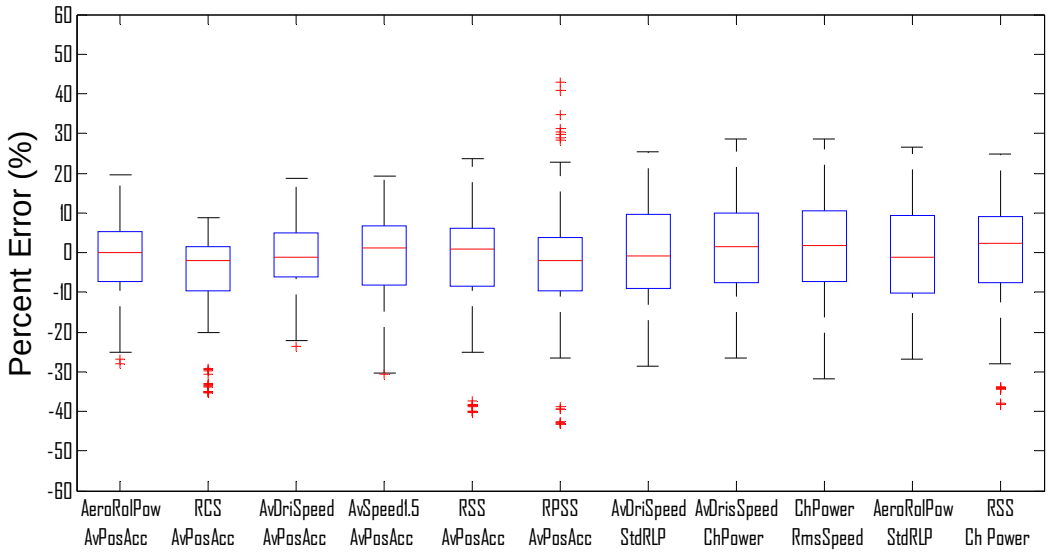

Figure 30 Box plots showing distribution of percent error for CO_2 mass rate predictions for two diesel buses using different metrics combinations

Figure 31 shows a parity plot of the case with lowest prediction error in Table 24. AeroRolPow and AvPosAcc were used and Idle, OCTA and KCM were used. Note that the combination of cycle properties contain information related to the three components of the road load equation considered in chassis dynamometer testing (AeroRolPow quantifies the rolling resistance and aerodynamic drag, while AvPosAcc quantifies the inertial power). The predictions were made for the five transit buses even though the results presented so far were based only on data from the conventional diesel vehicles[49]. Fifty four out of 67 predictions resulted in errors within ±10%. Only three tests were predicted with errors above 20%. The average prediction error was 5.72%, a satisfactory result taking into account the fact that expected fuel consumption measurement run-to-run variations (COV) are on the order of 4.4% for these chassis dynamometer tests.

[49] Buses 39 and 41 in Table 14.

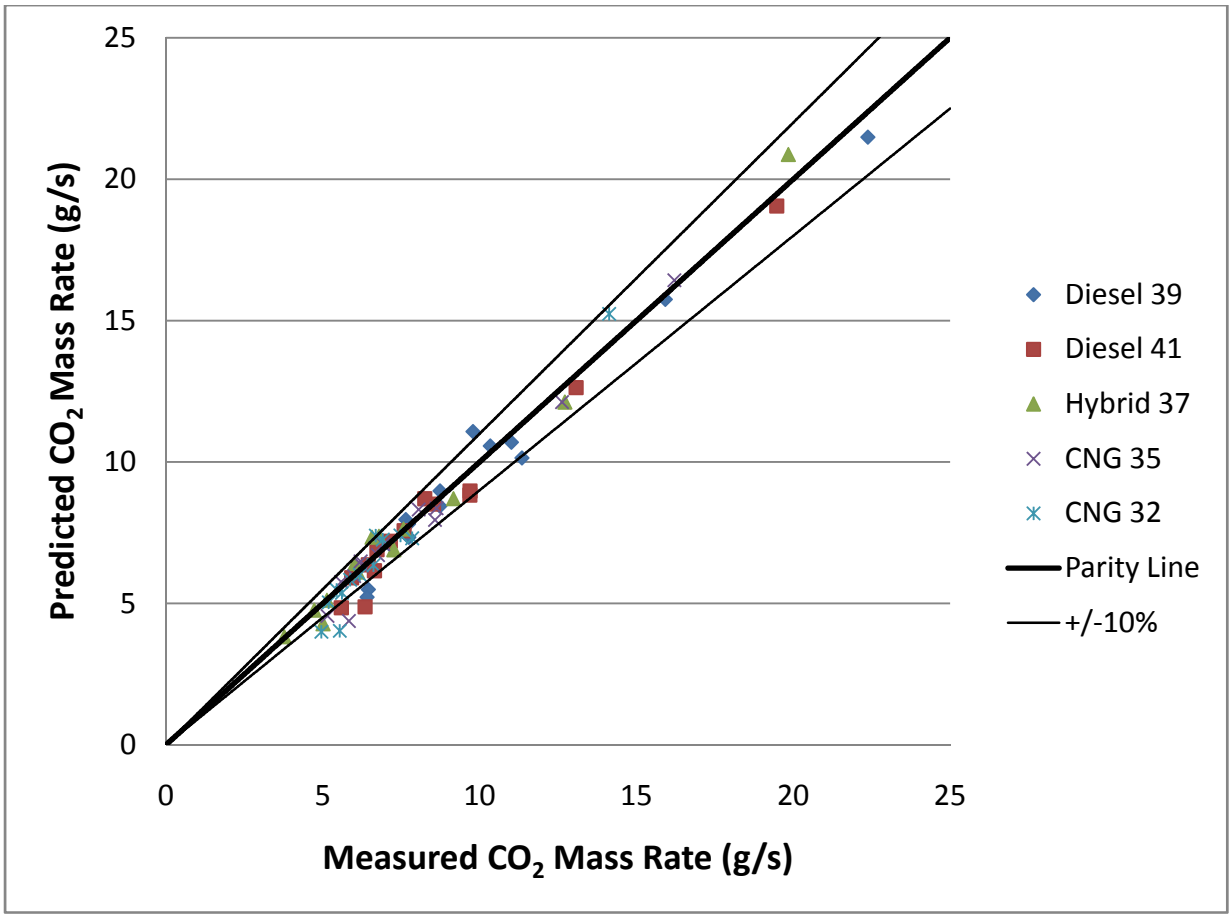

Figure 31 Results for CO_2 mass rate prediction for five transit buses using Idle, OCTA and KCM as baseline cycles and AeroRolPow and AvPosAccel as properties

6.2.3 NOx Mass Rate Prediction Using Two Baseline Cycles

The modeling methodology was applied using all possible combinations of two baseline cycles and one cycle property to predict NOx mass rate emissions over the remaining fourteen or fifteen cycles. Predictions were made for the five transit buses in Table 14 (two conventional diesel buses, two lean-burn CNG buses, and one diesel hybrid bus). Figure 32 shows the overall distribution of absolute percentage error over the 702,241 predictions made. The distribution is similar to the one obtained for CO_2 mass rate predictions using two baseline cycles. It was noted, however, that the prediction results were dependent on the type of vehicle technology. Particularly, predictions errors for the two lean-burn CNG buses followed a different distribution than the one observed for diesel and diesel hybrid buses. Figure 33 shows separate error distributions for the lean-burn CNG buses and for a category including the two conventional diesels and the diesel hybrid bus. Prediction errors lower than 20% were obtained

for the diesel and diesel hybrid buses in about 50% of the cases, but only in 20% of the cases for lean-burn CNG buses. NOx production may vary substantially due to air/fuel ratio variations and or as a result of the aftertreatment (See Section 6.2.4.1). Therefore, prediction of NOx mass rate for lean-burn CNG vehicles is expected to be more difficult than for conventional diesel vehicles.

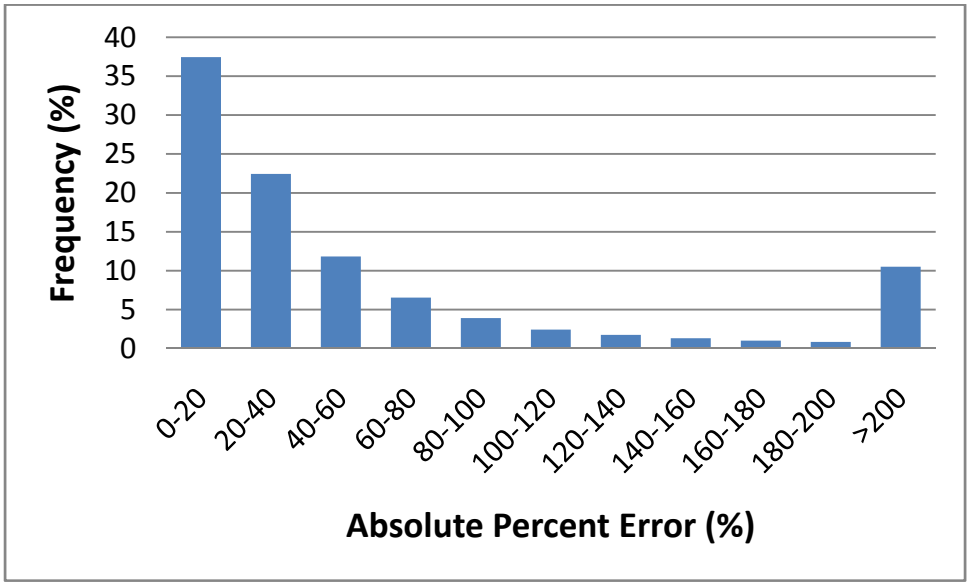

Figure 32 Distribution of error for NOx mass rate prediction using two baseline cycles for five transit buses

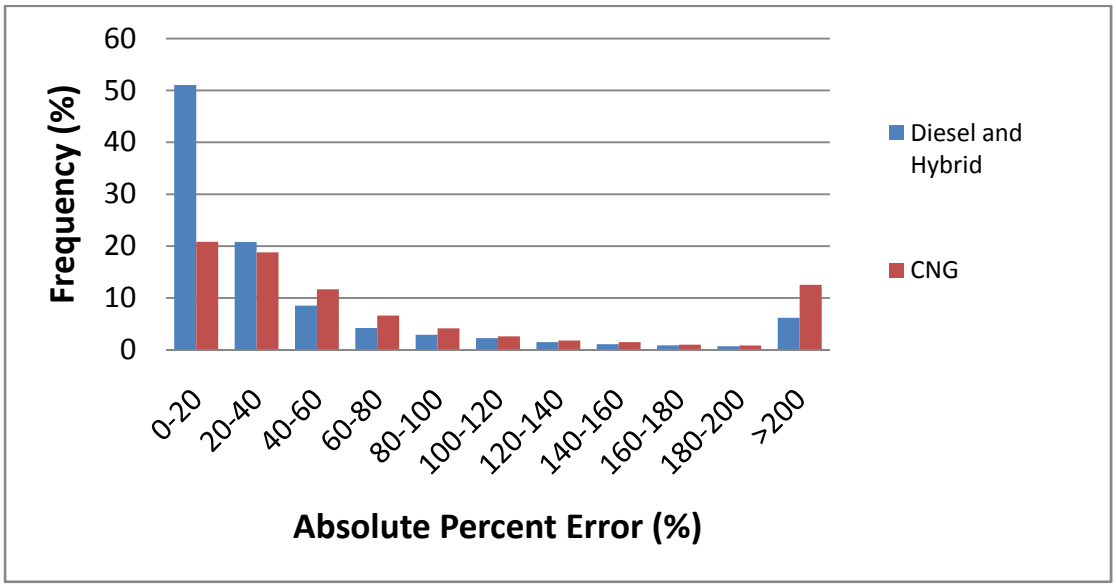

Figure 33 Distribution of error for NOx mass rate prediction using two baseline cycles for diesel, diesel hybrid, and lean-burn CNG buses

The results were filtered and organized using Microsoft Excel's pivot tables to obtain an error matrix in which rows represent the cycle property used and columns represent the cycle combinations used. The matrix was analyzed using the MATLAB routine described in Section 5.4 with the purpose of finding the cases that consistently produced errors lower than a threshold value. The initial threshold value selected was 20%, in an attempt to use the same threshold as for CO_2 predictions. However, the routine couldn't find a single case that complied with such value. Consequently, a 25% error threshold was selected. Table 26 shows the average absolute percentage error for the identified metrics and baseline cycles combinations for the five transit buses considered. It can be seen that similar results were obtained with power related metrics, speed related metrics, and metrics that account for variations in speed or power demand.

Table 26 Average absolute percentage error (%) of predicted NOx for five transit buses using two baseline cycles with a 25% threshold value

Property	Baseline Cycles				
	IDLE OCTA	IDLE CSHVC	IDLE BRAUN	IDLE TRANS	*TOTAL*
ChPower	21.38	23.62	24.68	22.52	***23.05***
ChEnergy	21.40	23.64	24.70	22.54	***23.07***
KI	22.07	23.39	23.19	23.88	***23.13***
StdRLP	21.83	24.22	23.88	22.65	***23.14***
CovInePow	22.26	24.60	23.42	24.32	***23.65***
StdSpeed	25.86	24.88	22.94	21.32	***23.75***
CovSpeed	22.60	24.65	23.54	24.24	***23.76***
StdInePow	22.42	24.76	24.62	23.54	***23.84***
RSS	27.83	23.95	24.40	21.36	***24.39***
StdDriSpeed	26.49	24.87	24.55	22.40	***24.58***
RPSS	26.58	24.93	23.93	23.52	***24.74***
TOTAL	***23.70***	***24.32***	***23.99***	***22.94***	***23.74***

Figure 34 show box and whisker plots for the distribution of prediction errors for each of the cycle properties presented in Table 26. The results show large variance in the prediction errors and a tendency to under predict NOx mass rate values. Interestingly, the distributions of error are very similar for very differently defined metrics. Outliers with errors as high as 100% were observed. Based on the

criteria defined previously[50] the overall prediction errors using two baseline cycles are unsatisfactory. Additional information should be included into the model to increase its predictive accuracy. The next section assesses the results when using an additional baseline cycle and cycle property for NOx.

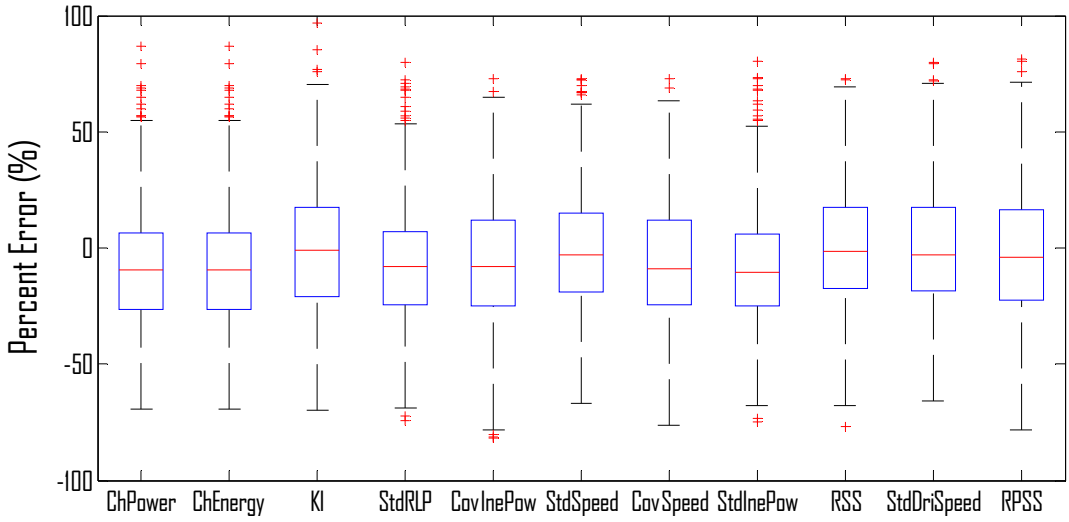

Figure 34 Box plots showing distribution of percent error for NOx mass rate predictions for five transit buses using different metrics

6.2.4 NOx Mass Rate Prediction Using Three Baseline Cycles

The method was applied using all possible combinations of three baseline cycles and two cycle properties to predict NOx mass rate emissions over the remaining fourteen cycles of the chassis dynamometer data set. Only data from diesel buses 39 and 41 were considered. Nearly two million (2 x 10^6) predictions were made. Figure 35 shows the distribution of absolute percentage error of the predictions made for the diesel buses. The error distribution was almost identical to the distribution of error obtained for the case of fuel consumption predictions with three baseline cycles. About 50% of the predictions were within 20% absolute error while 87% of the predictions produced errors lower than 100%. Ill-posed models producing prediction errors higher than 200% accounted for 7% of the predictions made.

[50] First, at least 50% of the observations should be within ±10% error limits, second, the maximum errors should be bounded by ±20% error, and third, the value of 0% error should be bounded by the interquartile range (not showing any bias).

In order to identify the most suitable metrics and combinations when using three baseline cycles the results were filtered and organized using Microsoft Excel's pivot tables. A matrix of average absolute percentage error[51] was generated which rows represent the cycle property used and which columns represent the cycle combinations used. The obtained matrix[52] was further analyzed using the MATLAB routine discussed in Section 5.4 to identify columns and rows with consistently good results. The prediction results were expected to be better in this case because a third baseline cycle was added, as well as because potentially difficult predictions for lean-burn CNG buses were not made. Based on the previous considerations the threshold value was set to 12%. Table 27 shows the summary of metrics and baseline cycles combinations that consistently produced average errors lower than 12% for the two diesel buses. Speed related metrics such as RSS, RCS and AvDriSpeed when combined with metrics accounting for transient behavior such as AvPosAcc, RmsSpeed and IF, produced prediction errors with values of around 11%, which is close to the expected run-to-run variability of the chassis NOx data for these buses.

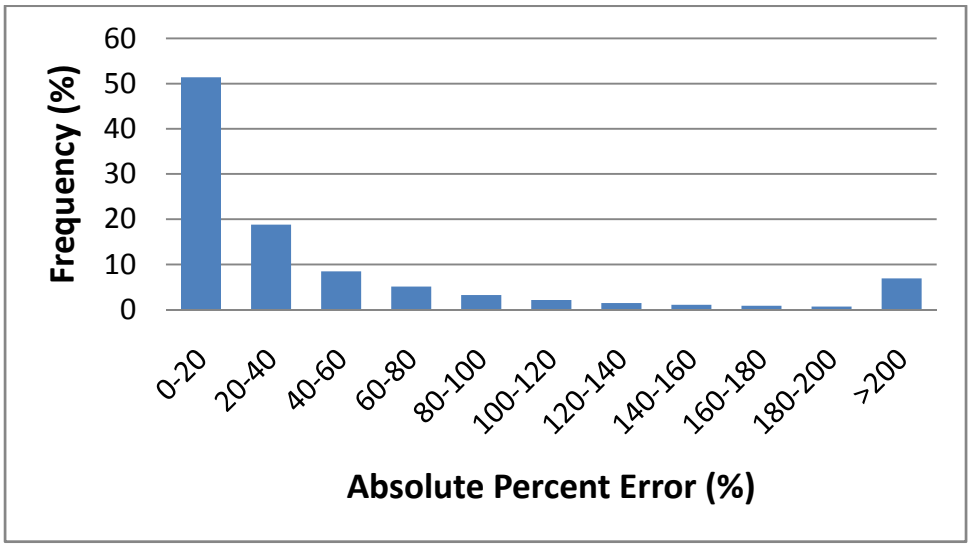

Figure 35 Distribution of error for NOx mass rate prediction for two diesel buses using three baseline cycles

[51] Average of 28 predictions: 14 "unseen" cycles for 2 vehicles.

[52] Matrix size: 105 x 680.

Table 27 Average absolute percentage error (%) of predicted NOx for two diesel buses using three baseline cycles with a 12% threshold value

			Baseline Cycles							
			NYComp Manhatt KCM	NYComp OCTA KCM	NYComp BRAUN KCM	NYComp Manhatt OCTA	NYComp OCTA UDDS	NYComp Manhatt BRAUN	NYComp BRAUN UDDS	AV.
Properties	AvDriSpeed	AvPosAcc	10.22	10.40	10.59	10.58	10.82	10.63	11.03	***10.61***
	AvPosRLP	RSS	10.79	10.61	10.06	11.26	11.11	11.56	10.57	***10.85***
	AvDriSpeed	IF	10.73	10.82	10.97	10.89	11.32	10.93	11.74	***11.06***
	RmsSpeed	AvPosAcc	10.74	10.89	11.09	11.00	11.26	11.53	11.51	***11.15***
	RSS	AvPosAcc	10.94	10.88	11.04	11.74	10.65	12.60	10.93	***11.25***
	AvPosRLP	RmsSpeed	10.87	10.86	10.79	11.45	11.76	11.59	11.54	***11.27***
	RmsSpeed	IF	11.02	11.03	11.27	11.02	11.48	11.29	12.01	***11.30***
	AvPosRLP	RCS	11.25	11.08	11.02	11.17	11.97	11.54	11.66	***11.39***
	$AvSpeed^{1.5}$	AvPosAcc	10.61	10.59	11.18	11.54	11.95	12.01	12.36	***11.46***
	RSS	IF	11.25	11.27	11.46	11.21	11.56	11.77	12.25	***11.54***
	AvPosRLP	AvPosAcc	11.02	11.15	11.72	11.10	12.69	11.27	12.94	***11.70***
	AVERAGE		***10.86***	***10.87***	***11.02***	***11.18***	***11.51***	***11.52***	***11.69***	***11.23***

The only identifiable trend in the baseline cycle combinations is that all of them include NYComp. Surprisingly, the Idle cycle is not present in any of them. Idle cycle NOx emissions for diesel buses were found to be outside the general trends observed for the other chassis dynamometer cycles. In Figure 39a, note that the Idle cycle (0 kW) NOx mass rates for the two diesel buses are far from the trends presented by the linear regression lines. This fact can explain the absence of the Idle cycle as a suitable baseline cycle for NOx mass rate prediction for these buses. It is speculated that engine and or aftertreatment control[53] may have lead to different idle NOx emissions rates but no investigations were done to support this.

To analyze possible bias and outliers in the predictions, Figure 36 shows box and whisker plots for the distribution of NOx prediction errors for the two diesel buses for each combination of metrics presented in Table 27 (each box plot represents 196 predictions). The Figure shows the presence of errors (outliers as red crosses) with absolute values as high as 100%. Further exploration of the data revealed that most

[53] Engine manufacturers may implement a shut off of the EGR valve during extended idling to prevent fouling of the EGR and intake systems, consequently increasing the NOx production levels at idle (Khan et al., 2006).

of these outliers were obtained when attempting to predict the Idle cycle. From the author's perspective, idle emissions should be measured and attempts to predict them on the basis of vehicle activity would be difficult. Figure 37 is the same data as Figure 36 but excludes the predictions of Idle cycle. Most of the predictions are within ±20%. Moreover, predictions are within ±10% for at least 50% of the predictions for the metrics combinations shown.

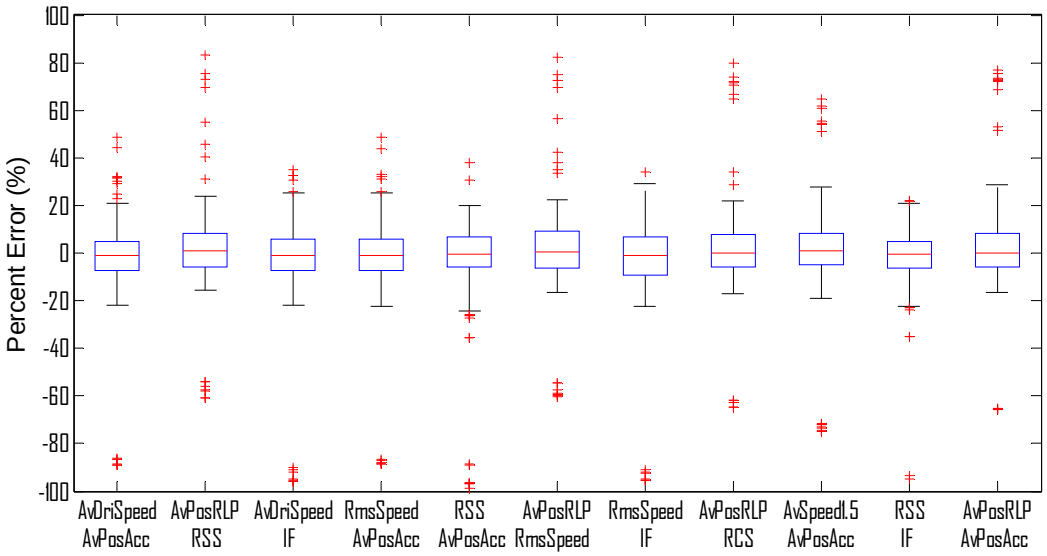

Figure 36 Box plots showing distribution of percent error for NOx mass rate predictions for two diesel buses using different metrics combinations

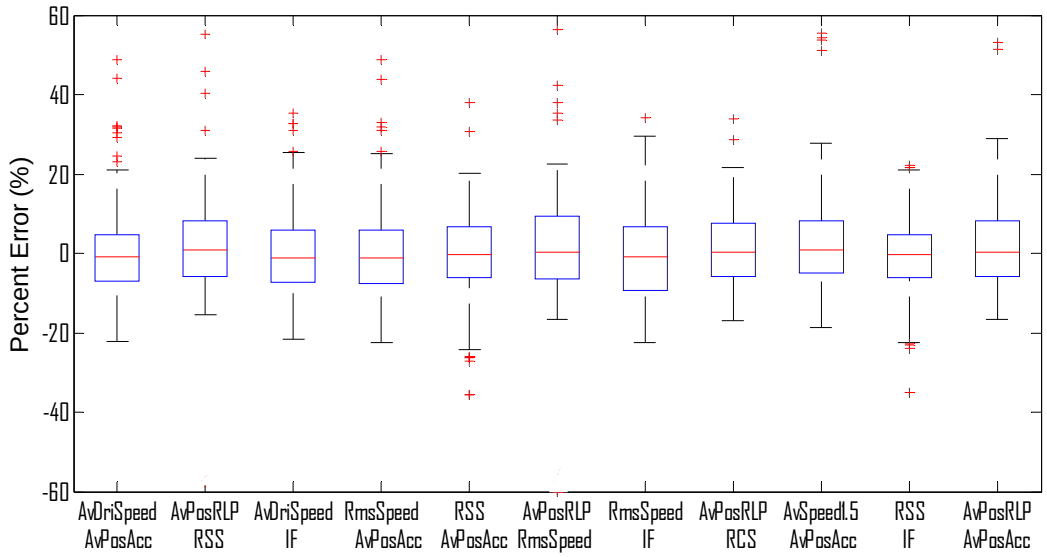

Figure 37 Box plots showing distribution of percent error for NOx mass rate predictions for two diesel buses using different metrics combinations, idle predictions excluded

Prediction results for the five buses using AvDriSpeed and AvPosAcc as properties and NYComp, OCTA, and KCM cycles baseline cycles are presented in Figure 38. Prediction results for diesel and diesel hybrid buses showed an average error of about 12%, with about 70% of the predictions within 10% error. However, very different results were observed for the two lean-burn CNG buses (buses 32 and 35). Most of the outliers shown (with a strong bias towards over prediction) correspond to lean-burn CNG buses. An average error of 270% was observed for these vehicles which are known for their NOx production sensitivity to air/fuel ratios[54]. Moreover, Figure 39 presents the relationship between power demand (using AvPosRLP as surrogate) and NOx mass rate production for a) diesel buses and b) lean-burn CNG buses. The correlation between NOx production and power demand is poor for lean-burn CNG buses (R^2 values of about 0.35) when compared to the correlation for diesel buses (R^2 values of about 0.75). Different metric combinations should be assessed to increase the NOx predictive accuracy for lean-burn CNG buses and the metric combinations shown in Table 27 should be only used for diesel and diesel hybrid vehicles NOx prediction. The next section was included to separately assess the prediction of NOx mass rate for lean-burn CNG buses.

[54] See Section 4.1.1.4.

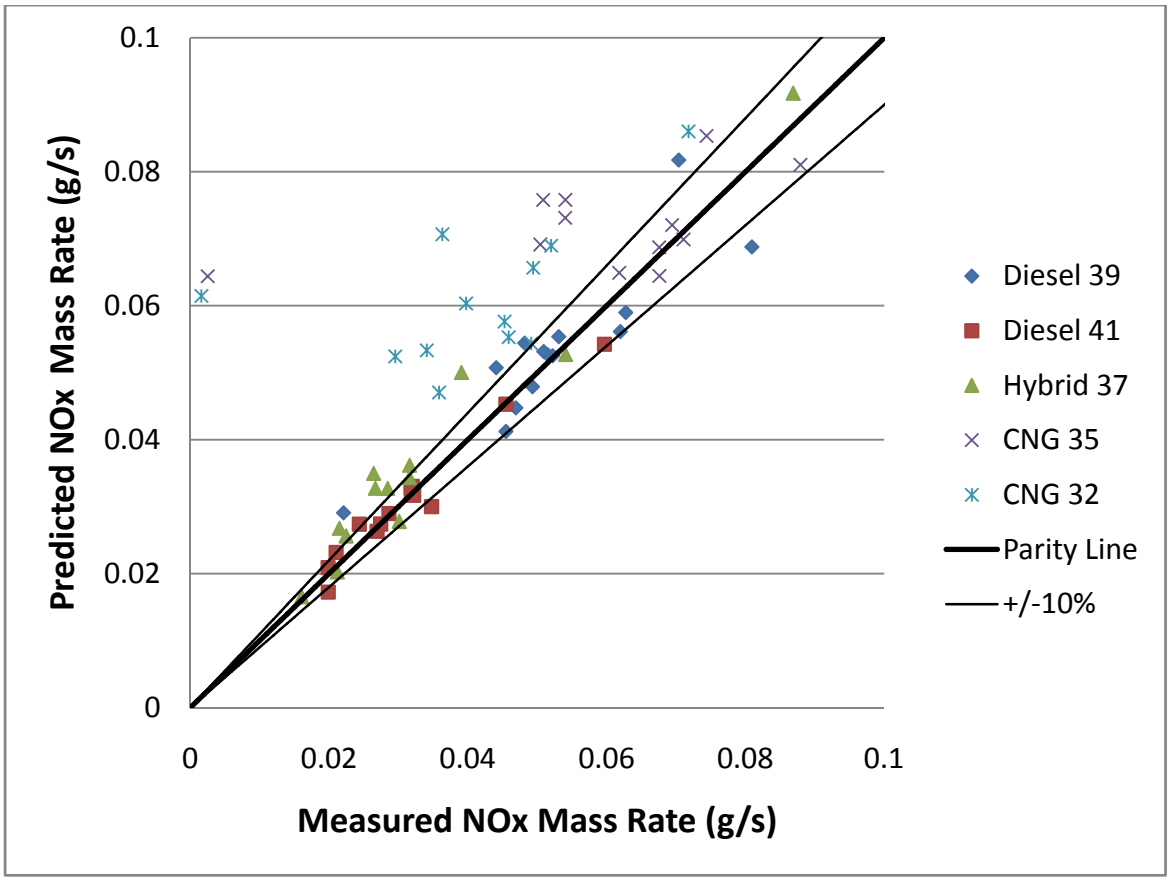

Figure 38 Results for NOx mass rate prediction for five transit buses using NYComp, OCTA and KCM as baseline cycles and Average Speed and AvPosAccel as properties

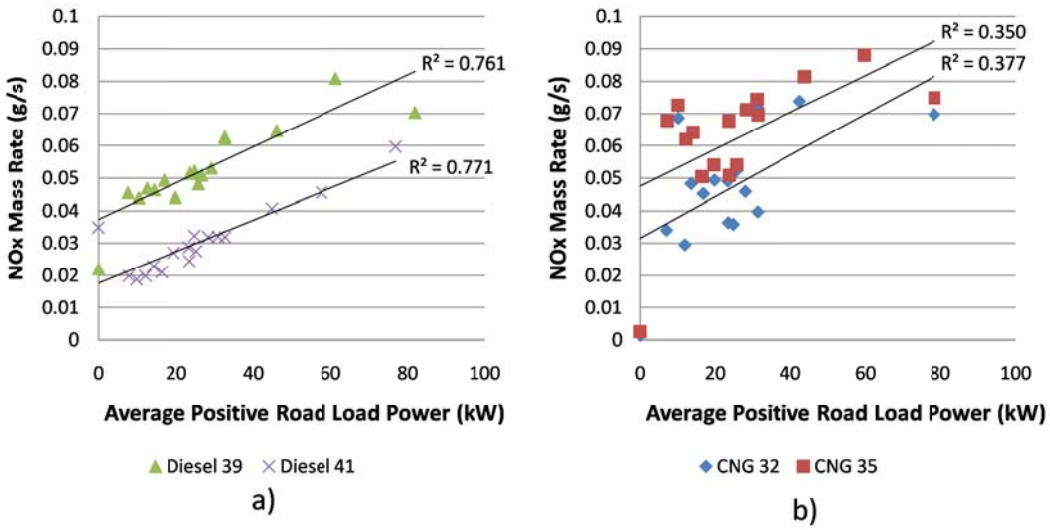

Figure 39 Relationship between power demand and NOx mass rate emissions for a) diesel buses, and b) CNG buses

6.2.4.1 NOx Mass Rate Predictions for Lean-burn CNG Vehicles

Based on the unsatisfactory results for NOx prediction of lean-burn natural gas fueled vehicles in the previous section, a separate assessment was performed for the two available lean-burn CNG vehicles in an attempt to find metrics that better translate NOx emissions for such vehicles. Note that this was a difficult task given the low correlation that was found between power demand and NOx emissions for these vehicles (Figure 39).

The results were analyzed using the routine described in Section 5.4. An attempt to use the same threshold value used for diesel vehicles (12%) did not produce any cases below this threshold for the two lean-burn CNG vehicles evaluated. Consequently, a higher threshold value of 25% was selected and the identified cases are summarized in Table 28. Run-to-run NOx measurement variability for the lean-burn CNG vehicles was difficult to estimate because only two repeated tests were available for some of the analyzed cycles (Idle, OCTA, Paris, and WMATA). It was found that test-to-test COV for Idle cycle NOx emissions were about 12% while COV for the remaining cycles ranged from 2% to 7%.

The combinations of metrics that produced the lowest average errors (of about 20%) for lean-burn natural gas vehicles are shown in Table 28. Errors were higher than the values observed for diesel vehicles by about 10% and only four combinations of baseline cycles were identified. Kinetic intensity in combination with a speed-related metric seems to be an appropriate choice for NOx mass rate prediction for lean-burn spark-ignited CNG vehicles. Figure 40 shows a parity plot with the results of NOx mass rate prediction for the two CNG buses using kinetic intensity and relative positive square speed as metrics. More than 50% of the predictions are outside the 10% error limits. However, the prediction bias has been reduced when compared to the results shown in Figure 38. If the same set of metrics is to be used for prediction of diesel and lean-burn CNG buses, a combination of metrics that is present in both Table 27 (diesel buses) and Table 28 (lean-burn CNG buses) should be used. The only combination of metrics that is present in both tables is RSS and AvPosAcc. That combination of metrics produced an average error of 11.25% for diesel vehicles and 19.11% for lean-burn CNG vehicles.

The relationship between vehicle activity and NOx production proved to be difficult to capture for the two lean-burn CNG vehicles examined. The lack of correlation between NOx emissions and power demand was attributed to two facts. First, the added uncertainty in NOx emissions measurements due to aftertreatment effects[55], and second, the NOx production sensitivity to the degree of throttling for lean-burn, natural gas spark ignited engines.

Even with closed loop air-fuel control[56], the engines may be forced to operate with richer mixtures in certain situations (e.g. high accelerations or low engine speeds). Very high levels of NOx may be emitted

[55] Exhaust from most combustion sources contains NOx composed primarily of NO. However, for lean-burn natural gas engines, there are two scenarios in which the NO_2/NOx ratio can be significant: (1) when the engine is operated at very lean conditions and (2) when an oxidation catalyst is used. Large NO_2/NOx ratios may result in additional uncertainty in NOx emissions measurements because the chemiluminescence technique was developed for low NO_2/NOx ratios (Olsen et al., 2010)

[56] Closed loop control systems use an oxygen sensor feedback to control the air/fuel ratio for lean-burn, spark-ignited engines. Closed loop control attempts to run the engine at constant exhaust oxygen content at a given point in its operating map. As some conditions change (humidity, temperature, or natural gas composition) the engine changes the air mass flow to provide the same oxygen content, thus affecting in-cylinder temperatures and NOx emission levels. (McCormick et al., 1997). Mixtures near stoichiometric produce high NOx levels, increased fuel consumption and knock conditions while very lean mixtures may not combust reliably causing misfiring and

as the engine air-to-fuel ratios approach stoichiometric conditions (Einewall et al., 2005). The highly transient nature of some of the chassis dynamometer cycles could have affected the NOx production and thus the corresponding NOx mass rate predictions. Moreover, lean-burn engines are subject to cyclic variations of in-cylinder pressure due to cyclic variations in the combustion process. These variations also results in variations in NOx emissions especially at very lean conditions (Cho and He, 2007). It should be noted that natural gas bus engine technology has gradually moved from lean to stoichiometric combustion starting in 2007. The lean-burn data are unlikely to be indicative of stoichiometric performance, where three way catalysts may be used for NOx reduction and CO, and HC oxidation (Wayne et al., 2008).

Table 28 Average absolute percentage error (%) of predicted NOx for two lean-burn CNG vehicles using three baseline cycles with a 25% threshold value

			Baseline Cycles				
			Beeline TRANS WMATA	Idle BRAUN UDDS	Idle OCTA COMM	Idle OCTA UDDS	*TOTAL*
Properties	RPSS	KI	17.83	17.88	18.23	18.28	***18.05***
	RSS	IF	18.05	18.44	18.20	18.63	***18.33***
	RSS	KI	18.07	17.99	18.60	18.99	***18.41***
	RPSS	IF	19.00	19.09	18.82	18.54	***18.86***
	RCS	KI	18.77	18.72	18.97	19.68	***19.04***
	RCS	RSS	18.32	19.02	19.17	19.79	***19.08***
	RSS	AvPosAcc	18.58	19.34	18.64	19.90	***19.11***
	RPSS	AvPosAcc	19.57	19.75	19.26	19.09	***19.42***
	RmsSpeed	KI	18.19	23.40	18.27	19.78	***19.91***
	$AvSpeed^2$	KI	19.42	23.29	19.34	22.53	***21.14***
	AeroRolPow	KI	19.31	23.94	19.23	22.56	***21.26***
	$AvSpeed^{1.5}$	KI	19.08	26.54	19.03	22.81	***21.87***
	AvDriSpeed	KI	18.70	30.34	18.84	22.01	***22.48***
	TOTAL		***18.68***	***21.36***	***18.82***	***20.20***	***19.77***

lack of combustion stability. The air/fuel ratio must be controlled within a narrow operating window (Cho and He, 2007).

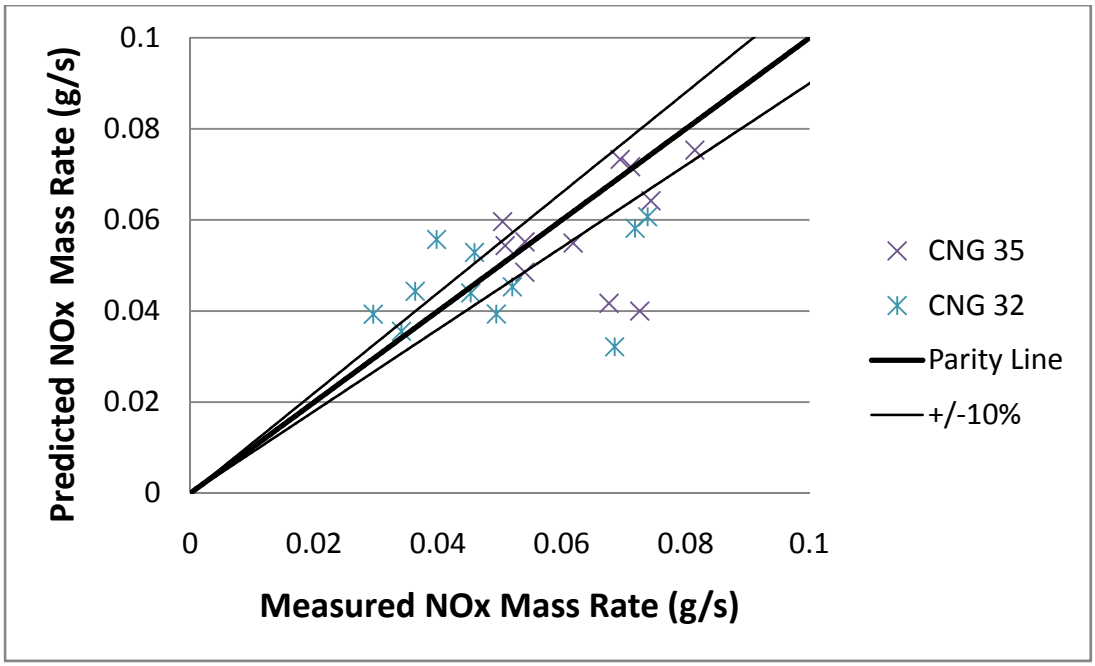

Figure 40 Parity plot of NOx mass rate prediction for two lean-burn CNG buses using Idle, OCTA, and COMM as baseline cycles and RPSS and KI as metrics

6.3 Predictions Using In-Use Data

The following sections discuss the results of applying the methodology to in-use data gathered with PEMS with a focus on the identification of suitable route's properties. The main difference between the chassis dynamometer and the in-use data approaches is the presence of grade information for the latter case. It should also be noted that while chassis dynamometer data included buses with different technologies (diesel hybrid, lean-burn CNG, and conventional diesel); the in-use data only contain information about diesel fueled Class 8 HD trucks. Additionally, the buses incorporated newer technology such as EGR, variable geometry turbochargers, and exhaust aftertreatment while the in-use Class 8 HD trucks examined in this section incorporated engine technologies from the mid to late 1990's.

6.3.1 Fuel Consumption Prediction Using Two Baseline Routes

All the possible combinations of two baseline routes and one route property were used to generate linear models to predict CO_2 mass rate emissions over the remaining six routes for the eighteen trucks summarized in Table 16. The results were analyzed using the average of absolute percentage error as the main parameter to measure goodness of fit between predicted and measured values. Figure 41 shows the distribution of absolute percentage error for a total of 232,848 predictions. The distribution is

similar to the one observed for CO_2 mass rate prediction for chassis dynamometer data[57]. About 77% of the predictions were below 100% absolute error, while 17% of the predictions were above 200%.

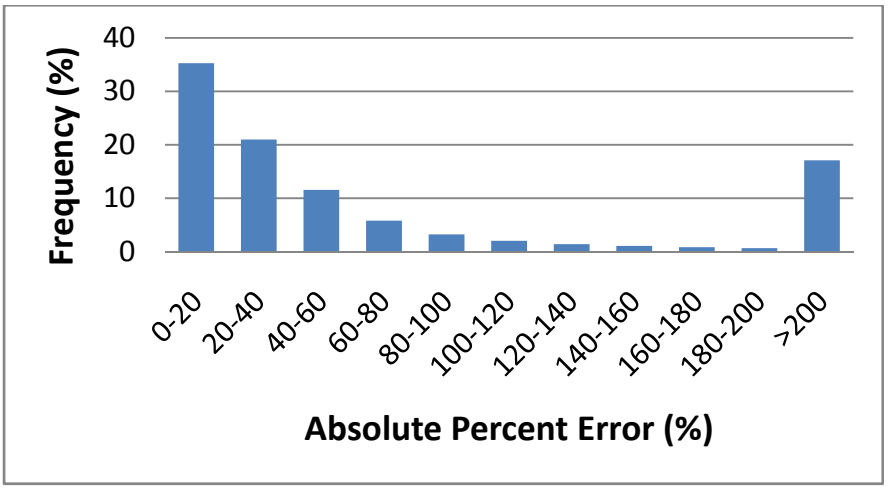

Figure 41 Distribution of error for fuel consumption prediction for eighteen trucks using two baseline routes

An error matrix was obtained using Microsoft Excel pivot tables. For the error matrix, columns represented route combinations and rows represented the properties used. The matrix was further analyzed using the MATLAB routine discussed in Section 5.4 to extract the combinations of rows and columns that consistently produced errors below a threshold value. A threshold value of 20% was selected (the same threshold value selected for chassis dynamometer fuel consumption prediction using two baseline cycles). Table 29 shows the obtained absolute average percent error[58] matrix.

[57] See Section 6.2.1.

[58] Average of 108 predictions corresponding to 18 vehicles and 6 predicted routes.

Table 29 Average absolute percentage error (%) of predicted fuel consumption for eighteen trucks using two baseline routes with a 20% threshold value

		Baseline Routes							
		Idle	Idle	Idle	Idle	Idle	Idle	Idle	*AVERAGE*
		BM2Sab	SW2Sab	Sab2SW	WashPA2	WashPA1	WashPA3	Sab2BM	
Properties	AvPosRLP	5.26	7.01	5.73	6.47	6.95	7.23	6.03	***6.38***
	GradePow	9.76	9.41	8.95	14.77	13.14	13.01	11.55	***11.51***
	ChPower	9.10	12.50	14.12	9.44	10.62	14.34	11.56	***11.67***
	RSS	11.04	9.74	11.85	12.04	10.89	9.67	27.53	***13.25***
	RPSS	10.99	10.39	14.27	12.66	9.72	10.24	27.64	***13.70***
	RmsSpeed	10.15	11.14	10.84	9.39	12.54	11.90	31.12	***13.87***
	AvDriSpeed	9.96	11.72	10.51	10.16	11.21	14.28	33.64	***14.50***
	AvSpeed	12.39	14.99	12.23	13.81	15.56	18.65	35.23	***17.55***
	RPCS	14.74	20.07	14.23	16.43	42.19	15.36	25.72	***21.25***
	RCS	14.67	19.92	14.55	17.87	48.39	15.99	28.46	***22.84***
	StdInePow	16.04	17.81	15.38	16.72	20.66	37.09	36.58	***22.90***
	PercDecel	19.09	19.28	25.22	25.32	19.45	19.77	39.91	***24.01***
	StdSpeed	19.94	16.96	21.13	25.38	17.07	44.58	23.47	***24.08***
	CovPosAcc	19.35	19.32	19.50	23.67	27.15	28.31	42.69	***25.71***
	InePow	18.66	21.96	18.78	20.70	19.23	32.05	50.97	***26.05***
	IPS	18.73	22.01	18.83	20.79	19.31	32.02	51.05	***26.11***
	AVERAGE	***13.74***	***15.26***	***14.76***	***15.98***	***19.00***	***20.28***	***30.20***	***18.46***

Use of average positive road load power (AvPosRLP) produced excellent predictive accuracies, with average errors consistently below 8%. These errors are close to the value of measurement variations (COV) estimated at 6.4%[59]. This fact indicates that this metric has enough predictive power to produce reasonable predictions by itself.

Road grade related metrics such as characteristic power and grade power showed good potential with errors bounded by 15% across the different baseline routes combinations. The remaining metrics (RSS, RPSS, RMS Speed, and AvSpeed) are only based on the speed-time trace, not containing any grade-related information. Their results are not as consistent as the grade-based metrics, especially when one of the baseline routes contains a pronounced grade (errors as high as about 50% when Sab2BM is a baseline route). Table 29 also indicates that suitable combinations of two baseline routes should include

[59] See section 4.2.2.

an idle "route." No combination of baseline routes with routes other than idle resulted on predictions with average errors below 20%.

Figure 42 show box plots with the distribution of prediction error for the first seven metrics in Table 29. Each box plot represents 756 predictions (18 vehicles, 7 baseline routes combinations, and 6 unseen routes). Note that the predictions are well centered on the value of 0% error showing no apparent bias. It can be seen also that AvPosRLP produced errors with a more narrow distribution (interquartile range is well within 10% error) when compared to other metrics.

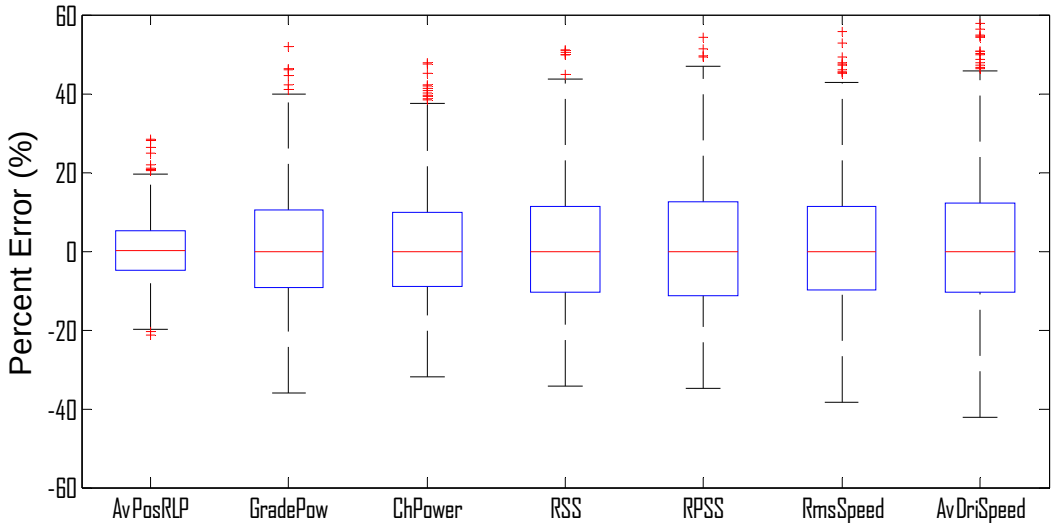

Figure 42 Box plots showing distribution of percent error for CO_2 mass rate predictions for eighteen trucks using different metrics

Overall, when compared with equivalent results obtained with chassis dynamometer data[60], the prediction results for in-use data have lower errors. However, the results are not entirely comparable because the averages are calculated on the basis of a different number of predictions (seventeen available chassis dynamometer cycles compared to eight available in-use routes). Moreover, these results are for typical truck operation on highways, while most of the chassis dynamometer cycles used were representative of city and suburban operation.

[60] See Section 6.2.1.

A parity plot for CO_2 mass rate prediction using the combination of baseline routes and route property that produced the lowest average error (5.26%) is presented in Figure 43. Idle and BM2Sab routes, in conjunction with AvPosRLP property, were used to predict the remaining six routes' CO_2 mass rate. The plot shows predicted values as a function of measured values. The parity line and the limits of ±10% error in the prediction are also shown. Interestingly, the choice of a route with a prolonged downhill grade did not negatively affect the prediction of routes without pronounced changes in altitude or of the route with prolonged uphill grade (Sab2BM). Note also that while many of the WashPA1 (city driving) predictions were below the parity line, many of the WashPA3 (highway driving) predictions were higher than their measured CO_2 mass rate values suggesting a bias of under-prediction for a city route and over-prediction for highway route. The two Saltwell routes (Sab2SW and SW2Sab) also exhibited an over-prediction bias for these two highway routes.

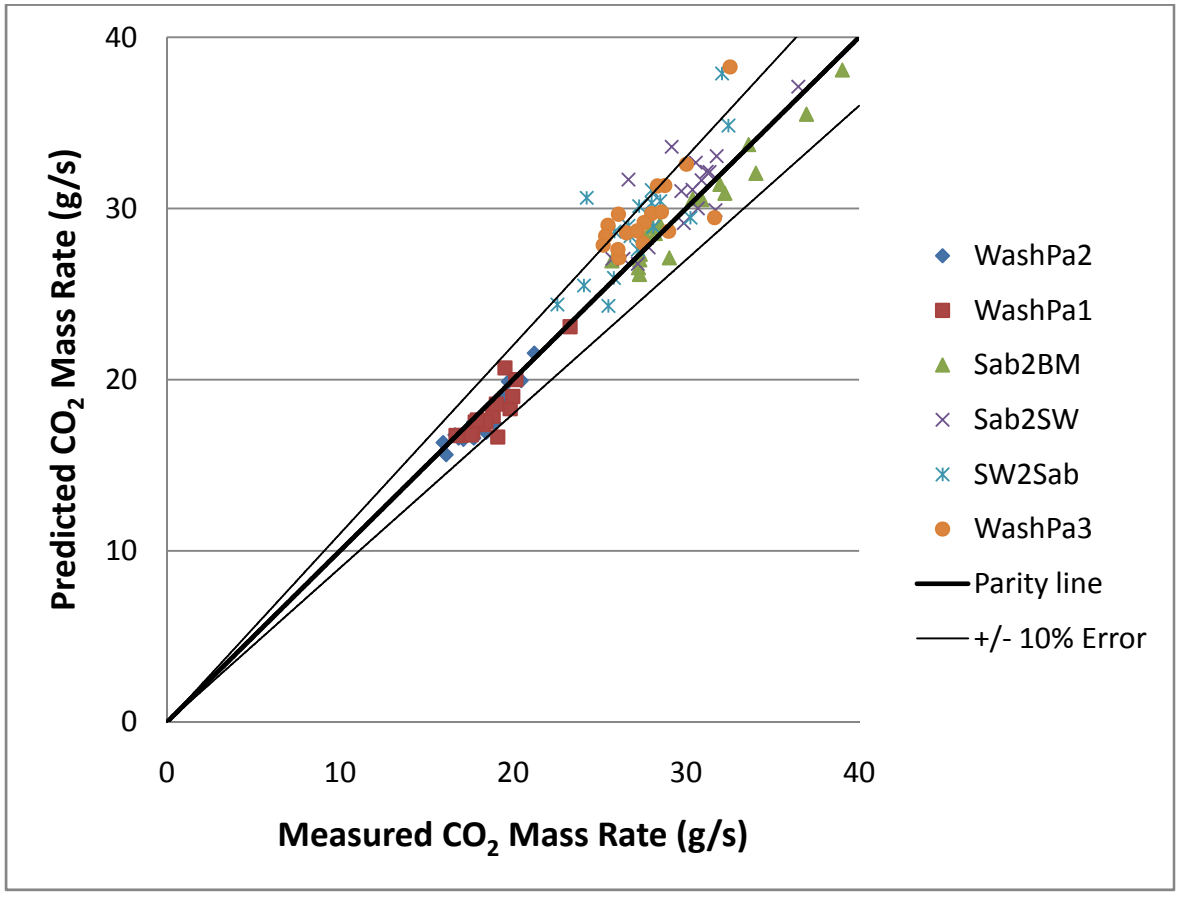

Figure 43 Parity plot of CO_2 mass rate prediction for eighteen trucks using Idle and BM2Sab as baseline routes, and RLP as metric

Table 30 shows the average weights for the baseline routes (average over eighteen vehicles), the bias, and the average absolute error for each predicted route. Note that the Idle "route" has negative weights for some of the predicted values, indicating extrapolation. Note also that Sab2BM and WashPA3 have similar weight coefficients. This means that the value of AvPosRLP is very similar between them. A second metric should be added to the model to help differentiate between these dissimilar routes (Sab2BM has a consistent hill climb at a rather low average speed, while WashPA3 contain highway speeds driving with general rolling terrain). Addition of one more metric to the model is explored in the next section.

Table 30 Average baseline route weights, bias and error for predicted routes

Predicted Route	w (Idle)	w (BM2Sab)	Bias (%)	Error (%)
WashPA2	0.21	0.79	-2.83	3.42
WashPA1	0.19	0.81	-3.27	3.97
Sab2BM	-0.38	1.38	-1.10	2.69
Sab2SW	-0.45	1.45	4.06	5.42
SW2Sab	-0.35	1.35	7.21	8.02
WashPA3	-0.38	1.38	7.16	8.04

6.3.2 Fuel Consumption Prediction Using Three Baseline Routes

The modeling methodology was applied to in-use data using all the possible combinations of three baseline routes and two route properties to generate linear models to predict the remaining five routes. The results were analyzed using the average absolute percentage error as the main parameter to measure goodness of fit between predicted and measured values. A histogram showing the distribution of error for a total of 14,747,040 total predictions is presented in Figure 44. When compared with the results obtained using two baselines cycles, adding a third baseline cycle increased the frequency of errors below 20%, from 35% to 38%.

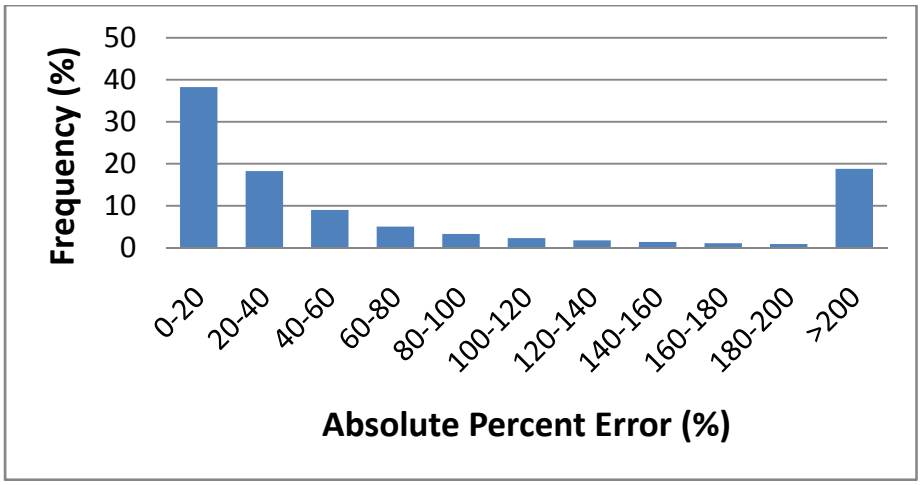

Figure 44 Distribution of error for fuel consumption prediction for eighteen trucks using three baseline cycles

An error matrix[61] was obtained using Excel pivot tables. Matrix columns represent baseline route combinations and matrix rows represent routes' properties combinations. The error matrix was further processed by using the routine discussed in Section 5.4 to identify the columns and rows that consistently produced results with errors below a selected threshold value. Initially, the threshold value was set to 12% (the same value used for fuel consumption prediction using three baseline cycles). The resultant matrix after processing contained 825 metric combinations and six route combinations, corresponding to about 3% of the cases of the original 2926 x 56 matrix. This matrix was too large to be shown. The threshold value was then reduced to 5% to focus on the most suitable metric combinations. Table 31 shows the error matrix after processing. Note that Table 31 corresponds to the first nine metric combinations of the 825 obtained when the threshold was set to 12%.

The addition of a third baseline route to the model increased predictive accuracy with average errors lower than the expected measurement variation (COV) for in-use testing. Average positive road load power is present in all the combinations shown in Table 31 and seems to be the metric of choice for translation of fuel consumption between different driving routes. When this metric was combined with metrics such as characteristic acceleration or average speed to the third power the results were improved when compared to the use of AvPosRLP as the only metric. Figure 45 shows the distribution of prediction errors for each of the metric combinations shown in Table 31. Each box plot represents 540

[61] Matrix size: 2926 x 56.

predictions (18 vehicles, 6 baseline routes combinations, and 5 unseen routes). The results are similar to each other suggesting that the resulting models are more sensitive to the values of AvPosRLP than to the values of the accompanying metric. However, the average errors are lower than when using AvPosRLP as the only metric.

Table 31 Average absolute percentage error (%) of predicted fuel consumption for eighteen trucks using three baseline routes with a 5% threshold value

			Baseline Routes						
			Idle WashPA2 WashPA3	Idle WashPA2 Sab2SW	Idle WashPA2 SW2Sab	Idle WashPA1 Sab2SW	Idle WashPA1 WashPA3	Idle WashPA1 SW2Sab	*AVERAGE*
Percent Route Properties	AvPosRLP	ChAccel	3.58	3.82	3.71	3.86	3.66	3.81	***3.74***
	AvPosRLP	$AvSpeed^3$	3.63	4.21	3.57	4.01	3.64	3.56	***3.77***
	AvPosRLP	$AvSpeed^{3.5}$	3.70	4.12	3.55	3.98	3.73	3.56	***3.77***
	AvPosRLP	$AvSpeed^4$	3.78	4.08	3.55	3.97	3.81	3.57	***3.79***
	AvPosRLP	$AvSpeed^{2.5}$	3.58	4.42	3.66	4.09	3.55	3.58	***3.81***
	AvPosRLP	AvPosGrade	3.81	4.07	4.38	3.86	3.65	4.17	***3.99***
	AvPosRLP	StdGrade	3.97	4.05	4.60	4.18	4.04	4.76	***4.27***
	AvPosRLP	FreqAccD	4.18	4.06	4.54	4.10	4.20	4.59	***4.28***
	AvPosRLP	FreqAccT	4.06	4.20	4.69	4.24	4.16	4.89	***4.37***
	AVERAGE		***3.81***	***4.12***	***4.03***	***4.03***	***3.83***	***4.05***	***3.98***

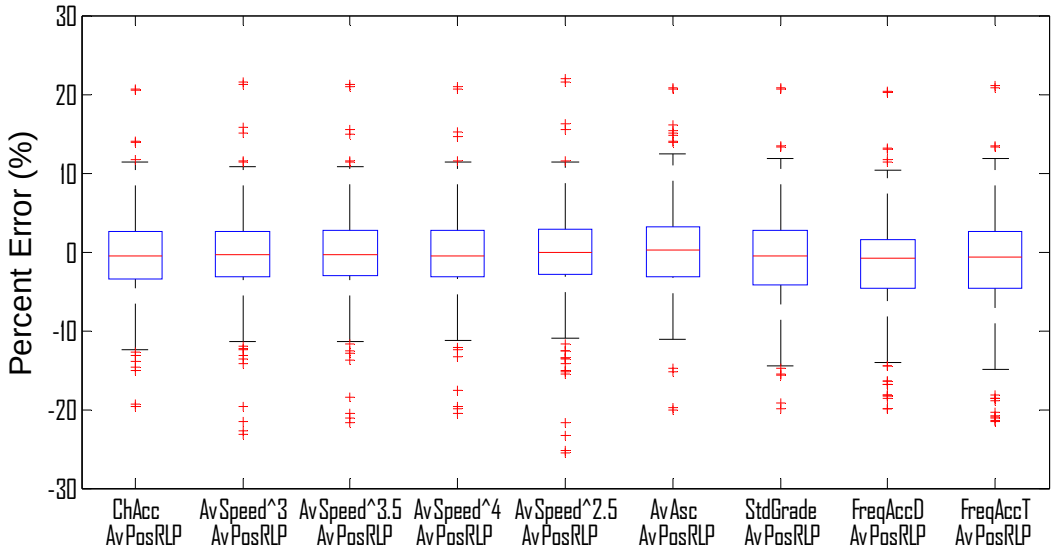

Figure 45 Box plots showing distribution of percent error for CO_2 mass rate predictions for eighteen trucks using different metrics

Figure 46 shows a parity plot with the results obtained when using the case with lowest error in Table 31. No apparent bias was observed and 87 out of 90 predictions were within the 10% error boundaries. The average prediction error (3.6%) is lower than the estimated run-to-run variability for in-use data (6.4%). Table 32 shows average weight coefficients, bias and percent errors for each predicted route. Note that idle weight coefficients are negative which suggest that extrapolation is being performed. However, the level of extrapolation is subtle since the highest weight coefficient value is just 1.13. The next section discusses allowable limits for weight coefficient values to obtain accurate predictions.

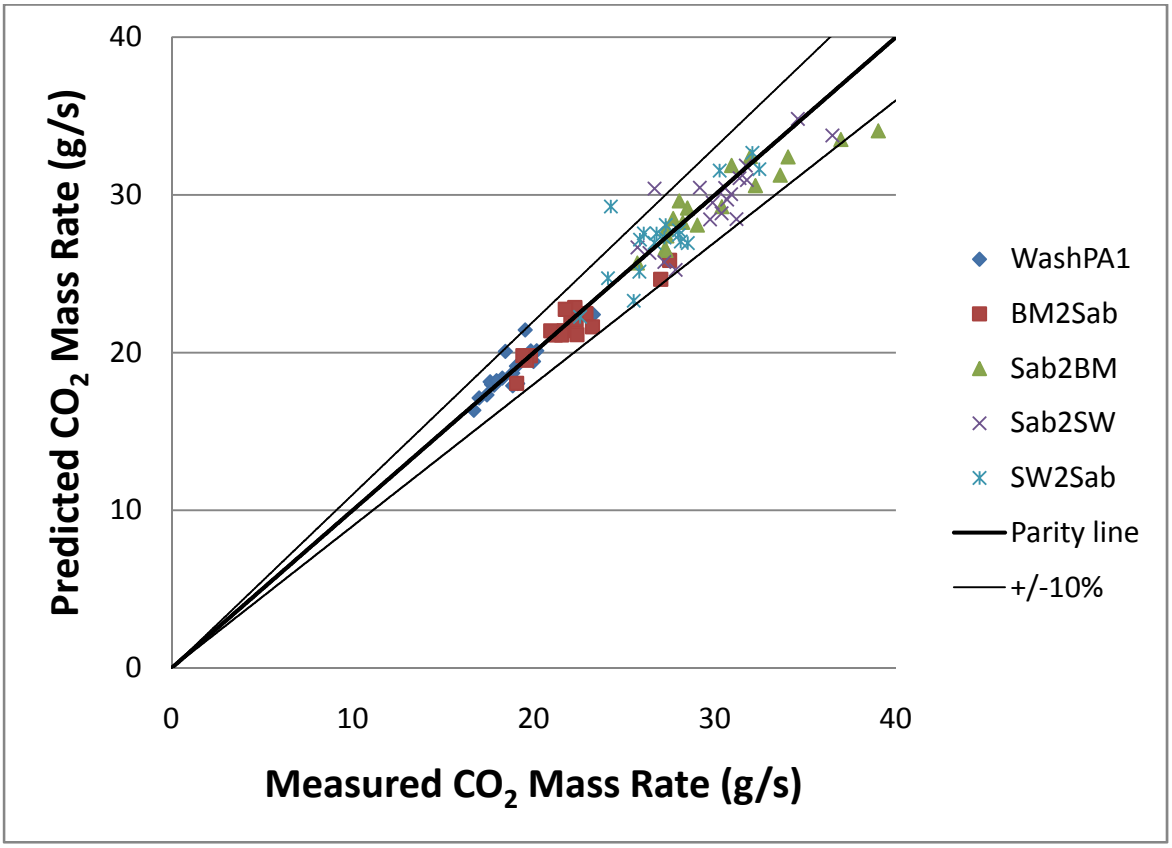

Figure 46 Parity plot of CO_2 mass rate prediction for eighteen trucks using Idle, WashPA2, and WashPA3 as baseline routes, and AvPosRLP and ChAcc as metrics

Table 32 Average baseline route weights, bias and error for predicted routes

Predicted Route	w Idle	w WashPA2	w WashPA3	Bias (%)	Error (%)
WashPA1	-0.07	1.13	-0.06	0.47	2.78
BM2Sab	-0.02	0.67	0.35	-1.37	2.98
Sab2BM	-0.46	1.06	0.41	-1.88	3.85
Sab2SW	-0.15	0.23	0.93	-1.56	4.15
SW2Sab	-0.05	0.15	0.89	1.12	4.16

6.3.2.1 Weight Coefficient Values

Figure 47 shows the distribution of weight coefficient values (excluding outliers) for CO_2 mass rate predictions with a) absolute errors below 5%, and b) absolute errors above 50%. High values (above an absolute value of three) of weight coefficients occur when heavy extrapolations are attempted. On the other hand, weight coefficients values for predictions below 5% error are below an absolute value of three. This value can be useful as a measure for determining allowable extrapolations. Predictions with models that result in weight coefficients larger than an absolute value of three should be avoided.

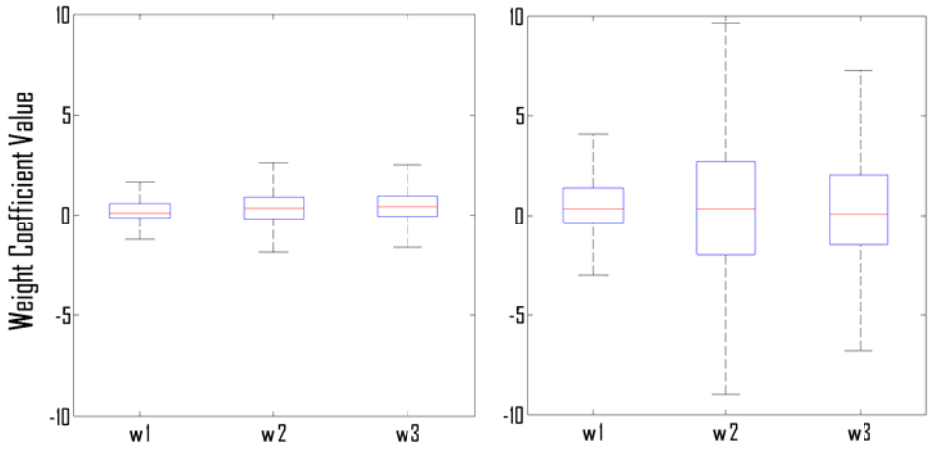

a) **b)**

Figure 47 Box plots for weight coefficients; a) predictions with errors below 5% and b) predictions with errors above 50%

6.3.3 NOx Mass Rate Prediction Using Two Baseline Routes

With the objective of identifying the most suitable route properties and route combinations to predict NOx, all the possible combinations of two baseline routes and one route property were used to generate linear models to predict the remaining six routes (232,848 total predictions). The results were analyzed using the average of absolute percentage error as the main parameter to measure goodness of fit between predicted and measured values. Figure 48 shows the distribution of errors where 30% of the predictions produced errors lower than 20%.

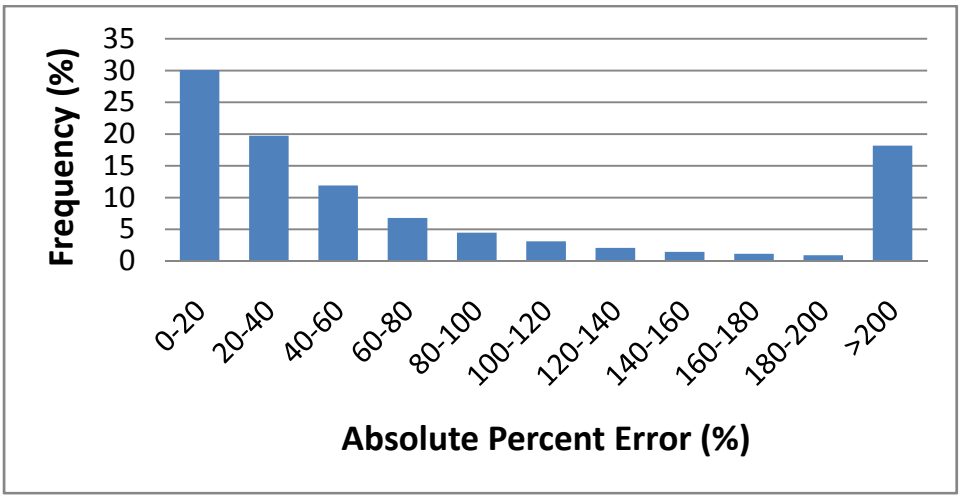

Figure 48 Distribution of error for NOx prediction for eighteen trucks using two baseline cycles

Table 33 shows the average of the absolute percentage error for the metrics and combinations of baseline routes that consistently produced average errors[62] lower than 20%.

[62] Average between 108 predictions.

Table 33 Average absolute percentage error (%) of predicted NOx for eighteen trucks using two baseline routes with a 20% threshold value

		Baseline Routes							
		Idle WashPA2	Idle WashPA1	Idle BM2Sab	Idle Sab2BM	Idle Sab2SW	Idle SW2Sab	Idle WashPA3	AVERAGE
Properties	**AvPosRLP**	10.22	15.61	9.83	12.94	9.85	9.88	16.68	***12.13***
	GradePow	13.75	16.07	13.51	12.61	11.98	12.16	34.09	***16.31***
	RPCS	13.32	19.36	15.87	28.49	13.24	16.99	16.33	***17.66***
	AvSpeed	12.20	15.73	13.20	41.75	14.38	13.48	13.47	***17.74***
	RolPow	12.20	15.71	13.24	41.73	14.39	13.48	13.54	***17.76***
	RCS	13.37	22.37	15.02	30.26	12.51	16.43	15.44	***17.91***
	AvDriSpeed	13.90	18.57	13.45	40.69	15.51	13.98	15.40	***18.79***
	RmsSpeed	15.31	17.20	14.61	38.16	16.73	14.34	16.90	***19.03***
	AvSpeed$^{1.5}$	17.00	16.43	13.84	42.31	13.04	16.98	15.45	***19.29***
	AeroRolPow	17.92	17.76	14.32	41.69	13.42	18.22	15.86	***19.89***
	AVERAGE	***13.59***	***17.21***	***13.35***	***29.68***	***13.06***	***14.00***	***18.65***	***17.08***

Average road load power was the metric that produced lowest NOx prediction errors among the cases considered. However, the results obtained by using only this property are not completely satisfactory. Figure 49 presents a parity plot for NOx mass rate predictions using the combination of baseline routes and route property that produced the lowest average error (9.83%) in Table 33. Table 34 shows the average weights for the baseline routes, the bias, and the average absolute error for each predicted route. These averages were based over a total of eighteen vehicles. Considerable positive bias was observed for WashPA1 (city driving) while considerable negative bias was observed for WashPA3 (rolling hills highway) and Sab2BM (significant grade, highway) routes. The two-dimensional model (equation of a line) is not sufficient to appropriately describe the emissions-activity relationship. Addition of a third baseline route and a second metric is explored and discussed in the next section.

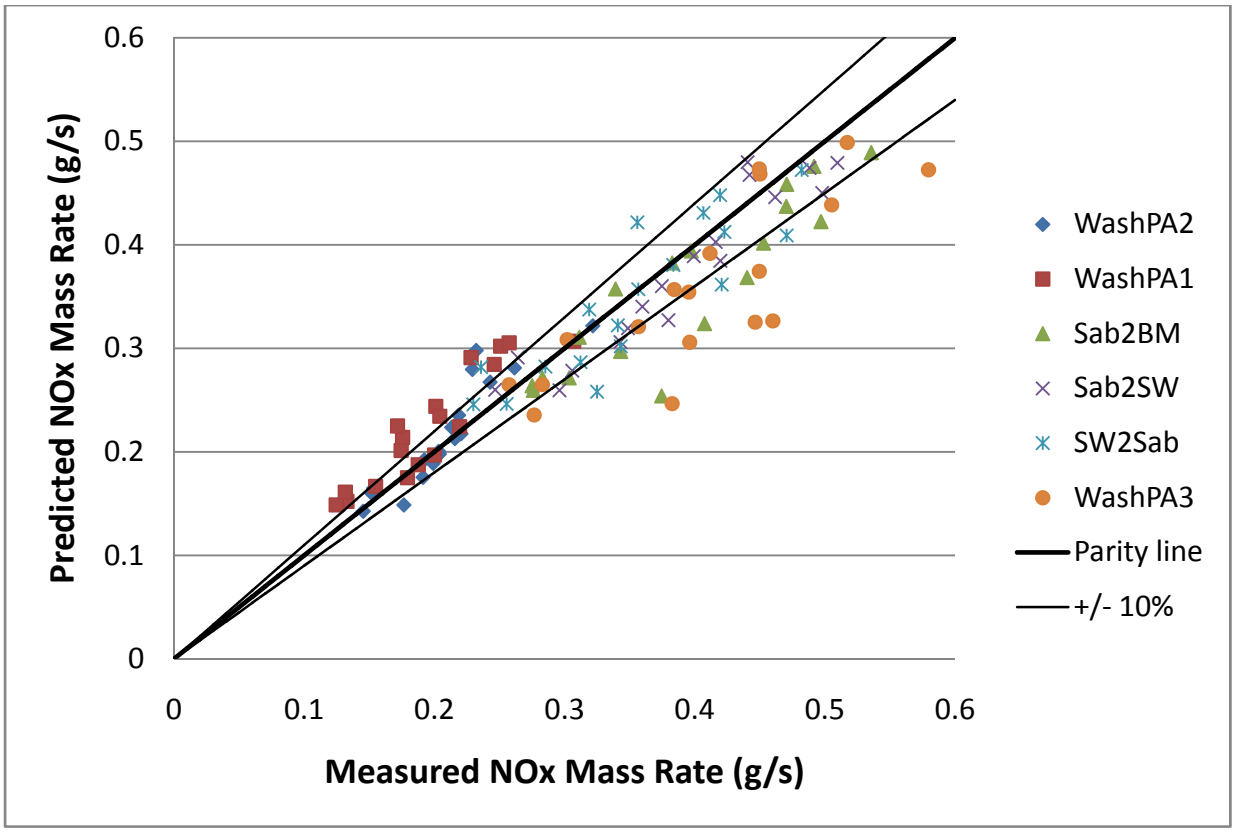

Figure 49 Parity plot of NOx mass rate prediction for eighteen trucks using Idle and BM2Sab as baseline routes, and AvPosRLP as metric

Table 34 Average baseline route weights, bias and error for predicted routes using AvPosRLP as metric, and baseline routes Idle and BM2Sab

Predicted Route	w (idle)	w (BM2Sab)	Bias (%)	Error (%)
WashPA2	0.21	0.79	3.07	7.29
WashPA1	0.19	0.81	13.90	14.33
Sab2BM	-0.38	1.38	-8.38	8.97
Sab2SW	-0.45	1.45	-3.81	7.20
SW2Sab	-0.35	1.35	-1.05	8.16
WashPA3	-0.38	1.38	-11.37	13.00

6.3.4 NOx Mass Rate Predictions Using Three Baseline Routes

The modeling methodology was applied to in-use data using all the possible combinations of three baseline routes and two route properties to generate linear models to predict the remaining five routes. The results were analyzed using the average of absolute percentage error as the main parameter to measure goodness of fit between predicted and measured values. A histogram showing the distribution of error for a total of 14,747,040 total predictions is presented in Figure 50. When compared with the results obtained using two baselines cycles, adding a third baseline cycle reduced the frequency of errors below 20%, from 30% to 28%.

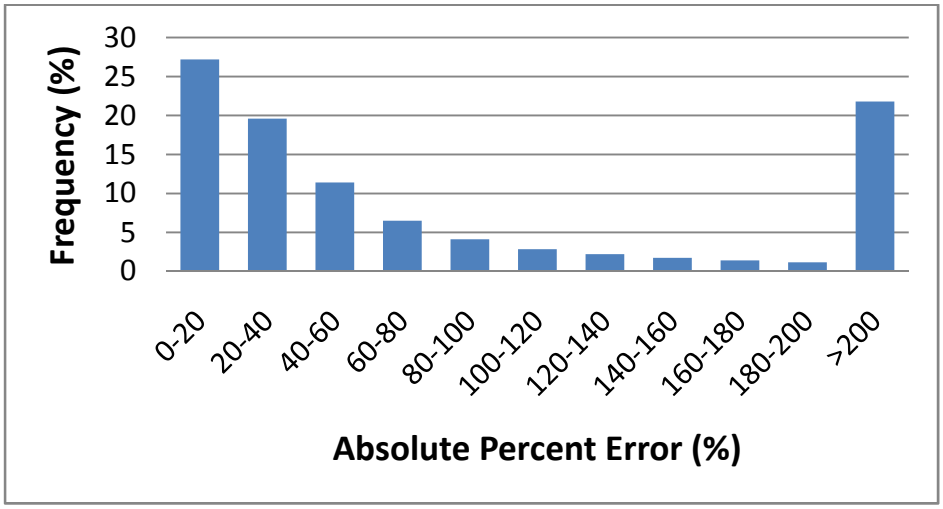

Figure 50 Distribution of error for NOx prediction for eighteen trucks using three baseline cycles

An error matrix was obtained using Excel pivot tables. Matrix columns represent baseline route combinations and matrix rows represent routes' properties combinations. The error matrix was further processed by using Section 5.4 MATLAB routine to identify the columns and rows that consistently produced results with errors below a threshold of 10%. Table 35 shows the error matrix after data processing.

The addition of a third baseline route to the model increased predictive accuracy as presented in Table 35. Average percentage errors of about 8% were obtained (errors of about 17% were obtained when using two baseline routes). Average positive road load power is present in all the combinations and seems to be the metric of choice for translation of NOx emissions rates between different driving routes. Figure 51 shows the distribution of prediction errors for each metrics combinations in Table 35. The

results are similar to each other suggesting that the resulting models are more sensitive to the values of AvPosRLP than to the values of the accompanying metric.

Table 35 Average absolute percentage error (%) of predicted NOx for eighteen trucks using three baseline routes with a 10% threshold value

			Baseline Routes					
			Idle WashPA1 Sab2SW	Idle WashPA1 Sab2BM	Idle WashPA1 SW2Sab	Idle WashPA2 Sab2SW	Idle WashPA2 Sab2BM	*AVERAGE*
Route Properties	**AvPosRLP**	**AvPosAcc**	7.48	7.16	8.35	9.10	8.61	***8.14***
	AvPosRLP	**StdAcc**	7.54	8.07	8.59	8.64	9.27	***8.42***
	AvPosRLP	**RmsAcc**	7.54	8.07	8.59	8.64	9.27	***8.42***
	AvPosRLP	**CovPosAcc**	8.19	7.45	8.86	9.76	8.45	***8.54***
	AvPosRLP	**PercAcc**	8.43	8.85	8.96	8.42	9.34	***8.80***
	AvPosRLP	**CovRLP**	8.30	9.09	8.72	8.55	9.53	***8.84***
	AvPosRLP	**FreqAccT**	8.17	9.25	8.80	8.74	9.35	***8.86***
	AvPosRLP	**FreqAccD**	8.00	9.19	8.86	8.68	9.74	***8.89***
	AvPosRLP	**RPS**	8.30	9.20	8.97	8.42	9.58	***8.89***
	AVERAGE		***7.99***	***8.48***	***8.74***	***8.77***	***9.24***	***8.64***

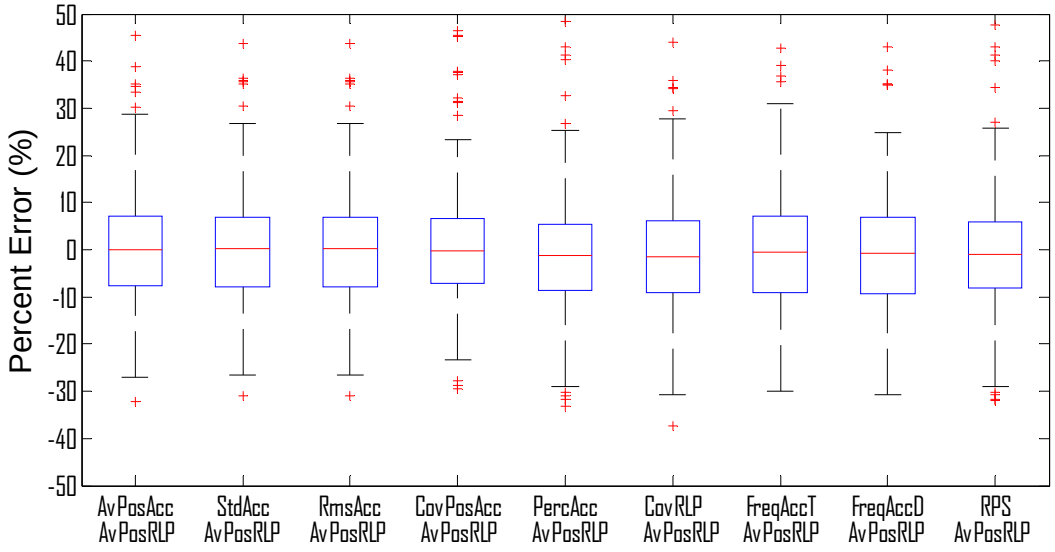

Figure 51 Box plots showing distribution of percent error for NOx mass rate predictions for eighteen trucks using different metrics

Figure 52 shows a parity plot with the results obtained when using the case with lowest error in Table 35. No apparent bias was observed (except for WashPA2 route) and 75 out of 90 predictions were within the ±10% error boundaries. Average weight coefficients, bias and percent errors for each predicted route are presented in Table 36. Considerable bias was observed for the prediction of WashPA2 (suburban-highway) route. However, the average prediction errors are about the same value of estimated run-to-run variability (COV) of the data (8.6%). WashPA2 and BM2Sab (significant grade, highway) are the worst and best predicted routes, respectively. Interestingly both routes correspond to interpolations, as shown by their positive weight coefficients.

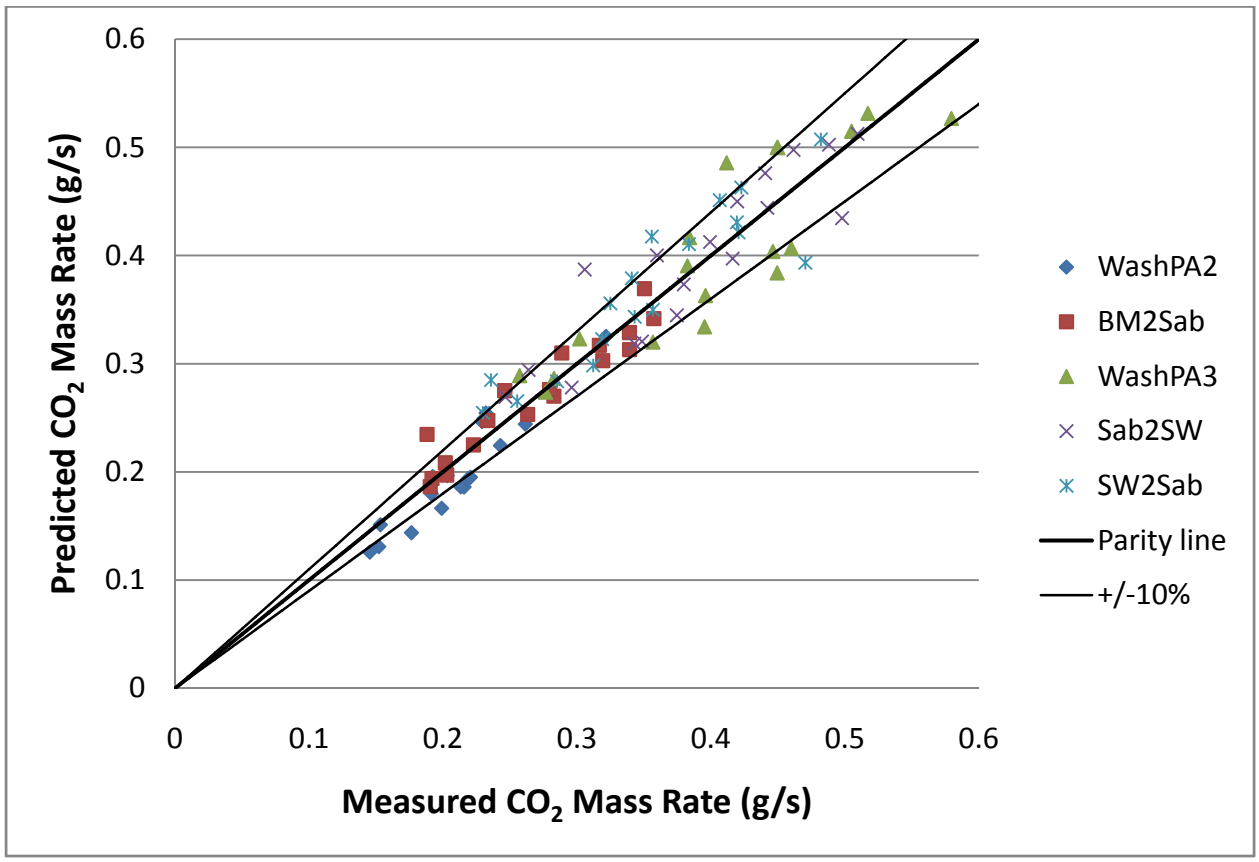

Figure 52 Parity plot of NOx mass rate prediction for eighteen trucks using Idle, WashPA1, and Sab2BM as baseline routes, and RLP and AvPosAccl as metrics

Table 36 Average baseline route weights, bias and error for predicted routes

Predicted Route	w (Idle)	w (WashPA1)	w (Sab2BM)	Bias (%)	Error (%)
WashPA2	0.07	0.88	0.05	-6.34	8.79
BM2Sab	0.07	0.50	0.43	1.52	5.33
Sab2SW	-0.18	0.31	0.87	2.29	7.61
SW2Sab	-0.09	0.29	0.81	4.88	7.45
WashPA3	0.13	-0.32	1.19	-0.21	8.67

6.3.5 Effects of Including Grade-Related Properties

For in-use data, all the suitable combinations of metrics included at least one metric with grade information. Figure 53 show parity plots of 540 CO_2 mass rate predictions for two different approaches. The first approach uses driving speed and average positive acceleration as suggested by a previous research (Delgado et al., 2012). The second approach includes grade information using average road load power and characteristic acceleration. The inclusion of grade improved the predictive capabilities of the model, decreasing the average percent error from 10.4% to 3.7% for the 540 predictions. Figure 54 show parity plots of 540 NOx mass rate predictions for two different approaches. The first approach does not include grade information by using average driving speed and average positive acceleration. The second approach includes grade information using average road load power and average positive acceleration. The inclusion of grade improved the predictive capabilities of the model, decreasing the average percent error from 21.7% to 8.1%. In both figures (53 and 54) a best fit line is shown along with a regression coefficient. It is evident that topography is a very important factor in determining fuel use and NOx emissions for HD vehicles and grade information should be included in the predictive models to improve their accuracy.

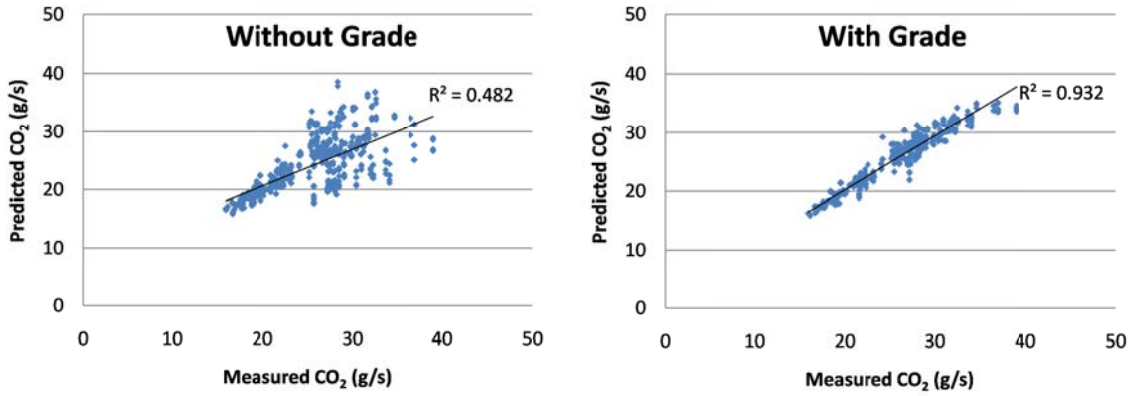

Figure 53 Effects of using grade related metrics in fuel consumption predictions

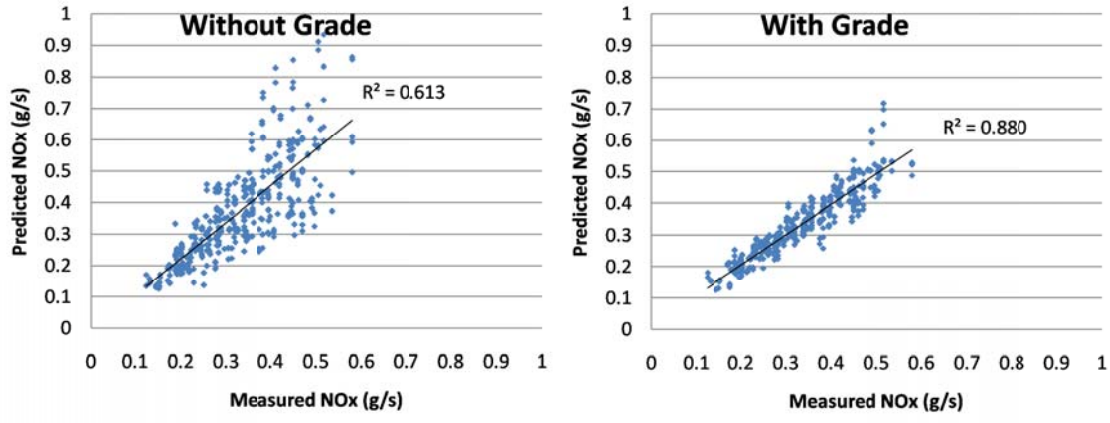

Figure 54 Effects of using grade related metrics in NOx predictions

6.4 Model Comparison to GEM-Generated Fuel Consumption Data

The GEM version 1.0, an open source MATLAB/Simulink-based program, was available for download from the EPA's website at the moment of writing (circa 2012). While version 1.0 was used for this part of the study, version 2.0 (which is an executable program, and is not open source) is used in the final EPA/NHTSA GHG rule. GEM 2.0 incorporates additional test data including a new driver model, a simplified electrical system model, and revised engine fuel maps that better characterize MD and HD vehicles. Additional details of the model can be found elsewhere (Lee et al., 2011). Figure 55 shows the graphic user interface (GUI) for the GEM model v1.0.

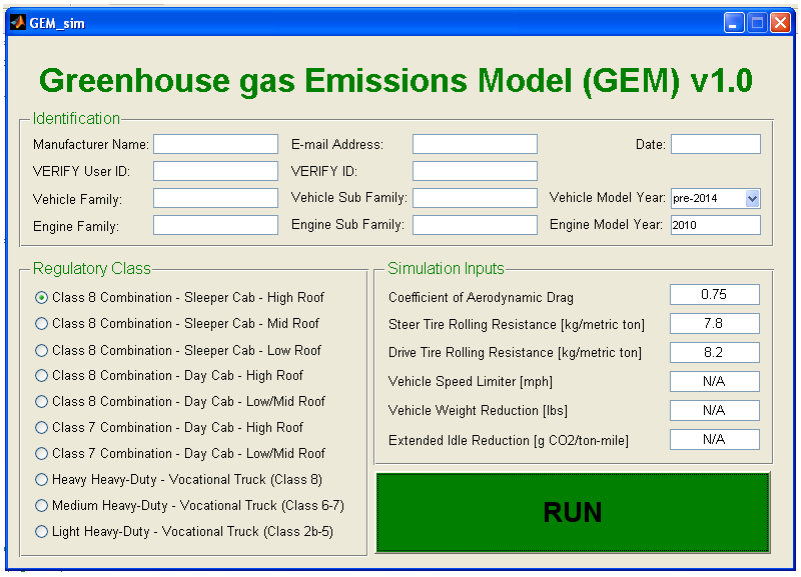

Figure 55 GEM graphical user interface (US EPA, 2010d)

EPA has programmed GEM with predefined parameters such as electric loads, engine maps, transmission configurations, and vehicle parameters for twelve regulatory subcategories. The regulatory class selected for this analysis was a Class 8 combination truck, sleeper cab, and high roof. GEM model uses a predefined 15L engine fuel consumption map. The vehicle parameters used for simulation are summarized in Table 37[63]. A baseline 2010 model year was selected for analysis. The truck was simulated over eighteen different driving cycles[64] to generate fuel consumption data. Table 38 presents the simulated cycles, relevant properties, and the results of the simulations.

Table 37 GEM baseline 2010 Class 8 truck vehicle parameters

GEM Vehicle Parameter	
Vehicle Model Year	2010
Engine Model Year	2010
Coefficient of Aerodynamic Drag	0.75
Steer Tire Rolling Resistance (kg/ton)	7.8
Drive Tire Rolling Resistance (kg/ton)	8.2

[63] GEM assumes a frontal area of 10.4m^2 for Class 8, sleeper cab, high roof for a C_DA=7.8m^2. Vehicle total weight is 70,500lbs.

[64] The seventeen cycles described in Table 15, Section 5.1 plus the Creep and Cruise modes of the Heavy-Duty Diesel Truck Schedule (HHDDTS). Idle cycle was not simulated. Speed-time traces are available in Appendix B.

The last column of Table 38 indicates the percentage of time that the simulated speed failed to be within 2mph from the target speed. Note that some cycles were more difficult to follow by the simulated GEM model driver. Figure 56 shows demanded and actual speed for the NYBus cycle. This cycle presented differences between target and simulated speed values higher than 2mph for 10.9% of the simulated time. Simulations of cycles such as CRUISE (Figure 57) or COMM followed the target speed-time trace without deviations higher than 2mph.

Table 38 GEM-simulated fuel consumption for a baseline 2010 Class 8 truck over nineteen driving cycles

Cycle	Cycle Properties				Simulation Results			
	AvSpeed (mph)	AvPosAcc (mph/s)	AvPosRLP (kW)	Distance (mi)	Fuel Economy (mpg)	CO_2 (g/ton-mile)	CO_2 (g/s)	% time missed by 2mph
ART	26.59	1.01	96.72	1.99	2.74	195.80	27.47	10.66
Beeline	14.19	0.91	52.36	6.80	2.40	222.87	16.69	10.11
BRAUN	13.95	0.86	45.18	6.74	2.47	217.18	15.99	9.55
CBD	12.33	0.98	38.44	2.01	2.27	236.31	15.37	5.85
COMM	46.34	0.52	110.89	3.99	5.52	97.07	23.74	0.00
CSHVC	13.58	0.56	34.77	6.72	3.20	167.62	12.02	0.45
ETCURBAN	14.18	0.54	30.91	2.36	3.64	147.01	11.00	2.45
KCM	23.42	0.78	65.50	12.78	3.29	162.98	20.15	6.24
Manhattan	6.74	0.75	23.11	2.35	1.85	288.90	10.27	5.62
NYBus	3.68	0.69	13.14	0.61	1.36	394.84	7.67	10.90
NY-Comp	8.76	0.35	15.96	2.50	2.28	234.72	10.86	2.05
OCTA	12.07	0.76	36.99	6.54	2.49	214.86	13.69	6.56
PARIS	6.62	0.66	19.16	3.51	1.98	270.87	9.46	3.31
UDDS	18.81	0.39	44.69	5.54	3.70	144.80	14.37	3.39
TRANS	14.90	0.50	37.81	2.85	3.50	153.30	12.05	0.92
WMATA	8.34	0.70	26.31	4.26	2.46	217.51	9.57	2.33
CREEP	1.64	0.19	2.04	0.12	2.18	246.22	2.13	1.32
CRUISE	39.86	0.20	78.54	23.06	6.36	84.18	17.72	0.00

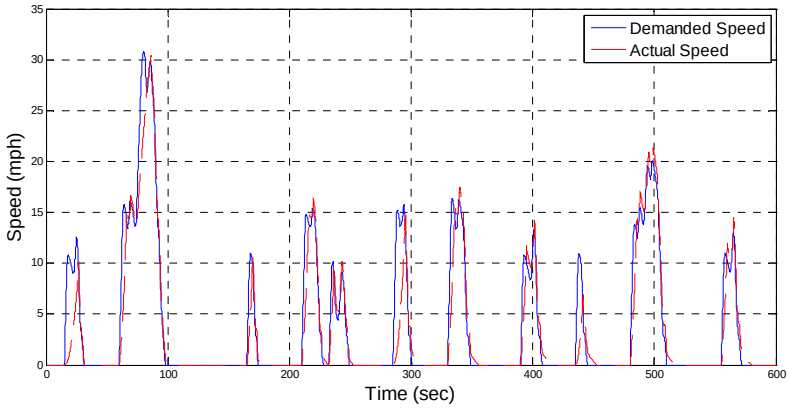

Figure 56 Actual and demanded speed for NYBus cycle[65]

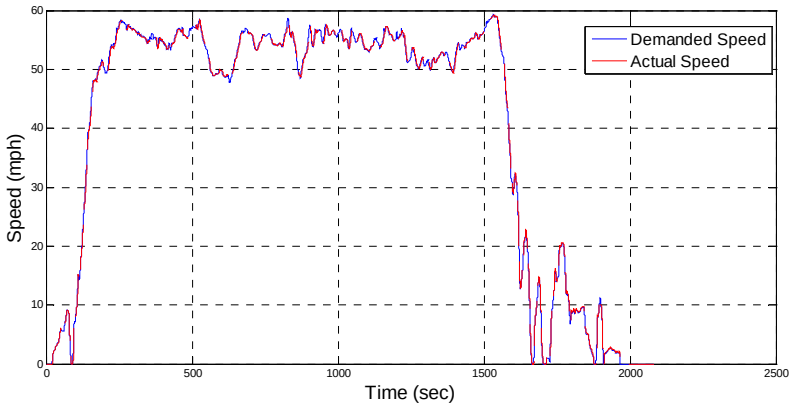

Figure 57 Actual and demanded speed for CRUISE cycle[66]

The obtained fuel consumption data was used to challenge the linear interpolation model. The main objective was to demonstrate if the modeling methodology could be used in conjunction with dynamic vehicle models to help fill possible information gaps and to reduce simulation computational time and avoiding the need to perform simulations for each and every type of vehicle activity. As an example, if one hundred of dynamic vehicle simulations would need to be performed for diverse vehicle activities, the requirements may be reduced by using the linear interpolation methodology by using the results of only three dynamic simulations to predict the remaining 97 vehicle activities. With this in mind, a linear interpolation model was generated using average road load power and average acceleration as

[65] 10.9% time missed by 2mph.

[66] 0% time missed by 2mph.

properties. The GEM-simulated Idle, OCTA, and KCM cycles were used as baseline cycles and the remaining 16 cycles were predicted. Figure 58 shows a parity plot showing the prediction results. The results are encouraging since the model was able to translate fuel consumption between different simulated driving activities within 10% error for 16 out of 19 simulated cycles, with an average percentage error of 8.8%.

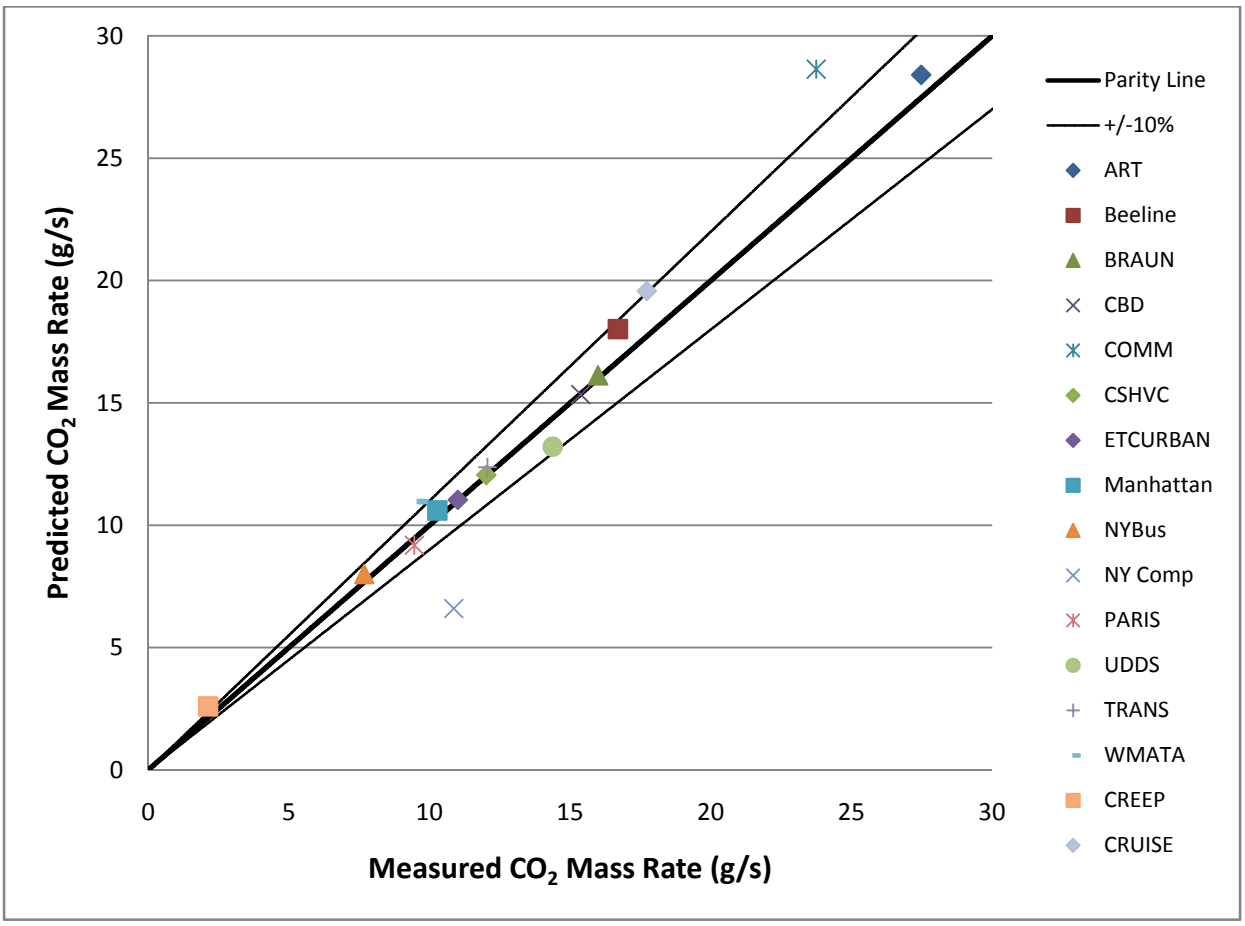

Figure 58 Parity plot of fuel consumption prediction using Idle, OCTA, and KCM as baseline cycles, and AvPosRLP and AvPosAccl as metrics

Among the cycles that failed to be predicted within 10% error, COMM cycle (with the highest value of AvPosRLP in Table 38) was identified as being outside the region of safe extrapolation, with one of its weight coefficients absolute values being higher than three (w_{IDLE}=0.42, w_{KCM}=3.13, w_{OCTA}=-2.55). The CREEP and NY-Comp cycles also failed to produce predictions within 10%, with errors of about 22% and 40%, respectively. Note that CREEP cycle property values in Table 38 are the lowest of the cycles used for this part of the study. NY-Comp cycle has similar CO_2 mass rate to cycles such as ETCURBAN or Paris,

but it has low property values with respect to them. These facts caused NY-Comp CO_2 mass rate to be under predicted.

6.5 Expected Benefits and Outcomes

The linear interpolation technique may support regulatory policy programs as well as estimating future emissions inventories. It allows estimation of emissions for new or "unseen" driving activity on the basis of a limited number of measurements. It can also be used to translate emissions and fuel consumption between diverse types of activity, avoiding the need to re-test vehicles.

With the level of accuracy achieved so far (prediction error values close to the values of the test-to-test measurement variations), the requirement to test vehicles according to representative cycles (aimed at reproducing real world operating conditions) can be reduced. A number of baseline test cycles would be enough to reproduce emissions and fuel consumption for a broad range of vehicle activity. In this way, a unique set of driving cycles can be used by regulatory agencies to test different configurations of HD vehicles, and then apply a different weighting of the emissions results depending on vehicle vocation. The technique may support regulatory programs reducing the number of test to perform and allowing the harmonization of emission databases that were created using different test cycles. The method can also be used by transit and fleet operators to evaluate fuel consumption benefits as a result of changes in routing or to estimate their emissions profile or footprint.

Sophisticated engine and emissions control technologies used to meet stricter emissions and fuel efficiency regulations (2007 and newer vehicles) are going to be difficult to simulate using pure simulation with complete vehicle models such as GEM because new models should be developed and validated. The approach discussed in this study may simplify regulations, without the need to develop new models to accommodate for newer technologies[67]. Testing is still going to be necessary in the future. In-use measurements are going to be useful to capture the constantly evolving duty cycle of different applications and a combination of limited vehicle testing with the linear interpolation modeling approach may prove more effective than use of pure simulation.

[67] Use of Selective Catalytic Reduction active aftertreatment systems will very likely confound NOx prediction with this approach due to their dependence on thermal conditions of the system.

Other advantages of the technique with respect to other models are:

The technique avoids the use of specialized software or time consuming computational routines. Calculations are relatively simple and can be implemented using a spreadsheet or even by "paper and pencil hand calculations."

The inputs to the model are cycle-averaged (or route-averaged) emissions and cycle (or route) properties. These inputs are more readily available than detailed component models required for other types of model (e.g. dynamic vehicle simulators). By using averages, the model also avoids the use of second-by-second emissions data which have to be time-aligned with second-by-second power to account for possible delays while the exhaust gases are transported through the measurement systems.

When all the obtained weighting factors are positive, their values provide a more physically meaningful weighting of test cycles than weightings values provided in some regulations (e.g. the harmonic averaging of 55% city and 45% highway operation for light-duty CAFE regulations).

6.6 Model Limitations

The author has found the following limitations of the modeling methodology:

The accuracy of the modeling approach depends heavily on the baseline cycles (or routes) and the properties being used. Knowledge of the level of accuracy that can be expected and the amount of extrapolation that can be managed by the model are important for reliable predictions. Good engineering judgment is needed in analyzing the data.

When results are reported on a trip average basis, typical driving cycle data cannot be used to evaluate emissions at a higher temporal resolution. This modeling approach cannot be used for the same purposes of microscopic models because it cannot (or has not been shown to) produce second-by-second emissions or fuel consumption data.

The technique has been verified for individual vehicles. Application of the technique to a group of vehicles with similar characteristics has yet to be done and is expected to produce less accurate predictions than when applied to individual vehicles.

Because of their transient nature, pollutant emissions like PM, THC or NMHC, and CO may be difficult to capture with this kind of modeling.

This approach may simplify actual fuel economy testing, but would still require prior knowledge of duty cycles for the various major types of MD and HD vehicles. In order to develop appropriate weighting factors for each application in-use testing may prove useful to capture the real world duty cycles of different applications such as transit buses, delivery vehicles, utility service trucks, refuse trucks, and long-haul tractor trailers.

If the proposed methodology is to be used with regulatory purposes, negative weights would be a potential issue because vehicle manufacturers (or any other groups that are subject to regulation) may "cheat" the model by creating artificial emissions and additional fuel consumption in the baseline cycles with negative weights. Potential "gaming" on any specific cycle/route would be diminished if negative weights are avoided. This can be accomplished by selecting baseline cycles that cover sufficiently wide range of vehicle operation, and thus minimizing extrapolation.

6.7 Guidelines for Appropriate Selection of Baseline Cycles or Routes

A given baseline cycle is not "good" or "bad" by itself. Rather, it is the combination of individual baseline cycles and metrics that makes the predictive approach suitable or not. However, the following guidelines are proposed to select appropriate test cycles or in-use routes to be used with the linear interpolation methodology.

Number of baseline cycles/routes

Based on the results discussed in Section 6.1, in order to minimize testing requirements and at the same time obtain accurate predictions, the recommended number of baseline cycles or routes to include in the model is three. Addition of dimensions to the model will complicate it and will reduce the interpolation region with respect to the whole space (see Section 3.5).

Idle information

Results showed that inclusion of idle information as a baseline cycle or route produced satisfactory results. Idle represents the minimum amount of activity possible, as well as the expected minimum emission rates[68]. In this way, the idle cycle or route acts as the intercept for the linear model.

Avoid or minimize extrapolation

The baseline cycles or routes should cover a wide range of operation. Ideally, all the predicted cycles should be inside the envelope of operation (e.g. their properties should be between the minimum and maximum values of the baseline properties). Weight coefficient values can be used as a quantitative measure of extrapolation. Based on the results so far, weight coefficients with absolute values larger than three (3) should be avoided.

Use independent cycles

Use of linearly independent cycles or routes will avoid ill-posed models. Linear dependency/independency depends on the relative values of the properties. If two properties are used, it will be advantageous to select baseline activity with relative metrics values opposite to each other. For example, it is better to use a baseline cycle with relatively low speed and high acceleration and another baseline cycle with relatively high speed and low acceleration than using one baseline cycle with relatively low speed and low acceleration and another baseline cycle with relatively high speed and relatively high acceleration. The former case will avoid baseline cycles to be multiple of each other (i.e. linearly dependent).

A decision-making structure (flowchart) is presented in Appendix D as a reference guide for application of the modeling methodology and summarizes the findings and contributions of this study. Testing type is divided between chassis dynamometer and in-use for the prediction of fuel consumption (CO_2 emission as surrogate) and NOx emissions. The "best" combinations of properties (as observed for the data sets used in this study) are presented for each case. Users of this model should be able to obtain accurate predictions for fuel consumption and NOx emissions from MD and HD diesel-fueled on-road vehicles using the decision structure with the flow chart. If the engine technology is different from

[68] Knowledge of idle emissions will be also useful for the specific case of combination trucks equipped with sleeper cabs because these vehicles usually idle for long periods of time in order to provide cabin hotel loads.

diesel, a study of metrics and cycles/routes for the specific technology should be performed. Additionally, newer technology such as selective catalyst reduction for diesel NOx control, as well as prediction of other pollutants should be explored as new data become available.

7 Conclusions and Recommendations

A model was extended to predict HD vehicle fuel consumption and NOx emissions employing chassis dynamometer data and in-use data gathered with PEMS. Data for five transit buses tested over up to 17 chassis dynamometer cycles, and data for 18 over-the-road HD trucks over up to eight in-use routes were used for model development and validation.

7.1 Conclusions

It was determined that when suitable metrics and baseline activity are used, the model is able to predict NOx within 10% of the measured values and CO_2 within 5% of the measured values. These percentage differences between measured and the predicted emissions values are on the same level of the variance in measured emissions between repeated chassis or in-use tests.

It was found that the modeling methodology should be implemented using three baseline cycles or routes. Three is recommended number of baseline tests to perform since no significant gains in accuracy are expected when using additional baseline activity.

Average road load power was identified as a suitable property to be used with in-use data. This property consistently produced predictions with average errors near the measurement run-to-run variations for both NOx and CO_2 emissions.

It was demonstrated that the model could be successfully applied to in-use data gathered with PEMS. Topography is a very important factor in determining fuel use and emissions for HD vehicles. Fuel consumption predictive accuracy improved from 10.4% to 3.7% and NOx mass rate predictive accuracy improved from 21.7% to 8.1% when including grade information into the model. The use of in-use measurements including grade information can generate a new approach for emissions inventory allowing users to access real-world emissions from a vehicle that is operated over a roadway route that is very different from the chassis dynamometer test schedules usually used for emission characterization.

The method was challenged using fuel consumption simulation data from a dynamic vehicle simulator (GEM). The method was able to predict 16 out of 19 simulated cycles within 10% error, with an average

absolute error of 8.8%. The model can be used in conjunction with more detailed models to save simulation time and to fill possible gaps of information instead of performing simulations for each possible application and vehicle class.

7.2 Recommendations for Future Work

As more in-use data becomes available for present technology vehicles, the modeling methodology should be validated and updated accordingly. Additional data are needed for the various MD and HD vocations and technologies.

Use of shorter pieces of vehicle activity would provide additional opportunities (even less tests requirements and shorter scale applications). For example, a unique driving cycle or route could be broken up into short trips (microtrips) related to specific types of driving activity. In this way a single test could be performed to extract all the baseline activity needed to generate the model. It is recommended that future work be conducted to estimate the minimum time window or route length that is required for this method to be satisfactory implemented.

Explore the potential of use of the model to include new technologies like selective catalytic reduction (SCR) and other advanced aftertreatment systems for post 2007 model year MD and HD vehicles. Alternative fuels such as compressed natural gas should be expanded for lean-burn and stoichiometric combustion engines. The method should be challenged using bio-derived fuels.

Theoretically, other influent factors (as weight, or accessory loads) can be added to the model at the cost of using an additional baseline cycle. Moreover, the method could be expanded to predict different emissions such as PM, ammonia (NH_3), N_2O, CH_4 and to define appropriate properties to make these predictions and to quantify the model's predictive capabilities.

8 References

Ahn, K., Rakha, H., Trani, A., and Van Aerde, M. (2002) "Estimating vehicle fuel consumption and emissions based on instantaneous speed and acceleration levels." Journal of Transportation Engineering, 128, 182-190.

Antonacci, G., Todeschini, I., and Cemin, A. (2008) "Influence of road gradient on emissions factors." Proceedings of 21st TFEIP Meeting, Milan, Italy.

Barlow, T.J., Latham, S., McCrae, I.S., and Boulter, P.G. (2009) "A reference book of driving cycles for use in the measurement of road vehicle emissions." TRL Limited. Published Project Report PPR354. Berkshire, England.

Barth, M., An, F., Norbeck, J., and Ross, M. (1996) "Modal emissions modeling: a physical approach." Transportation Research Record, 1520, 81-88.

Barth, M., G. Scora, and Younglove, T. (2004) "Modal emissions model for heavy-duty diesel vehicles." Transportation Research Record, 1880, 10–20.

Bedick, C.R. (2009) "Optimization of a retrofit urea-SCR System." Ph.D. Dissertation. West Virginia University, Morgantown, WV.

Bradley, R. (2000) "Technology roadmap for the 21st century truck program." US Department of Energy. Energy Efficiency and Renewable Energy. Report 21CT-001. Washington, DC.

Cappiello, A., Chabini, I., Nam, E., Abou-Zeid, M., and Lue, A. (2002) "A statistical model of vehicle emissions and fuel consumption." Proceedings 5th IEEE International Conference on Intelligent Transportation Systems, Singapore.

Cho, H.M. and He, B.Q. (2007) "Spark ignition natural gas engines – A review." Energy Conversion and Management, 48, 608-618.

Ciccarelli, T. and Toossi, R. (2002) "Assessment of hybrid configuration and control strategies in planning future metropolitan urban transit systems." Final Report, California State University, Long Beach, CA. Also available at: http://www.metrans.org/research/final/00-06_Final.pdf

Clark, N.N., Gautam, M., Bata, R.M., Wang, W.G., Loth, J.L., Palmer, G.M., and Lyons, D.W. (1995) "Design and operation of a new transportable laboratory for emissions testing of heavy-duty trucks and buses." International Journal of Vehicle Design, Heavy Vehicle Systems, 2, 308-322.

Clark, N.N., Tehranian, A., Jarrett, R.P., and Nine, R.D. (2002a) "Translation of distance-specific emissions rates between different heavy-duty vehicle chassis test schedules." SAE Technical Paper 2002-01-1754.

Clark, N.N., Kern, J.M., Atkinson, C.M., and Nine, R.D. (2002b) "Factors affecting heavy-duty diesel vehicle emissions." Journal of the Air & Waste Management Association, 52, 84-94.

Clark, N.N., Gajendran, P., and Kern, J.M. (2003) “A predictive tool for emissions from heavy-duty diesel vehicles.” Environmental Science & Technology, 37, 1, 7-15.

Clark, N.N., Khan, A.S., Wayne, W.S., Lyons, D.W., Gautam, M., McKain, D.L., Thompson, G.J., and Barnett, R. (2007a) “Weight effect on emissions and fuel consumption from diesel and lean-burn natural gas transit buses.” SAE Technical Paper 2007-01-3626.

Clark, N.N., Gautam, M., Wayne, W.S., Lyons, D.W., Thompson, G.J., and Zielinska, B. (2007b) “Heavy-duty vehicle chassis dynamometer testing for emissions inventory, air quality modeling, source apportionment and air toxics emissions inventory.” Coordinating Research Council Report E 55/59, Alpharetta, GA.

Clark, N.N., Vora, K.A., Wang, L., Gautam, M., Wayne, W.S., and Thompson, G. (2010) “Expressing cycles and their emissions on the basis of properties and results from other cycles.” Environmental Science & Technology, 44, 5986-5992.

Code of Federal Regulations (2008) “Emission standards and supplemental requirements for 2007 and later model year diesel heavy-duty engines and vehicles.” 40 CFR 86.007-11, Washington, DC.

Delgado, O.F., Clark, N.N., and Thompson, G.J. (2012) “Heavy-duty truck fuel consumption prediction based on driving cycle properties.” International Journal of Sustainable Transportation, 6, 1-24.

Delgado, O.F., Clark, N.N., and Thompson, G.J. (2011a) “Modeling transit bus fuel consumption on the basis of cycle properties.” Journal of the Air & Waste Management Association, 61, 443-452.

Delgado, O.F., Clark, N.N., and Thompson, G.J. (2011b) “Method for translation of in-use fuel consumption and NOx emissions between different heavy-duty vehicle routes.” Proceedings of the ASME 2011 Internal Combustion Engine Division Fall Technical Conference, Morgantown, WV.

Delgado, O.F., Clark, N.N., and Thompson, G.J. (2010) “Modeling heavy-duty vehicle fuel economy based on cycle properties.” 20th CRC On-road Vehicle Emissions Workshop, San Diego, CA.

Einewall, P., Tunestal, P., and Johansson, B. (2005) “Lean burn gas operation vs. stoichiometric operation with EGR and a three way catalyst.” SAE Technical Paper 2005-01-0250.

Energy Information Administration (EIA). (2011) “Annual Energy Outlook.” US Department of Energy, Washington, DC.

Federal Register. (1998) "Notice of filing of consent decree under the Clean Air Act." Federal Register, 63, 212, Office of the Federal Register, National Archives and Records Administration, Washington, DC.

Federal Register. (2009) “Fuel economy regulations for automobiles: technical amendments and corrections.” Federal Register, 74 226, Office of the Federal Register, National Archives and Records Administration, Washington, DC.

Fomunung, I., Washington, S., and Guensler, R. (1999) “A statistical model for estimating oxides of nitrogen emissions from light-duty motor vehicles.” Transportation Research Part D, 4, 333-352.

Frey, H.C., Unal, A., Chen, J., Li. S, and Xuan, X. (2002) “Methodology for developing modal emission rates for EPA’s multi-scale motor vehicle & equipment emission system.” US Environmental Protection Agency Document EPA-420-R-02-027, Washington, DC.

Frey, H.C., Rouphail, N.M., and Zhai, H. (2006) “Speed- and facility-specific emission estimates for on road light-duty vehicles based on real-world speed profiles.” Transportation Research Record, 1987, 128-137.

Frey, H.C., Rouphail, N.M., Zhai, H., Farias, T.L., and Goncalves, G.A. (2007) “Comparing real-world fuel consumption for diesel- and hydrogen-fueled transit buses and implication for emissions.” Transportation Research Part D, 12, 281-291.

Frey, H.C., Rouphail, N.M., and Zhai, H. (2008) “Link-based emission factors for heavy-duty diesel trucks based on real-world data.” Transportation Research Record 2058, 23–32.

Gajendran, P. (2005) “Development of a heavy-duty diesel vehicle emissions inventory prediction methodology.” Ph.D. Dissertation, West Virginia University, Morgantown, WV.

Gao, D.W., Mi, C., and Emadi, A. (2007) “Modeling and simulation of electric and hybrid vehicles.” Proceedings of the IEEE, 95, 4, 729–745.

Gautam, M., Clark, N.N., Thompson, G.J., Carder, D.K., and Lyons, D.W. (2000a) “Evaluation of mobile monitoring technologies for heavy-duty diesel-powered vehicle emissions.” Phase I Final Report Submitted to the Settling Heavy-Duty Diesel Engine Manufacturers, Department of Mechanical and Aerospace Engineering, West Virginia University, Morgantown, WV.

Gautam, M., Clark, N.N., Thompson, G.J., Carder, D.K., and Lyons, D.W. (2000b) “Development of in-use testing procedures for heavy-duty diesel-powered vehicle emissions.” Phase II Final Report Submitted to the Settling Heavy-Duty Diesel Engine Manufacturers, Department of Mechanical and Aerospace Engineering, West Virginia University, Morgantown, WV.

Gautam, G., Thompson, G.J., Carder, D.K., Clark, N.N., Shade, B.C., Riddle, W.C., and Lyons, D.W. (2001) “Measurement of in-use, on-board emissions from heavy-duty diesel vehicles: Mobile Emissions Measurement System.” SAE Technical Paper 2001-01-3643.

Giannelli, R., Nam, E., Helmer, K., Scora, G., Younglove, T., and Barth, M.J. (2005) “Heavy-duty diesel vehicle fuel consumption modeling based on road load and power train parameters.” SAE Technical Paper 2005-01-3549.

Gillespie, T. (1992) Fundamentals of Vehicle Dynamics. Society of Automotive Engineers, Warrendale, PA.

Genta, G. (1997) Motor Vehicle Dynamics: Modeling and Simulation. World Scientific Publications, Singapore.

Hiranuma, S., Takeda, Y., Kawatani, T., Doumeki, R., Nagasaki, K., and Tatsuya, I. (2003) “Development of DPF system for commercial vehicle – basic characteristic and active regenerating performance.” SAE Technical Paper 2003-01-3182.

Jimenez-Palacios, J.L. (1999) “Understanding and quantifying motor vehicle emissions with vehicle specific power and TILDAS remote sensing.” Ph.D. Dissertation, Massachusetts Institute of Technology, Cambridge, MA.

Karbowski, D., Delorme, A., and Rousseau, A. (2010) “Modeling the hybridization of a class 8 line-haul truck.” SAE Technical Paper 2010-01-1931.

Kern, J. M. (2000) “Inventory and prediction of heavy-duty diesel vehicle emissions.” M.Sc. Thesis, West Virginia University, Morgantown, WV.

Khan, A.S., Clark, N.N., Thompson, G.J., Wayne, W.S., Gautam, M., Lyon, D.W., and Hawelti, D. (2006) “Idle emissions from heavy-duty diesel vehicles: review and recent data.” Journal of the Air & Waste Management Association, 56, 1404-1419.

Koupal, J., Michaels, H., Cumberworth, M., Bailey, C., and Brzezinski, D. (2002) “EPA’s plan for MOVES: A comprehensive mobile source emissions model.” Proceedings of the 12th CRC On-Road Vehicle Emissions Workshop, San Diego, CA.

Koupal, J., Cumberworth, M., Michaels, H., Beardsley, M., and Brzezinski, D. (2003) “Design and implementation of MOVES: EPA’s new generation mobile source emission model.” EPA’s Annual Emission Inventory Conference, San Diego, CA.

Koupal, J., Landman, L., Nam, E., Warila J., Scarbro, C., Glover, E., and Giannelli, R. (2005) “MOVES 2004 energy and emission inputs.” US Environmental Protection Agency Document EPA-420-P-05-003, Washington, DC.

Lee, S., Lee, B., Zhang, H., Sze, C., Quinones, L., and Sanchez, J. (2011) “Development of greenhouse gas emission model for 2014-2017 heavy- and medium-duty vehicle compliance.” SAE Technical Paper 2011-01-2188.

Krishnamurthy, M. (2000) “Characterization of in-use emissions from on-highway heavy-duty diesel engines.” M.Sc. Thesis. West Virginia University, Morgantown, WV.

Krishnamurthy, M. (2006) “Development of predictive NOx model for on-road heavy-duty diesel engines.” Ph.D. Dissertation, West Virginia University, Morgantown, WV.

Lowell, D., Parsley, W., Bush, C., and Zupo, D. (2003) “Comparison of clean diesel buses to CNG buses.” Ninth Diesel Engine Emissions Reduction (DEER) Workshop, Newport, RI.

McCormick, R.L., Graboski, M.S., Newlin, A.W., and Ross, J.D. (1997) “Effect of humidity on heavy-duty transient emissions from diesel and natural gas engines at high altitude.” Journal of the Air & Waste Management Association, 47, 784-791.

McKain, D.L., Clark, N.N., Balon, T.H., Moynihan, P.J., Lynch, S.A., and Webb, T.C. (2000) "Characterization of emissions from hybrid-electric and conventional transit buses." SAE Technical Paper 2000-01-2011.

Melendez, M., Taylor, J., Zuboy, J., Wayne, W.S., and Smith, D. (2005) "Emission testing of Washington Metropolitan Area Transit Authority (WMATA) natural gas and diesel transit buses." Technical Report NREL/TP-540-36355, Golden, CO.

Morris, M. (2011) "Development of an artificial neural network to predict in-use engine emissions." Ph.D. Dissertation, West Virginia University, Morgantown, WV.

National Research Council (NRC) (2000) "Modeling mobile-source emissions." Committee to review EPA's mobile source emissions factor (MOBILE) model. National Academy Press, Washington, DC.

National Research Council (NRC) (2010) "Technologies and approaches to reducing the fuel consumption of medium- and heavy-duty vehicles." Committee to assess fuel economy technologies for medium- and heavy-duty vehicles, Transportation Research Board, Washington, DC.

Nine, R.D., Clark, N.N., Daley, J.J., and Atkinson, C.M. (1999) "Development of a heavy-duty chassis dynamometer driving route." Proceedings of the Institution of Mechanical Engineers, Part D, 213, 561–574.

Ntziachristos, L. and Samaras, Z. (2000) "COPERT III computer programme to calculate emissions from road transport. Methodology and emission factors (Version 2.1)." European Environment Agency, Technical Report No. 49, Copenhagen, Denmark.

O'Keefe, M.P., Simpson, A., Kelly, J., and Pedersen, D.S. (2007) "Duty cycle characterization and evaluation towards heavy hybrid vehicle applications." SAE Technical Paper 2007-01-0302.

Olsen, D.B., Kohls, M., and Arney, G. (2010) "Impact of oxidation catalysts on exhaust NO_2/NO_x ratio from lean-burn natural gas engines." Journal of the Air & Waste Management Association, 60, 867-874.

Petrushov, V.A. (1997) "Coast down method in time-distance variables." SAE Technical Paper 970408.

Portland State Aerospace Society (PSAS) (2004) "A quick derivation relating altitude to air pressure." Portland, OR. Also available at: http://psas.pdx.edu/RocketScience/PressureAltitude_Derived.pdf

Post, K., Kent, J.H., Tomlin, J., and Carruthers, N. (1984) "Fuel consumption and emission modeling by power demand and a comparison with other models." Transportation Research Part A, 18, 191-213.

Rakha, H., Kyoungha, A., and Trani, A. (2004) "Development of VT-Micro model for estimating hot stabilized light-duty vehicle and truck emissions." Transportation Research Part D, 9, 49–74.

Ramamurthy, R., Clark, N.N., Lyons, D.W., and Atkinson, C.M. (1998) "Models for predicting transient heavy-duty vehicle emissions." SAE Technical Paper 982652.

Shade, B.C. (2000) “A performance evaluation of the MEMS - An on-road emissions measurement system study.” M.Sc. Thesis, West Virginia University, Morgantown, WV.

Simpson, A.G. (2005) “Parametric modeling of energy consumption in road vehicles.” Doctoral Thesis, University of Queensland, Brisbane, Australia.

Smit R., Smoker R., Schoen, E., and Henseman, A. (2006) “A new modeling approach for road traffic emissions: VERSIT+LD – Background and methodology.” TTNO Report 06.OR.PT.016.1/RS, Delft, Netherlands.

Smit, R., Smoker, R., and Rab, E. (2007) “A new modeling approach for road traffic emissions: VERSIT+.” Transportation Research Part D, 12, 414–422.

Smith, E.D., Szidarovszky, F., Karnavas, W.J., and Bahill, A.T. (2008) “Sensitivity analysis, a powerful system validation technique.” The Open Cybernetics and Systemics Journal, 2, 39-56.

Society of Automotive Engineers (SAE) (1981) “Recommended practice truck and bus wind tunnel testing.” SAE Standard J1252, Warrendale, PA.

Society of Automotive Engineers (SAE) (2002) “Recommended practice for measuring fuel economy and emissions of hybrid-electric and conventional heavy-duty vehicles.” SAE Standard J2711, Warrendale, PA.

Sovran, G. and Blaser, D. (2003) “A contribution to understanding automotive fuel economy and its limits.” SAE Technical Paper 2003-01-2070.

Sydbom, A., Blomberg, A., Parnia, S., Stenfors, N., Sandstrom, T., and Dahlen, S.E. (2001) “Health effects of diesel exhaust emissions.” European Respiratory Journal, 17, 733-746.

Taylor, S.T., Clark, N.N., Gautam, M., and Wayne, W.S. (2004) “Diesel emissions prediction from dissimilar cycle scaling.” Journal of Automobile Engineering, 218, 341-352.

Thompson, G.J., Atkinson, C.M., Clark, N.N., Long, T.W., Hanzevack, E. (2000) “Neural network modeling of the emissions and performance of a heavy-duty diesel engine.” Proceedings of the Institution of Mechanical Engineers, Part D: Journal of Automobile Engineering, 214, 2, 111-126.

Thompson, G.J., Clark, N.N., Atkinson, R.J., Luzader, Z., VanScoy, F.L., Baker, V., and Chandler, J. (2004) “Development of an interface method for implementing road grade in chassis dynamometer testing.” ASME Internal Combustion Engine Division Fall Technical Conference, Long Beach, CA.

Thompson, G.J., Carder, D.K., Clark, N.N., and Gautam M. (2008) “Summary of in-use NOx emissions from heavy-duty diesel engines.” Journal of Commercial Vehicles, 117, 162-184.

Tóth-Nagy, C., Conley, J.J., Jarrett, R.P., and Clark. N.N. “Further validation of artificial neural network-based emissions simulation models for conventional and hybrid electric vehicles.” Journal of the Air & Waste Management Association 56, 7, 898-910.

Traver, M.L., Atkinson, R.J., and Atkinson, C.M. (1999) “Neural network-based diesel engine emissions prediction using in-cylinder combustion pressure.” SAE Technical Paper 1999-01-1532.

US Environmental Protection Agency. (US EPA) (1980) "Passenger car fuel economy: EPA and road." US Environmental Protection Agency Document 460/3-80-010, Washington, DC.

US Environmental Protection Agency. (2001) “EPA’s new generation mobile source emissions model: initial proposal and issues.” US Environmental Protection Agency Document EPA420-R-01-007, Washington, DC.

US Environmental Protection Agency. (2002) “Draft design and implementation plan for EPA’s multi-scale motor vehicle and equipment emission system (MOVES).” US Environmental Protection Agency Document EPA420-P-02-006, Washington, DC.

US Environmental Protection Agency. (2004a) “Advanced technology vehicle modeling in PERE.” US Environmental Protection Agency Document 420-D-04-002, Washington, DC.

US Environmental Protection Agency. (2004b) “Smartway transport partnership overview.” US Environmental Protection Agency Document 420-F-02-052, Washington, DC.

US Environmental Protection Agency. (2005) “Fuel consumption modeling of conventional and advanced technology vehicles in the Physical Emission Rate Estimator (PERE).” US Environmental Protection Agency Document 420-P-05-001, Washington, DC.

US Environmental Protection Agency. (2008) “Advance notice of proposed rulemaking: regulating greenhouse gas emissions under the clean air act.” US Environmental Protection Agency Document EPA-HQ-OAR-2008-0318, Washington, DC.

US Environmental Protection Agency. (2010a) “Inventory of US greenhouse gas emissions and sinks: 1990-2008.” US Environmental Protection Agency Document EPA-430-R-10-006, Washington, DC.

US Environmental Protection Agency. (2010b) “Technical guidance on the use of MOVES2010 for emission inventory preparation in state implementation plans and transportation conformity.” US Environmental Protection Agency Document EPA-420-B-10-023, Washington, DC.

US Environmental Protection Agency. (2010c) “MOVES2010 highway vehicle population and activity data.” US Environmental Protection Agency Document EPA-420-R-10-026, Washington, DC.

US Environmental Protection Agency. (2010d) “Greenhouse gas emission model (GEM) user guide.” US Environmental Protection Agency Document EPA-420-B-10-039, Washington, DC.

US Environmental Protection Agency and National Highway Traffic Safety Administration. (2011) “Regulatory impact analysis: final rulemaking to establish greenhouse gas emissions standards and fuel efficiency standards for medium- and heavy-duty engines and vehicles.” US Environmental Protection Agency Document EPA-420-R-11901, Washington, DC.

Vora, K.A., Clark, N.N., Nine, R.D., Gautam, M., Wayne, W.S., Thompson, G.J., and Lyons, D.W. (2004) "Correlation study of PM and NOx for heavy-duty vehicles across multiple drive schedules." SAE Technical Paper 2004-01-3022.

Wang, H. and Fu, L. (2010) "Developing a high-resolution vehicular emission inventory by integrating an emission model and a traffic model: Part 1—modeling fuel consumption and emissions based on speed and vehicle-specific power." Journal of the Air & Waste Management Association 60, 12, 1463-1470.

Wang, L., Clark, N., and Chen, P. (2010) "Modeling and validation of an over-the-road truck." SAE Technical Paper 2010-01-2001.

Wayne, W.S., Clark, N.N., Nine, R.D., and Rosepiler, S. (2002) "Washington metropolitan area transit authority diesel emissions control retrofit project." Final Report. West Virginia University, Morgantown, WV.

Wayne, W.S., Clark, N.N., Nine, R.D., Elefante, D. (2004) "A comparison of emissions and fuel economy from hybrid-electric and conventional drive transit buses." Energy & Fuels, 18, 257-270.

Wayne, W.S., Clark, N.N., Khan, A.S., Gautam, M., Thompson, G., and Lyons, D. (2008) "Regulated and non-regulated emissions and fuel economy from conventional diesel, hybrid-electric diesel, and natural gas transit buses." Journal of Transportation Research Forum, 47, 3.

Weinblatt, H., Dulla, R.G., and Clark, N.N. (2003) "Vehicle activity based procedure for estimating emissions of heavy-duty vehicles." Transportation Research Record, 1842, 64-72.

Wipke, K.B., Cuddy, M.R., and Burch, S.D. (1999) "ADVISOR 2.1: A user-friendly advanced powertrain simulation using a combined backward/forward approach." IEEE Transactions on Vehicular Technology, 48, 6, 1751-1761.

Wu, Y., Carder, D., Shade, B., Atkinson, R., Clark, N., and Gautam. M. (2009) "A CFR1065-compliant transportable/on-road low emissions measurement laboratory with dual primary full-flow dilution tunnels." Proceedings of ASME Internal Combustion Engine Division 2009 Spring Technical Conference, Milwaukee, WI.

Yanowitz, J., Graboski, M., and McCormick, R. (2002) "Prediction of in-use emissions of diesel vehicles from engine testing." Environmental Science and Technology, 36, 2, 270-275.

Yoon, S., Li, H., Jun, J., Ogle, J.H., Guensler, R.L., and Rodgers, M.O. (2005) "Methodology for developing transit bus speed-acceleration matrices for load-based mobile source emissions models." Transportation Research Record, 1941, 26-33.

Zervas, E. and Bikas, G. (2008) "Impact of the driving cycle on the NOx and particulate matter exhaust emissions of diesel passenger cars." Energy & Fuels, 22, 1707-1713.

Zhai, H., Frey, H.C., and Rouphail, N.M. (2008) "A vehicle-specific power approach to speed- and facility-specific emissions estimates for diesel transit buses." Environmental Science & Technology, 42, 7985-7991.

Zhang, K and Frey, H.C. (2006) “Road grade estimation for on-road vehicle emissions modeling using LIDAR data.” Journal of the Air & Waste Management Association, 56, 777-788.

Appendix A – Properties Definitions

a_i Acceleration at time step i

$\bar{a}_+$ Average positive acceleration

$\bar{a}_-$ Average negative acceleration

f Sample frequency

n Total number of observations

$n_{v>0}$ Total number of observations with positive speeds

$n_{a>0}$ Total number of observations with positive accelerations

$n_{a<0}$ Total number of observations with negative accelerations

N_{stops} Total number of stops

T Total cycle time

T_{idle} Total idle time (speeds less than 0.5mph)

$T_{a>0}$ Total time with positive accelerations

$T_{a<0}$ Total time with negative accelerations

$\bar{v}$ Average speed

v_i Instantaneous speed at time step i

v_{i-1} Instantaneous speed at time step i-1

x Total distance traveled

$$f = \frac{1}{\Delta t}$$

$$T = \frac{n}{f}$$

$$x = \int v_i \, dt \approx \frac{\sum v_i}{f}$$

1. Average Speed

$$AvSpeed = \bar{v} = \frac{1}{T}\int v_i \, dt \approx \frac{x}{T} \quad \text{[mph]}$$

2. Average Driving Speed

$$AvDriSpeed = \frac{1}{T}\int v_{i>0} \, dt \approx \frac{x}{T - T_{idle}} \quad \text{[mph]}$$

3. Relative Positive Speed

$$RPS = \frac{1}{x}\int v_{i,a>0}\, dt \approx \frac{\sum v_{i,a>0}}{x\, f} \qquad \text{[non dimensional]}$$

4. Relative Square Speed

$$RSS = \frac{1}{x}\int v_i^2\, dt \approx \frac{\sum v_i^2}{x\, f} \qquad \text{[m/s]}$$

5. Relative Positive Square Speed

$$RPSS = \frac{1}{x}\int v_{i,a>0}^2\, dt \approx \frac{\sum v_{i,a>0}^2}{x\, f} \qquad \text{[m/s]}$$

6. Relative Cubic Speed

$$RCS = \frac{1}{x}\int v_i^3\, dt \approx \frac{\sum v_i^3}{x\, f} \qquad [m^2/s^2]$$

7. Relative Positive Cubic Speed

$$RPCS = \frac{1}{x}\int v_{i,a>0}^3\, dt \approx \frac{\sum v_{i,a>0}^3}{x\, f} \qquad [m^2/s^2]$$

8. Average of Speed to the n Power (n from 1.5 to 4 in 0.5 increments)

$$AvSpeed^n = \frac{1}{T}\int v_i^n\, dt \qquad [mph^n]$$

14. Standard Deviation of Speed

$$StdSpeed = \sqrt{\frac{\sum_{i=1}^{n}(v_i - \bar{v})^2}{n-1}} \qquad \text{[mph]}$$

15. Coefficient of Variation of Speed

$$CovSpeed = \frac{StdSpeed}{AvSpeed} \times 100\% \qquad [\%]$$

16. Interquartile Range of Speed

$$IqrSpeed = 75th - 25th \qquad \text{[mph]}$$

17. Root Mean Square Speed

$$RmsSpeed = \sqrt{\frac{\sum v_i^2}{f\,T}}$$ [mph]

20. Average Acceleration

$$AvAccel = \bar{a} = \frac{1}{T}\int a_i\,dt$$ [mph/s]

21. Average Positive Acceleration

$$AbsPosAcc = \overline{a_+} = \frac{1}{T}\int a_+ dt \approx \frac{\sum a_{i,a>0}}{n}$$ [mph/s]

22. Average Negative Acceleration

$$AbsNegAcc = \overline{a_-} = \frac{1}{T_{a<0}}\int a_- dt \approx \frac{\sum a_{i,a<0}}{n_{a<0}}$$ [mph/s]

23. Average Acceleration Squared

$$AvAccel^2 = \overline{a^2} = \frac{1}{T}\int a_{i,a>0}^2\,dt$$ [mph^2/s^2]

24. Indicator factor

$$IF = \frac{1}{T}\sum\frac{a_i}{v_i}$$ [1/s]

25. Standard Deviation Acceleration

$$StdAccel = \sqrt{\frac{\sum_{i=1}^{n}(a_i-\bar{a})^2}{n-1}}$$ [mph/s]

27. RMS of Acceleration

$$RMSacc = \sqrt{\frac{\sum a_i^2}{f\,T}}$$ [mph/s]

32. Jerk

$$\overline{\frac{\partial a}{\partial t}} = \frac{\sum_{i=1}^{n}\frac{a_{i+1}-a_i}{\Delta t}}{n}$$ [mph/s^2]

33. Number of accelerations per unit distance

$$FreqAccD = \frac{Number\ of\ accelerations{>}2mph/s}{x} \quad [1/mile]$$

34. Number of accelerations per unit time

$$FreqAccT = \frac{Number\ of\ accelerations{>}2mph/s}{T} \quad [1/s]$$

35. Percent Time at Idle

$$PercIdle = \frac{100 \times T_{idle}}{T} \quad [\%]$$

36. Percent Time Accelerating

$$\mathrm{PercAccel} = \frac{100 \times \mathrm{T_{a>0}}}{\mathrm{T}} \quad [\%]$$

37. Percent Time Decelerating

$$\mathrm{PercAccel} = \frac{100 \times \mathrm{T_{a<0}}}{\mathrm{T}} \quad [\%]$$

38. Kinetic Intensity

$$KI = \frac{ChAccel}{RCS} \quad [km^{-1}]$$

39. Stops per unit distance

$$FreqStopsD = \frac{number\ of\ stops}{x} \quad [mile^{-1}]$$

40. Relative Positive Acceleration

$$RPA = \frac{1}{x}\int va\ dt \approx \frac{\sum v_i a_{i,a>0}}{x\ f} \quad [m/s^2]$$

41. Inertial Power Surrogate

$$IPS = \frac{1}{T}\int va\ dt \approx \frac{\sum v_i a_{i,a>0}}{n} \quad [m^2/s^3]$$

42. Positive Kinetic Energy

$$PKE = \frac{\sum(v_{i+1}^2 - v_i^2)_{for\ v_{i+1} > v_i}}{x}$$ [m/s²]

43. Inertial Power

$$InePow = \frac{1}{n}\sum_{i=1}^{n} m v_i a_i$$ [kW]

44. Rolling Resistance Power

$$RolPow = \frac{1}{n}\sum_{i=1}^{n} \mu m g v_i \cos\theta_i$$ [kW]

45. Drag Power Surrogate

$$DPS = \frac{1}{T}\int v^2 a\ dt \approx \frac{\sum v^2 a_{i,a>0}}{n}$$ [m³/s⁴]

46. Aerodynamic Resistance Power

$$AeroPow = \frac{1}{n}\sum_{i=1}^{n} 0.5 \rho C_D A v_i^3$$ [kW]

47. Aerodynamic and Rolling Resistance Power

$$AeroRolPow = AeroPow + RolPow$$ [kW]

48. Characteristic Acceleration

$$ChAccel = \frac{1}{x}\sum_{i=2}^{n} \left[\frac{1}{2}\left(v_i^2 - v_{i-1}^2\right) + g(h_i - h_{i-1})\right]^+$$ [m/s²]

49. Characteristic Power

$$ChPower = \frac{1}{T}\sum_{i=2}^{n} \left[\frac{1}{2}\left(v_i^2 - v_{i-1}^2\right) + g(h_i - h_{i-1})\right]^+$$ [W/kg]

50. Characteristic Energy

$$ChEnergy = \frac{1}{n}\sum_{i=2}^{n} \left[\frac{1}{2}\left(v_i^2 - v_{i-1}^2\right) + g(h_i - h_{i-1})\right]^+$$ [J/kg]

51. Average Positive Road Load Power

$$AvPosRLP = \frac{1}{n}\sum_{i=1}^{n}\left[\mu m g v_i \cos\theta_i + 0.5\rho C_D A v_i^3 + m v_i a_i + m g v_i \sin\theta_i\right]^+ \quad \text{[kW]}$$

52. Average Positive Vehicle Specific Power

$$AvPosVSP = \frac{1}{n}\sum_{i=1}^{n}\left[\frac{A\cdot v_i + B\cdot v_i^2 + C\cdot v_i^3}{m} + (a_i + g\sin\theta_i)\cdot v_i\right]^+ \quad \text{[W/kg]}$$

53. Petrushov Power

$$AvPet = \frac{1}{n}\sum_{i=1}^{n} A v_i + B {v_i}^2 + C {v_i}^3 \quad \text{[kW]}$$

56. Time Derivative of Road Load Power

$$\frac{dRLP}{dt} = \frac{\sum_{i=1}^{n}\frac{RLP_{i+1} - RLP_i}{\Delta t}}{n} \quad \text{[W/s]}$$

59. Average Positive Grade

$$AvPosGrade = \frac{1}{x}\int G_+ ds \approx \frac{1}{x}\sum_{G_i>0} G_i \cdot \Delta s_i \quad \text{[\%]}$$

60. Average Negative Grade

$$AvNegGrade = \frac{1}{x}\int G_- ds \approx \frac{1}{x}\sum_{G_i<0} G_i \cdot \Delta s_i \quad \text{[\%]}$$

61. Average Climb Rate

$$AvClimbRate = \frac{1}{T}\sum_{G_i>0} G_i \cdot \Delta s_i \quad \text{[m/s]}$$

62. Average Grade

$$AvGrade = \frac{1}{n}\sum_{v_i>0} G_i \quad \text{[\%]}$$

64. Average Ascent

$$AvAsc = \sum_{G_i>0}\frac{G_i\cdot\Delta s_i}{v_i\cdot\Delta t} \quad \text{[\%]}$$

65. Average Descent

$AvAsc = \sum_{G_i<0} \frac{G_i \cdot \Delta s_i}{v_i \cdot \Delta t}$ [%]

66. Altitude change per unit distance

$AltDist = \frac{\Delta h}{x} \times 100\%$ [%]

67. Grade Power

$GradePow = \frac{1}{n} \sum_{i=1}^{n} mgv_i \sin\theta_i$ [kW]

68. Other Metrics

$Acc^1Speed^3 = \frac{1}{T} \int v^3 a \, dt \approx \frac{\sum v^3 a_{i,a>0}}{n}$ [m^4/s^5]

$Acc^2Speed^1 = \frac{1}{T} \int v a^2 \, dt \approx \frac{\sum v a_{i,a>0}^2}{n}$ [m^3/s^5]

$Acc^2Speed^2 = \frac{1}{T} \int v^2 a^2 \, dt \approx \frac{\sum v^2 a_{i,a>0}^2}{n}$ [m^4/s^6]

$Acc^2Speed^3 = \frac{1}{T} \int v^3 a^2 \, dt \approx \frac{\sum v^3 a_{i,a>0}^2}{n}$ [m^5/s^7]

$Acc^3Speed^1 = \frac{1}{T} \int v a^3 \, dt \approx \frac{\sum v a_{i,a>0}^3}{n}$ [m^4/s^7]

$Acc^3Speed^2 = \frac{1}{T} \int v^2 a^3 \, dt \approx \frac{\sum v^2 a_{i,a>0}^3}{n}$ [m^5/s^8]

$Acc^3Speed^3 = \frac{1}{T} \int v^3 a^3 \, dt \approx \frac{\sum v^3 a_{i,a>0}^3}{n}$ [m^6/s^9]

Appendix B - Chassis Dynamometer Cycles

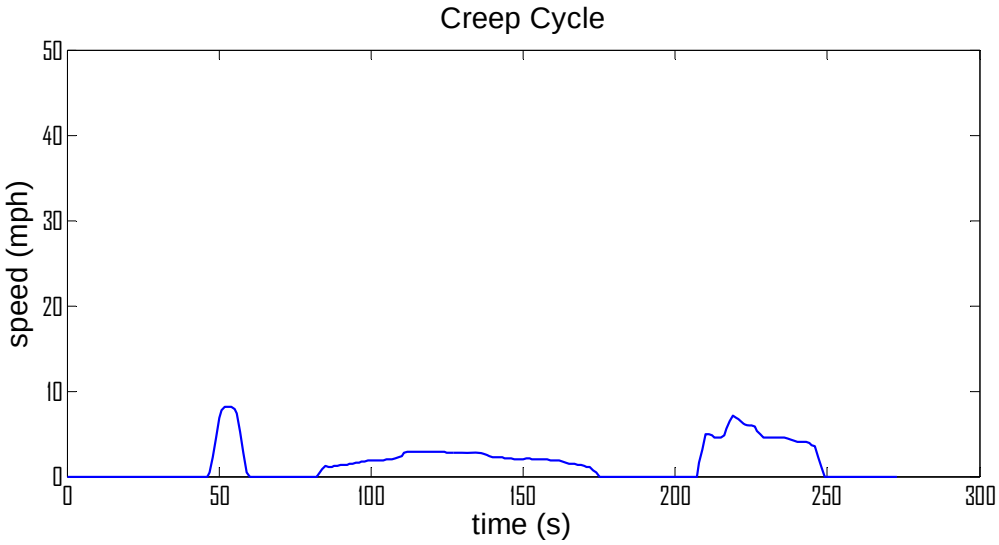

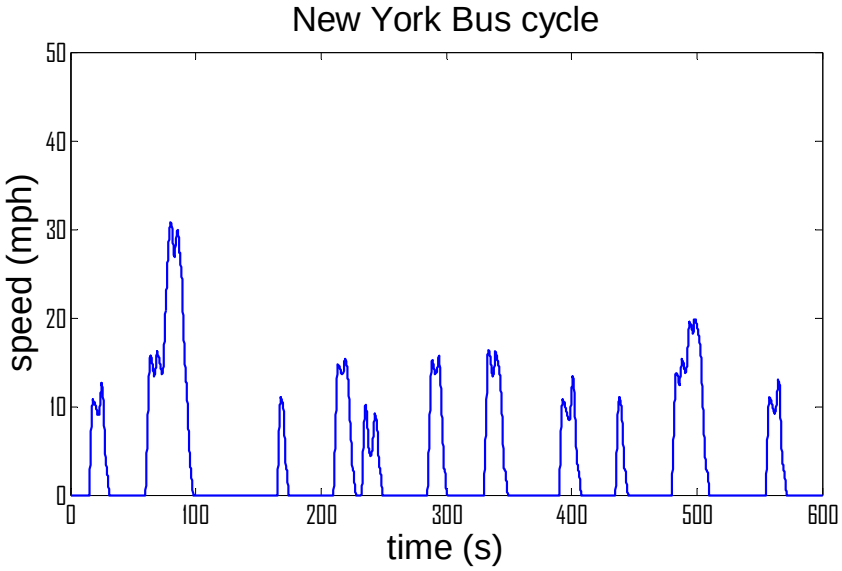

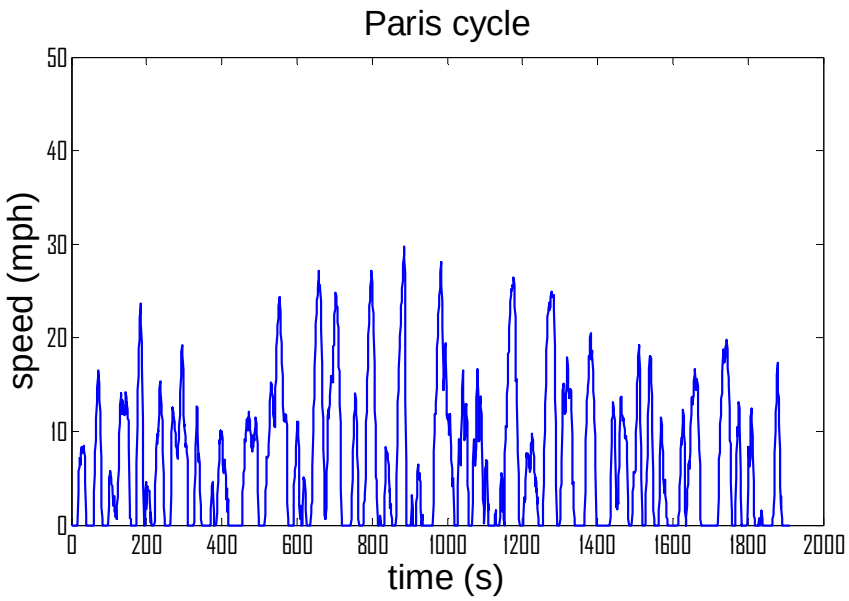
Paris cycle
speed (mph)
time (s)
0
10
20
30
40
50
0
200
400
600
800
1000
1200
1400
1600
1800
2000

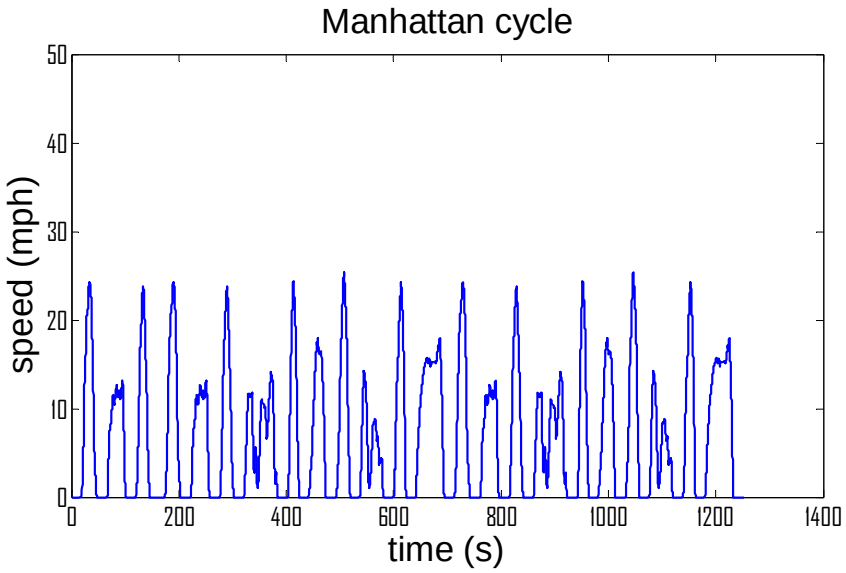
Manhattan cycle
speed (mph)
time (s)
0
10
20
30
40
50
0
200
400
600
800
1000
1200
1400

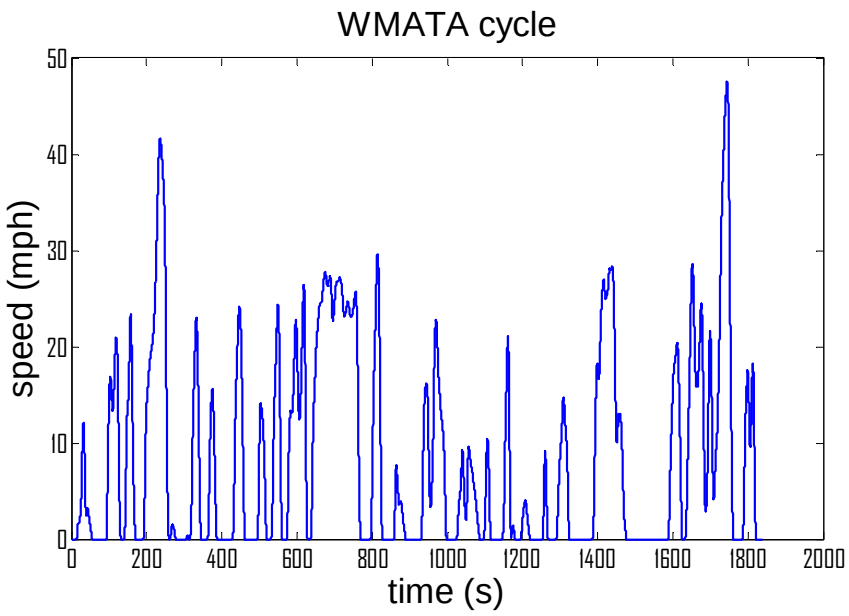
WMATA cycle
speed (mph)
time (s)
0
10
20
30
40
50
0
200
400
600
800
1000
1200
1400
1600
1800
2000

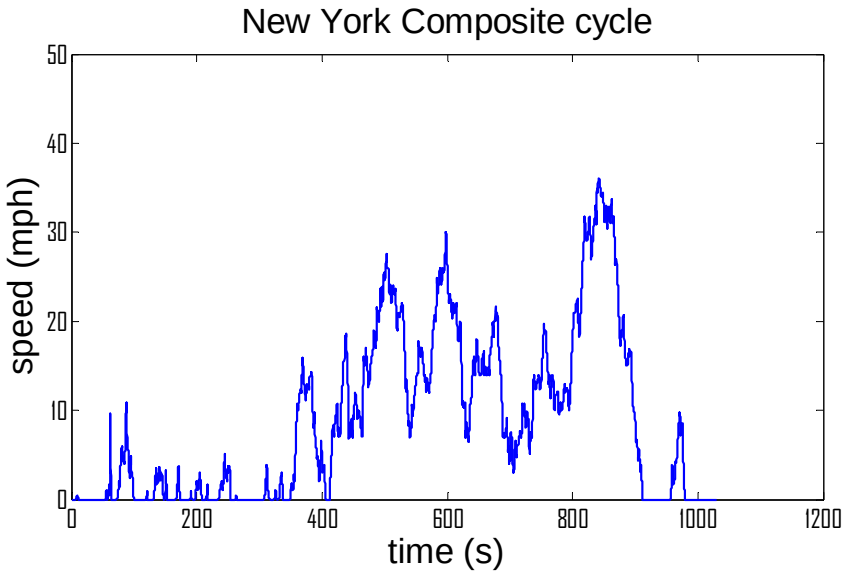
New York Composite cycle
speed (mph)
time (s)
0
10
20
30
40
50
0
200
400
600
800
1000
1200

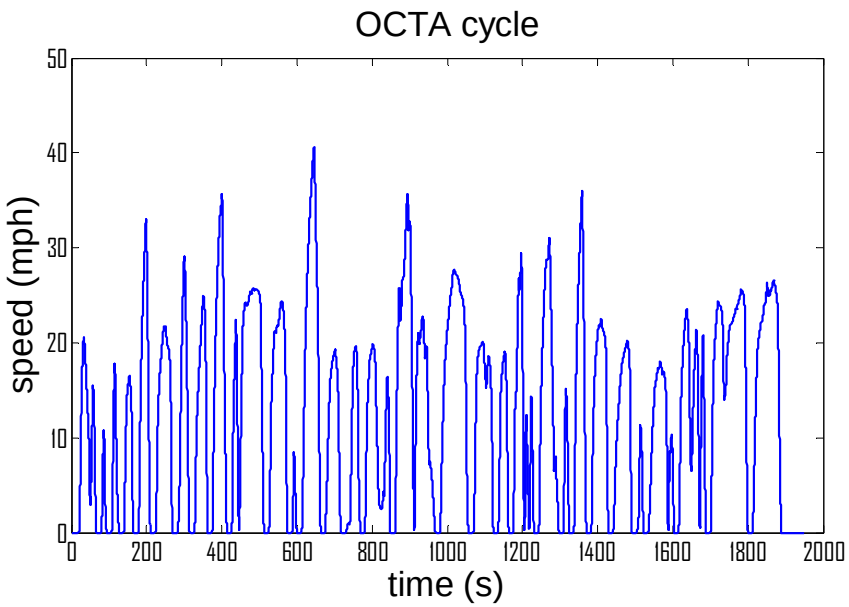
OCTA cycle
speed (mph)
time (s)
0
10
20
30
40
50
0
200
400
600
800
1000
1200
1400
1600
1800
2000

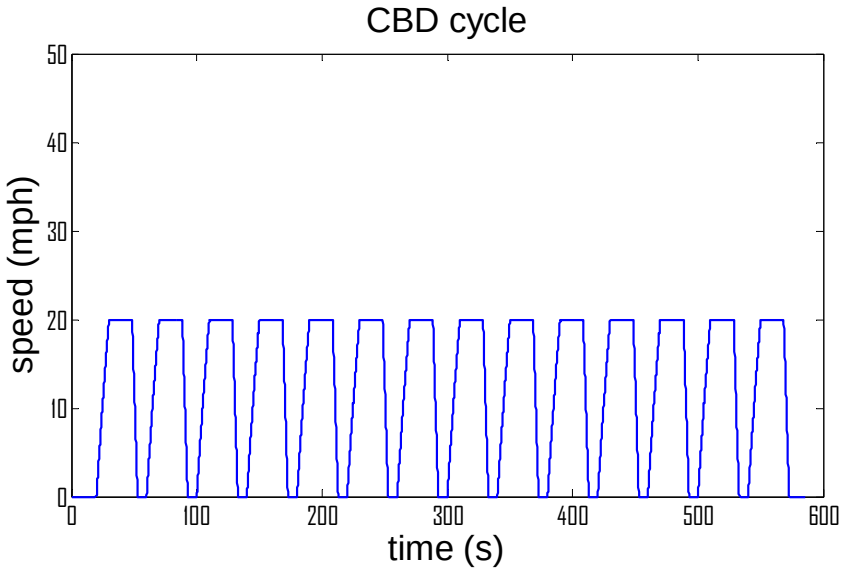
CBD cycle
speed (mph)
time (s)
0
10
20
30
40
50
0
100
200
300
400
500
600

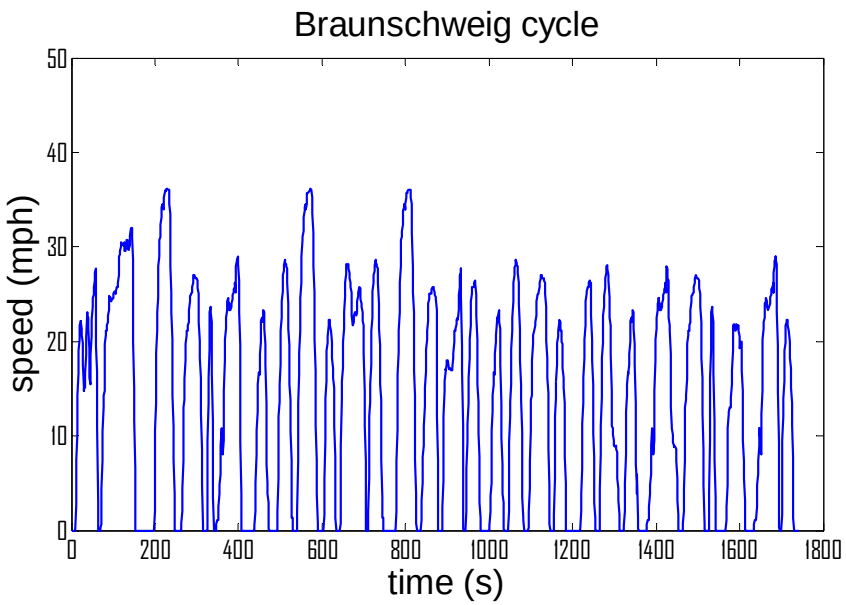
Braunschweig cycle
speed (mph)
time (s)
0
10
20
30
40
50
0
200
400
600
800
1000
1200
1400
1600
1800

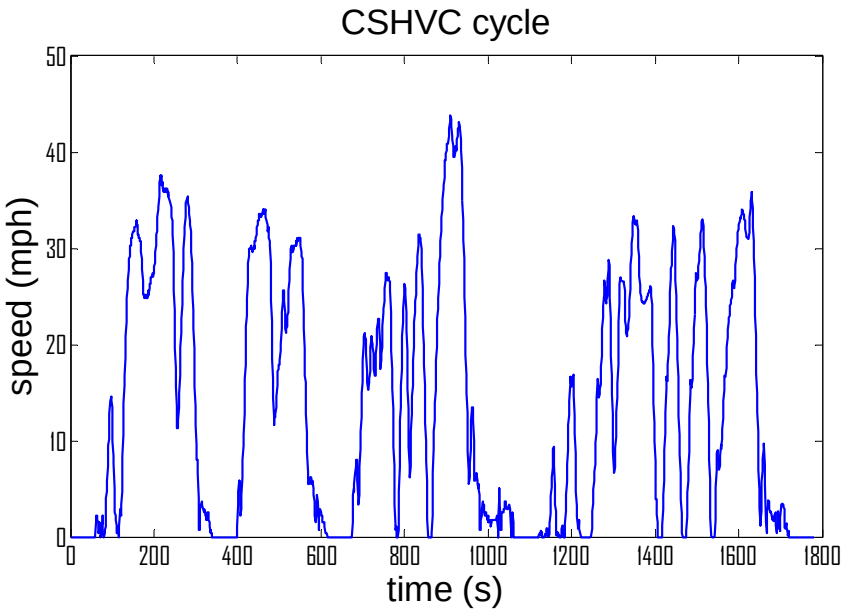
CSHVC cycle
speed (mph)
time (s)
0
10
20
30
40
50
0
200
400
600
800
1000
1200
1400
1600
1800

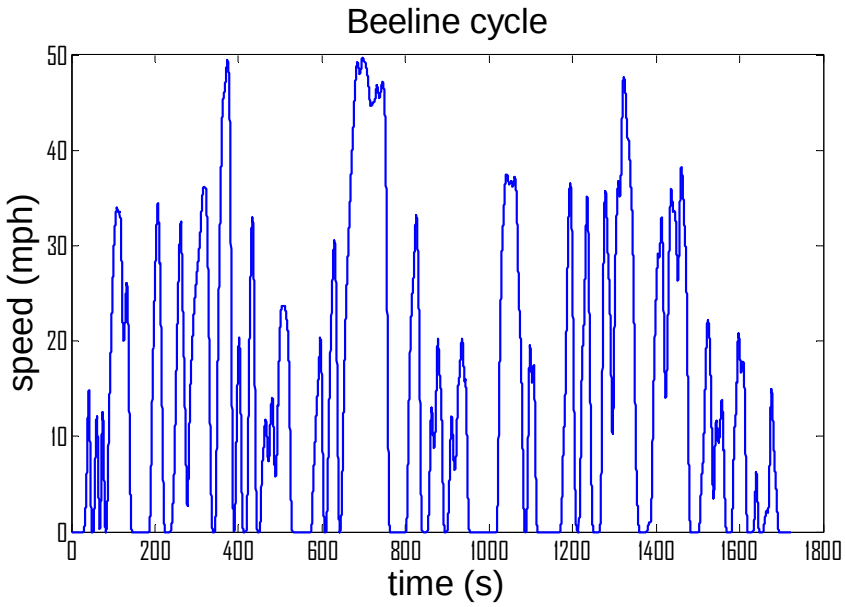
Beeline cycle
speed (mph)
time (s)
0
10
20
30
40
50
0
200
400
600
800
1000
1200
1400
1600
1800

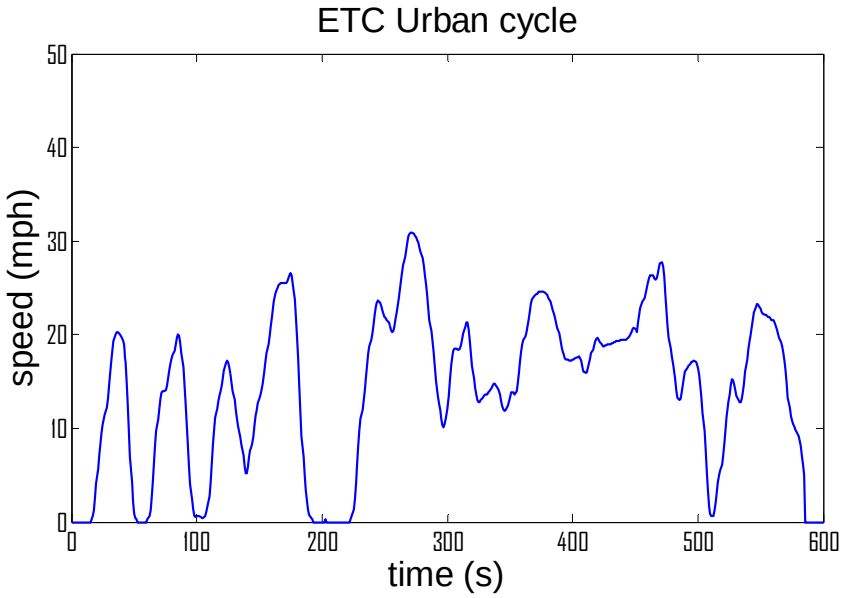
ETC Urban cycle
speed (mph)
time (s)
0
10
20
30
40
50
0
100
200
300
400
500
600

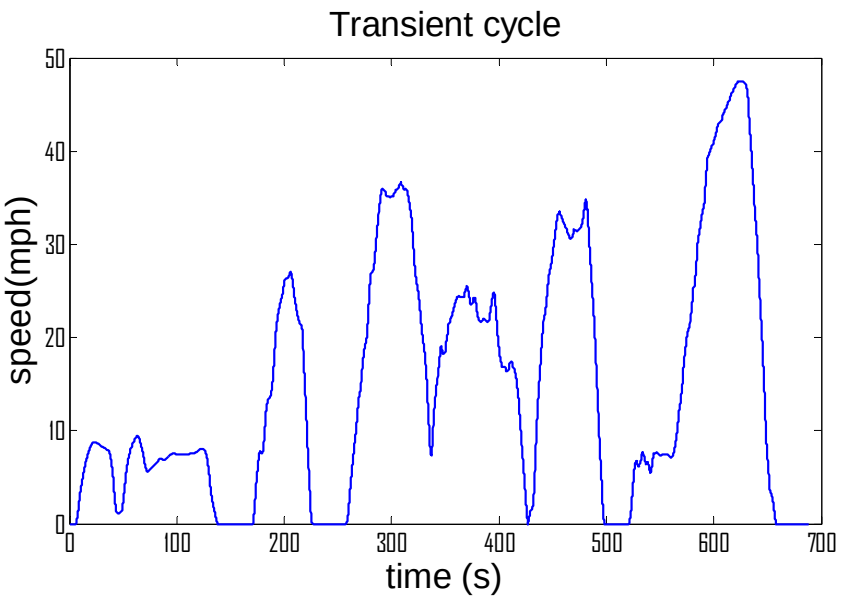
Transient cycle
speed(mph)
time (s)
0
10
20
30
40
50
0
100
200
300
400
500
600
700

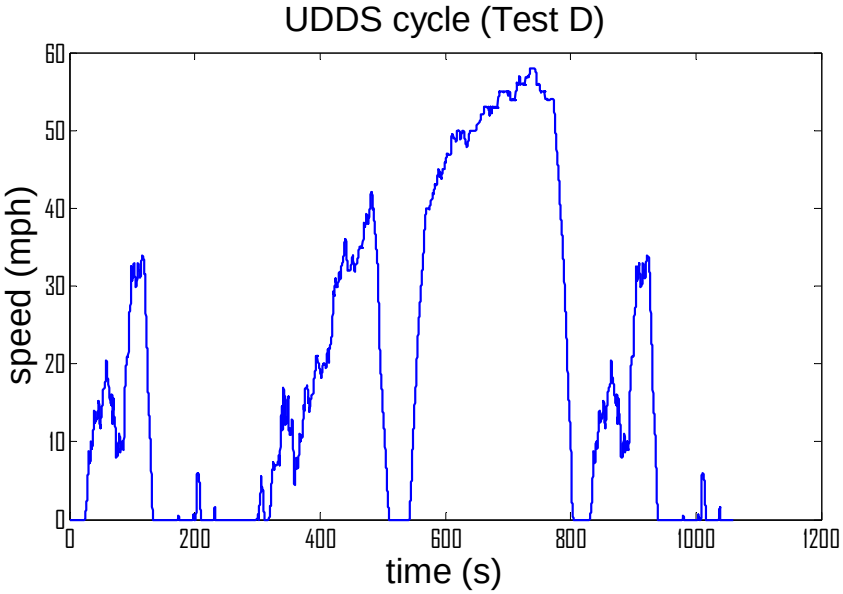
UDDS cycle (Test D)
speed (mph)
time (s)
0
10
20
30
40
50
60
0
200
400
600
800
1000
1200

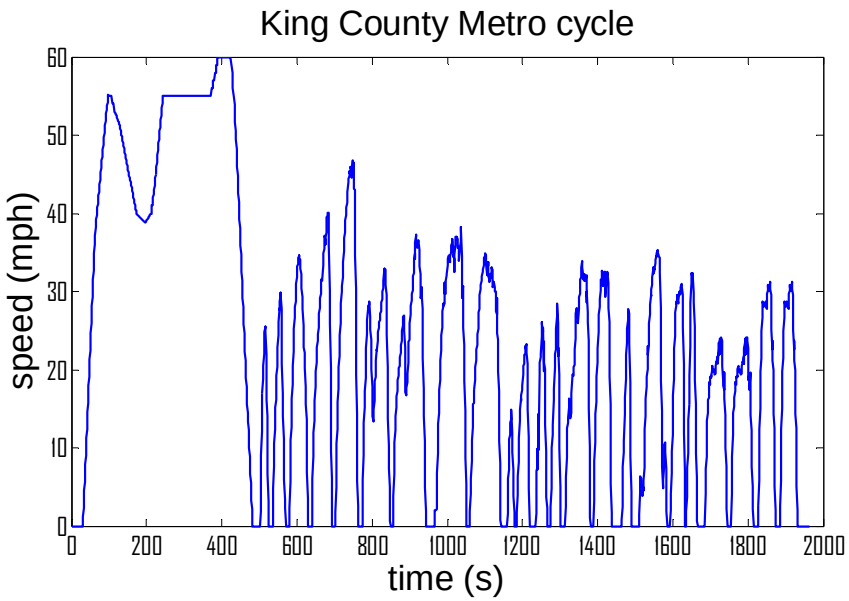
King County Metro cycle
speed (mph)
time (s)
0
10
20
30
40
50
60
0
200
400
600
800
1000
1200
1400
1600
1800
2000

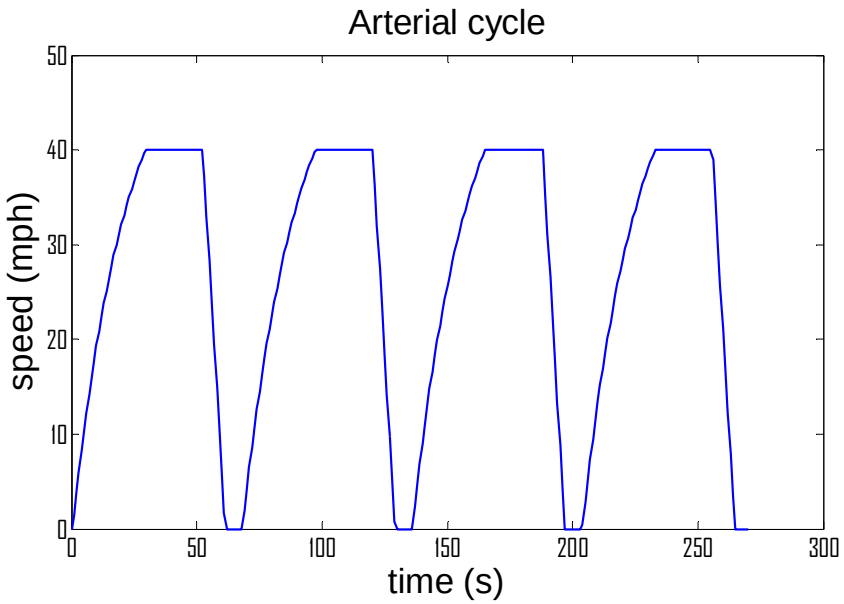
Arterial cycle
speed (mph)
time (s)
0
10
20
30
40
50
0
50
100
150
200
250
300

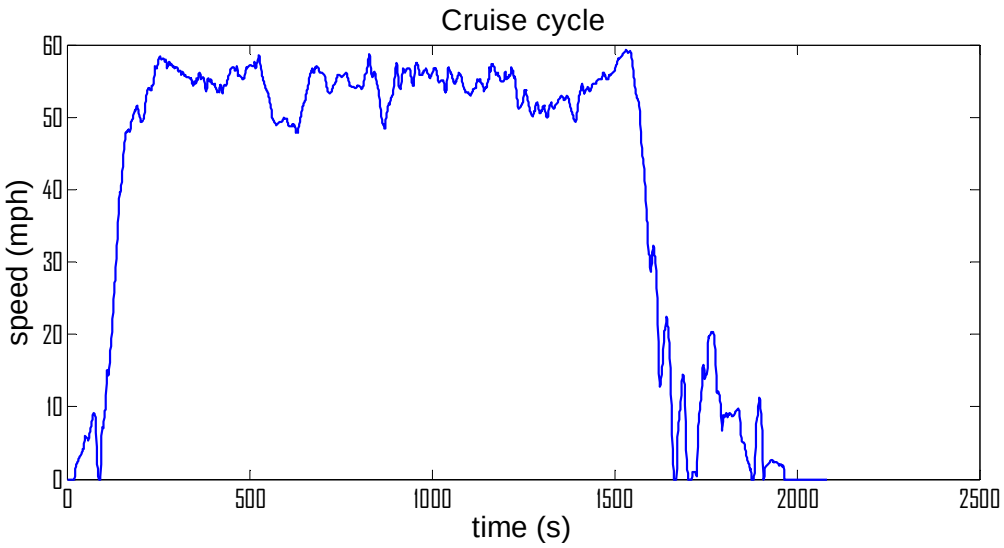
Cruise cycle
speed (mph)
time (s)
0
10
20
30
40
50
60
0
500
1000
1500
2000
2500

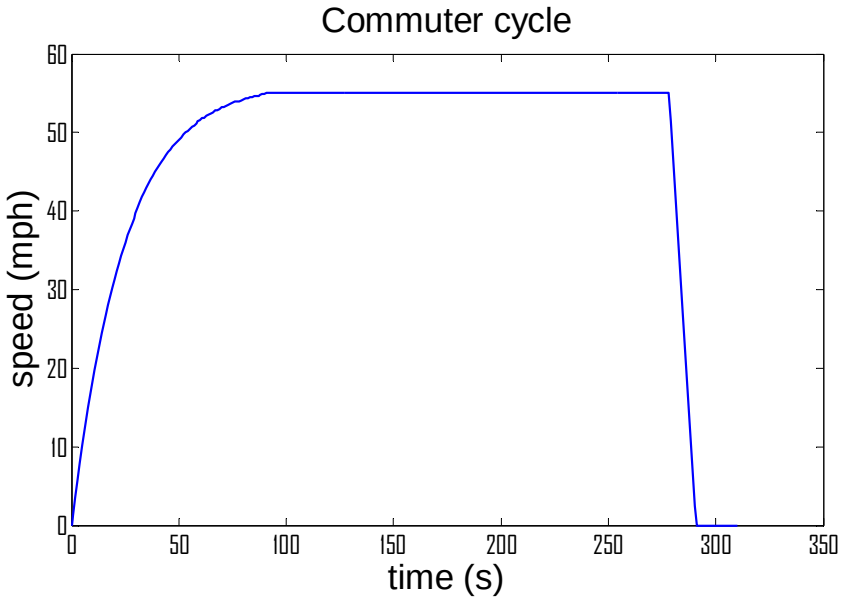
Commuter cycle
speed (mph)
time (s)
0
10
20
30
40
50
60
0
50
100
150
200
250
300
350

Cycle Properties (Averaged over 5 vehicles)

Metric ID	Metric	Units	Chassis Dynamometer Cycles																
			ART	Beeline	BRAUN	CBD	COMM	CSHVC	ETCURBAN	Idle	KCM	Manhattan	NYBus	NYComp	OCTA	PARIS	UDDS	TRANS	WMATA
1	AvSpeed	mph	25.55	14.04	13.75	13.11	44.37	14.02	14.11	0.00	23.34	6.86	3.51	8.75	12.17	6.64	18.73	15.33	8.45
2	AvDriSpeed	mph	27.87	17.85	16.53	14.11	47.58	17.28	15.60	0.00	26.20	9.26	6.56	11.52	14.63	8.97	24.81	17.47	11.97
3	RPS	none	0.63	0.57	0.60	0.55	0.59	0.56	0.54	0.00	0.56	0.53	0.55	0.48	0.59	0.52	0.63	0.58	0.55
4	RSS	m/s	15.32	12.54	10.14	7.99	23.13	11.55	8.47	0.00	16.41	6.30	6.26	8.29	9.24	6.40	17.61	11.92	9.14
5	RPSS	m/s	9.55	7.10	6.11	4.37	13.43	6.44	4.59	0.00	8.78	3.31	3.42	3.94	5.45	3.36	10.92	7.16	5.04
6	RCS	m^2/s^2	249.00	186.07	113.08	67.12	546.07	149.91	77.86	0.00	311.67	45.64	48.07	82.15	95.72	49.80	356.33	170.76	99.68
7	RPCS	m^2/s^2	153.03	105.60	68.34	36.46	313.59	82.24	41.92	0.00	161.22	23.70	25.50	38.57	56.06	26.02	217.43	106.28	54.63
8	$AvSpeed^{1.5}$	$mph^{1.5}$	147.96	72.30	64.45	54.87	317.96	69.74	60.66	0.00	138.19	25.18	12.71	36.57	54.29	24.35	114.66	76.69	37.10
9	$AvSpeed^2$	mph^2	8.8E02	3.9E02	3.1E02	2.3E02	2.3E03	3.6E02	2.7E02	0.0E00	8.6E02	9.7E01	4.9E01	1.6E02	2.5E02	9.5E01	7.4E02	4.1E02	1.7E02
10	$AvSpeed^{2.5}$	$mph^{2.5}$	5.3E03	2.2E03	1.5E03	1.0E03	1.7E04	1.9E03	1.2E03	0.0E00	5.5E03	3.8E02	2.0E02	7.5E02	1.2E03	3.9E02	4.9E03	2.3E03	8.4E02
11	$AvSpeed^3$	mph^3	3.2E04	1.3E04	7.8E03	4.4E03	1.2E05	1.1E04	5.5E03	0.0E00	3.6E04	1.6E03	8.5E02	3.6E03	5.8E03	1.7E03	3.3E04	1.3E04	4.2E03
12	$AvSpeed^{3.5}$	$mph^{3.5}$	1.9E05	7.8E04	4.0E04	1.9E04	8.8E05	5.8E04	2.6E04	0.0E00	2.5E05	6.5E03	3.7E03	1.8E04	2.9E04	7.3E03	2.3E05	7.7E04	2.2E04
13	$AvSpeed^4$	mph^4	1.2E06	4.8E05	2.1E05	8.5E04	6.5E06	3.3E05	1.2E05	0.0E00	1.7E06	2.8E04	1.7E04	8.9E04	1.5E05	3.3E04	1.6E06	4.6E05	1.2E05
14	StdSpeed	mph	14.91	14.03	11.08	7.90	18.08	12.87	8.27	0.00	17.67	7.05	6.07	9.26	10.17	7.14	19.69	13.20	10.07
15	CovSpeed	%	58.47	99.93	80.58	60.35	40.78	91.85	58.60	0.00	75.67	102.65	172.93	105.84	83.57	107.45	105.10	86.09	119.27
16	IqrSpeed	mph	27.04	24.15	22.83	14.60	11.66	25.44	11.44	0.00	26.90	12.18	5.41	14.59	19.99	11.07	33.57	19.08	15.57
17	RmsSpeed	mph	29.58	19.85	17.66	15.30	47.91	19.03	16.35	0.00	29.27	9.84	7.01	12.73	15.86	9.75	27.17	20.22	13.14
18	StdDriSpeed	mph	13.35	13.49	10.08	7.29	14.08	12.15	7.23	0.00	16.60	6.69	6.99	8.99	9.40	6.92	19.04	12.69	10.08
19	CovDriSpeed	%	47.94	75.63	60.98	51.70	29.59	70.43	46.36	0.00	63.35	72.24	106.70	78.06	64.21	77.14	76.77	72.66	84.23
20	AvAcc	mph/s	-0.02	0.00	0.00	0.01	0.00	0.00	0.00	0.00	0.00	0.00	0.00	0.00	0.00	0.00	0.00	0.00	0.00
21	AvPosAcc	mph/s	0.89	0.78	0.81	0.97	0.32	0.53	0.53	0.00	0.72	0.71	0.49	0.30	0.74	0.63	0.35	0.51	0.59
21	AvPosAcc	mph/s	0.55	0.43	0.46	0.52	0.19	0.28	0.28	0.00	0.41	0.37	0.25	0.15	0.41	0.32	0.20	0.28	0.30
22	AvNegAcc	mph/s	1.49	0.97	1.06	1.11	0.45	0.59	0.61	0.00	0.94	0.78	0.51	0.30	0.94	0.65	0.48	0.62	0.62
23	$AvAcc^2$	mph^2/s^2	1.23	1.03	1.09	1.46	0.32	0.51	0.43	0.00	0.88	0.89	0.51	0.18	0.92	0.64	0.28	0.43	0.67
24	IF	s^{-1}	0.05	0.05	0.06	0.08	0.01	0.03	0.03	0.00	0.04	0.06	0.04	0.02	0.06	0.05	0.02	0.03	0.04
25	StdAcc	mph/s	1.49	1.15	1.18	1.27	0.78	0.80	0.73	0.00	1.11	0.99	0.76	0.43	1.08	0.83	0.67	0.78	0.88
26	IqrAcc	mph/s	1.43	1.35	1.46	2.09	0.14	0.68	0.93	0.00	1.05	1.14	0.45	0.41	1.35	1.08	0.35	0.73	0.74
27	RmsAcc	mph/s	1.49	1.15	1.18	1.27	0.77	0.80	0.73	0.00	1.11	0.99	0.76	0.43	1.08	0.83	0.67	0.78	0.88

Metric ID	Metric	Units	Chassis Dynamometer Cycles																
			ART	Beeline	BRAUN	CBD	COMM	CSHVC	ETCURBAN	Idle	KCM	Manhattan	NYBus	NYComp	OCTA	PARIS	UDDS	TRANS	WMATA
28	StdPosAcc	mph/s	0.66	0.64	0.66	0.72	0.46	0.48	0.38	0.00	0.60	0.62	0.52	0.29	0.61	0.50	0.40	0.42	0.56
29	CovPosAcc	%	136.07	121.73	123.25	133.69	68.39	110.70	138.70	0.00	120.68	114.66	94.78	103.26	122.99	126.29	87.63	120.71	105.40
30	StdNegAcc	mph/s	1.28	0.88	0.83	0.77	0.91	0.67	0.53	0.00	0.90	0.68	0.62	0.33	0.76	0.56	0.68	0.65	0.72
31	CovNegAcc	mph/s	116.48	110.13	127.40	144.71	49.63	88.90	114.79	0.00	105.04	114.22	82.30	92.89	124.04	117.44	71.27	94.99	87.25
32	Jerk	mph/s^2	-0.01	0.00	0.00	0.00	0.00	0.00	0.00	0.00	0.00	0.00	0.00	0.00	0.00	0.00	0.00	0.00	0.00
33	FreqAccD	$mile^{-1}$	18.14	24.33	28.22	48.86	2.08	5.29	0.25	0.00	12.29	36.10	23.95	0.00	24.64	18.20	3.29	3.03	20.45
34	FreqAccT	s^{-1}	0.13	0.09	0.11	0.18	0.03	0.02	0.00	0.00	0.08	0.07	0.02	0.00	0.08	0.03	0.02	0.01	0.05
35	PercIdle	%	7.39	23.64	16.23	4.84	6.44	23.58	10.82	100.00	10.05	28.19	53.06	33.17	15.33	26.31	30.74	14.57	35.58
36	PercAcc	%	61.68	54.64	56.55	53.70	58.72	51.90	53.46	0.00	56.53	52.35	50.72	49.96	55.73	50.56	57.88	55.20	51.17
37	PercDecel	%	38.32	44.39	43.24	46.30	41.28	46.46	46.54	0.00	43.46	47.65	49.25	49.96	44.21	48.77	41.82	44.71	48.71
38	KI	km^{-1}	1.70	2.72	3.99	5.85	0.23	2.33	3.77	0.00	1.00	11.76	13.70	4.19	4.56	9.85	0.73	1.87	4.69
39	FreqStopsD	$mile^{-1}$	1.36	3.66	4.41	6.78	0.15	2.27	1.96	0.00	1.85	9.68	18.86	7.22	4.82	12.44	2.05	1.62	6.20
40	RPA	m/s^2	0.20	0.22	0.20	0.19	0.05	0.15	0.12	0.00	0.14	0.21	0.22	0.09	0.19	0.18	0.09	0.14	0.19
41	IPS	m^2/s^3	2.33	1.37	1.24	1.10	1.00	0.92	0.77	0.00	1.42	0.65	0.35	0.36	1.01	0.54	0.80	0.96	0.72
42	PKE	m/s^2	0.42	0.51	0.45	0.39	0.13	0.35	0.29	0.00	0.31	0.54	0.66	0.34	0.44	0.49	0.26	0.32	0.47
43	InePow	kW	41.17	24.14	21.90	19.46	17.70	16.28	13.57	0.00	25.14	11.41	6.16	6.43	17.83	9.60	14.04	16.88	12.72
44	RolPow	kW	15.07	8.28	8.11	7.73	26.17	8.27	8.32	0.00	13.77	4.05	2.07	5.16	7.18	3.92	11.05	9.04	4.98
45	DPS	m^3/s^4	28.77	14.37	10.78	7.26	17.14	9.43	6.00	0.00	16.60	3.84	2.12	2.92	8.29	3.36	10.84	10.68	6.06
46	AeroPow	kW	10.52	4.32	2.57	1.45	40.07	3.47	1.82	0.00	12.03	0.52	0.28	1.19	1.93	0.55	11.04	4.33	1.39
47	AeroRolPow	kW	25.60	12.60	10.68	9.19	66.24	11.74	10.14	0.00	25.80	4.57	2.35	6.35	9.11	4.47	22.09	13.37	6.37
48	ChAcc	m/s^2	0.21	0.25	0.23	0.20	0.06	0.17	0.15	0.00	0.16	0.27	0.33	0.17	0.22	0.25	0.13	0.16	0.23
49	ChPower	W/kg	2.42	1.59	1.39	1.15	1.27	1.10	0.93	0.00	1.63	0.82	0.52	0.67	1.19	0.73	1.09	1.10	0.88
50	ChEnergy	J/kg	2.41	1.59	1.39	1.15	1.26	1.09	0.92	0.00	1.63	0.82	0.52	0.67	1.19	0.73	1.09	1.10	0.88
51	AvPosRLP	kW	60.20	32.09	28.79	25.31	79.48	23.95	19.76	0.00	44.55	14.05	7.51	10.17	23.71	12.08	31.68	25.78	16.55
52	AvPosVSP	W/kg	3.58	1.91	1.71	1.51	4.73	1.42	1.18	0.00	2.65	0.84	0.45	0.61	1.41	0.72	1.88	1.53	0.98
53	AvPet	kW	9.2E03	3.8E03	2.2E03	1.3E03	3.5E04	3.0E03	1.6E03	0.0E00	1.0E04	4.5E02	2.4E02	1.0E03	1.7E03	4.8E02	9.6E03	3.8E03	1.2E03
54	StdRLP	kW	115.72	77.65	65.59	53.65	82.88	54.65	37.83	0.00	78.01	39.51	29.01	24.53	57.37	34.02	59.81	57.91	48.61
55	CovRLP	%	192.25	241.83	227.77	211.97	104.13	228.16	191.41	0.00	175.00	281.19	385.82	241.16	241.94	281.63	188.83	224.60	293.79
56	dRLP/dt	W/s	5.6E03	3.9E03	3.7E03	3.6E03	1.8E03	2.5E03	2.2E03	0.0E00	3.4E03	2.4E03	1.3E03	1.0E03	3.1E03	1.8E03	1.8E03	2.1E03	2.3E03
57	StdInePow	kW	115.01	76.29	65.09	53.75	76.99	53.34	37.33	0.00	73.23	39.30	28.83	23.33	56.98	33.74	52.30	56.06	48.02

Metric ID	Metric	Units	Chassis Dynamometer Cycles																
			ART	Beeline	BRAUN	CBD	COMM	CSHVC	ETCURBAN	Idle	KCM	Manhattan	NYBus	NYComp	OCTA	PARIS	UDDS	TRANS	WMATA
58	CovInePow	%	279.39	315.81	297.22	276.25	434.31	327.58	275.08	0.00	291.04	344.35	467.97	363.02	319.48	351.36	372.50	332.03	377.55
68	$Acc^{1}Speed^{3}$	m^{4}/s^{5}	395.98	178.91	106.39	53.34	328.09	109.43	52.21	0.00	236.47	26.43	15.71	27.74	79.16	24.98	179.45	141.12	62.20
69	$Acc^{2}Speed^{1}$	m^{3}/s^{5}	1.24	0.79	0.71	0.67	0.33	0.38	0.26	0.00	0.66	0.40	0.18	0.10	0.55	0.27	0.26	0.36	0.37
70	$Acc^{2}Speed^{2}$	m^{4}/s^{6}	13.23	7.43	5.50	3.96	4.29	3.55	1.86	0.00	6.23	2.31	1.07	0.83	4.15	1.65	2.81	3.70	2.89
71	$Accel^{2}Speed^{3}$	m^{5}/s^{7}	161.09	82.34	48.73	26.46	65.98	37.70	15.33	0.00	71.64	15.38	7.90	7.73	36.68	11.82	36.57	44.17	27.94
72	$Acc^{3}Speed^{1}$	m^{4}/s^{7}	0.80	0.54	0.50	0.48	0.16	0.19	0.10	0.00	0.41	0.29	0.10	0.04	0.37	0.16	0.13	0.17	0.22
73	$Acc^{3}Speed^{2}$	m^{5}/s^{8}	7.51	4.72	3.66	2.63	1.75	1.69	0.69	0.00	3.34	1.67	0.60	0.28	2.63	0.96	1.25	1.59	1.65
74	$Acc^{3}Speed^{3}$	m^{6}/s^{9}	82.01	47.76	30.12	16.47	22.55	16.65	5.37	0.00	32.29	10.80	4.46	2.60	21.86	6.67	13.90	17.63	14.94
75	Distance	mi	2.06	6.72	6.68	2.06	4.04	6.62	2.34	0.00	12.72	2.09	0.58	2.50	6.59	3.52	5.51	2.84	4.31
76	CO_2	g/s	13.58	8.88	8.19	7.88	18.41	6.81	6.51	1.71	11.44	6.47	5.33	5.68	7.65	5.42	9.59	7.43	6.23
77	NOx	g/s	0.07	0.05	0.04	0.04	0.07	0.04	0.04	0.01	0.06	0.05	0.04	0.05	0.05	0.03	0.05	0.04	0.04
78	FE	mpg	4.67	3.78	4.23	4.14	5.71	5.03	5.09	0.08	4.83	2.41	1.62	3.65	3.79	2.77	4.80	4.85	3.24

Appendix C – In-use Routes

WashPA2

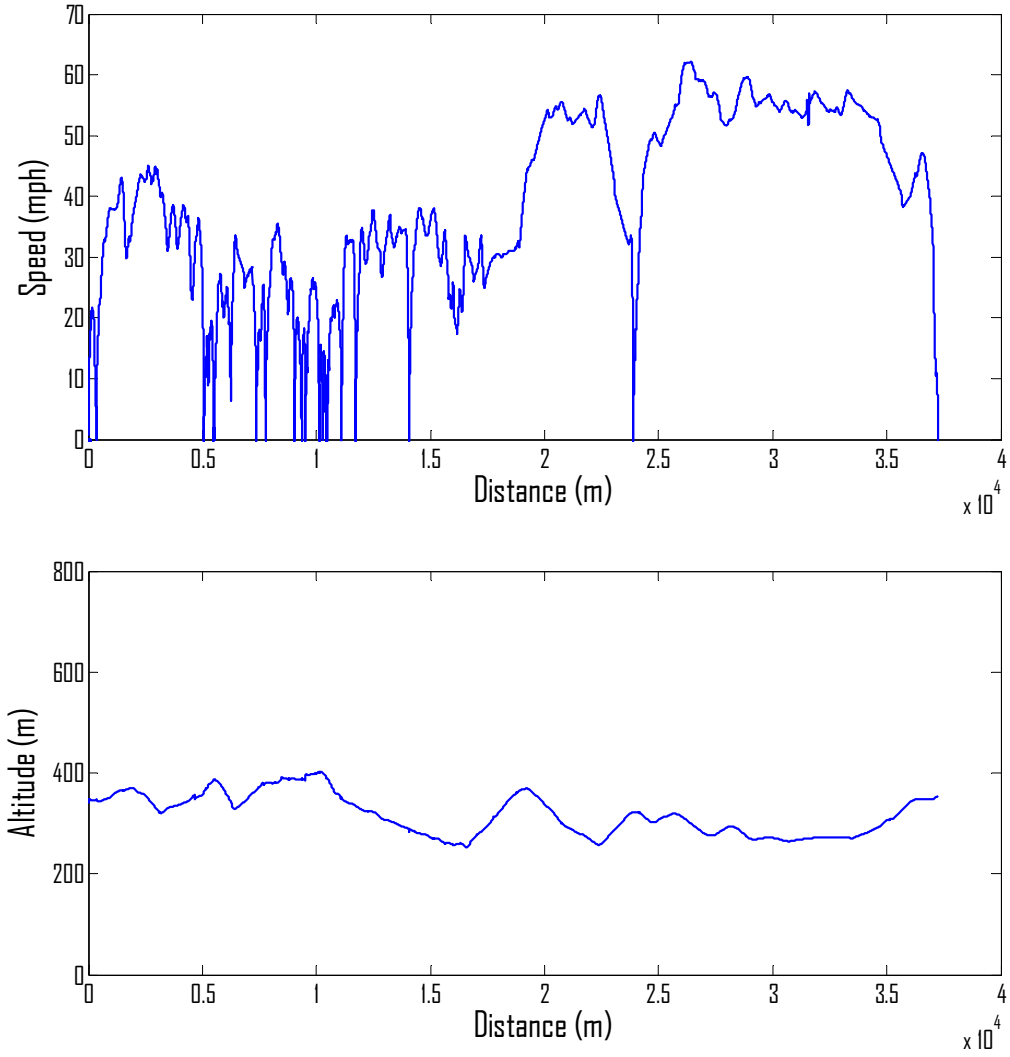

WashPA1

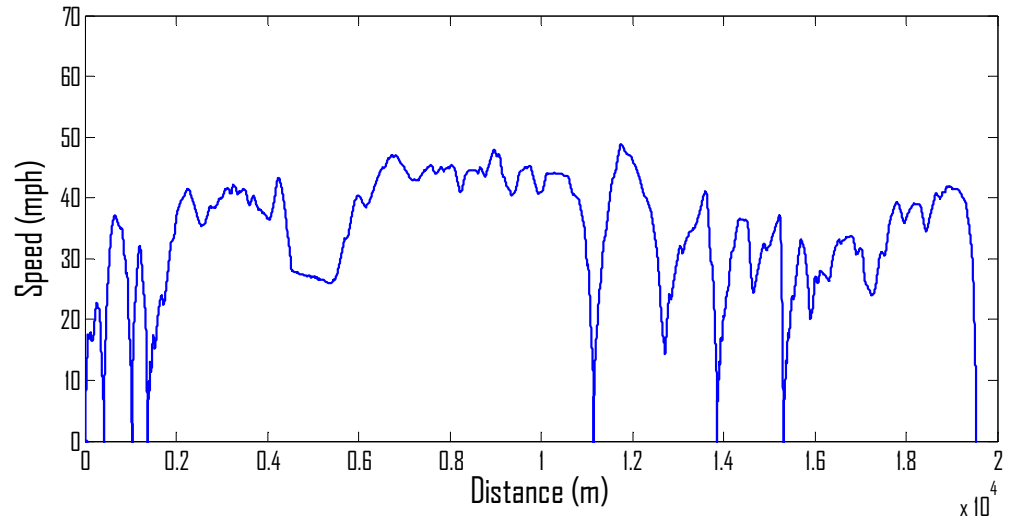
Speed (mph)
70
60
50
40
30
20
10
0
0
0.2
0.4
0.6
0.8
1
1.2
1.4
1.6
1.8
2
Distance (m)
x 10^4

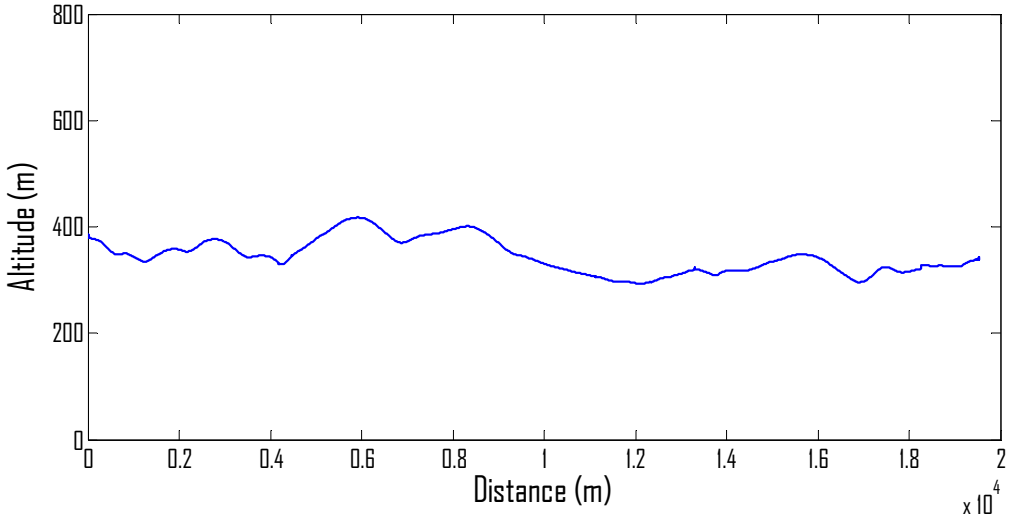
Altitude (m)
800
600
400
200
0
0
0.2
0.4
0.6
0.8
1
1.2
1.4
1.6
1.8
2
Distance (m)
x 10^4

BM2Sab

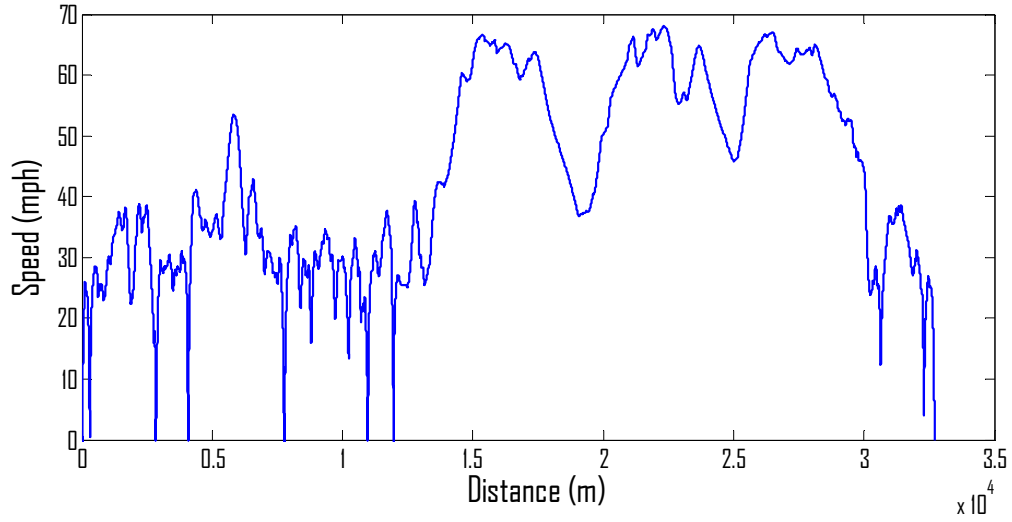
Speed (mph)
70
60
50
40
30
20
10
0
0
0.5
1
1.5
2
2.5
3
3.5
Distance (m)
x 10^4

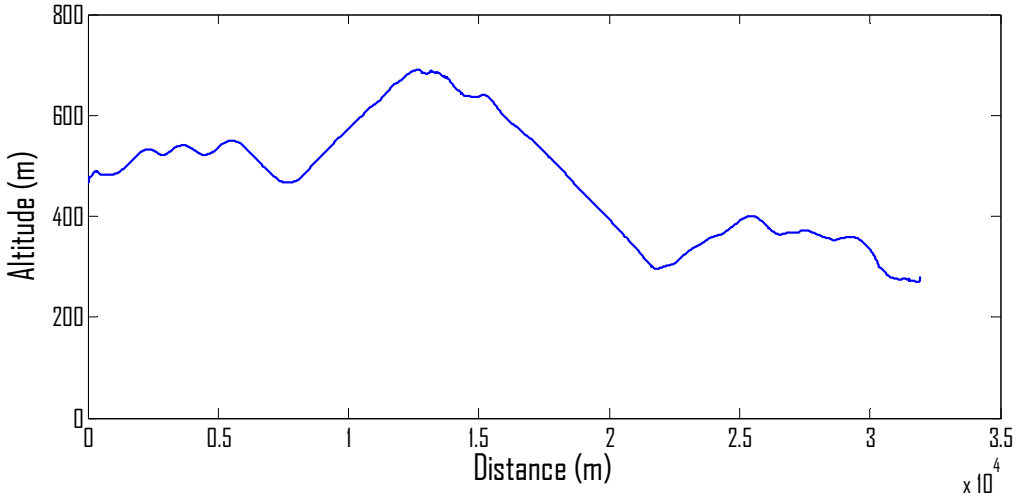
Altitude (m)
800
600
400
200
0
0
0.5
1
1.5
2
2.5
3
3.5
Distance (m)
x 10^4

Sab2BM

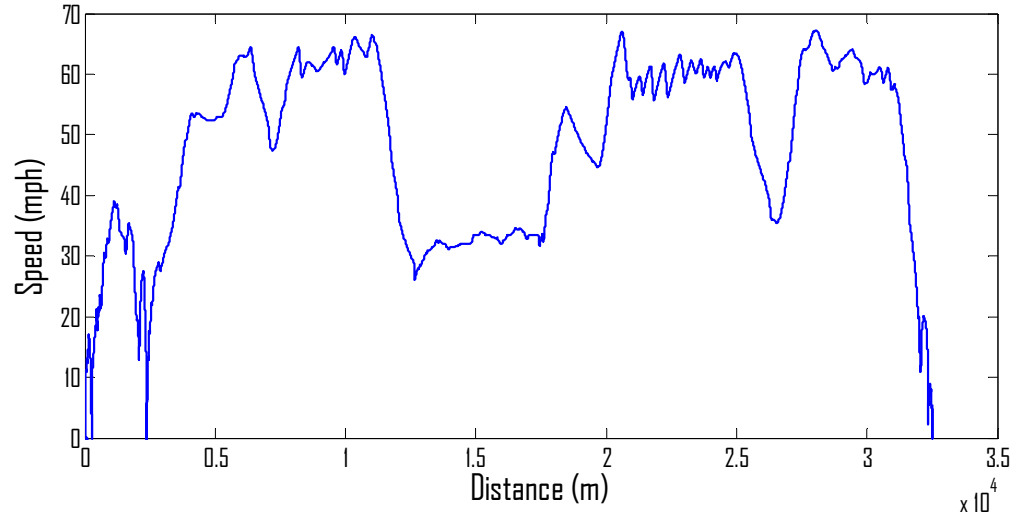
Speed (mph)
70
60
50
40
30
20
10
0
0
0.5
1
1.5
2
2.5
3
3.5
Distance (m)
x 10^4

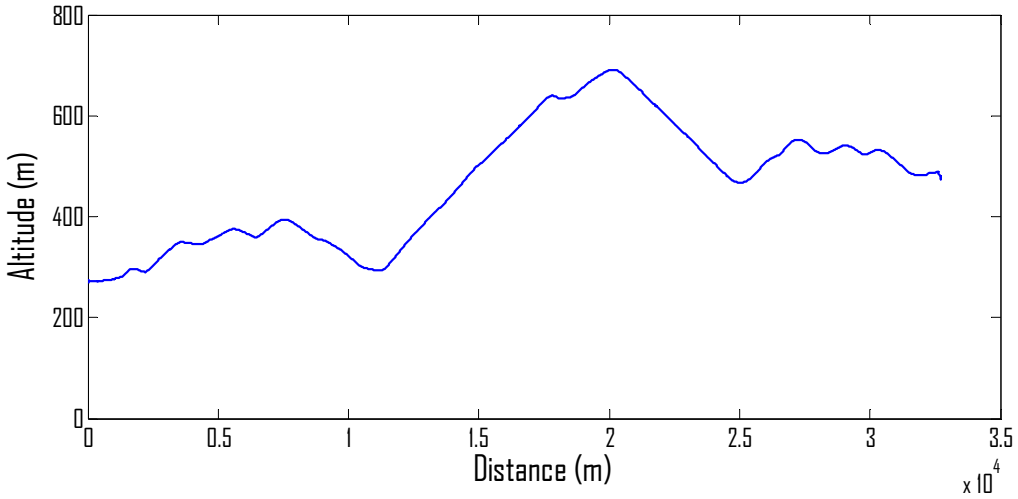
Altitude (m)
800
600
400
200
0
0
0.5
1
1.5
2
2.5
3
3.5
Distance (m)
x 10^4

Sab2SW

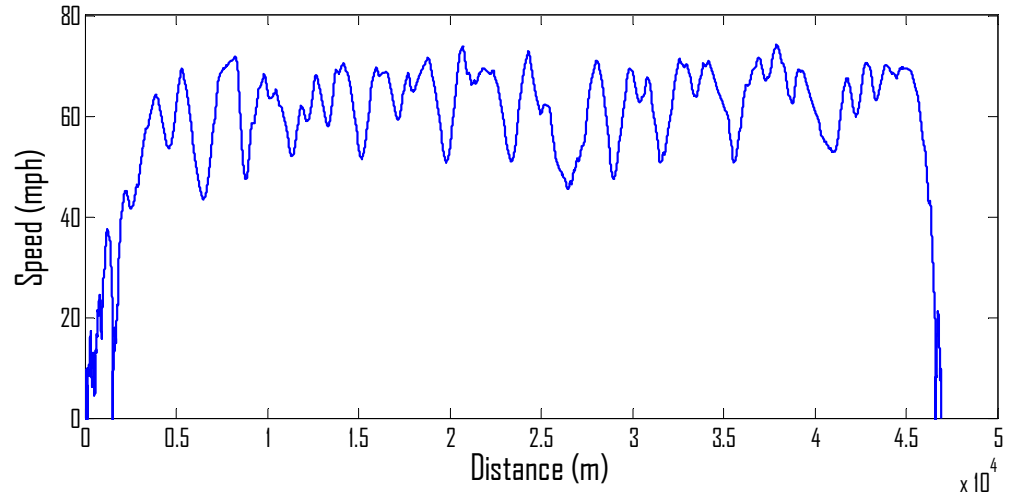
Speed (mph)
0
20
40
60
80
0
0.5
1
1.5
2
2.5
3
3.5
4
4.5
5
Distance (m)
x 10^4

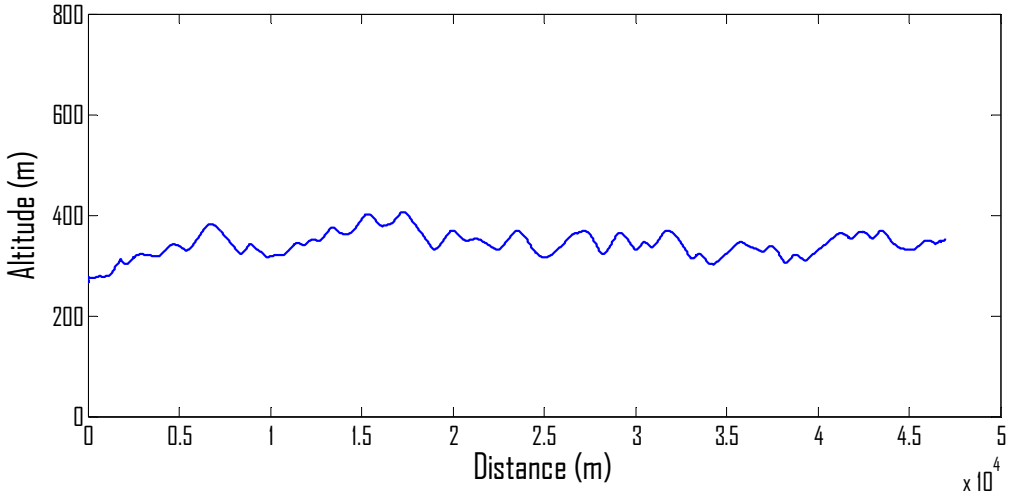
Altitude (m)
0
200
400
600
800
0
0.5
1
1.5
2
2.5
3
3.5
4
4.5
5
Distance (m)
x 10^4

SW2Sab

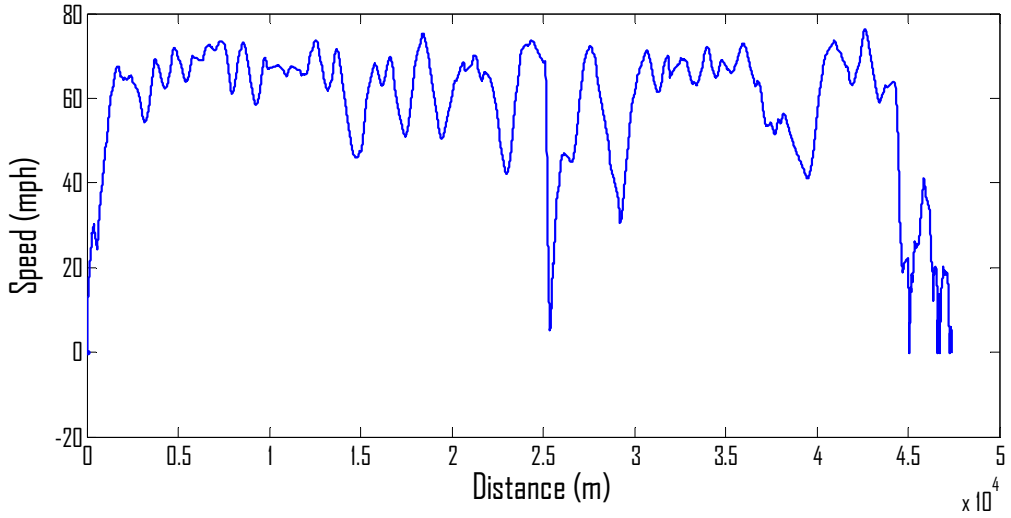
Speed (mph)
80
60
40
20
0
-20
0
0.5
1
1.5
2
2.5
3
3.5
4
4.5
5
Distance (m)
x 10^4

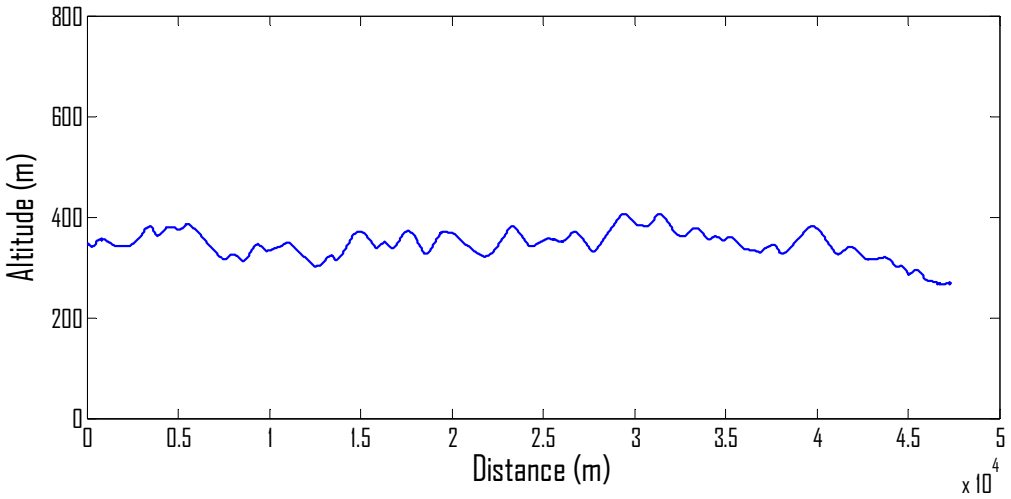
Altitude (m)
800
600
400
200
0
0
0.5
1
1.5
2
2.5
3
3.5
4
4.5
5
Distance (m)
x 10^4

WashPA3

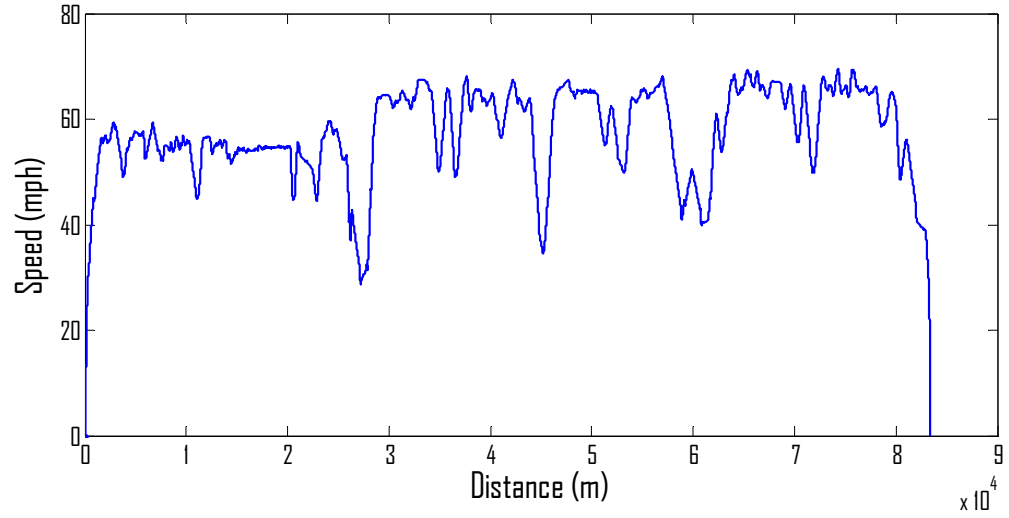
Speed (mph)
0
20
40
60
80
0
1
2
3
4
5
6
7
8
9
Distance (m)
x 10^4

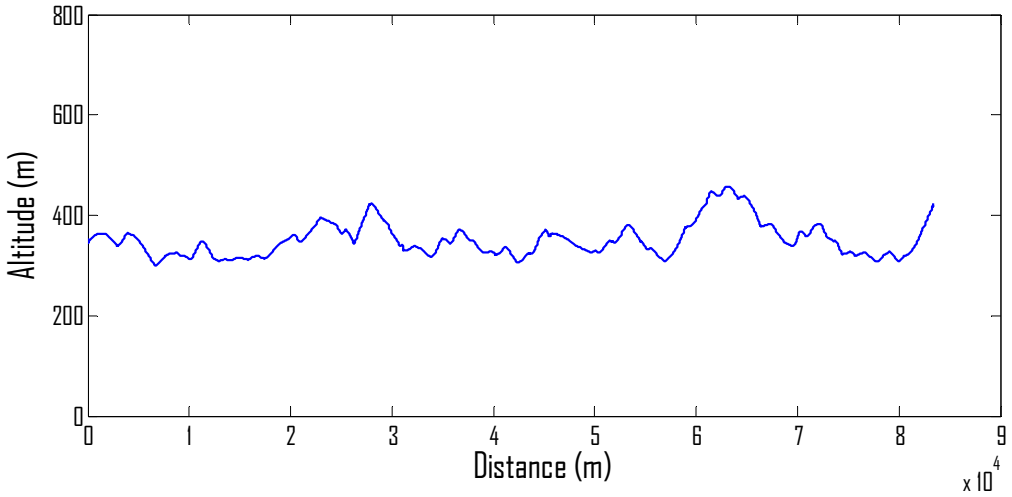
Altitude (m)
0
200
400
600
800
0
1
2
3
4
5
6
7
8
9
Distance (m)
x 10^4

Route Properties (averaged over 18 vehicles)

Metric ID	Metric	Units	In-use Routes						
			WashPA2	WashPA1	BM2Sab	Sab2BM	Sab2SW	SW2Sab	WashPA3
1	AvSpeed	mph	25.94	26.13	35.60	36.01	46.94	48.06	52.19
2	AvDriSpeed	mph	30.29	30.70	39.11	40.45	51.72	51.84	55.24
3	RPS	none	0.51	0.54	0.50	0.50	0.49	0.51	0.49
4	RSS	m/s	17.82	15.98	21.59	22.10	25.91	26.20	25.82
5	RPSS	m/s	9.10	8.50	10.91	11.22	12.74	13.27	12.83
6	RCS	m^2/s^2	363.26	274.30	512.29	542.83	700.18	719.12	682.44
7	RPCS	m^2/s^2	185.31	145.16	262.14	280.98	344.67	365.11	340.78
8	$AvSpeed^{1.5}$	$mph^{1.5}$	1.6E02	1.5E02	2.4E02	2.5E02	3.6E02	3.7E02	4.0E02
9	$AvSpeed^2$	mph^2	1.0E03	9.4E02	1.7E03	1.8E03	2.7E03	2.8E03	3.0E03
10	$AvSpeed^{2.5}$	$mph^{2.5}$	6.9E03	5.8E03	1.2E04	1.3E04	2.1E04	2.2E04	2.3E04
11	$AvSpeed^3$	mph^3	4.7E04	3.6E04	9.2E04	9.9E04	1.7E05	1.7E05	1.8E05
12	$AvSpeed^{3.5}$	$mph^{3.5}$	3.3E05	2.3E05	6.8E05	7.5E05	1.3E06	1.4E06	1.4E06
13	$AvSpeed^4$	mph^4	2.3E06	1.4E06	5.2E06	5.8E06	1.0E07	1.1E07	1.1E07
14	StdSpeed	mph	18.93	15.73	21.18	21.83	22.53	22.43	16.69
15	CovSpeed	%	73.43	60.68	59.78	61.17	48.39	46.82	32.21
16	IqrSpeed	mph	30.36	25.94	35.44	34.72	29.24	31.23	14.12
17	RmsSpeed	mph	32.14	30.54	41.45	42.17	52.14	53.07	54.89
18	StdDriSpeed	mph	16.97	12.37	18.91	18.96	17.89	18.68	11.38
19	CovDriSpeed	%	56.26	40.49	48.47	47.28	34.68	36.14	20.77
20	AvAcc	mph/s	0.00	0.00	0.00	0.00	0.00	0.00	0.00
21	AvPosAcc	mph/s	0.51	0.56	0.45	0.39	0.51	0.48	0.29
21	AvPosAcc	mph/s	0.23	0.26	0.20	0.17	0.23	0.22	0.14
22	AvNegAcc	mph/s	0.55	0.68	0.44	0.43	0.50	0.49	0.29
23	$AvAcc^2$	mph^2/s^2	0.55	0.59	0.43	0.32	0.45	0.42	0.24
24	IF	s^{-1}	0.02	0.02	0.01	0.01	0.01	0.01	0.00
25	StdAcc	mph/s	0.72	0.80	0.62	0.56	0.64	0.63	0.42
26	IqrAcc	mph/s	0.52	0.63	0.50	0.41	0.75	0.67	0.40
27	RmsAcc	mph/s	0.72	0.80	0.62	0.56	0.64	0.63	0.42
28	StdPosAcc	mph/s	0.52	0.51	0.46	0.39	0.41	0.42	0.31
29	CovPosAcc	%	100.54	111.88	98.69	101.51	131.56	119.01	107.18
30	StdNegAcc	mph/s	0.62	0.72	0.50	0.51	0.45	0.47	0.33
31	CovNegAcc	mph/s	89.04	94.85	92.44	84.06	115.33	107.00	97.19
32	Jerk	mph/s^2	0.00	0.00	0.00	0.00	0.00	0.00	0.00
33	FreqAccD	$mile^{-1}$	16.44	18.30	9.37	3.99	3.60	3.45	1.15
34	FreqAccT	s^{-1}	0.12	0.13	0.09	0.04	0.05	0.05	0.02
35	PercIdle	%	14.40	14.82	9.00	10.93	9.28	7.28	5.49
36	PercAcc	%	44.65	46.28	44.55	44.14	45.00	46.99	46.58
37	PercDecel	%	41.56	38.51	44.98	40.65	46.04	45.93	46.15
38	KI	km^{-1}	0.52	0.86	0.35	0.32	0.31	0.29	0.19
39	FreqStopsD	$mile^{-1}$	0.69	0.50	0.24	0.26	0.12	0.12	0.03
40	RPA	m/s^2	0.09	0.11	0.09	0.08	0.10	0.10	0.06

Metric ID	Metric	Units	In-use Routes						
			WashPA2	WashPA1	BM2Sab	Sab2BM	Sab2SW	SW2Sab	WashPA3
41	lPS	m^2/s^3	1.05	1.33	1.37	1.31	2.19	2.12	1.42
42	PKE	m/s^2	0.19	0.24	0.18	0.17	0.22	0.21	0.13
43	lnePow	kW	39.12	49.86	51.03	48.81	81.86	79.21	52.95
44	RolPow	kW	37.93	38.20	52.07	52.68	68.64	70.30	76.36
45	DPS	m^3/s^4	15.93	19.44	28.43	29.35	55.12	53.52	35.78
46	AeroPow	kW	14.21	10.80	27.53	29.60	49.63	52.11	53.60
47	AeroRolPow	kW	52.14	49.01	79.60	82.28	118.27	122.41	129.96
48	ChAcc	m/s^2	0.16	0.17	0.14	0.21	0.14	0.12	0.11
49	ChPower	m^2/s^3 or W/kg	1.85	2.03	2.31	3.42	2.94	2.67	2.58
50	ChEnergy	m^2/s^2 or J/kg	0.37	0.41	0.46	0.68	0.59	0.53	0.52
51	AvPosRLP	kW	96.04	99.08	122.73	169.76	179.12	165.70	168.17
52	AvPosVSP	W/kg	2.70	2.79	3.45	4.77	5.04	4.66	4.73
53	AvPet	kW	1.2E04	9.3E03	2.4E04	2.5E04	4.3E04	4.5E04	4.6E04
54	StdRLP	kW	194.73	215.79	263.12	253.00	264.13	261.73	219.35
55	CovRLP	%	202.11	218.03	214.52	149.18	146.15	156.40	128.24
56	dRLP/dt	W/s	1.8E04	2.0E04	1.9E04	1.9E04	2.4E04	2.4E04	2.1E04
57	StdlnePow	kW	127.05	153.36	163.39	163.51	225.13	223.94	159.25
58	CovlnePow	%	320.41	308.20	318.14	334.28	272.53	279.89	290.09
59	AvPosGrade	%	1.33	1.40	1.44	2.06	1.46	1.30	1.06
60	AvNegGrade	%	1.36	1.65	2.09	1.42	1.31	1.45	0.99
61	AvClimbRate	m/s	0.15	0.16	0.23	0.33	0.31	0.28	0.25
62	AvGrade	%	-0.07	-0.13	-0.48	1.24	0.41	-0.06	0.28
63	StdGrade	%	4.13	3.96	4.11	4.00	3.34	3.31	2.61
64	AvAsc	%	2.60	2.89	3.19	3.79	2.84	2.76	2.23
65	AvDes	%	2.82	3.22	3.81	3.13	2.70	2.76	1.89
66	AltDistance	%	-0.03	-0.25	-0.65	0.64	0.15	-0.15	0.07
67	GradePow	kW	53.50	56.91	79.81	115.60	106.61	97.23	86.12
68	Acc^1Speed^3	m^4/s^5	295.01	315.05	666.59	732.77	1463.98	1431.60	933.29
69	Acc^2Speed^1	m^3/s^5	0.41	0.52	0.50	0.41	0.79	0.77	0.49
70	Acc^2Speed^2	m^4/s^6	5.59	6.94	9.33	8.81	19.10	18.78	11.71
71	$Accel^2Speed^3$	m^5/s^7	97.59	106.69	206.84	215.19	496.60	490.45	294.68
72	Acc^3Speed^1	m^4/s^7	0.43	0.29	0.36	0.22	0.69	0.80	1.33
73	Acc^3Speed^2	m^5/s^8	6.86	3.58	6.64	4.44	15.88	18.24	28.41
74	Acc^3Speed^3	m^6/s^9	132.07	52.22	144.60	106.00	391.59	448.20	649.50
75	Distance	mi	22.90	12.03	19.77	20.16	29.07	29.30	51.42
76	CO_2	g/s	18.10	18.74	22.07	30.35	30.09	27.23	27.77
77	NOx	g/s	0.21	0.20	0.27	0.39	0.39	0.35	0.41

Appendix D – Modeling Methodology Flowchart